

Eye movement tracking in ocular, neurological, and mental diseases

Edited by

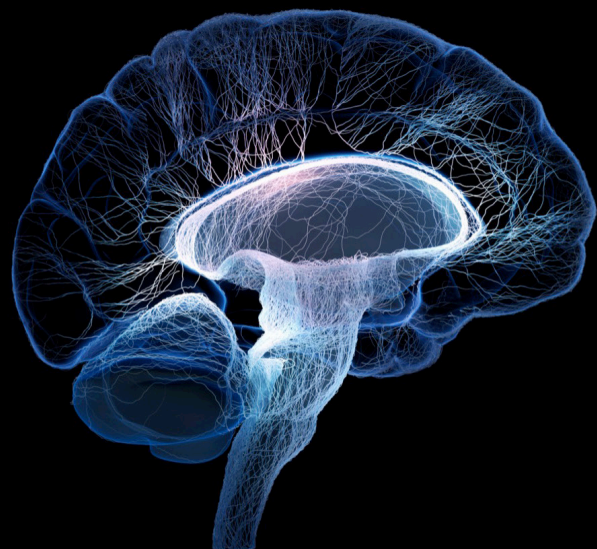
Xuemin Li, Joanne Fielding, Rong Zhang and
Xiaoyu Liu

Coordinated by

Yuxin Wang

Published in

Frontiers in Neuroscience



FRONTIERS EBOOK COPYRIGHT STATEMENT

The copyright in the text of individual articles in this ebook is the property of their respective authors or their respective institutions or funders. The copyright in graphics and images within each article may be subject to copyright of other parties. In both cases this is subject to a license granted to Frontiers.

The compilation of articles constituting this ebook is the property of Frontiers.

Each article within this ebook, and the ebook itself, are published under the most recent version of the Creative Commons CC-BY licence. The version current at the date of publication of this ebook is CC-BY 4.0. If the CC-BY licence is updated, the licence granted by Frontiers is automatically updated to the new version.

When exercising any right under the CC-BY licence, Frontiers must be attributed as the original publisher of the article or ebook, as applicable.

Authors have the responsibility of ensuring that any graphics or other materials which are the property of others may be included in the CC-BY licence, but this should be checked before relying on the CC-BY licence to reproduce those materials. Any copyright notices relating to those materials must be complied with.

Copyright and source acknowledgement notices may not be removed and must be displayed in any copy, derivative work or partial copy which includes the elements in question.

All copyright, and all rights therein, are protected by national and international copyright laws. The above represents a summary only. For further information please read Frontiers' Conditions for Website Use and Copyright Statement, and the applicable CC-BY licence.

ISSN 1664-8714
ISBN 978-2-8325-4400-6
DOI 10.3389/978-2-8325-4400-6

About Frontiers

Frontiers is more than just an open access publisher of scholarly articles: it is a pioneering approach to the world of academia, radically improving the way scholarly research is managed. The grand vision of Frontiers is a world where all people have an equal opportunity to seek, share and generate knowledge. Frontiers provides immediate and permanent online open access to all its publications, but this alone is not enough to realize our grand goals.

Frontiers journal series

The Frontiers journal series is a multi-tier and interdisciplinary set of open-access, online journals, promising a paradigm shift from the current review, selection and dissemination processes in academic publishing. All Frontiers journals are driven by researchers for researchers; therefore, they constitute a service to the scholarly community. At the same time, the *Frontiers journal series* operates on a revolutionary invention, the tiered publishing system, initially addressing specific communities of scholars, and gradually climbing up to broader public understanding, thus serving the interests of the lay society, too.

Dedication to quality

Each Frontiers article is a landmark of the highest quality, thanks to genuinely collaborative interactions between authors and review editors, who include some of the world's best academicians. Research must be certified by peers before entering a stream of knowledge that may eventually reach the public - and shape society; therefore, Frontiers only applies the most rigorous and unbiased reviews. Frontiers revolutionizes research publishing by freely delivering the most outstanding research, evaluated with no bias from both the academic and social point of view. By applying the most advanced information technologies, Frontiers is catapulting scholarly publishing into a new generation.

What are Frontiers Research Topics?

Frontiers Research Topics are very popular trademarks of the *Frontiers journals series*: they are collections of at least ten articles, all centered on a particular subject. With their unique mix of varied contributions from Original Research to Review Articles, Frontiers Research Topics unify the most influential researchers, the latest key findings and historical advances in a hot research area.

Find out more on how to host your own Frontiers Research Topic or contribute to one as an author by contacting the Frontiers editorial office: frontiersin.org/about/contact

Eye movement tracking in ocular, neurological, and mental diseases

Topic editors

Xuemin Li — Peking University Third Hospital, China

Joanne Fielding — Monash University, Australia

Rong Zhang — Peking University, China

Xiaoyu Liu — Beihang University, China

Topic Coordinator

Yuxin Wang — Peking University Third Hospital, China

Citation

Li, X., Fielding, J., Zhang, R., Liu, X., Wang, Y., eds. (2024). *Eye movement tracking in ocular, neurological, and mental diseases*. Lausanne: Frontiers Media SA.
doi: 10.3389/978-2-8325-4400-6

Table of contents

- 05 **Editorial: Eye movement tracking in ocular, neurological, and mental diseases**
Yuexin Wang and Xuemin Li
- 07 **Vigilance or avoidance: How do autistic traits and social anxiety modulate attention to the eyes?**
Wei Ni, Haoyang Lu, Qiandong Wang, Ci Song and Li Yi
- 18 **Development of a quantitative measurement on visual clutter in see through display**
Qingfeng Liu, Yanyan Wang, Yu Bai, Mengsun Yu, Zhengtao Cao, Xinli Yu and Li Ding
- 24 **The impact of different corneal refractive surgeries on binocular dynamic visual acuity**
Yuexin Wang, Yining Guo, Yuanting Li, Yu Zhang, Yifei Yuan, Tingyi Wu, Yueguo Chen and Xuemin Li
- 34 **Binocular dynamic visual acuity in dry eye disease patients**
Xiaotong Ren, Yuexin Wang, Tingyi Wu, Dalan Jing and Xuemin Li
- 41 **Eye movement characteristics in a mental rotation task presented in virtual reality**
Zhili Tang, Xiaoyu Liu, Hongqiang Huo, Min Tang, Xiaofeng Qiao, Duo Chen, Ying Dong, Linyuan Fan, Jinghui Wang, Xin Du, Jieyi Guo, Shan Tian and Yubo Fan
- 52 **Eye movement characteristics and visual fatigue assessment of virtual reality games with different interaction modes**
Lei Fan, Junjie Wang, Qi Li, Zhenhao Song, Jinhui Dong, Fangjun Bao and Xiaofei Wang
- 60 **Influence of hypobaric hypoxic conditions on ocular structure and biological function at high attitudes: a narrative review**
Yuchen Wang, Xinli Yu, Ziyuan Liu, Zhongsheng Lv, Huaqin Xia, Yiren Wang, Jiayi Li and Xuemin Li
- 71 **Eye movement changes as an indicator of mild cognitive impairment**
Julius Opwonya, Boncho Ku, Kun Ho Lee, Joong Il Kim and Jaeuk U. Kim
- 81 **Motor synchronization and impulsivity in pediatric borderline personality disorder with and without attention-deficit hyperactivity disorder: an eye-tracking study of saccade, blink and pupil behavior**
Olivia G. Calancie, Ashley C. Parr, Don C. Brien, Jeff Huang, Isabell C. Pitigoi, Brian C. Coe, Linda Booij, Sarosh Khalid-Khan and Douglas P. Munoz

- 99 **Attentional bias for high-calorie food cues by the level of hunger and satiety in individuals with binge eating behaviors**
Ji-Min Woo, Gi-Eun Lee and Jang-Han Lee
- 111 **How do patients with Parkinson's disease and cerebellar ataxia read aloud? -Eye-voice coordination in text reading**
Yasuo Terao, Shin-ichi Tokushige, Satomi Inomata-Terada, Tai Miyazaki, Naoki Kotsuki, Francesco Fisicaro and Yoshikazu Ugawa
- 136 **Machine learning-based early diagnosis of autism according to eye movements of real and artificial faces scanning**
Fanchao Meng, Fenghua Li, Shuxian Wu, Tingyu Yang, Zhou Xiao, Yujian Zhang, Zhengkui Liu, Jianping Lu and Xuerong Luo



OPEN ACCESS

EDITED AND REVIEWED BY
Benjamin Thompson,
University of Waterloo, Canada

*CORRESPONDENCE
Xuemin Li
✉ lxmxm66@sina.com

RECEIVED 01 January 2024
ACCEPTED 03 January 2024
PUBLISHED 19 January 2024

CITATION
Wang Y and Li X (2024) Editorial: Eye
movement tracking in ocular, neurological,
and mental diseases.
Front. Neurosci. 18:1364078.
doi: 10.3389/fnins.2024.1364078

COPYRIGHT
© 2024 Wang and Li. This is an open-access
article distributed under the terms of the
[Creative Commons Attribution License \(CC
BY\)](#). The use, distribution or reproduction in
other forums is permitted, provided the
original author(s) and the copyright owner(s)
are credited and that the original publication
in this journal is cited, in accordance with
accepted academic practice. No use,
distribution or reproduction is permitted
which does not comply with these terms.

Editorial: Eye movement tracking in ocular, neurological, and mental diseases

Yuexin Wang^{1,2} and Xuemin Li^{1,2*}

¹Department of Ophthalmology, Peking University Third Hospital, Beijing, China, ²Beijing Key Laboratory of Restoration of Damaged Ocular Nerve, Beijing, China

KEYWORDS

eye movement, eye tracking, ocular disease, neurological disease, mental disease, dynamic vision

Editorial on the Research Topic

Eye movement tracking in ocular, neurological, and mental diseases

Eye movement and dynamic vision abnormalities could be seen in various ocular, neurological, and mental disorders. Therefore, eye movement tracking and accurate evaluation and interpretation of eye movement patterns are significant to disease assessment, diagnosis and treatment. Now, eye-tracking-based tasks and dynamic vision can effectively be integrated into visual and cognitive function evaluation that contributes to assessing several ocular and mental diseases. To further promote the standardized application of the eye movement tracking-based assessment paradigm, the relationship between eye movement patterns and disease parameters should be elucidated qualitatively and quantitatively. The present Research Topic contains a representative collection of studies regarding eye movement tracking and dynamic vision and its interpretation in various ocular and mental disorders.

The majority of the articles in the Research Topic combine various tasks and measurements of eye movement in patients with neurological or mental diseases. The coordination between eye movement and daily tasks might be affected in patients with these disorders. Terao et al. investigated the role of the cerebellum and basal ganglia in eye-voice coordination during reading aloud in patients with Parkinson's disease and spinocerebellar degeneration (SCD). They found that SCD patients have restricted ability to advance text processing ahead of the gaze due to slowed vocal output, and PD patients have slowed scanning but effectively utilize advanced processing of upcoming text. Opwonya et al. developed machine learning-based models for classifying mild cognitive impairment (MCI) using eye movement data during prosaccade/antisaccade and go/no-go tasks. The models achieved an outstanding performance combining eye movement metrics, demographics, and cognitive test scores for MCI classification, and they found that changes in eye movement metrics in MCI are mainly attentional and executive function deficits. Ni et al. explored the influence of autistic traits and social anxiety on different temporal stages of attention to the eyes in college students, and their movement was recorded during the virtual face viewing. The study suggested the separate and interactive roles of autistic traits and social anxiety in ocular attention that highlight the application of eye-tracking techniques in psychiatric diagnosis. Calancie et al. enrolled pediatric patients with borderline personality disorder (BPD) symptoms with and without a comorbid attention deficit and hyperactivity disorder (ADHD) diagnosis and quantified

their temporal learning and performance to predictable or unpredictable stimuli in metronome tasks combined with video-based eye tracking. The research supports normal temporal motor prediction in patients with BPD and a reduced response inhibition in BPD combined with ADHD. [Meng et al.](#) applied eye movement patterns to cartoon characters or real persons in identifying children with autism spectrum disorder (ASD) and found that machine learning algorithms provide promising results in identifying ASD with eye movement metrics. [Woo et al.](#) investigate the relationship between attentional bias for food cues and hunger in individuals with binge eating problems with the eye tracker. The research demonstrated that attentional bias for high-calorie food occurred in individuals with binge eating problems without awareness.

As for ocular diseases, conventional visual function assessment mainly focuses on static vision. Dynamic vision, involving the coordination of complicated eye movement, is limited evaluated in clinical ophthalmology. [Wang, Guo et al.](#) investigated the impact of different corneal refractive surgeries on dynamic visual acuity (DVA) and found that postoperative DVA was better than before the surgery in adult myopic patients. [Ren et al.](#) examined DVA in dry eye patients and demonstrated that DVA is significantly associated with symptoms and signs of dry eye disease. The patients with corneal fluorescein staining and severe meibomian gland dropout have worse DVA than those without the signs. These studies demonstrate that DVA is a promising indicator for functional vision in patients with ocular diseases or surgeries that might better reflect the vision in real-life scenarios.

Conventionally, eye-tracking research presents visual tasks on a two-dimensional screen. With the development of virtual reality (VR), it could present three-dimensional objects in versatile surroundings and simultaneously record eye movement. In the Research Topic, two studies applied VR technology in eye movement research. [Fan et al.](#) explored the eye movement characteristics during virtual reality games of primary mode or 360 modes. They found that the saccade duration and amplitude were greater in the mode with visual stimulus from all around the subjects, and the primary mode is more likely to cause visual fatigue. [Tang et al.](#) designed a virtual reality-based mental rotation task using 3D stimuli and applied an eye tracker to record eye movement during task. The result showed that the fixation time and number of within-object fixation and saccades for mirrored objects were lower than that for identical objects.

Outstanding dynamic vision and accurate object tracking are crucial in some occupations, including driver, pilot and athletes. As shown in the Research Topic, [Liu et al.](#) enrolled pilots to complete

visual search tasks with various clutter factors using an eye tracker to record the viewing path in a timely manner. The research found a significant difference among eye movement metrics at different clutter and developed a quantitative measurement for declutter design and appraisal of cockpit displays. Besides the original articles, the Research Topic also includes a review of dynamic vision. [Wang, Yu et al.](#) reviewed the dynamic visual and eye movement changes in high-altitude environments. They illustrated that dynamic vision performance gradually decreased as the altitude increased, and the pupil saccade function did not differ under different hypoxic conditions.

The present Research Topic demonstrates that eye movement and dynamic vision evaluation potentially provide important information in the assessment and diagnosis of ocular diseases, neurological diseases, and mental disorders. Further research is required to standardize the paradigm and integrate eye-tracking and dynamic vision evaluation into conventional medical systems to better interpret and understand the disease.

Author contributions

YW: Conceptualization, Validation, Writing—original draft.
XL: Conceptualization, Validation, Writing—review & editing.

Funding

The author(s) declare that no financial support was received for the research, authorship, and/or publication of this article.

Conflict of interest

The authors declare that the research was conducted in the absence of any commercial or financial relationships that could be construed as a potential conflict of interest.

Publisher's note

All claims expressed in this article are solely those of the authors and do not necessarily represent those of their affiliated organizations, or those of the publisher, the editors and the reviewers. Any product that may be evaluated in this article, or claim that may be made by its manufacturer, is not guaranteed or endorsed by the publisher.



OPEN ACCESS

EDITED BY

Xuemin Li,
Peking University Third Hospital, China

REVIEWED BY

Vivien Günther,
Leipzig University, Germany
Toru Fujioka,
University of Fukui, Japan

*CORRESPONDENCE

Li Yi
✉ yilipku@pku.edu.cn

SPECIALTY SECTION

This article was submitted to
Visual Neuroscience,
a section of the journal
Frontiers in Neuroscience

RECEIVED 27 October 2022

ACCEPTED 16 December 2022

PUBLISHED 11 January 2023

CITATION

Ni W, Lu H, Wang Q, Song C and Yi L
(2023) Vigilance or avoidance: How
do autistic traits and social anxiety
modulate attention to the eyes?
Front. Neurosci. 16:1081769.
doi: 10.3389/fnins.2022.1081769

COPYRIGHT

© 2023 Ni, Lu, Wang, Song and Yi. This
is an open-access article distributed
under the terms of the [Creative
Commons Attribution License \(CC BY\)](#).
The use, distribution or reproduction in
other forums is permitted, provided
the original author(s) and the copyright
owner(s) are credited and that the
original publication in this journal is
cited, in accordance with accepted
academic practice. No use, distribution
or reproduction is permitted which
does not comply with these terms.

Vigilance or avoidance: How do autistic traits and social anxiety modulate attention to the eyes?

Wei Ni¹, Haoyang Lu¹, Qiandong Wang^{2,3}, Ci Song¹ and
Li Yi^{1,4*}

¹School of Psychological and Cognitive Sciences and Beijing Key Laboratory of Behavior and Mental Health, Peking University, Beijing, China, ²Beijing Key Laboratory of Applied Experimental Psychology, National Demonstration Center for Experimental Psychology Education, Faculty of Psychology, Beijing Normal University, Beijing, China, ³Education Research Center for Children With ASD, Faculty of Education, Beijing Normal University, Beijing, China, ⁴IDG/McGovern Institute for Brain Research at PKU, Peking University, Beijing, China

Introduction: Social anxiety disorder (SAD) and autism spectrum disorder (ASD) are highly overlapping in symptoms and have a high rate of comorbidity, posing challenges in diagnosis and intervention for both disorders. Both disorders are linked to abnormal attention to the eyes, yet how they interactively modulate the attentional process to the eyes remains unclear.

Methods: In this study, we explored how autistic traits and social anxiety in college students separately and together affected different temporal stages of attention to the eyes. Participants were instructed to view virtual faces for 10 s and make an emotional judgment, while their eye movements were recorded.

Results: We found that social anxiety and autistic traits affected different temporal stages of eye-looking. Social anxiety only affected the first fixation duration on the eyes, while autistic traits were associated with eye avoidance at several time points in the later stage. More importantly, we found an interactive effect of autistic traits and social anxiety on the initial attention to the eyes: Among people scoring high on autistic traits, social anxiety was related to an early avoidance of the eyes as well as attention maintenance once fixated on the eyes.

Discussion: Our study suggests the separate and interactive roles of social anxiety and autistic traits in attention to the eyes. It contributes to a deeper understanding of the mechanisms of social attention in both SAD and ASD and highlights the application of psychiatric diagnoses using eye-tracking techniques.

KEYWORDS

autism spectrum disorder, social anxiety disorder, attention to the eyes, eye avoidance, attention maintenance, eye movement

1. Introduction

Social anxiety disorder (SAD), characterized by fear and anxiety of social contexts, is one of the most common mental disorders, with a lifetime prevalence of 4% and a 12-month prevalence of 2.4% across countries (Stein et al., 2017). People with SAD worry that their behaviors will be negatively evaluated by others and thus show anxiety and avoidance of various social situations (American Psychiatric Association [APA], 2013). SAD is commonly reported in the typical population (Stein and Stein, 2008) and also among people with special needs, such as people with autism spectrum disorder (ASD), a neurodevelopmental disorder involving social communication impairments and repetitive, restricted behavior and interests (American Psychiatric Association [APA], 2013). Similar to SAD, autistic people also show social avoidance and withdrawn behavior (Kleberg et al., 2017). Moreover, these two disorders have a high rate of comorbidity: Social anxiety affected 12–56% of autistic adults (Rosbrook and Whittingham, 2010; Bejerot et al., 2014; Maddox and White, 2015) and 7–57% of autistic children and adolescence (Leyfer et al., 2006; Kuusikko et al., 2008; White et al., 2015). The overlap of symptoms (e.g., avoidance of social interaction and eye contact) and the high rate of comorbidity between ASD and SAD pose challenges to diagnosis and intervention for both disorders. Hence, an investigation of how these two traits influence social behaviors separately and together becomes necessary. This study focused on the effects of autistic traits and social anxiety on social attention, especially attention to the eyes.

Abnormal attention to the eyes, such as eye avoidance, is commonly reported in people with autistic traits or ASD (e.g., Pelphrey et al., 2002; Chen and Yoon, 2011; Freeth et al., 2013; Yi et al., 2013, 2014), as well as people with SAD (e.g., Schneier et al., 2011; Weeks et al., 2013). The *eye avoidance* hypothesis of autism believes that avoidance of the eyes can cause severe social impairment in autistic people, since the eye region contains the most important social information (Tanaka and Sung, 2016). Autistic people may perceive the eyes as socially threatening, thus avoiding the eyes as an adaptive strategy. Similarly, the *avoidance* hypothesis of SAD proposes that people with SAD use safe actions like avoidance of eye contact to prevent feelings of fear and anxiety in social contexts (Clark and Wells, 1995).

Despite the similar eye avoidance patterns found in autistic people and people with SAD, people with SAD have specific attentional bias to the eyes at the early stages of face processing (e.g., Boll et al., 2016; Keil et al., 2018; Kleberg et al., 2021; Wieser et al., 2009b). The attentional biases in SAD could be explained by *vigilance* theory (Clark and Wells, 1995; Mogg and Bradley, 1998) and *maintenance* or *delayed disengagement* theory (Fox et al., 2002). The *vigilance* theory suggests that people with SAD tend to initially orient their attention toward threatening social information (Bögels and Mansell, 2004). The *maintenance* or *delayed disengagement* theory emphasizes their difficulty in

shifting their attention away from social threats (Fox et al., 2002; Amir et al., 2003; Pergamin-Hight et al., 2016; Fernandes et al., 2018). Rapee and Heimberg (1997) suggested that both attentional processes within the same social anxiety model of enhanced attention to the social threats, but the underlying cognitive mechanisms of the two processes differ, which can be differentiated by eye-tracking evidence. Particularly, *vigilance* has been reflected in more first fixations on the eyes (Boll et al., 2016) and shorter latency to the eyes (Keil et al., 2018) in SAD at all ages, while the *maintenance* of attention has been indicated by a longer latency to shift their attention away from threatening faces in adults (Buckner et al., 2010) and from the eye region in children and adolescents with SAD (Kleberg et al., 2021).

Beside the early attentional bias toward the eyes, people with SAD may also experience a later avoidance of the eyes, according to *vigilance-avoidance* hypothesis (Amir et al., 1998; Bögels and Mansell, 2004). Previous studies in SAD have suggested the importance of distinguishing early (*vigilance* or *maintenance*) and late (*avoidance*) attentional patterns regarding the eyes. This dynamic process has been explored using temporal analyses looking at the attentional patterns in different stages (e.g., Wieser et al., 2009a; Keil et al., 2018), but has not been proved by other studies (e.g., Boll et al., 2016; Capriola-Hall et al., 2021). Different from SAD, autistic people show a persistent eye avoidance across time (e.g., Wang et al., 2018).

In summary, although autism and SAD both display atypical attention to the eyes, their gaze patterns and underlying mechanisms could differ. More importantly, autistic traits and social anxiety were highly correlated in both clinical samples and healthy people (Bellini, 2006; Freeth et al., 2013; Bejerot et al., 2014), resulting in their interactive impacts on the gaze pattern to the eyes. On one hand, social anxiety is one of the most common comorbidities of autism (e.g., Maddox and White, 2015), and thus could affect the eye-looking patterns in autistic people. One previous study found that the fear of negative evaluation, a symptom of social anxiety, was related to longer gaze duration to social threats in autism (White et al., 2015). On the other hand, co-occurring autistic traits could contribute to the heterogeneity of attentional patterns to the eyes in people with high social anxiety. Given that autistic traits were related to avoidance of eyes (Chen and Yoon, 2011), socially anxious people with high autistic traits may exhibit more avoidant instead of vigilant or maintained eye-looking patterns. Therefore, exploring the influence of autistic traits and social anxiety on the attention to the eyes is necessary not only for a better understanding of the mechanisms of social attention, but also for the diagnosis and treatment of both disorders.

Autistic traits and social anxiety affect not only clinical samples, but also the general population. Non-autistic people who have familial risks or show more features of autism than the average but do not meet the diagnostic criteria of ASD are defined as the broader autism phenotype (BAP; Wheelwright et al., 2010; Sucksmith et al., 2011). Anxiety disorder, could also

be defined as continuums, as suggested by Research Domain Criteria framework (RDoC; Insel et al., 2010). The severity of SAD or ASD symptoms could be reflected by social anxiety and autistic traits, obtained by psychometric measures. These two traits could affect many aspects of social cognitive processes of two disorders in the broader population. More importantly, we could explore how these traits interactively affect cognition by regarding the traits as continuous variables, which would bring insights to the cognitive mechanism of comorbidity.

The current study examined how autistic traits and social anxiety in the general population separately and interactively affected attention to the eyes. We aimed to address the following research questions. First, how do autistic traits and social anxiety separately or interactively modulate attention to the eyes? Here we focus on the interactive effects of these two traits, which have rarely been explored in previous investigations. We hypothesized that social anxiety and autistic traits may interactively influence the attention to the eyes. Second, we separated the stimulus display time into different stages and examined the roles of autistic traits and social anxiety at different times in the stimulus. We examined the roles of autistic traits and social anxiety in attention to the eyes at the very early stages, including the proportion, duration, and latency of the first fixations on the eyes. At the later stages of face processing, we investigated whether autistic traits and social anxiety were associated with more eye avoidance.

2. Materials and methods

2.1. Participants

Sixty-four healthy college students participated in our experiment. Forty-seven were recruited directly from the campus internal forum at Peking University. To match the number of participants in the high and low autistic traits group, we posted another recruitment advertisement online to screen participants with high AQ scores. Forty-one students completed the online AQ and Social Phobia Inventory (SPIN) questionnaires, out of which 17 scored high in AQ (averaged score >26) and were included in our formal experiment. All the participants were required to be nearsighted below 5.0 diopters, and without colorblindness or color weakness. All participants were required not to be diagnosed with any psychiatric disorders, according to self-report. Four participants were excluded from data analysis for missing data in the questionnaire, eye-tracking calibration problems (See section “2.3 Procedures” for details), or computer crashes during the experiments. The final sample size was 60 (21 males, aged 18–29, mean age = 22.02, $SD_{age} = 2.45$). We separated our participants into high and low autistic traits groups and high and low social anxiety groups. The high autistic traits group consisted of 27 participants, and the high social anxiety group consisted

of 37 participants. Twenty-one participants were in both high autistic and high social anxiety groups. More information of our participants was shown in Table 1. The study was approved by the Committee for Protecting Human and Animal Subjects at School of Psychological and Cognitive Sciences at Peking University, China (protocol number: 2020-03-09).

2.2. Materials

2.2.1. Psychometric measures

We used a Chinese version of the Autism-spectrum Quotient (Baron-Cohen et al., 2001) scale to measure participants' autistic traits. It was a self-report scale with 50 items containing five different autistic dimensions: social skill, attention switching, attention to detail, communication, and imagination (Baron-Cohen et al., 2001). Two scoring approaches were widely used in ASD researches. The first one was the 4-point scoring system (1 = *definitely disagree* to 4 = *definitely agree*), a continuous approach that extended well in the non-clinical samples (Murray et al., 2016). The second one was the dichotomous system (0 = *definitely disagree* or *slightly disagree* and 1 = *slightly agree* or *definitely agree*), which was optimal for diagnosing individuals (Thomas, 2011). We adopted the 4-point version to accurately represent the continuity of autistic traits when conducting linear mixed models (LMMs). In the temporal analysis, we divided our participants into the high and low AQ groups by a cut-off value of 26 in the original AQ dichotomous scale and compared the two groups (Woodbury-Smith et al., 2005). The cut-off value at 26 was found to be a more sensitive score to screen ASD and broader autism phenotype (Woodbury-Smith et al., 2005).

We also used a Chinese version of the Social Phobia Inventory (SPIN) by Connor et al. (2000) to assess social anxiety. It was a self-report scale with 17 items measuring three dimensions: fear, avoidance, and physiological discomfort (Connor et al., 2000). Participants rated from 0 (not at all) to 4 (extremely) according to their situations during the last 3 months (Connor et al., 2000). The higher SPIN score represented, the higher the level of social anxiety. We used the SPIN score as a continuous variable in LMMs, and divided the participants into the high and low SPIN groups according to the cut-off score 19 in temporal analysis (Connor et al., 2000). The correlation between SPIN score and 4-point AQ score was $r = 0.44$ ($p < 0.001$).

2.2.2. Stimulus materials and apparatus

Face stimuli were virtual Asian male faces generated by FaceGen Modeller 3.5 (Singular Inversions, 2010) randomly, including five emotions: angry, fearful, happy, sad, and neutral. Each emotion consisted of eight different face images (400 × 400 pixels). We used the Tobii Pro Spectrum (TobiiTech, Stockholm, Sweden) eye-tracker to collect the eye gaze data with a sample

TABLE 1 Means (standard deviations) of demographic information and clinical test scores of participants.

	Full sample (N = 60)	Group by AQ score		Group by SPIN score	
		High AQ (N = 27)	Low AQ (N = 33)	High SPIN (N = 37)	Low SPIN (N = 23)
Age	22.02 (2.45)	21.63 (2.30)	22.33 (2.52)	21.73 (2.37)	22.48 (2.50)
Gender (female/male)	39/21	18/9	21/12	23/14	16/7
AQ					
Four-point scale	120.35 (14.28)	131.07 (8.25)	111.58 (12.01)	124.30 (12.84)	114 (14.44)
Binary scale	23.03 (6.52)	28.33 (2.92)	18.70 (5.33)	24.76 (5.81)	20.26 (6.77)
SPIN	24.37 (12.47)	29.85 (13.23)	19.88 (9.91)	31.70 (9.76)	12.57 (4.97)

rate of 300 Hz. Stimuli were presented on a 24-inch screen with a resolution of $1,920 \times 1,080$ pixels.

2.3. Procedures

Participants sat in a chair 60 cm away from the screen and were asked to keep their head and body still during the task. Before the experiment, participants needed to perform an eye movement calibration designed by Tobii Pro Spectrum. The calibration was accepted only if the errors of all five points for two eyes were less than 1° visual angle.

Participants were asked to complete an emotion discrimination task, including four blocks with 20 trials in each block. Each trial began with a $3^\circ \times 3^\circ$ animated fixation that appeared randomly on either the left or the right side of the screen to catch participants' attention. Participants had to fixate on the animation for 1.5 s before a $20^\circ \times 20^\circ$ central face picture appeared. The face picture was presented for 10 s, during which participants were instructed to view the face freely. We used 10 s to explore the temporal dynamics of gaze patterns (van der Geest et al., 2002). After that, participants needed to press the key "1" or "3" to choose the right facial emotion from two options presented on the screen (see Figure 1A). The task was set up to engage the participants.

2.4. Data analysis

Eye movement data were analyzed in R (Version 4.0.2). Missing data were filled by linear interpolation with a maximum time gap of 75 ms (Olsen, 2012). We averaged the gaze data from both eyes when calculating fixations. Areas of interest (AOIs) were defined in Figure 1B.

We excluded invalid trials according to the following criteria: (1) trials with more than 30% missing valid eye gaze data (Wang et al., 2020); (2) trials with less than 50% of the time looking at the face out of the whole screen. According to these criteria, a total of 874 (18.2%) invalid trials were excluded. The mean accuracy of emotion judgment was 88.5% (SD = 0.13). ANOVA test revealed no effect of AQ or SPIN on

the judgment accuracy ($ps > 0.05$). We excluded incorrect trials in the analyses.

To explore the roles of autistic traits and social anxiety in the attention to the eyes, we focused on three aspects of eye movement data: the overall eye-looking time, the initial attention to the eyes, and the temporal dynamics of eye-looking time. First, for the overall eye-looking time, we calculated the proportional fixation time on the eyes out of the whole face (eyes + rest of the face) during the whole 10 s of the trial. We adopted a linear mixed model with z-transformed AQ, SPIN, and facial emotion as fixed variables and subjects as the random variable to examine the impacts of AQ, SPIN, and facial emotion on the overall eye-looking time. We also included sex of the participants as a covariate in the model since the majority of the participants were female. The LMM was estimated in the "afex" package (Singmann et al., 2021), and *post hoc* comparisons were made in the "emmeans" package (Lenth, 2020). Second, to examine how the two traits separately or interactively affect the initial attention to the eyes, we computed the proportion of first fixations on the eyes when participants looked away from the peripheral fixation to the face, by dividing the trials where the first fixation was on the eyes by the individual number of valid trials with correct answers. Instead of exploring the attentional process of the whole face, we calculated the latency to the eyes (the time from the facial stimulus appearing to the onset of the first fixations on the eyes) and the duration (the eye-looking time of the first fixation on the face) of the first fixations on the eyes because we intended to focus on examining the vigilance, maintenance, and avoidance of the eyes in this study. These theories emphasized on how the individual's attention was first attracted by the socially threatening stimuli in the environment, which was the eye gaze in our study. Therefore, the first fixation on the eye region was a precondition to our research question. Several studies used the same methods to investigate the early attentional process to the human eye region (e.g., Keil et al., 2018; Capriola-Hall et al., 2021). We then conducted three LMMs to examine the impacts of AQ, SPIN, and facial emotion on the proportion of first fixations on the eyes, first fixation duration, and latency. The descriptive data of overall eye-looking time, proportion of first fixations on the eyes, first fixation duration, and first fixation latency

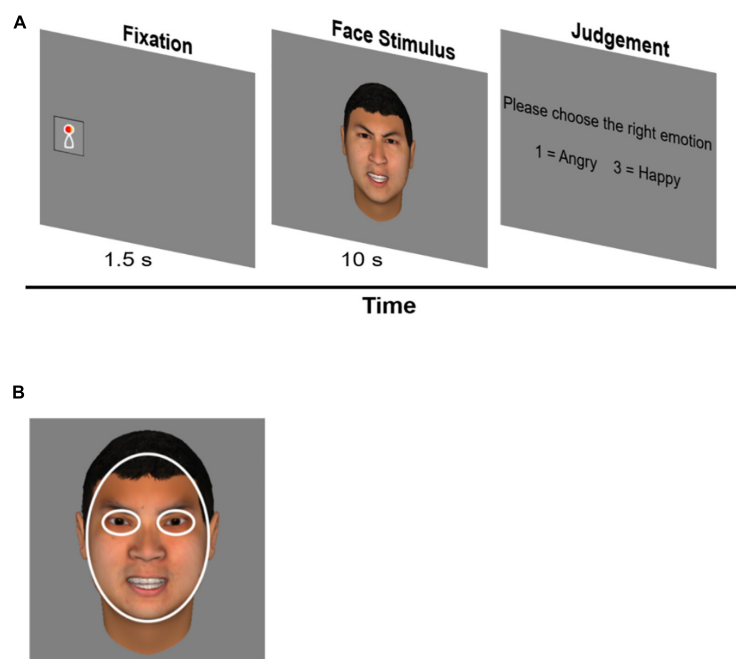


FIGURE 1

Emotion discrimination task and definition of AOs. (A) Each trial started with an animated fixation that appeared randomly on either left or right side of the screen. Participants needed to fix the fixation for 1.5 s before a central face appeared. This step was designed to measure the latency time and the position of the participant's first fixations to the central face. The face was presented for 10 s. After that, participants needed to choose the right facial emotion from two options by pressing a key. (B) Areas of interest were eyes and face. Fixation data on both eyes of the face were computed together when analyzing data.

under five emotions were shown in [Supplementary Table 1](#). To better understand how AQ modulate the effect of SPIN, we chose three Z-transformed scores of AQ (-1,0,1) to represent low, medium, and high level of autistic traits in our further simple slope analyses of SPIN. Third, to further explore the temporal dynamics of eye-looking time, we used a moving-average approach (e.g., [Dankner et al., 2017](#); [Wang et al., 2018](#)) to calculate the proportional eye-looking time of each 250 ms epoch. We then separated our participants into the high and low autistic trait groups by the cut-off value of 26 in the AQ scale ([Woodbury-Smith et al., 2005](#)), or the high and low social anxiety groups by the cut-off value of 19 in SPIN ([Connor et al., 2000](#)). We adopted a cluster-based permutation test to compare the differences between different groups of participants (e.g., [Wang et al., 2018, 2020](#)).

3. Results

3.1. Autistic traits or social anxiety do not modulate the overall eye-looking time

We used the proportion of eye-looking time out of face-looking time during the 10 s of the face stimulus as the index

of overall eye-looking time. The original full model consisted of the random slopes of emotion within participants and the random intercept of participants. However, the model failed to converge. The ANOVA indicated an insignificant difference between the original and nested models with the random intercept of participants as the only random effect. Therefore, the final model used the main and interaction of autistic traits, social anxiety, and emotion as fixed effects, participants as the random effect, and sex as the covariate. The LMMs below used the same fixed, random, and controlling effects.

The complete LMM result was shown in [Supplementary Table 2](#). We found no main effect of either autistic traits, $F(1, 53.82) = 0.99, p = 0.33$, SPIN, $F(1, 54.31) = 0.37, p = 0.55$, or the interaction of autistic traits and social anxiety, $F(1, 54.26) = 1.32, p = 0.26$. However, autistic traits, social anxiety, and emotion revealed a significant interaction on the overall eye-looking time, $F(4, 3384.86) = 3.29, p = 0.01$. We then compared slopes of social anxiety under five emotions between high (1 SD above the mean AQ), medium (mean AQ), and low levels of autistic traits (-1 SD below the mean AQ), and found no difference under any emotions ($ps > 0.05$, see [Supplementary Table 3](#) for details). Even so, as shown in [Figure 2](#), participants with lower autistic traits tended to look at eyes more as they scored more on social anxiety, while those with higher autistic traits tended to look at eyes less as they scored more on social anxiety. Moreover, sex

had an effect on the overall eye-looking time, $F(1, 54.62) = 4.79$, $p = 0.033$. Female participants looked longer at the eyes than male participants.

In sum, we did not find direct evidence of impacts of autistic traits and social anxiety on the overall attention to the eyes, independently or interactively. Thus, we focused on their effects on the temporal dynamics of eye-looking patterns in the following analyses.

3.2. Autistic traits and social anxiety interactively modulated the first fixations to the eyes

To investigate how autistic traits and social anxiety impacted the first fixations on the eyes, we adopted three LMMs with dependent variables of the proportion of first fixations on the eyes, the first fixation durations on the eyes, and the latency to the eyes. As shown in [Supplementary Table 4](#), the LMM showed a significant interaction between autistic traits and social anxiety on the proportion of first fixations on the eyes, $F(1, 50.79) = 4.52$, $p = 0.038$. Simple slope analyses revealed that the effect of social anxiety on the proportion of first fixations on the eyes was significant at the high level of autistic traits (1 SD above the mean AQ), $B = -0.058$, $t = -2.055$, $\beta = -0.314$, $p = 0.045$. No effect of social anxiety was found at the low (-1 SD below the mean AQ) or medium level of autistic traits (mean AQ), $B = 0.029$, $t = 0.825$, $\beta = 0.156$, $p = 0.413$, and $B = -0.014$, $t = -0.599$, $\beta = -0.079$, $p = 0.552$, respectively (see [Figure 3A](#)). The main effect of social anxiety or autistic traits was not significant, $F(1, 51.79) = 0.36$, $p = 0.552$, and $F(1, 50.54) = 0.01$, $p = 0.923$, respectively. These results indicated that participants with both high autistic and high social anxiety looked less at eyes when they attended to the face, compared to individuals with high autistic traits and low social anxiety.

Then, we selected trials in which participants' first fixations (29 percent of valid trials) were on the eyes and made log-transformations of the first fixation duration and the latency of first fixation because of non-normality (Shapiro–Wilk normality test, $W = 0.252$, $p < 0.001$, and $W = 0.657$, $p < 0.001$, respectively). We conducted another two LMMs with log-transformed first fixation duration and log-transformed latency as dependent variables of each model.

As shown in [Supplementary Table 5](#), the interaction between autistic traits and social anxiety on log-transformed first fixation duration was significant, $F(1, 56.26) = 7.10$, $p = 0.010$. Simple slope analyses showed that social anxiety had a positive effect on the first fixation duration at the eyes at the high level of autistic traits ($B = 0.219$, $t = 3.434$, $\beta = 0.380$, $p = 0.001$), as well as the medium level of autistic traits ($B = 0.095$, $t = 2.007$, $\beta = 0.165$, $p = 0.0496$). Social anxiety did not show any effect on first fixation duration at the low level of autistic traits ($B = -0.029$, $t = -0.415$, $\beta = -0.050$, $p = 0.680$, see [Figure 3B](#)). Social

anxiety also had a significant main effect, $F(1, 51.22) = 4.05$, $p = 0.050$, indicating that with higher social anxiety, people tended to look at eyes longer on their first fixations (see [Figure 4](#)). However, the main effect of autistic traits was not significant, $F(1, 39.14) = 0.33$, $p = 0.569$.

As shown in [Supplementary Table 6](#), social anxiety and autistic traits had a marginal interaction on log-transformed latency, $F(1, 53.80) = 3.13$, $p = 0.083$. Simple slope analyses revealed a positive effect of social anxiety on latency at the high level of autistic traits ($B = 0.111$, $t = 2.352$, $\beta = 0.265$, $p = 0.022$), but not at the low ($B = -0.011$, $t = -0.206$, $\beta = -0.025$, $p = 0.837$) or the medium levels of autistic traits ($B = 0.050$, $t = 1.430$, $\beta = 0.120$, $p = 0.158$, see [Figure 3C](#)). The main effect of social anxiety or autistic traits was not significant, $F(1, 49.49) = 2.05$, $p = 0.158$, and $F(1, 38.11) = 0.01$, $p = 0.936$, respectively.

In sum, we found that social anxiety was related to longer first fixation durations on the eyes. In addition, autistic traits and social anxiety had an interactive effect on the first fixations on the eyes. Among people with high autistic traits, social anxiety was related to fewer first fixations on the eyes, longer latency to the eyes, and longer first fixation duration on the eyes. However, among people with low autistic traits, social anxiety was not related to any indices of first fixations on the eyes.

3.3. Autistic traits, but not social anxiety, was associated with eye avoidance across time

Besides the initial attention to the eyes, we also explored how autistic traits and social anxiety impacted eye-looking time at later stages. To this end, we compared temporal dynamics of eye-looking time between the high and low autistic trait groups as well as between the high and low social anxiety groups. The results are shown in [Figure 5](#). People in the low autistic traits group generally looked less at eyes, but the differences were significant at around 2, 4, and 8 s ($p < 0.05$, see [Figure 5A](#)). However, there was no difference between high and low social anxiety groups across all time intervals (see [Figure 5B](#)).

4. Discussion

We aimed to address two research questions in this study to investigate how social anxiety and autistic traits influenced the attention to the eyes. First, we explored how autistic traits and social anxiety separately and interactively influenced the overall attention to the eyes. Our results revealed that the overall eye-looking time was not modulated by either of these two traits. Second, we separated the eye looking by different temporal stages and examined how these two traits affected the attention to the eyes for each stage. We found that these two traits had an interactive impact on the first fixations on the

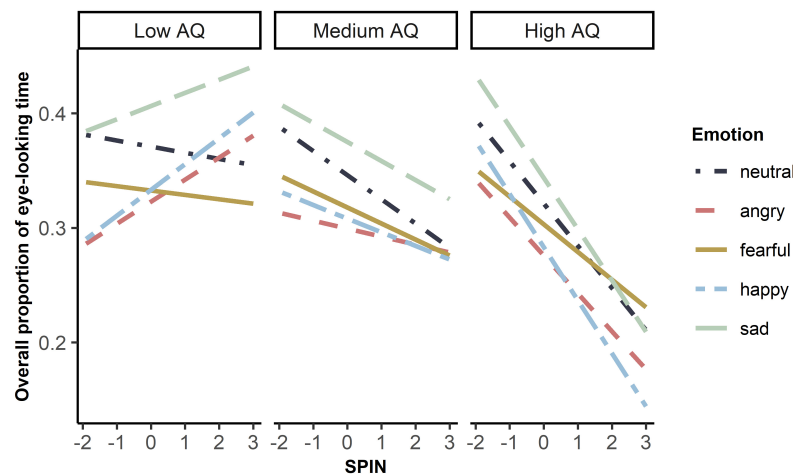


FIGURE 2

Simple slope plot of interaction between autistic traits, social anxiety, and emotion on overall eye-looking time. Low autistic traits referred to -1 standard deviation below mean AQ (original score: 106). Medium autistic traits referred to mean AQ (original score: 120). High autistic traits referred to 1 standard deviation above mean AQ (original score: 135). X-axis was the z-standardized score of SPIN. Y-axis was the original data of overall eye-looking time.

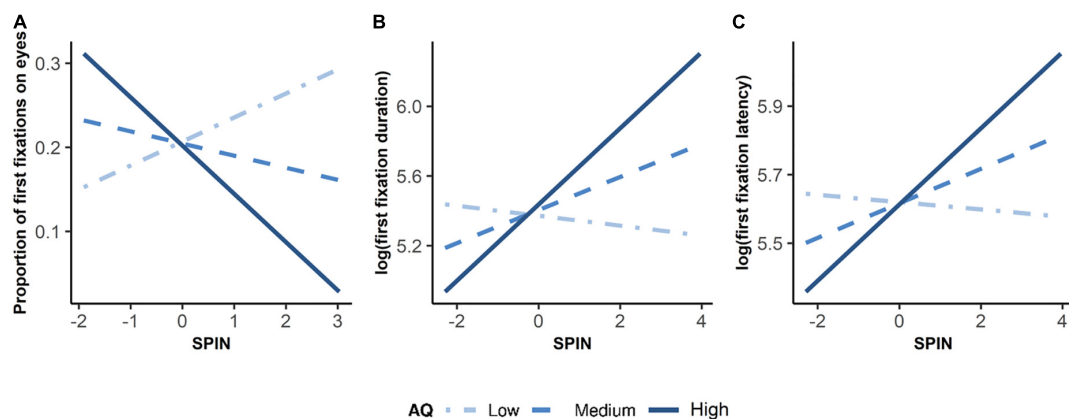


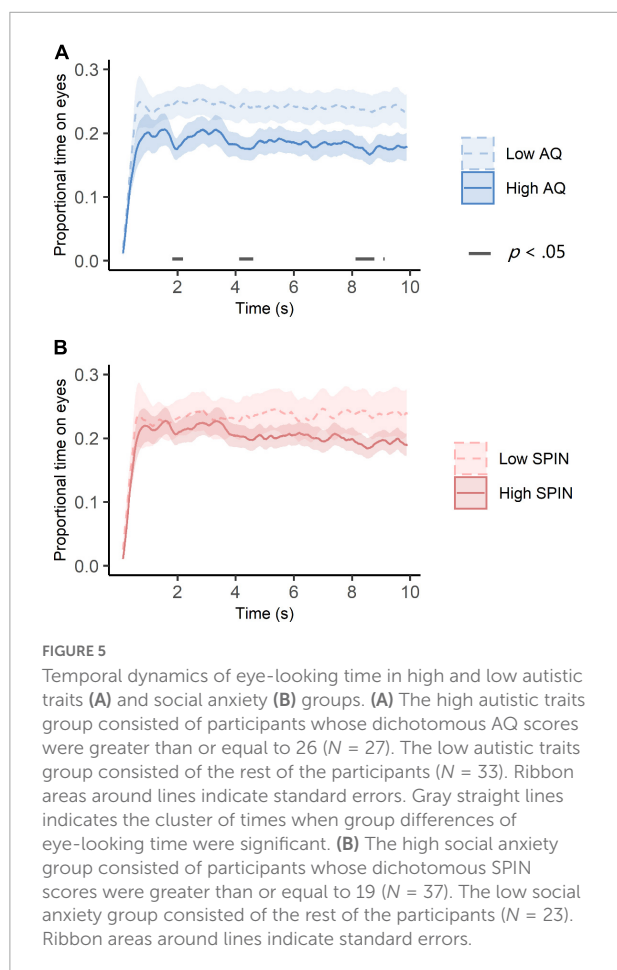
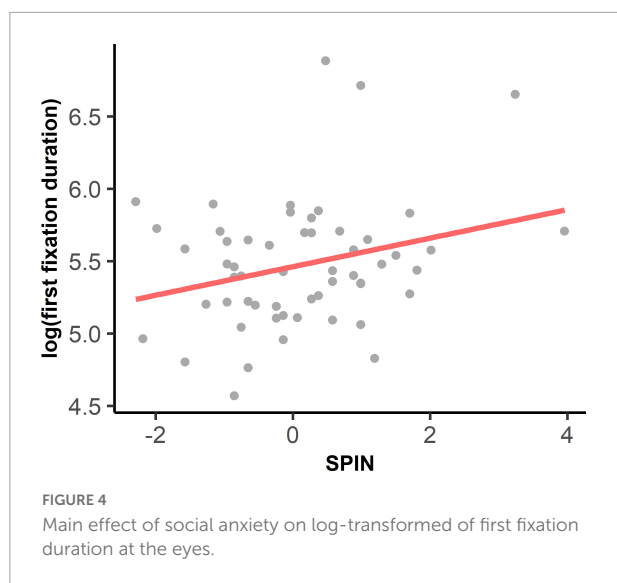
FIGURE 3

Simple Slope Plots of Interaction between Autistic Traits and Social Anxiety on Initial Attention to the Eyes. Low autistic traits referred to -1 standard deviation below mean AQ. Medium autistic traits referred to mean AQ. High autistic traits referred to 1 standard deviation above mean AQ. X-axis was the z-standardized score of SPIN. Three plots show interactions between autistic traits and social anxiety on (A) proportion of first fixations on eyes, (B) log-transformed duration of first fixation, and (C) log-transformed latency of first fixation.

eyes: among people with relatively high autistic traits, social anxiety was related to the avoidance of eyes as well as the early attention maintenance on the eyes. In addition, we found that social anxiety only affected the attention to the eyes on first fixations, while autistic traits affected the avoidance of the eyes significantly at several time points during the 10 s trial.

We found that the effects of social anxiety on attention to the eyes were mainly in the early stage. Specifically, we found that social anxiety could affect first fixation duration on the eyes—the higher the social anxiety, the longer the first fixation duration on the eyes (see Figure 4). Social anxiety did not affect the latency of the first fixation on the eyes or the

proportion of the first fixation on the eyes. This finding does not support the *vigilance* hypothesis of SAD, which suggests that the initial vigilance to the eyes is reflected by shorter latency or more first fixations to the eyes in people with SAD (Boll et al., 2016; Keil et al., 2018) and people with relatively high social anxiety (Gutiérrez-García et al., 2018). Instead, our finding of longer first fixation durations on the eyes in high social anxiety indicated an early maintenance of attention to the eyes. The result could be explained by the *maintenance* hypothesis of SAD, which emphasizes the attentional inflexibility of people with SAD when facing social threats (Kleberg et al., 2021). The *maintenance* theory has also been supported by previous studies,



which revealed an attentional disengaging problem from socially threatening stimuli in people with SAD (e.g., Fox et al., 2002; Moriya and Tanno, 2011; McGlade et al., 2020) and people with high social anxiety (Wieser et al., 2009a). Although our

finding of longer first fixation duration on the eyes in individuals with higher social anxiety was consistent with a previous study in youth with SAD (Capriola-Hall et al., 2021), contradictory findings in Keil et al. (2018) indicated that children with SAD oriented to the eyes faster but their first fixation duration on the eyes was shorter. To further examine the underlying mechanisms of attentional bias in SAD, future studies should use more sophisticated paradigms of disengagement, such as cueing the participants' initial fixation to the eyes or other socially threatening stimuli, to measure their disengaging time in shifting from the eyes (Boll et al., 2016; Kleberg et al., 2021).

More importantly, we found an interactive effect of social anxiety and autistic traits on the initial attention to the eyes: In people with high autistic traits, social anxiety was related to fewer first fixations and longer latency to the eyes, while in people with low autistic traits, social anxiety did not affect the first fixations on the eyes (as shown in Figures 3A, C). This result indicated that the early *vigilance* to the eyes was not present in people with high social anxiety co-occurring high autistic traits. Instead, autistic traits could enhance the avoidance of the eyes at the early stages of face processing in people with high social anxiety. In addition, social anxiety was related to longer first fixation duration on the eyes in people with high and medium levels of autistic traits, but not in people with low levels of autistic traits (as shown in Figure 3B), indicating the early maintenance of attention to the eyes in people with high social anxiety and relatively high autistic traits. This *maintenance* eye-looking pattern may reflect an early enhanced attention to social stimuli or an impaired disengagement of early attention in people with high social anxiety. Summarizing the results above, our findings suggest that people with high levels of autistic traits and social anxiety tend to avoid looking at the eyes at the early stage, but once they fixated on the eyes, they displayed a tendency to maintain their attention on the eyes. This avoidance-maintenance eye-looking pattern in people with comorbidity of ASD and SAD could interfere the normal interpersonal communication, especially the non-verbal communication, which largely relies on eye contacts and social information processing. Our findings highlight the importance of viewing the effects of the two traits on social attention as interactive rather than separate. Future studies should take into account comorbidities of social anxiety, such as autism, when describing clinical samples, and interpreting the results in future investigations of social attention. Notably, different experimental paradigms should be used to confirm the findings. In Kleberg et al. (2017), participants were presented with the human eye region with three non-social stimuli. After controlling autistic traits, researchers found that people with high social anxiety oriented their attention away from the eyes more quickly. The experimental paradigm and the materials we used might have caused inconsistent findings.

Different from the initial attention to the eyes, later attention to the eyes was only affected by autistic traits, not social anxiety.

People with relatively high autistic traits avoided the eyes at several time points at later stage of the trial. This finding supported the *eye avoidance* hypothesis of autism (Tanaka and Sung, 2016), and was consistent with the findings in non-autistic adults with high autistic traits (Chen and Yoon, 2011; Hessels et al., 2018). Inconsistent with the *vigilance-avoidance* account of social anxiety (e.g., Keil et al., 2018), we did not find a later avoidance of the eyes in people with social anxiety. Thus, our findings only support the attentional bias of social anxiety in the early stage, reflecting the subjects' difficulty in shifting their attention from the eyes (Kleberg et al., 2021). Autistic traits, on the other hand, could be related to an uncomfortable tension elicited by viewing socially threatening stimuli, resulting in a sustained avoidance of the eyes (Tanaka and Sung, 2016). Our study suggests that attention to the eyes in social anxiety among those with autistic traits should be considered as a dynamic process, and different traits could affect different stages of attention to the eyes. However, the underlying neural and physiological mechanisms needs further investigations.

Our study has several implications for the underlying mechanisms and clinical practices regarding SAD and ASD. First, the results contribute to the understanding of heterogeneity of eye-looking patterns in people with SAD. The existing theories have proposed that people with SAD could be vigilant or avoidant of the eyes, or they may be difficult to disengage their attention from the eyes. However, these various gaze patterns could be affected by comorbid situations. Thus, the investigation of social information processing should consider comorbidities, such as co-occurring autism. Second, comorbidity could make the diagnosis of ASD and SAD highly complicated, given their similarities in deficient social information processing. Our study suggests different mechanisms underlying these two traits affecting social attention and may provide an objective tool of eye-tracking techniques for distinguishing the two disorders. Last, our study implies that interventions for autism should also consider co-occurring social anxiety or other disorders for a more individualized and precise intervention approach. Similarly, it is also important for the treatment of social anxiety to consider co-occurring autistic traits.

Our study also had some limitations. First, participants in this study were all college students with different levels of autistic traits and social anxiety. Although people with high level of autistic traits and social anxiety have been found to show similar cognitive processes with clinical samples (e.g., Moriya and Tanno, 2011; Hessels et al., 2018), caution needs to be taken when interpreting the findings and generalizing the conclusions to clinical samples. Second, we recruited a second set of participants with relatively high AQ to match the numbers of participants in the high and low AQ group. Because autistic traits have a moderate correlation with social anxiety (Wainer et al., 2011), the mean scores of SPIN in our participants were therefore higher than the neurotypically

sample (Connor et al., 2000). Although the mean score of low SPIN group (i.e., 12) was consistent with previous non-clinical sample data (Connor et al., 2000), it might still be important to note that our sample may not be representative enough. Third, caution should also be taken when generalizing our findings to people in different cultures. Cultural differences could contribute to the differences between our findings and those of previous studies, which were mostly conducted outside of China. Our participants were Chinese college students, who were thought to show more avoidance of eye contacts than Western people in daily communication (Blais et al., 2008; Fu et al., 2012). Therefore, similar studies should be conducted with people from different cultures to confirm our findings (Blais et al., 2008; Fu et al., 2012). Fourth, we had a relatively high rate of invalid trials in the current study which was probably caused by the relatively large trial numbers, simple stimuli and task, and long trial duration. Future studies should use a variety of real human faces with shorter trial duration. We also included only a few trials where the first fixation was on the eyes (21 percent of the original trials) to explore the initial attention to the eyes. Fifth, the measurement of social anxiety in our study (i.e., SPIN) refers to socially anxious symptoms during the last 3 months and could not clearly be considered as a trait measure. Therefore, more research was needed on the effect of trait social anxiety on face processing.

In conclusion, we found that autistic traits and social anxiety could affect different stages of attention to the eyes: social anxiety only affected the first fixations, while autistic traits affected the attention to the eyes across the whole time. More importantly, we found an interactive effect between social anxiety and autistic traits on the attention to the eyes: People with high autistic traits and high social anxiety were initially avoidant of the eyes, but once they looked at the eyes, they maintained their attention on the eyes. Our study suggests an interactive role of different traits on the same cognitive process and emphasizes the importance of considering the temporal dynamic process when investigating the roles of different traits in social attention. Our study also has important implications for the clinical practices of autism and social anxiety.

Data availability statement

The datasets presented in this study can be found in online repositories. The names of the repository/repositories and accession number(s) can be found below: <https://osf.io/eu6rs/>.

Ethics statement

The studies involving human participants were reviewed and approved by Committee for Protecting Human and Animal

Subjects at School of Psychological and Cognitive Sciences at Peking University, China. The patients/participants provided their written informed consent to participate in this study.

Author contributions

WN and CS designed experiments and collected data. WN, HL, and QW conducted the eye-tracking data analysis. WN and HL completed the statistical analysis. WN wrote the manuscript. LY revised the manuscript. All authors contributed to the article and approved the submitted version.

Funding

This work was supported by grants from the Key-Area Research and Development Program of Guangdong Province (2019B030335001), National Natural Science Foundation of China (31871116), Postdoctoral Science Foundation (2021M690443), and Clinical Medicine Plus X – Young Scholars Project in Peking University, the Fundamental Research Funds for the Central Universities.

References

- American Psychiatric Association [APA] (2013). *Diagnostic and statistical manual of mental disorders. Fifth Edition*. Washington, DC: American Psychiatric Association, doi: 10.1176/appi.books.9780890425596
- Amir, N., Elias, J., Klumpp, H., and Przeworski, A. (2003). Attentional bias to threat in social phobia: Facilitated processing of threat or difficulty disengaging attention from threat? *Behav. Res. Ther.* 41, 1325–1335. doi: 10.1016/S0005-7967(03)00039-1
- Amir, N., Foa, E. B., and Coles, M. E. (1998). Automatic activation and strategic avoidance of threat-relevant information in social phobia. *J. Abnorm. Psychol.* 107, 285–290. doi: 10.1037/0021-843X.107.2.285
- Baron-Cohen, S., Wheelwright, S., Skinner, R., Martin, J., and Clubley, E. (2001). The autism-spectrum quotient (AQ): Evidence from Asperger syndrome/high-functioning autism, males and females, scientists and mathematicians. *J. Autism Dev. Disord.* 31, 5–17. doi: 10.1023/A:1005653411471
- Bejerot, S., Eriksson, J. M., and Mörtberg, E. (2014). Social anxiety in adult autism spectrum disorder. *Psychiatry Res.* 220, 705–707. doi: 10.1016/j.psychres.2014.08.030
- Bellini, S. (2006). The development of social anxiety in adolescents with autism spectrum disorders. *Focus Autism Other Dev. Disabl.* 21, 138–145. doi: 10.1177/10883576060210030201
- Blais, C., Jack, R. E., Scheepers, C., Fiset, D., and Caldara, R. (2008). Culture shapes how we look at faces. *PLoS One* 3:e3022. doi: 10.1371/journal.pone.0003022
- Bögels, S. M., and Mansell, W. (2004). Attention processes in the maintenance and treatment of social phobia: Hypervigilance, avoidance and self-focused attention. *Clin. Psychol. Rev.* 24, 827–856. doi: 10.1016/j.cpr.2004.06.005
- Boll, S., Bartholomaeus, M., Peter, U., Lupke, U., and Gamer, M. (2016). Attentional mechanisms of social perception are biased in social phobia. *J. Anxiety Disord.* 40, 83–93. doi: 10.1016/j.janxdis.2016.04.004
- Buckner, J. D., Maner, J. K., and Schmidt, N. B. (2010). Difficulty disengaging attention from social threat in social anxiety. *Cogn. Ther. Res.* 34, 99–105. doi: 10.1007/s10608-008-9205-y
- Capriola-Hall, N. N., Ollendick, T. H., and White, S. W. (2021). Attention deployment to the eye region of emotional faces among adolescents with and without social anxiety disorder. *Cogn. Ther. Res.* 45, 456–467. doi: 10.1007/s10608-020-10169-2
- Chen, F. S., and Yoon, J. M. D. (2011). Brief report: Broader autism phenotype predicts spontaneous reciprocity of direct gaze. *J. Autism Dev. Disord.* 41, 1131–1134. doi: 10.1007/s10803-010-1136-2
- Clark, D. M., and Wells, A. (1995). “A cognitive model of social phobia,” in *Social phobia: Diagnosis, assessment, and treatment*, (New York, NY: The Guilford Press), 69–93.
- Connor, K. M., Davidson, J. R. T., Churchill, L. E., Sherwood, A., Weisler, R. H., and Foa, E. (2000). Psychometric properties of the Social Phobia Inventory (SPIN): New self-rating scale. *Br. J. Psychiatry* 176, 379–386. doi: 10.1192/bjp.176.4.379
- Dankner, Y., Shalev, L., Carrasco, M., and Yuval-Greenberg, S. (2017). Prestimulus inhibition of saccades in adults with and without attention-deficit/hyperactivity disorder as an index of temporal expectations. *Psychol. Sci.* 28, 835–850. doi: 10.1177/0956797617694863
- Fernandes, C., Silva, S., Pires, J., Reis, A., Ros, A. J., Janeiro, L., et al. (2018). Eye-tracking evidence of a maintenance bias in social anxiety. *Behav. Cogn. Psychother.* 46, 66–83. doi: 10.1017/S1352465817000418
- Fox, E., Russo, R., and Dutton, K. (2002). Attentional bias for threat: Evidence for delayed disengagement from emotional faces. *Cogn. Emot.* 16, 355–379. doi: 10.1080/02699930143000527
- Freeth, M., Foulsham, T., and Kingstone, A. (2013). What affects social attention? Social presence, eye contact and autistic traits. *PLoS One* 8:e53286. doi: 10.1371/journal.pone.0053286
- Fu, G., Hu, C. S., Wang, Q., Quinn, P. C., and Lee, K. (2012). Adults scan own and other-race faces differently. *PLoS One* 7:e37688. doi: 10.1371/journal.pone.0037688
- Gutiérrez-García, A., Calvo, M. G., and Eysenck, M. W. (2018). Social anxiety and detection of facial untrustworthiness: Spatio-temporal oculomotor profiles. *Psychiatry Res.* 262, 55–62. doi: 10.1016/j.psychres.2018.01.031
- Hessels, R. S., Holleman, G. A., Cornelissen, T. H. W., Hooge, I. T. C., and Kemner, C. (2018). Eye contact takes two—autistic and social anxiety traits predict

Conflict of interest

The authors declare that the research was conducted in the absence of any commercial or financial relationships that could be construed as a potential conflict of interest.

Publisher's note

All claims expressed in this article are solely those of the authors and do not necessarily represent those of their affiliated organizations, or those of the publisher, the editors and the reviewers. Any product that may be evaluated in this article, or claim that may be made by its manufacturer, is not guaranteed or endorsed by the publisher.

Supplementary material

The Supplementary Material for this article can be found online at: <https://www.frontiersin.org/articles/10.3389/fnins.2022.1081769/full#supplementary-material>

- gaze behavior in dyadic interaction. *J. Exp. Psychopathol.* 9:je062917. doi: 10.5127/jep.062917
- Insel, T., Cuthbert, B., Garvey, M., Heinssen, R., Pine, D. S., Quinn, K., et al. (2010). Research domain criteria (RDoC): Toward a new classification framework for research on mental disorders. *AJP* 167, 748–751. doi: 10.1176/appi.ajp.2010.09091379
- Keil, V., Hepach, R., Vierrath, S., Caffier, D., Tuschen-Caffier, B., Klein, C., et al. (2018). Children with social anxiety disorder show blunted pupillary reactivity and altered eye contact processing in response to emotional faces: Insights from pupillometry and eye movements. *J. Anxiety Disord.* 58, 61–69. doi: 10.1016/j.janxdis.2018.07.001
- Kleberg, J. L., Högström, J., Nord, M., Bölte, S., Serlachius, E., and Falck-Ytter, T. (2017). Autistic traits and symptoms of social anxiety are differentially related to attention to others' eyes in social anxiety disorder. *J. Autism Dev. Disord.* 47, 3814–3821. doi: 10.1007/s10803-016-2978-z
- Kleberg, J. L., Högström, J., Sundström, K., Frick, A., and Serlachius, E. (2021). Delayed gaze shifts away from others' eyes in children and adolescents with social anxiety disorder. *J. Affect. Disord.* 278, 280–287. doi: 10.1016/j.jad.2020.09.022
- Kuusikko, S., Pollock-Wurman, R., Jussila, K., Carter, A. S., Mattila, M.-L., Ebeling, H., et al. (2008). Social anxiety in high-functioning children and adolescents with autism and Asperger syndrome. *J. Autism Dev. Disord.* 38, 1697–1709. doi: 10.1007/s10803-008-0555-9
- Lenth, R. V. (2020). *emmeans: Estimated marginal means, aka least-squares means. R package version 1.5.3*. Available online at: <https://cran.r-project.org/web/packages/emmeans/index.html>
- Leyfer, O. T., Folstein, S. E., Bacalman, S., Davis, N. O., Dinh, E., Morgan, J., et al. (2006). Comorbid psychiatric disorders in children with autism: Interview development and rates of disorders. *J. Autism Dev. Disord.* 36, 849–861. doi: 10.1007/s10803-006-0123-0
- Maddox, B. B., and White, S. W. (2015). Comorbid social anxiety disorder in adults with autism spectrum disorder. *J. Autism Dev. Disord.* 45, 3949–3960. doi: 10.1007/s10803-015-2531-5
- McGlade, A. L., Craske, M. G., and Niles, A. N. (2020). Temporal trends in attention disengagement from social threat as a function of social anxiety. *J. Behav. Ther. Exp. Psychiatry* 68:101529. doi: 10.1016/j.jbtep.2019.101529
- Mogg, K., and Bradley, B. P. (1998). A cognitive-motivational analysis of anxiety. *Behav. Res. Ther.* 36, 809–848. doi: 10.1016/S0005-7967(98)00063-1
- Moriya, J., and Tanno, Y. (2011). The time course of attentional disengagement from angry faces in social anxiety. *J. Behav. Ther. Exp. Psychiatry* 42, 122–128. doi: 10.1016/j.jbtep.2010.08.001
- Murray, A. L., Booth, T., McKenzie, K., and Kuenssberg, R. (2016). What range of trait levels can the Autism-Spectrum Quotient (AQ) measure reliably? An item response theory analysis. *Psychol. Assess.* 28, 673–683. doi: 10.1037/pas0000215
- Olsen, A. (2012). *The tobii I-VT fixation filter*. Danderyd Municipality: Tobii Technology, 21.
- Pelphrey, K. A., Sasson, N. J., Reznick, J. S., Paul, G., Goldman, B. D., and Piven, J. (2002). Visual scanning of faces in autism. *J. Autism Dev. Disord.* 32, 249–261. doi: 10.1023/A:1016374617369
- Pergamin-Hight, L., Bitton, S., Pine, D. S., Fox, N. A., and Bar-Haim, Y. (2016). Attention and interpretation biases and attention control in youth with social anxiety disorder. *J. Exp. Psychopathol.* 7, 484–498. doi: 10.5127/jep.053115
- Rapee, R. M., and Heimberg, R. G. (1997). A cognitive-behavioral model of anxiety in social phobia. *Behav. Res. Ther.* 35, 741–756.
- Rosbrook, A., and Whittingham, K. (2010). Autistic traits in the general population: What mediates the link with depressive and anxious symptomatology? *Res. Autism Spectr. Disord.* 4, 415–424. doi: 10.1016/j.rasd.2009.10.012
- Schneier, F. R., Rodebaugh, T. L., Blanco, C., Lewin, H., and Liebowitz, M. R. (2011). Fear and avoidance of eye contact in social anxiety disorder. *Compr. Psychiatry* 52, 81–87. doi: 10.1016/j.comppsy.2010.04.006
- Singmann, H., Bolker, B., Westfall, J., and Aust, F. (2021). *afex: Analysis of factorial experiments. R package version 0.28-1*. Available online at: <https://cran.r-project.org/web/packages/afex/index.html>
- Singular Inversions, (2010). *FaceGen Modeller*. Available online at: www.facegen.com (accessed January 21, 2021).
- Stein, D. J., Lim, C. C. W., Roest, A. M., de Jonge, P., Aguilar-Gaxiola, S., Al-Hamzawi, A., et al. (2017). The cross-national epidemiology of social anxiety disorder: Data from the world mental health survey initiative. *BMC Med.* 15:143. doi: 10.1186/s12916-017-0889-2
- Stein, M. B., and Stein, D. J. (2008). Social anxiety disorder. *Lancet* 371, 1115–1125. doi: 10.1016/S0140-6736(08)60488-2
- Sucksmith, E., Roth, I., and Hoekstra, R. A. (2011). Autistic traits below the clinical threshold: Re-examining the broader autism phenotype in the 21st century. *Neuropsychol. Rev.* 21, 360–389. doi: 10.1007/s11065-011-9183-9
- Tanaka, J. W., and Sung, A. (2016). The “eye avoidance” hypothesis of autism face processing. *J. Autism Dev. Disord.* 46, 1538–1552. doi: 10.1007/s10803-013-1976-7
- Thomas, M. L. (2011). The value of item response theory in clinical assessment: A review. *Assess.* 18, 291–307. doi: 10.1177/1073191110374797
- van der Geest, J. N., Kemner, C., Verbaten, M. N., and van Engeland, H. (2002). Gaze behavior of children with pervasive developmental disorder toward human faces: A fixation time study. *J. Child Psychol. Psychiat.* 43, 669–678. doi: 10.1111/1469-7610.00055
- Wainer, A. L., Ingersoll, B. R., and Hopwood, C. J. (2011). The structure and nature of the broader autism phenotype in a non-clinical sample. *J. Psychopathol. Behav. Assess.* 33, 459–469. doi: 10.1007/s10862-011-9259-0
- Wang, Q., Hoi, S. P., Wang, Y., Song, C., Li, T., Lam, C. M., et al. (2020). Out of mind, out of sight? Investigating abnormal face scanning in autism spectrum disorder using gaze-contingent paradigm. *Dev. Sci.* 23:e12856. doi: 10.1111/desc.12856
- Wang, Q., Lu, L., Zhang, Q., Fang, F., Zou, X., and Yi, L. (2018). Eye avoidance in young children with autism spectrum disorder is modulated by emotional facial expressions. *J. Abnorm. Psychol.* 127, 722–732. doi: 10.1037/abn0000372
- Weeks, J. W., Howell, A. N., and Goldin, P. R. (2013). Gaze avoidance in social anxiety disorder. *Depress. Anxiety* 30, 749–756. doi: 10.1002/da.22146
- Wheelwright, S., Auyeung, B., Allison, C., and Baron-Cohen, S. (2010). Defining the broader, medium and narrow autism phenotype among parents using the Autism Spectrum Quotient (AQ). *Mol. Autism* 1:10. doi: 10.1186/2040-2392-1-10
- White, S. W., Maddox, B. B., and Panneton, R. K. (2015). Fear of negative evaluation influences eye gaze in adolescents with autism spectrum disorder: A pilot study. *J. Autism Dev. Disord.* 45, 3446–3457. doi: 10.1007/s10803-014-2349-6
- Wieser, M. J., Pauli, P., Alpers, G. W., and Mühlberger, A. (2009a). Is eye to eye contact really threatening and avoided in social anxiety?—An eye-tracking and psychophysiology study. *J. Anxiety Disord.* 23, 93–103. doi: 10.1016/j.janxdis.2008.04.004
- Wieser, M. J., Pauli, P., Weyers, P., Alpers, G. W., and Mühlberger, A. (2009b). Fear of negative evaluation and the hypervigilance-avoidance hypothesis: An eye-tracking study. *J. Neural Transm.* 116, 717–723. doi: 10.1007/s00702-008-0101-0
- Woodbury-Smith, M. R., Robinson, J., Wheelwright, S., and Baron-Cohen, S. (2005). Screening adults for Asperger syndrome using the AQ: A preliminary study of its diagnostic validity in clinical practice. *J. Autism Dev. Disord.* 35, 331–335. doi: 10.1007/s10803-005-3300-7
- Yi, L., Fan, Y., Quinn, P. C., Feng, C., Huang, D., Li, J., et al. (2013). Abnormality in face scanning by children with autism spectrum disorder is limited to the eye region: Evidence from multi-method analyses of eye tracking data. *J. Vision* 13, 5–5. doi: 10.1167/13.10.5
- Yi, L., Feng, C., Quinn, P. C., Ding, H., Li, J., Liu, Y., et al. (2014). Do individuals with and without autism spectrum disorder scan faces differently? A new multi-method look at an existing controversy: Face processing in autism spectrum disorder. *Autism Res.* 7, 72–83. doi: 10.1002/aur.1340



OPEN ACCESS

EDITED BY
Xuemin Li,
Peking University Third Hospital, China

REVIEWED BY
Liu Liping,
Tianjin University, China
Edmond Q. Wu,
Shanghai Jiao Tong University, China

*CORRESPONDENCE
Li Ding
✉ 07441@buaa.edu.cn

SPECIALTY SECTION
This article was submitted to
Visual Neuroscience,
a section of the journal
Frontiers in Neuroscience

RECEIVED 05 January 2023
ACCEPTED 20 January 2023
PUBLISHED 06 February 2023

CITATION
Liu Q, Wang Y, Bai Y, Yu M, Cao Z, Yu X and
Ding L (2023) Development of a quantitative
measurement on visual clutter in see through
display.
Front. Neurosci. 17:1138225.
doi: 10.3389/fnins.2023.1138225

COPYRIGHT
© 2023 Liu, Wang, Bai, Yu, Cao, Yu and Ding.
This is an open-access article distributed under
the terms of the [Creative Commons Attribution
License \(CC BY\)](#). The use, distribution or
reproduction in other forums is permitted,
provided the original author(s) and the
copyright owner(s) are credited and that the
original publication in this journal is cited, in
accordance with accepted academic practice.
No use, distribution or reproduction is
permitted which does not comply with
these terms.

Development of a quantitative measurement on visual clutter in see through display

Qingfeng Liu¹, Yanyan Wang², Yu Bai², Mengsun Yu^{1,2},
Zhengtao Cao², Xinli Yu¹ and Li Ding^{1*}

¹School of Biological Science and Medical Engineering, Beihang University, Beijing, China, ²AirForce Medical Center, Fourth Military Medical University, Beijing, China

Objective: With the wide use of transmission displays to improve operation performance, the display information highlights clutter because of the contradiction between the massive amount of information and limited display area. Our study aimed to develop a quantitative measurement for declutter design and appraisal.

Methods: Using the ergonomics research system of characters and symbols in a see-through cockpit display, we set the simulated flight task interface at four pixel scale levels by enlarging all the display elements in a certain ratio. Flight task videos of 12 clutter degrees were recorded using each flight interface matched with three flight scene complexity levels. A total of 60 pilots completed the visual search tasks in the flight task video while the eye tracker was used to record the view path in real time. Visual search performance was analyzed to study the effect of various clutter factors and levels on pilots' performance in visual search tasks, and acquire quantitative clutter measure parameters.

Results: GLM univariate test revealed that there were significant differences among the fixation time in areas of interest (AOI), total Fixation point number, total fixation time at four pixel scale levels, and three flight scene complexity levels ($P < 0.05$). Visual search performance declined after the cutoff point, while the clutter degree increased. According to the visual search performance data, the recommend feature congestion upper pixel number limit in a 600*800 display was 18,576, and the pixel ratio was 3.87%.

Conclusion: A quantitative measurement for declutter design and appraisal of cockpit displays was developed, which can be used to support see-through display design.

KEYWORDS

visual clutter, eye track, cockpit, display, ergonomics

1. Introduction

Modern air combat involves system operation, during which, information regarding the war field state, the two-sided situation and the command order need to be interchangeable and allow comprehensive perception. Therefore, human aircraft interface design has become a key factor for operation performance. The narrow cockpit of a military fighter limits the display space. Innovative display technologies characterized by see-through displays such as the head-up display (HUD) (Betts, 1975; Doucette, 2012) and helmet-mounted display (HMD) (Newman and Greeley, 1997) have been applied to improve the operation performance.

However, display information clutter has been highlighted because of the contradiction between the massive amount of information and the limited display area. Federal Aviation Administration (2014) pointed out that a cluttered display may result in an increased processing time for flight crew to obtain display information, so clutter should be minimized during display design. As the pilot must see through the HUD, special attention is needed to avoid display clutter that would otherwise unduly obscure the outside view. SAE International (1998) also stresses that a decluttered design is a necessary requirement for HUD.

Several clutter measures have been used in advanced cockpit displays. Subjective impressions of clutter may be collected with a multidimensional measure of clutter (Kaber et al., 2008) or overall perceived clutter rating (Doyon-Poulin et al., 2014). Rosenholtz et al. (2005) created an objective measure of clutter based on the feature congestion theory and image analysis technology. The image feature is calculated after being transformed to perceptual base International Commission on Illumination (CIE) lab color space and Gaussian pyramids. Kim et al. (2011) used this method to measure nine HUD configurations in a simulation landing flight of a civil aircraft. Consequently, the outside scene remained relatively stable and screenshot images of each configuration were extracted from videos recorded during the simulation flight and analyzed to calculate the clutter score. However, for fighter see-through displays, the outside view is successively changing during a maneuver task. Therefore the display element and flight scene, which are two clutter factors, could not be integrated into one image. Tullis (1983) proposed that active pixel numbers were an available method to measure the clutter of a black and white display. This method should be applied to see-through aviation displays since the border of characters and symbols are clear with no background.

In our study, we aimed to develop a quantitative measurement based on pixel numbers for declutter design and appraisal for see through displays in fighter cockpits.

2. Methods article types


2.1. Subjects

A total of 60 male pilots [mean (SD), age 22.14 ± 9.24 y, flight hours $1,250.68 \pm 1,522.84$ h] participated the experiment. All subjects were medically qualified. The study was approved by the Logistics Department of the Civilian Ethics Committee of Beihang University. All subjects who participated in the experiment were provided with and signed an informed consent form. All relevant ethical safeguards were met with regard to subject protection.

2.2. Equipment and test setting

2.2.1. Experiment flight task design

An ergonomics research system of display characters and symbols in the military cockpit was developed based on an analysis of display factors, layout and arrangement of the interface in modern military cockpits using Microsoft Visual Studio, 2013 edit. Display elements, the vector data set and the typical flight visual scene database were edited. We designed and edit the display elements including shape, size, location, color, salience etc., and recorded a flight task video with a dynamic flight scene using ergonomics evaluation and research. The total pixels of each and all elements were calculated by the program.

Using an ergonomics research system, we set simulation flight task images at four clutter levels by enlarging all of the display elements in a certain ratio (Figure 1). A target symbol  was inserted in each display image for the search task. Dynamic flight scene videos of three complexity levels (night, day and a complex environment) were constructed (Figure 2). Flight task videos of 12 clutter degrees were recorded using each flight interface matched with three complexity levels flight scenes (Figure 3). The video format was Windows Media Video (WMV) and the duration was 45 s. A 4×3 experiment design was used.

2.2.2. Eye tracker

A Tobii Pro X2-30 eye tracker was used in the experiment. This is a small, full-feature eye tracking system that can be mounted below the PC monitor. The fixation angle could be up to 36° .

2.2.3. Procedure

The pilots signed a statement of informed consent, which outlined the purpose of the experiment and informed the subjects of their rights when they were recruited. The pilots were seated 70 cm in front of a computer monitor with a Tobii X2-30 eye tracker mounted below the screen. They were given instructions and completed the eye tracker calibration. Then, they completed three practice trials to ensure the correct operation of the search task. Pilots then pressed the enter key on the keyboard to start the search task. They were asked to find the given target as soon as possible and press the enter key when they found it. Then, the next trial would begin. Each pilots completed 48 trials. The eye tracker recorded the eye movement behavior and fixation time in areas of interest (AOI), and total fixation point numbers, total fixation time, and saccade length were analyzed. The experiment was carried out in daylight with normal laboratory illumination.

2.3. Statistical analysis

The Statistical Product and Service Solutions (SPSS) 19.0 statistical software package was used to analyze the data. All the test data were expressed as M or $M \pm SD$ (s). The general linear model (GLM) univariate test, χ^2 test, and Pearson correlation were used for analysis; $P < 0.05$ was set as the threshold value of significant difference in the statistical analysis.

3. Results

3.1. Descriptive analysis

As eye tracking data including fixation time in AOI, total fixation point numbers and total fixation time did not conform with the normal distribution, log transformation was carried out to normalize the data. The data of the mean saccade length were near the normal distribution.

3.2. Clutter effects of varied clutter levels and flight scene complexity levels

A 4×3 GLM univariate test revealed that the fixation time in AOI, total fixation numbers and total fixation time were significantly

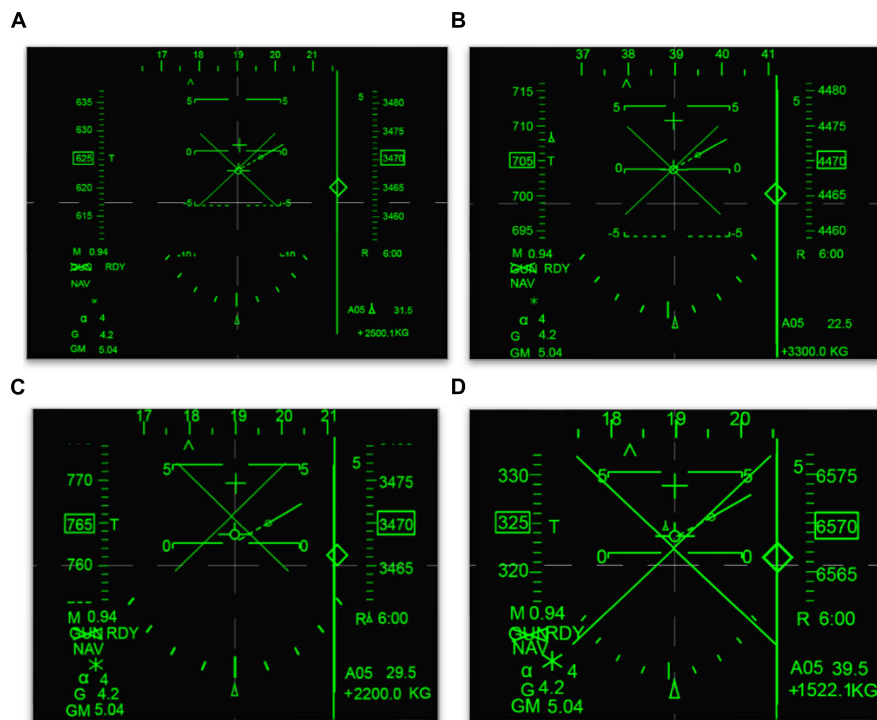


FIGURE 1
Four clutter level displays. (A) Clutter level 1. (B) Clutter level 2. (C) Clutter level 3. (D) Clutter level 4.



FIGURE 2
Dynamic flight scene videos of night, day, and complex environment. (A) Night scene. (B) Day scene. (C) Complex environment scene.

different among the four clutter levels [$F_{\text{Fixation time in AOI}}(4, 812) = 47.907$, $F_{\text{Total Fixation point number}}(4, 812) = 46.714$, $F_{\text{Total Fixation time}}(4, 812) = 49.556$, $P < 0.01$] and three flight scene complexities [$F_{\text{Fixation time in AOI}}(4, 812) = 21.402$, $F_{\text{Total Fixation number}}(4, 812) = 16.878$, $F_{\text{Total Fixation time}}(4, 812) = 32.743$, $P < 0.01$]. The mean saccade lengths were significantly different among the four clutter levels [$F_{\text{Mean saccade length}}(4, 812) = 3.179$, $P < 0.05$], but not the three flight scene complexities [$F_{\text{Mean saccade length}}(4, 812) = 0.676$, $P > 0.05$], as shown in Figures 4–7.

Results of the *post hoc* least significant difference (LSD)-t on clutter levels indicated that there were no significant differences between level 1 and level 2 in terms of all eye tracking data ($P > 0.05$). The fixation time in AOI, total fixation number and total fixation time data for levels 3 and 4 were higher than those of levels 1 and 2. The saccade length data of level 4 were higher than those of level 1 and level 2 ($P < 0.05$). The *post hoc* LSD-t on flight scene complexity levels indicated that the fixation time in AOI, total fixation point number and total Fixation time data of level 2 were

higher than level 1, and those of level 3 were higher than level 2 ($P < 0.01$). Therefore, the visual search performance declined after the cutoff point while the clutter degree (pixel factor and flight scene factor) increased.

3.3. Analysis of delayed reaction

In the experiment, the duration of each task video was 45 s, which was long enough for the target search. In a real flight task, the available search time maybe transient because of the rapid speed of the aircraft. Therefore, we set 10 s as the cutoff value which meant that tasks with a search time higher than 10 s were invalid or represented a delayed reaction. The delayed reaction rate is important for search performance just as the error rate is important for a reaction time task. The χ^2 test showed that delayed reaction numbers increased with the clutter degree ($\chi^2 = 53.390$, $P = 0.000$), as shown in Table 1.

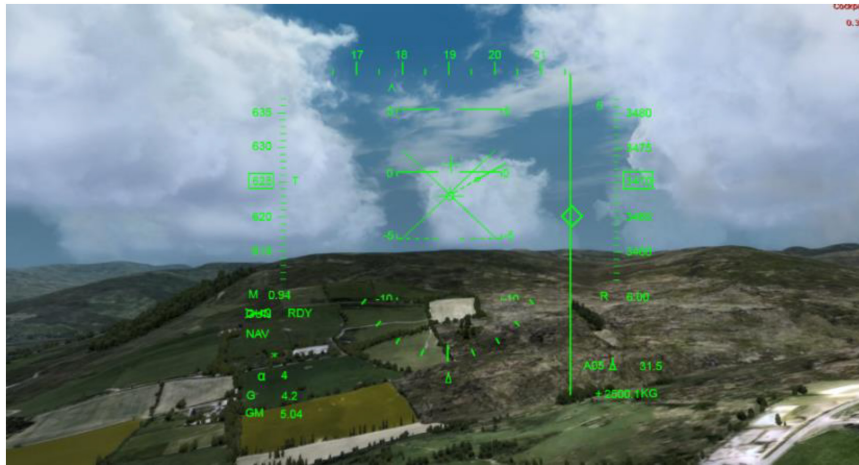


FIGURE 3
Screenshot of dynamic flight scene videos.

3.4. Quantitative clutter measure parameters calculation

According to visual search performance data, method of linear interpolation was used to calculate the quantitative parameters. Table 2 presents pixel numbers and pixel ratio of each clutter levels.

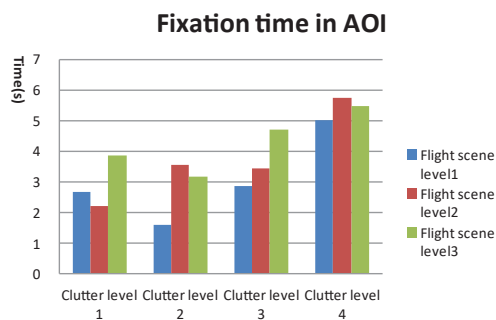


FIGURE 4
General linear model (GLM) Univariate test of fixation time in areas of interest (AOI).

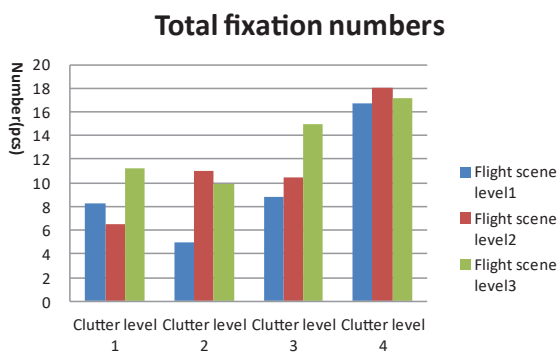


FIGURE 5
General linear model (GLM) Univariate test of total fixation numbers.

Table 3 presents estimated marginal mean of Fixation time in AOI which is equal to searching time and will be used to calculate the clutter measure parameters.

According to the GLM univariate test results, the search performance decreased after clutter level 2, since the eye tracking data showed no significant difference between level 1 and level 2, but did show a significant difference between level 2 and level 3. The clutter cutoff point should therefore be between level 2 and level 3.

According to method of linear interpolation:

The clutter of pixel numbers (CPN) cutoff point formula is:

$$CIR = AVE(PN_2 + PN_3)$$

$$\therefore PN_2 = 15,631, PN_3 = 21,545$$

$$\therefore CPR = AVE(15,631 + 21,545) = 18,756$$

The clutter of pixel ratio (CPR) cutoff point formula is:

$$CIR = AVE(PR_2 + PR_3)$$

$$\therefore PR_2 = 3.26, PR_3 = 4.49$$

$$\therefore CPR = AVE(3.26 + 4.49) = 3.87\%$$

The clutter of reaction time (CRT) cutoff point formula is:

$$CRTP = AVE(RT_2 + RT_3)$$

$$\therefore RT_2 = 2.610, 95\% CI = 2.387, 2.854$$

$$RT_3 = 3.585, 95\% CI = 3.266, 3.934$$

$$\therefore CRTP = AVE(2.610 + 3.585) = 3.097 \text{ s}, 95\% CI = 2.827, 3.394$$

The results revealed that the recommended feature congestion upper pixel number limit for a 600*800 display was 18,576 px, and the pixel ratio was 3.87%. When using a search task to evaluate the clutter of a see-through display, the search time should not be over 3.097 s, 95% CI = 2.827, 3.394.

4. Discussion

Clutter is a key concern in the design of aviation displays because it is not only a perceived crowding sense, but also a potential negative factor on flight performance, especially in fighter see-through displays whose scale is limited by the cockpit space. Though it is widely accepted that human performance is particularly sensitive to visual clutter in searching tasks, results of studies on aviation display visual clutter are somewhat contradictory. Ververs and Wickens (1998) found that a cluttered display could cause a

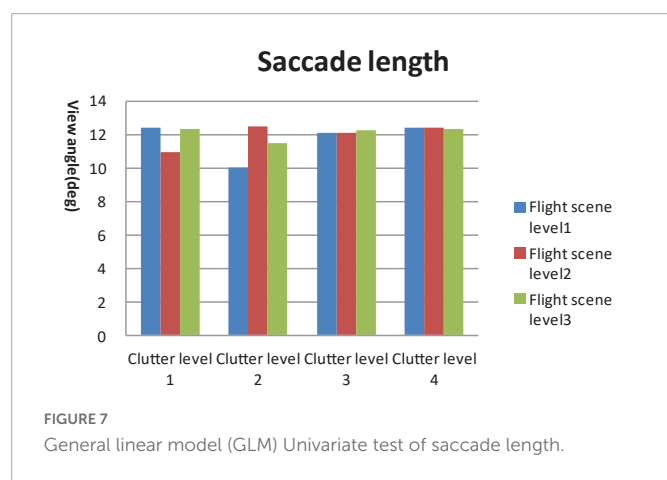
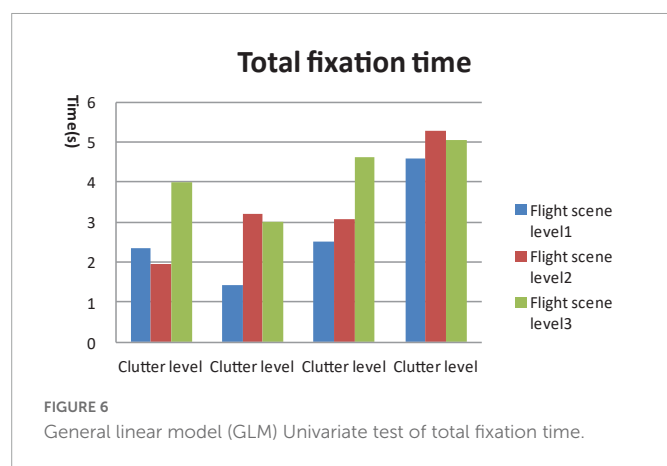


TABLE 1 Delayed reaction of varied clutter degrees.

	Clutter level 1	Clutter level 2	Clutter level 3	Clutter level 4
> 10 s	2	8	14	40
< 10 s	196	203	189	161

little longer change detection time, but have no effect on flight performance. Doyon-Poulin et al. (2014) found that middle clutter display can lead to better simulation flight performance, as measured by localizer deviation, but this effect was not found in other flight indices. Kim et al. (2011) also suggested that middle clutter HUD configurations were better for a pilot's landing performance, and that cognitive complexity and a lack of information for high and low clutter displays may cause higher workload and less stable operation, respectively. Rarely, studies have focused on fighter see-through displays, and middle clutter is still a concept with less quantitative criterion. Subjective rating is the most common clutter evaluation method for aviation displays since both the visual density and task-relevant dimensions of clutter are considered. The disadvantage is that subjective evaluation can only be carried out in a later design process, when the displays have been provided with their main functions.

Our study aimed to develop a quantitative measurement for declutter design and appraisal that can be used in the early design stage of see-through displays in fighter cockpits. Pixel numbers and ratio were selected as the quantitative measurements for see-through display clutter for three reasons.

TABLE 2 Estimated marginal mean of Fixation time in (AOI) (s).

Clutter levels	Mean reaction time (RT, s)	SE	CI 95% Upper	CI 95% lower
Level 1	2.831	1.049	2.578	3.109
Level 2	2.610	1.047	2.387	2.854
Level 3	3.585	1.049	3.266	3.934
Level 4	5.408	1.049	4.924	5.940

TABLE 3 Pixel numbers and pixel ratio of each clutter levels.

Clutter levels	Pixel number (PN, px)	Pixel ratio (PR, %)
Level 1	10,254	2.14
Level 2	15,631	3.26
Level 3	21,545	4.49
Level 4	28,353	5.91

Firstly, active pixel numbers is a valid visual clutter measurement on information density. Grahame et al. (2004) measured webpage clutter in pixels as a percentage of the total page space that was occupied by meaningful elements. This method should be applied to see-through aviation displays since the borders of characters and symbols are clear with no colorful background. Nickerson (1994) also suggested that the ratio of the space that is occupied by meaningful units to that of background can evaluate information clutter. Frank and Timpf (1994) even used ink dosage to measure the information density on a black and white map.

Secondly, this simple method is sufficient for fighter see-through display clutter measurement. There are several image analysis methods and software for clutter measurement, for example, Insight (Arents et al., 2010). Display image properties such as color, luminosity, and orientation can be analyzed by an image processing program. Rosenholtz et al. (2005, 2011) has proposed a feature congestion theory and a measure of display clutter and validated such tools during the aviation display design process. Finally, the outside flight scene is difficult to measure using image analysis methods since the fighter moves successively in multi-degrees and the outside scene changes rapidly during a maneuver. Therefore, the flight scene may have an effect on see-through display clutter and it cannot be measured by image analysis.

We develop an ergonomics research system of display characters and symbols in a military cockpit, where we designed and constructed simulation flight task images of four pixel levels by enlarging all the display elements in a certain ratio, and dynamic flight scene videos of three complexity levels (night, day, and a complex environment). An eye tracker was used to record visual search behaviors. The experiment using pilots showed that the visual search performance declined after the cutoff point, while the clutter degree (pixel number factor) increased. The flight scene complexity had a negative effect on visual clutter. Delayed reaction numbers increased gradually as clutter degree grew. The ratio even arrived at 20% at clutter level 4 in the experiment, which is totally unacceptable for military flights. Higher active pixel numbers or ratio should be avoided in see-through display design.

According to the visual search performance data, the method of linear interpolation was used to calculate the quantitative parameters.

Feature congestion and performance indices were calculated. Feature congestion measured by pixel number reflected the information density, which can guide design directive. The performance index acquired from the eye tracker can be used in ergonomics evaluation by pilots. The recommended upper limit of the pixel number in a 600*800 display is 18,576 px, and the pixel ratio is 3.87%. When using a search task to evaluate the clutter of a see-through display, the search time should not be over 3.097 s, 95% CI = 2.827, 3.394.

In our study, a quantitative measurement based on pixel numbers was developed and validated for declutter design and appraisal of see-through cockpit displays. The method could be used to evaluate the clutter level of interfaces for ergonomic improvement.

Data availability statement

The original contributions presented in this study are included in the article/supplementary material, further inquiries can be directed to the corresponding author.

Ethics statement

The studies involving human participants were reviewed and approved by the Logistics Department of the Civilian Ethics Committee of Beihang University. The patients/participants provided their written informed consent to participate in this study.

References

- Arents, R. R. D., Merwe, G. K. V. D., Verhoeven, R. P. M., and Zon, G. D. R. (2010). *Insight: Assisting aviation display designers by measuring visual clutter*. Amsterdam: National Aerospace Laboratory NLR.
- Betts, J. F. (1975). *Head-up display/gun camera for the F-15 aircraft, Disneyland*. Bellingham, WA: International Society for Optics and Photonics.
- Doucette, A. R. (2012). Military/avionics: Design decisions for a head-up display: This F-14 fighter optics retrofit case history is a prime example of analyzing and selecting design options. *IEEE Spectrum* 13, 29–32. doi: 10.1109/MSPEC.1976.6369296
- Doyon-Poulin, P., Ouellette, B., and Robert, J. (2014). "Effects of visual clutter on pilot workload, flight performance and fixation pattern," in *Proceedings of the international conference on human-computer interaction in aerospace. HCI-Aero '14*, (New York, NY: Association for Computing Machinery). doi: 10.1145/2669592.2669656
- Federal Aviation Administration (2014). *AC 25-11B—Electronic flight displays*. Washington, DC: U.S. Department of Transportation Federal Aviation Administration.
- Frank, A. U., and Timpf, S. (1994). Multiple representations for cartographic objects in a multi-scale Tree—An intelligent graphical zoom. *Comput. Graph.* 18, 823–829. doi: 10.1016/0097-8493(94)90008-6
- Grahame, M., Laberge, J., and Scialfa, C. T. (2004). Age differences in search of web pages: The effects of link size, link number, and clutter. *Hum. Factors* 46, 385–398. doi: 10.1518/hfes.46.3.385.50404
- Kaber, D. B., Alexander, A. L., Stelzer, E. M., Kim, S.-H., Kaufmann, K., and Hsiang, S. M. (2008). Perceived clutter in advanced cockpit displays: Measurement and modeling with experienced pilots. *Aviat. Space Environ. Med.* 79, 1007–1018. doi: 10.3357/ASEM.2319.2008
- Kim, S. H., Prinzel, L. J., Kaber, D. B., Alexander, A. L., Stelzer, E. M., Kaufmann, K., et al. (2011). Multidimensional measure of display clutter and pilot performance for advanced head-up display. *Aviat. Space Environ. Med.* 82, 1013–1022. doi: 10.3357/ASEM.3017.2011
- Newman, R. L., and Greeley, K. W. (1997). *Helmet-mounted display design guide [S]*. San Marcos, TX: Crew Systems.
- Nickerson, J. V. (1994). *Visual programming*. Ph.D. dissertation. New York, NY: New York University.
- Rosenholtz, R., Dorai, A., and Freeman, R. (2011). Do predictions of visual perception aid design? *ACM Trans. Appl. Percept. (TAP)* 8, 1–20. doi: 10.1145/1870076.1870080
- Rosenholtz, R., Li, Y., Mansfield, J., and Jin, Z. (2005). "Feature congestion: A measure of display clutter," in *Proceedings of the ACM SIGCHI conference on human factors in computing systems*. (New York, NY: Association for Computing Machinery). doi: 10.1145/1054972.1055078
- SAE International (1998). *Head-up display human factor issues [S]*. Warrendale, PA: Society of Automotive Engineers, Inc.
- Tullis, T. S. (1983). Formatting of alphanumeric displays: A review and analysis. *Hum. Factors* 25, 657–682. doi: 10.1177/001872088302500604
- Ververs, P. M., and Wickens, C. D. (1998). Head-up displays: Effect of clutter, display intensity, and display location on pilot performance. *Int. J. Aviat. Psychol.* 8, 377–403. doi: 10.1207/s15327108ijap0804_4

Author contributions

QL: conceptualization, methodology, experiment, formal analysis, and writing—original draft. YW: data curation, methodology, experiment, and formal analysis. YB: experiment and data curation. MY: resources and supervision. ZC: experiment and validation. XY: visualization and writing—review editing. LD: conceptualization, funding acquisition, resources, supervision, and writing—review editing. All authors contributed to the article and approved the submitted version.

Conflict of interest

The authors declare that the research was conducted in the absence of any commercial or financial relationships that could be construed as a potential conflict of interest.

Publisher's note

All claims expressed in this article are solely those of the authors and do not necessarily represent those of their affiliated organizations, or those of the publisher, the editors and the reviewers. Any product that may be evaluated in this article, or claim that may be made by its manufacturer, is not guaranteed or endorsed by the publisher.



OPEN ACCESS

EDITED BY
Jiawei Zhou,
Wenzhou Medical University, China

REVIEWED BY
Lin Li,
Capital Medical University, China
Haixia Zhang,
Capital Medical University, China

*CORRESPONDENCE
Yueguo Chen
✉ chenyeuguo@263.net
Xuemin Li
✉ lxmxm66@sina.com

†These authors have contributed equally to this work

SPECIALTY SECTION
This article was submitted to
Visual Neuroscience,
a section of the journal
Frontiers in Neuroscience

RECEIVED 11 January 2023
ACCEPTED 20 February 2023
PUBLISHED 03 March 2023

CITATION
Wang Y, Guo Y, Li Y, Zhang Y, Yuan Y, Wu T,
Chen Y and Li X (2023) The impact of different
corneal refractive surgeries on binocular
dynamic visual acuity.
Front. Neurosci. 17:1142339.
doi: 10.3389/fnins.2023.1142339

COPYRIGHT
© 2023 Wang, Guo, Li, Zhang, Yuan, Wu, Chen
and Li. This is an open-access article
distributed under the terms of the [Creative
Commons Attribution License \(CC BY\)](#). The
use, distribution or reproduction in other
forums is permitted, provided the original
author(s) and the copyright owner(s) are
credited and that the original publication in this
journal is cited, in accordance with accepted
academic practice. No use, distribution or
reproduction is permitted which does not
comply with these terms.

The impact of different corneal refractive surgeries on binocular dynamic visual acuity

Yuxin Wang^{1,2†}, Yining Guo^{1,2†}, Yuanting Li^{1,2†}, Yu Zhang^{1,2},
Yifei Yuan^{1,2}, Tingyi Wu^{1,2}, Yueguo Chen^{1,2*} and Xuemin Li^{1,2*}

¹Department of Ophthalmology, Peking University Third Hospital, Beijing, China, ²Beijing Key Laboratory of Restoration of Damaged Ocular Nerves, Beijing, China

Purpose: To investigate the influence of different corneal refractive surgeries on dynamic visual acuity (DVA), and explore its potential influence factors.

Methods: This was a prospective non-randomized study. Adult myopic patients undergoing bilateral laser-assisted sub-epithelial keratomileusis (LASEK), femtosecond laser-assisted *in situ* keratomileusis (FS-LASIK), or small incision lenticule extraction (SMILE) with Plano refraction target were enrolled. Uncorrected and corrected distance visual acuity (UDVA/CDVA), manifest refraction and binocular optotype-moving DVA of 40 and 80 degrees per second (dps) were evaluated pre-operatively and post-operatively up to 3 months.

Results: The study included 264 eyes of 132 subjects, with an average age of 27.0 ± 6.7 years, and females accounted for 59% of the participants. Significant improvement was observed at the 3-month visit for 40 dps (SMILE, $P = 0.001$; LASEK, $P = 0.006$; FS-LASIK, $P = 0.010$) and 80 dps (SMILE, $P = 0.011$; LASEK, $P = 0.025$; FS-LASIK, $P = 0.012$) DVA. Adjusting for pre-operative DVA, there was no significant difference in DVA among groups at 3 months post-operatively ($P > 0.05$ for multiple comparisons). Overall, multiple linear models demonstrated that post-operative DVA at 3 months was correlated with pre-operative DVA (40 dps, $\beta = 0.349$, $P = 0.001$; 80 dps, $\beta = 0.447$, $P < 0.001$), pre-operative spherical equivalent (40 dps, $\beta = 0.311$, $P = 0.003$; 80 dps, $\beta = 0.261$, $P = 0.009$) and post-operative UDVA (40 dps, $\beta = -0.224$, $P = 0.024$; 80 dps, $\beta = -0.188$, $P = 0.05$).

Conclusion: Dynamic visual acuity at 3 months post-operatively of the three corneal refractive surgeries was better than that before the surgery in adult myopic patients, and there was no significant difference among different surgical techniques. Post-operative DVA at 3 months was found correlated with pre-operative DVA, pre-operative SE, and post-operative UDVA. With further improvement, DVA could be a promising functional visual indicator for myopic patients undergoing refractive surgeries.

KEYWORDS

myopia, dynamic visual acuity, laser-assisted sub-epithelial keratomileusis, femtosecond laser-assisted *in situ* keratomileusis, small incision lenticule extraction

Introduction

Laser corneal refractive surgery has become an effective alternative to refractive error correction. These types of surgery correct the refractive error by quantitatively removing corneal tissue and reshaping the cornea (Wen et al., 2017). Currently, it mainly includes three categories: corneal surface ablation techniques (such as laser-assisted sub-epithelial keratomileusis, LASEK), corneal stroma ablation surgery (such as femtosecond laser-assisted *in situ* keratomileusis, FS-LASIK), and refractive corneal lenticule extraction procedures (such as small incision lenticule extraction, SMILE) (Wen et al., 2017). Each of these types of surgery has its advantages and disadvantages. Previous studies have demonstrated that corneal surface ablation surgery exhibit better performance in visual quality-related outcomes, including higher-order aberrations (HOAs) and contrast sensitivity (CS) (Kirwan and O'Keefe, 2009; Wen et al., 2017), while corneal stromal ablation surgery, especially FS-LASIK, demonstrates relative advantages in efficacy and predictability (Wen et al., 2017). With the advent of femtosecond lasers, SMILE surgery has gradually emerged, which may have potentially better biomechanical outcomes without a corneal flap compared with LASIK (Reinstein et al., 2014; Chansue et al., 2015).

Current visual quality assessment for laser refractive surgery mainly focuses on static vision, including visual acuity, optical aberration and contrast sensitivity (Reinstein et al., 1995; Stulting et al., 2011; Yildirim et al., 2016). Dynamic visual acuity (DVA) refers to the ability to recognize objects with relative motion (Geer and Robertson, 1993; Long and Zavod, 2002; Hirano et al., 2017). DVA is a comprehensive reflection of visual function and perceptual judgment ability. Measuring visual acuity in dynamic situations, as well as the detail resolution of moving objects, can better reflect the visual function in real-life scenes (Long and Zavod, 2002). Therefore, DVA is now gradually recognized as an important evaluation index for functional vision (Ao et al., 2014; Wu et al., 2022), with important applications in sports performance (Uchida et al., 2012), driving safety evaluation (Wilkins et al., 2013; Lacherez et al., 2014), and ocular diseases (Wu et al., 2021). The previous study demonstrated that myopia significantly affects DVA when fully corrected with spectacles, and worse DVA was associated with more significant myopia (Wang et al., 2022b). Further research showed that the uncorrected DVA post-SMILE surgery is significantly better than the pre-operative corrected DVA (Wang et al., 2022a). However, the impact of different refractive surgeries on DVA remained to be explored in a controlled study.

The present study aims to compare the influence of different corneal refractive surgeries on DVA and investigate the associated factors. Measuring the DVA before and after three corneal refractive surgeries might help us to understand the impact of the different surgeries on functional vision so that DVA can be used as a supplement to the existing indicators to guide the selection of refractive surgery based on patients' requirements in the future.

Abbreviations: CDVA, corrected distance visual acuity; dps, degrees per second; DVA, dynamic visual acuity; DVAT, dynamic visual acuity test; FS-LASIK, femtosecond laser-assisted *in situ* keratomileusis; LASEK, laser-assisted sub-epithelial keratomileusis; SEQ, spherical equivalent; SMILE, small incision lenticule extraction; SVA, static visual acuity.

Materials and methods

Subjects

The present research was a prospective case series performed following the tenets of the Declaration of Helsinki. The protocol of the study was approved by the ethics committee of Peking University Third Hospital (IRB00006761-M2020431) and informed consent was obtained from all subjects. The trial was registered at [ClinicalTrials.gov](https://www.clinicaltrials.gov) (ChiCTR2000037814).

Consecutive patients undergoing bilateral SMILE, FS-LASIK or LASEK surgery were prospectively enrolled when they met the following inclusion criteria: (1) age 18 to 40 years, (2) correction of myopia or myopic astigmatism for Plano target; (3) pre-operative myopia less than 10 D, astigmatism less than 3 D and anisometropia less than 3D; and (4) pre-operative and 3-month post-operative corrected distance visual acuity (CDVA) could be fully corrected to 0 (LogMAR). Exclusion criteria were as follows: (1) history of severe ocular diseases, including keratoconus, glaucoma, retinal diseases, and severe ocular surface diseases; (2) complications including severe haze and irregular corneal topography; (3) vestibular dysfunction and extraocular muscle abnormalities that affect the free movement of eyes; and (4) cognitive disorders or other systemic diseases causing poor cooperation.

Pre-operative and post-operative evaluation

All recruited patients underwent a detailed pre-operative evaluation, including uncorrected distance visual acuity (UDVA), CDVA with LogMAR visual chart, cycloplegic and non-cycloplegic automatic (TOPCON KR8100, Japan) and manifest refraction, slit-lamp biomicroscopy (IM 900, Koniz), non-contact tonometer (NCT NIDEK Co., Ltd), dilated funduscopy, IOL master 700 (Carl Zeiss Meditec AG), corneal topography (Pentacam, Oculus, Germany). All patients were scheduled to be examined at 1 week, 1 month, and 3 months post-operatively. Non-contact intraocular pressure, slit-lamp biomicroscopy, UDVA, and non-cycloplegic automatic refraction were evaluated at each follow-up. Non-cycloplegic manifest refraction and CDVA were measured at 1 and 3 months post-operatively.

Dynamic visual acuity testing procedure

The DVA test procedure was consistent with previous studies (Ao et al., 2013, 2014; Liu et al., 2020; Wu et al., 2022). The optotypes were presented on a 24-inch In-Plane Switching screen with a resolution of 1920 × 1080 pixels (refresh rate of 60 Hz, brightness of 30 lux). The size and configuration of the moving optotype were designed according to the standard logarithmic visual chart, and the velocity was quantified with the viewing angle (degree) changes per second (dps). Optotype generation and presentation were controlled using Matlab2017b (MathWorks, United States).

Binocular DVA (abbreviated as DVA) of 40 and 80 dps was evaluated pre-operatively and post-operatively at each follow-up.

To avoid the impact of refractive errors, pre-operative DVA was examined with CDVA spectacles. Post-operative DVA was tested with the naked eye. Subjects were required to seat 2.5 m away from the screen to provide approximately 10° visual angle. The optotype moved horizontally from left to right in the middle of the screen with a random opening direction, and subjects were required to identify the direction. The DVA test logic was similar to the static visual acuity test. The test started with the optotypes three to four sizes larger than the static visual acuity. There were eight optotypes presented once per 2 s for a certain size. One size smaller optotype would be displayed only if no less than five of eight optotypes were identified correctly. The record consisted of two parts, the minimize size (A, LogMAR) that subjects could identify five or more optotypes and the number (B) of optotypes with one size smaller that could be recognized. The result was calculated using the following equation:

$$DVA = -\text{Log}_{10}A - \frac{0.1}{8} * B$$

Surgical procedures

The surgery was selected non-randomized according to the manifest refraction, corneal topography, and patients' intention based on sufficient informed consent. The same surgery was carried out in both eyes. All patients received standard sterile draping. After topical anesthesia using oxybuprocaine hydrochloride, the eyelids were prepared with the povidone-iodine 5% solution. The procedures of different surgery were as follows:

Laser-assisted sub-epithelial keratomileusis: Surgery began with epithelial removal after soaking in 20% ethanol for 20 s. The stroma was wiped with a sponge, and the ablation was performed by WaveLight EX500 excimer laser (Alcon Laboratories Inc., Fort Worth, TX, USA). Next, the 0.02% mitomycin C cotton pad was applied to the corneal stroma, and then the cornea was rinsed with normal saline. Finally, a bandage soft contact lens (Acuvue, Johnson Vision Care, Inc., FL, United States) was placed on the cornea.

Femtosecond laser-assisted *in situ* keratomileusis: Flaps were created by WaveLight FS200 laser (Alcon Laboratories Inc., Fort Worth, TX, USA) with a thickness of 110 µm, a diameter of 8.5 to 9.0 mm and a site-cut angle of 90°. Then corneal flaps were lifted, and the stroma bed was exposed. Ablation with WaveLight EX500 excimer laser (Alcon Laboratories Inc., Fort Worth, TX, USA) began when iris registration was activated. Afterward, the flaps were repositioned, and normal saline irrigation was used to remove debris. Finally, a slightly moistened sponge was used to ensure the flaps were in a good position with no striae.

Small incision lenticule extraction: The intrastromal lenticule was created using a 500 kHz VisuMax femtosecond laser (Carl Zeiss Meditec AG, Jena, Germany) with the following parameters: cap thickness of 120 µm, cap diameter of 7.5–7.8 mm, the optical zone of 6.5–6.6 mm and laser energy of 130 nanojoules (nJ). The thickness of the lenticule was dependent on the pre-operative manifest refraction. After the anterior and posterior surfaces of the lenticule were separated bluntly, the lenticule was extracted from a 2-mm incision at 10 o'clock manually.

After surgery, all patients were given 0.5% Levofloxacin drops (Santen Pharmaceutical Co., Ltd., Osaka, Japan) and 0.5%

Loteprednol Etabonate Ophthalmic Suspension (Bausch & Lomb Incorporated, FL, United States) four times a day for 1 month. The dosage of preservative-free artificial tears was adjusted according to patients' symptoms.

Statistical analysis

Statistical analysis was performed using IBM SPSS 26.0 (IBM, Armonk, NY, United States). The graphics were generated with Microsoft Excel (2020, Microsoft Corp). The astigmatism analysis was calculated using the Alpins method (Alpins, 1993). The sphere plus half of the cylinder diopter was equal to the spherical equivalent (SEQ). Continuous variables were shown in mean ± SD (range), and categorical variables were presented with the number (percentage). One-way analysis of variance was applied to compare the baseline clinical data, including age, sphere, cylinder, SEQ, central corneal thickness and average keratometry. Pre-operative and post-operative DVA at each visit time was compared with mixed linear models in consideration of the relevance of repeated measurements. The random effect was included for the subjects, and the time point was disposed of as the repeated factor. The post-operative DVA at each time point was also compared among groups with a linear mixed model adjusting for the pre-operative DVA. Changes in LogMAR between pre-operative and 3-month post-operative DVA were calculated. Spearman's correlation was conducted between 3-month post-operative DVA and DVA changes and their potential influential factors, including age, pre-operative DVA, pre-operative mean binocular SEQ, post-operative UDVA, CDVA and mean binocular SEQ at 3 months. Multiple linear models were applied to analyze associated factors for post-operative DVA at 3 months. Bonferroni's correction was conducted for multiple comparisons. $P < 0.05$ was considered statistically significant.

Results

Baseline clinical features

A total of 264 eyes of 132 patients (mean age 27.0 ± 6.7 years; 59% female) were included in the study. The baseline clinical characteristics are summarized in Table 1. Statistical differences existed in the pre-operative sphere, cylinder and SEQ among groups ($P < 0.001$) and *post hoc* comparison demonstrated that sphere, cylinder and SEQ were the greatest in FS-LASIK eyes ($P < 0.001$). The pre-operative central corneal thickness was 556.52 ± 27.64 µm, 528.15 ± 35.69 µm, and 545.83 ± 21.52 µm ($P < 0.001$) in SMILE, LASEK, and FS-LASIK group, respectively.

Static vision and refraction

In this study, 98% of SMILE, 92% of LASEK, and 88% of FS-LASIK eyes achieved SEQ within 0.5 D, and the cylinder within 0.5 D was 98, 90, and 85%, respectively (Supplementary Figures 1–4). No difference was found in 3-month post-operative UDVA

TABLE 1 Baseline clinical characteristics of recruited patients.

Surgery	SMILE	LASEK	FS-LASIK	P
Subjects (n)	46	40	46	
Eyes (n)	92	80	92	
Age (years)	27.24 ± 6.82 (18, 40)	26.10 ± 6.98 (18, 39)	26.61 ± 6.40 (18, 38)	0.734
Sphere (D)	−4.39 ± 1.10 (−6.25, −2.00)	−4.06 ± 1.24 (−7.00, −1.50)	−5.79 ± 1.70 (−9.00, −1.00)	<0.001*
Cylinder (D)	−0.56 ± 0.40 (−1.50, 0)	−0.68 ± 0.51 (−2.00, 0)	−1.36 ± 0.82 (−3.50, 0)	<0.001*
Spherical equivalent (D)	−4.67 ± 1.17 (−6.75, −2.25)	−4.40 ± 1.31 (−7.75, −1.88)	−6.47 ± 1.73 (−9.38, −1.75)	<0.001*
LogMAR CDVA	−0.06 ± 0.05 (−0.18, 0)	−0.05 ± 0.05 (−0.18, 0)	−0.06 ± 0.04 (−0.18, 0)	0.233
Central corneal thickness (μm)	556.52 ± 27.64 (507, 624)	528.15 ± 35.69 (475, 618)	545.83 ± 21.52 (503, 615)	<0.001*
Average keratometry (D)	43.11 ± 1.49 (38.79, 46.15)	43.52 ± 1.55 (40.04, 46.51)	43.43 ± 1.43 (40.28, 46.65)	0.161

CDVA, corrected distance visual acuity; D, diopter; FS-LASIK, femtosecond laser-assisted *in situ* keratomileusis; LASEK, laser-assisted sub-epithelial keratomileusis; SMILE, small incision lenticule extraction (SMILE). Continuous data are given as mean ± standard deviation (range).

*Statistically significant.

among groups (SMILE: 1.20 ± 0.12 , LASEK: 1.16 ± 0.15 , FS-LASIK: 1.19 ± 0.11 , $P = 0.195$). Overall, 89% of SMILE, 79% of LASEK and 86% of FS-LASIK eyes achieved the same or better post-operative UDVA compared with pre-operative CDVA.

Dynamic vision and refraction

The histogram of pre-operative and 3-month post-operative DVA for 40 and 80 dps is demonstrated in [Figures 1, 2](#). Compared with pre-operative DVA, more individuals achieved 0.2 LogMAR DVA at 3 months post-operatively. The percentage of individuals with better than 0.2 LogMAR pre-operative and 3-month post-operative DVA was 78 vs. 96%, 73 vs. 92%, 78 vs. 96% for 40 dps test in SMILE, LASEK, FS-LASIK groups, respectively, and that was 70 vs. 89%, 63 vs. 88%, 61 vs. 80% for 80 dps test. A total of 71, 66, and 72% of patients had better 40 dps DVA following SMILE, LASEK, or FS-LASIK at 3 months than before the surgery. As for 80 dps DVA, the percentage was 78, 77, and 68%, respectively ([Figures 1, 2](#)).

The pre-operative and post-operative DVA at each visit is shown in [Table 2](#), and the result of multiple comparisons is demonstrated in [Supplementary Table 1](#). No significant difference was found in pre-operative 40 and 80 dps DVA among SMILE, LASEK, and FS-LASIK groups (40 dps: 0.148 ± 0.077 , 0.161 ± 0.070 , 0.156 ± 0.088 , $P = 0.748$; 80 dps: 0.178 ± 0.065 , 0.185 ± 0.073 , 0.188 ± 0.094 , $P = 0.834$). At 1 week post-operatively, the patients receiving LASEK showed worse DVA (40 dps, $P = 0.022$, 80 dps, $P < 0.001$) than the pre-operative DVA measurement. Post-operatively at 1 month, a significantly improved 40 dps DVA was obtained in patients undergoing SMILE ($P = 0.033$) compared with the pre-operative DVA. Significant improvement was observed at 3 months post-operatively for 40 dps (SMILE 0.09 ± 0.068 , $P = 0.001$; LASEK 0.10 ± 0.076 , $P = 0.006$, FS-LASIK 0.10 ± 0.072 , $P = 0.010$) and 80 dps (SMILE 0.13 ± 0.072 , $P = 0.011$; LASEK 0.14 ± 0.072 , $P = 0.025$, FS-LASIK 0.14 ± 0.088 , $P = 0.012$) DVA compared with the pre-operative measurements.

Adjusting for the pre-operative DVA, the comparison between different surgical groups illustrated that LASEK patients presented significantly worse DVA than FS-LASIK and SMILE groups at 1-week visit (40 dps: $P = 0.003$; 80 dps: $P = 0.004$). At 1 month post-operatively, the adjusted DVA in patients undergoing LASEK

was significantly worse than in patients with SMILE for 40 dps ($P = 0.027$) measurements. There was no significant difference for the adjusted post-operative DVA at 3 months among three surgical procedures (40 dps, $P = 0.870$; 80 dps, $P = 0.859$).

Influential factors of DVA at 3 months post-operatively

Spearman's correlation between post-operative DVA at 3 months and potentially influential factors were illustrated in [Table 3](#). Post-operative DVA was correlated with pre-operative DVA in SMILE (40 dps: $R = 0.488$, $P = 0.008$; 80 dps: $R = 0.728$, $P < 0.001$) and FS-LASIK group (40 dps: $R = 0.410$, $P = 0.042$; 80 dps: $R = 0.509$, $P = 0.009$). A significant negative correlation was found between pre-operative SEQ and 80 dps post-operative DVA of SMILE patients ($R = -0.374$, $P < 0.001$). Post-operative UDVA was positively correlated with 40 dps DVA in the FS-LASIK group ($R = 0.478$, $P = 0.016$) and 80 dps DVA in the LASEK group ($R = 0.501$, $P = 0.009$).

[Table 4](#) summarizes multiple linear regression results for DVA at 3 months. The regression analysis illustrated that 3-month post-operative DVA was significantly correlated with pre-operative DVA in SMILE ($P = 0.001$ for 40 dps; $P < 0.001$ for 80 dps) and FS-LASIK ($P = 0.004$ for 40 dps; $P = 0.001$ for 80 dps) groups. Post-operative DVA was correlated with UDVA at 3 months for patients undergoing LASEK ($P = 0.005$ for 40 dps; $P = 0.001$ for 80 dps) and FS-LASIK ($P = 0.005$ for 40 dps), but not for 80 dps DVA in FS-LASIK group ($P = 0.373$). Besides, a significant correlation between pre-operative SEQ and post-operative DVA at 80 dps in SMILE ($P = 0.048$) and LASEK ($P = 0.040$) groups was observed.

Changes between pre- and post-operative DVA at 3 months were calculated, and its associated factors were analyzed using Spearman's correlation, and the results are shown in [Table 5](#). Pre-operative DVA was significantly positively correlated with DVA changes for both 40 dps (SMILE: $R = -0.644$, $P < 0.001$; LASEK: $R = -0.457$, $P = 0.019$; FS-LASIK: $R = -0.642$, $P = 0.001$) and 80 dps (LASEK: $R = -0.531$, $P = 0.005$; FS-LASIK: $R = -0.521$, $P = 0.008$), except for 80 dps DVA changes in SMILE group ($P = 0.386$). Meanwhile, age was negatively correlated with DVA changes in the SMILE group for 40 dps ($R = -0.411$, $P = 0.030$).

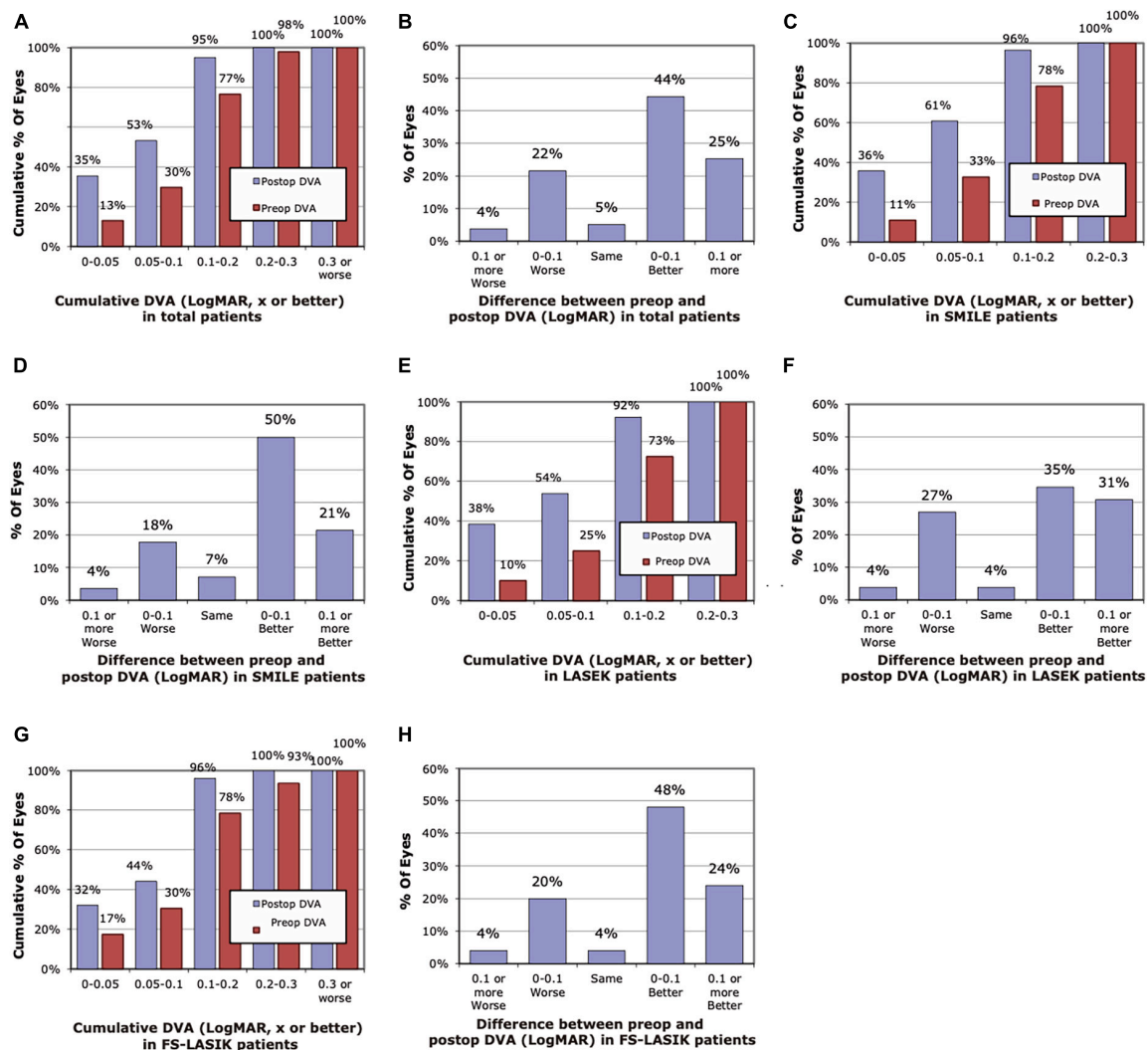


FIGURE 1

Histogram of pre-operative and post-operative dynamic visual acuity (DVA) of 40 dps at 3 months. (A) Cumulative pre-operative and post-operative DVA of total patients. (B) Changes in LogMAR between pre-operative and post-operative DVA of total patients. (C) Cumulative pre-operative and post-operative DVA of the SMILE group. (D) Changes in LogMAR between pre-operative and post-operative DVA of the SMILE group. (E) Cumulative pre-operative and post-operative DVA of the LASEK group. (F) Changes in LogMAR between pre-operative and post-operative DVA of the LASEK group. (G) Cumulative pre-operative and post-operative DVA of the LASIK group. (H) Changes in LogMAR between pre-operative and post-operative DVA of the LASIK group.

Discussion

Existing visual function assessment for corneal refractive surgery mainly focuses on static vision. DVA is a promising functional visual evaluation indicator. To our knowledge, this study is the first to compare DVA after SMILE, FS-LASIK, and LASEK surgeries, which can be used as a supplement to the existing indicators to guide refractive surgery visual function evaluation.

In the present study, the DVA of the LASEK group was worse than that of the FS-LASIK and SMILE groups 1 week post-operatively, and worse than that pre-operatively. During the early post-operative period, the patient receiving LASEK suffers from a corneal epithelial healing process (Ghirlando et al., 1995), and the irregular corneal surface might increase the optical scatter that induces decreased DVA. The DVA performance of the SMILE group was better at 1 month post-operatively compared with the

measurement before the surgery, but a significant improvement was not observed in the other two surgeries. The result indicates that the functional vision of the patient may recover faster after SMILE than other surgeries. The previous study has demonstrated that SMILE may cause less corneal biomechanical changes at the beginning of corneal wound healing in the early post-operative stage, which may be due to stiffer anterior stroma and the corneal integrity preservation (Yu et al., 2019a), and the refractive power was more uniform from central to peripheral cornea (Yu et al., 2019b). There was no significant difference in DVA among the three surgical procedures at 3 months after surgery, indicating that after the corneal remodeling, the three surgical methods had comparable effects on DVA.

This study discovered that DVA at 3 months post-operatively was significantly better than pre-operative DVA. The result is similar to our previous research enrolling myopic patients

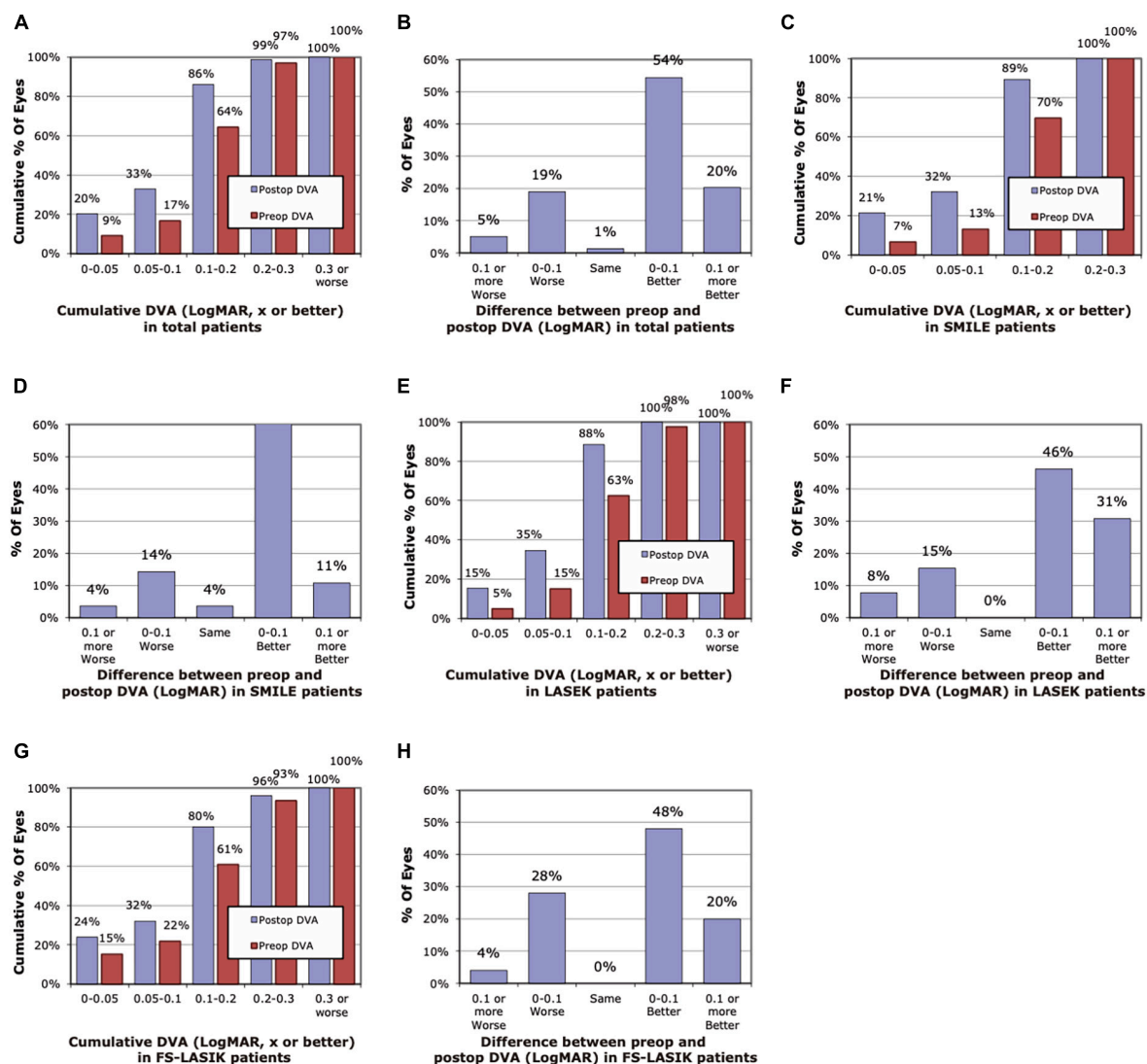


FIGURE 2

Histogram of pre-operative and post-operative dynamic visual acuity (DVA) of 80 dps at 3 months. (A) Cumulative pre-operative and post-operative DVA of the total. (B) Changes in LogMAR between pre-operative and post-operative DVA of the total. (C) Cumulative pre-operative and post-operative DVA of the SMILE group. (D) Changes in LogMAR between pre-operative and post-operative DVA of the SMILE group. (E) Cumulative pre-operative and post-operative DVA of the LASEK group. (F) Changes in LogMAR between pre-operative and post-operative DVA of the LASEK group. (G) Cumulative pre-operative and post-operative DVA of the LASIK group. (H) Changes in LogMAR between pre-operative and post-operative DVA of the LASIK group.

undergoing SMILE (Wang et al., 2022a). The outcome may indicate that the correction of DVA with corneal refractive surgeries was significantly better than that of spectacles. When observing a moving object, the eye needs to keep the object relatively stable on the retina through smooth tracking and saccade, and keep the fovea's fixation on the image as much as possible (Spering and Montagnini, 2011). Previous studies have demonstrated that the magnocellular (M) retinal ganglion cells responsible for motion perception are mainly distributed in the peripheral retina (Dacey, 1994; Skottun, 2016), and the perception of motion by the peripheral retina may affect eye tracking (Wang et al., 2021). Previous studies have shown that the resolution of the macular area to the optotype decreases with the increase of the speed of the optotype (Geer and Robertson, 1993; Lewis et al., 2011), which may be due to the macular image shift, resulting in a more

obvious drag effect (Geer and Robertson, 1993). Refractive surgery and spectacles differently affect the projection of objects on the central and peripheral retina. Spectacles have obvious peripheral defocus and prism effects that cause unclear images projected to the peripheral retina (Bakaraju et al., 2008; Lin et al., 2010; Backhouse et al., 2012; Lewerenz et al., 2018; Wang et al., 2022b), and more difficulties in predicting the trajectory of the object. Thus, DVA following refractive surgeries was significantly better than the use of spectacles pre-operatively.

Our study found that post-operative DVA at 3 months was correlated with pre-operative DVA, pre-operative SE, and post-operative UDVA, which was most consistent with previous studies (Wang et al., 2022a,b). Post-operative UDVA reflects the imaging ability of the macula, which is suggested to be related to DVA. We found that worse post-operative DVA was associated with

TABLE 2 Mean dynamic visual acuity (DVA) and comparison among surgical methods.

	Pre-operative	1 week	1 month	3 months	<i>p</i> [#]
SMILE					
Subjects (<i>n</i>)	46	46	42	28	
DVA (40 dps)	0.148 ± 0.077	0.151 ± 0.090	0.121 ± 0.066	0.093 ± 0.068	0.001*
DVA (80 dps)	0.178 ± 0.065	0.187 ± 0.090	0.170 ± 0.080	0.133 ± 0.072	0.017*
LASEK					
Subjects (<i>n</i>)	40	32	36	26	
DVA (40 dps)	0.161 ± 0.070	0.203 ± 0.081	0.174 ± 0.107	0.106 ± 0.076	<0.001*
DVA (80 dps)	0.185 ± 0.073	0.241 ± 0.069	0.215 ± 0.092	0.140 ± 0.072	<0.001*
FS-LASIK					
Subjects (<i>n</i>)	46	43	33	25	
DVA (40 dps)	0.156 ± 0.088	0.133 ± 0.085	0.145 ± 0.094	0.107 ± 0.072	0.059
DVA (80 dps)	0.188 ± 0.094	0.186 ± 0.066	0.177 ± 0.088	0.144 ± 0.088	0.056
Total					
Subjects (<i>n</i>)	132	121	111	79	
DVA (40 dps)	0.155 ± 0.078	0.158 ± 0.090	0.145 ± 0.091	0.102 ± 0.071	<0.001*
DVA (80 dps)	0.183 ± 0.078	0.201 ± 0.080	0.187 ± 0.088	0.138 ± 0.076	<0.001*
Comparison among surgical methods (<i>P</i>-value[#])					
DVA (40 dps)	0.748	0.003*	0.033*	0.870	
DVA (80 dps)	0.834	0.004*	0.051	0.859	

dps, degree per second; DVA, dynamic visual acuity; FS-LASIK, femtosecond laser-assisted *in situ* keratomileusis; LASEK, laser-assisted sub-epithelial keratomileusis; SMILE, small incision lenticule extraction (SMILE). Data was shown as Mean ± SD.

[#]Calculated using linear mixed model, and pre-operative DVA was adjusted as a covariant when analyzes the difference in post-operative DVA among surgical methods.

*Statistically significant, *P* < 0.05.

TABLE 3 Spearman's correlation between DVA at 3 months post-operatively and potential influential factors.

Parameters		DVA at 40 dps				DVA at 80 dps			
		SMILE	LASEK	FS-LASIK	Total	SMILE	LASEK	FS-LASIK	Total
Age (years)	R	0.029	−0.051	−0.088	−0.027	0.242	0.124	0.073	0.133
	P	0.882	0.804	0.677	0.815	0.215	0.546	0.727	0.243
Pre-operative DVA	R	0.488	0.158	0.410	0.402	0.728	0.295	0.509	0.529
	P	0.008*	0.440	0.042*	<0.001*	<0.001*	0.144	0.009*	<0.001*
Pre-operative SEQ [#]	R	−0.200	−0.201	−0.383	−0.242	−0.374	−0.137	−0.294	−0.216
	P	0.309	0.326	0.059	0.032*	<0.001*	0.504	0.154	0.056
Post-operative UDVA	R	0.270	0.320	0.478	0.353	0.364	0.501	0.297	0.403
	P	0.165	0.111	0.016*	0.001*	0.057	0.009*	0.149	<0.001*
Post-operative CDVA	R	−0.269	0.208	−0.091	−0.059	−0.185	0.409	−0.287	−0.040
	P	0.174	0.354	0.672	0.620	0.355	0.058	0.175	0.736
Post-operative SEQ [#]	R	0.065	0.144	0.299	0.160	−0.046	0.211	0.192	0.147
	P	0.747	0.524	0.156	0.177	0.821	0.346	0.369	0.215

dps, degree per second; DVA, dynamic visual acuity; FS-LASIK, femtosecond laser-assisted *in situ* keratomileusis; LASEK, laser-assisted sub-epithelial keratomileusis; SEQ, spherical equivalent; SMILE, small incision lenticule extraction (SMILE); UDVA, uncorrected distance visual acuity.

[#]Mean binocular SEQ (subjective refraction, diopter).

*Statistically significant.

smaller pre-operative SE measurements. Combining the previous evidence that severe myopia is associated with worse DVA (Wang et al., 2022b) for myopic adults corrected with spectacles, the current result manifested that individuals with more severe myopia pre-operatively still have worse post-operative DVA though

corrected with refractive surgery. Previous studies have shown that patients with severe myopia tend to have thinner retinal ganglion cell-inner plexiform layer (Mwanza et al., 2011; Seo et al., 2017; Lee et al., 2020). As mentioned above, the M ganglion cells play a key role in motion perception (Skottun, 2016). Thus,

TABLE 4 Multiple linear regression for DVA at 3 months.

	Dependent variable	Independent variable	Unstandardized coefficient	Standardized coefficient	P	R ²	Adjusted R ²
SMILE	DVA at 40 dps	Pre-operative DVA at 40 dps	0.487	0.613	0.001	0.376	0.351
	DVA at 80 dps	Pre-operative DVA at 80 dps	0.725	0.662	<0.001	0.581	0.546
		Pre-operative mean binocular SEQ [#]	−0.017	−0.279	0.048		
LASEK	DVA at 40 dps	Post-operative UDVA at 3 months	0.861	0.574	0.005	0.329	0.296
	DVA at 80 dps	Post-operative UDVA at 3 months	0.836	0.618	0.001	0.564	0.518
		Pre-operative mean binocular SEQ [#]	−0.031	−0.339	0.040		
FS-LASIK	DVA at 40 dps	Pre-operative DVA at 40 dps	0.401	0.508	0.004	0.488	0.439
		Post-operative UDVA at 3 months	1.074	0.450	0.009		
	DVA at 80 dps	Pre-operative DVA at 80 dps	0.580	0.632	0.001	0.400	0.373
Total	DVA at 40 dps	Pre-operative DVA at 40 dps	0.296	0.349	0.001	0.364	0.336
		Post-operative UDVA at 3 months	0.536	0.311	0.003		
		Pre-operative mean binocular SEQ [#]	−0.011	−0.224	0.024		
	DVA at 80 dps	Pre-operative DVA at 80 dps	0.434	0.447	<0.001	0.412	0.386
		Post-operative UDVA at 3 months	0.485	0.261	0.009		
		Pre-operative mean binocular SEQ [#]	−0.010	−0.188	0.05		

dps, degree per second; DVA, dynamic visual acuity; FS-LASIK, femtosecond laser-assisted *in situ* keratomileusis; LASEK, laser-assisted sub-epithelial keratomileusis; SEQ, spherical equivalent; SMILE, small incision lenticule extraction (SMILE); UDVA, uncorrected distance visual acuity.

[#]Mean binocular SEQ (subjective refraction, diopter).

TABLE 5 Spearman's correlation between DVA changes at 3 months and potential influential factors.

Parameters		DVA changes ^a at 40 dps				DVA changes ^a at 80 dps			
		SMILE	LASEK	FS-LASIK	Total	SMILE	LASEK	FS-LASIK	Total
Age (years)	R	−0.411	0.244	−0.258	−0.108	−0.289	0.083	0.131	0.025
	P	0.030*	0.229	0.214	0.343	0.136	0.688	0.533	0.824
Pre-operative DVA	R	−0.644	−0.457	−0.642	−0.597	−0.170	−0.531	−0.521	−0.415
	P	<0.001*	0.019*	0.001*	<0.001*	0.386	0.005*	0.008*	<0.001*
Pre-operative SEQ [#]	R	0.145	−0.155	−0.138	−0.088	−0.327	0.009	0.075	−0.041
	P	0.461	0.451	0.509	0.441	0.090	0.966	0.721	0.721
Post-operative UDVA	R	−0.203	0.124	0.234	0.030	−0.049	−0.010	0.129	0.044
	P	0.301	0.547	0.261	0.791	0.804	0.963	0.538	0.699

dps, degree per second; DVA, dynamic visual acuity; FS-LASIK, femtosecond laser-assisted *in situ* keratomileusis; LASEK, laser-assisted sub-epithelial keratomileusis; SEQ, spherical equivalent; SMILE, small incision lenticule extraction (SMILE); UDVA, uncorrected distance visual acuity.

^aThe DVA changes were calculated as post-operative minus pre-operative measurements, where a negative change indicated the improvement in DVA.

[#]Mean binocular SEQ (subjective refraction, diopter).

*Statistically significant.

the decline in the density of M ganglion cells might lead to the decline of DVA in individuals with severe myopia. Further research is required to explore the relationship between retinal neuronal anatomy and DVA. However, we found that pre-operative DVA was positively associated with DVA changes, which indicates that patients with more severe myopia obtain more gains in

DVA. The above-mentioned negative optical effect of spectacles is theoretically more obvious for higher myopia patients. Thus, correction with refractive surgery could be more beneficial in patients with higher myopia in DVA improvement.

Myopia is the most prevalent ocular disease to cause decreased uncorrected visual acuity. It could be corrected with several

methods, among which spectacles are mostly used. In the present research, we found that patients undergoing laser refractive surgery achieved improved DVA compared with that before the surgery corrected with spectacles. Therefore, for individuals with higher dynamic vision demands, such as those involved in athletic competition, driving and flight task, refractive surgery might be a better corrective option than spectacles. It is noted to mention that comprehensive pre-operative evaluation is required to screen eligible candidates for refractive surgery. Previous research has shown that motion perception may be more useful for driving safety than fine vision (Moharrer et al., 2020). With further research, DVA can not only be applied to evaluate the functional vision but can also guide the selection of myopia correction methods to supplement the existing indicators.

Certain limitations exist in the present study. Firstly, the follow-up was only extended to 3 months post-operatively. The DVA might change in a long-term post-operatively. Thus, measurement at 6 months and longer after refractive surgery is required in further research. In addition, the loss to follow-up rate at 3 months post-operatively is high in the present research, which might be due to the COVID-19 global pandemic. DVA is suggested to better reflect functional vision in daily life. Thus, subjective quality of life evaluation and its association with DVA is required for post-operative refractive surgery patients in the future study. In addition, this study only focused on distant DVA, and recent research suggested that dynamic defocus curves may also be promising indicators of functional vision assessing the DVA of difference distance (Wu et al., 2022). Future research can incorporate these novel indicators to evaluate the full-distance dynamic vision better.

In summary, from the 3-month observation, the DVA following three laser refractive surgeries was better than that before the surgery in adult myopic patients. There was no significant difference among different surgical techniques for post-operative DVA at 3 months. Post-operative DVA at 3 months was found correlated with pre-operative DVA, pre-operative SE, and post-operative UDVA. The present research provided the basis for applying the DVA test as an indicator for functional vision in refractive surgery and useful information for selecting the myopia correction method in a DVA-based way.

Data availability statement

The original data presented in this study are included in the article/**Supplementary material**, further inquiries can be directed to the corresponding authors.

References

- Alpins, N. A. (1993). A new method of analyzing vectors for changes in astigmatism. *J. Cataract Refract. Surg.* 19, 524–533. doi: 10.1016/s0886-3350(13)80617-7
- Ao, M., Li, X., Huang, C., Hou, Z., Qiu, W., and Wang, W. (2014). Significant improvement in dynamic visual acuity after cataract surgery: a promising potential parameter for functional vision. *PLoS One* 9:e115812. doi: 10.1371/journal.pone.0115812
- Ao, M. X., Wang, W., Li, X. M., Hou, Z. Q., and Huang, C. (2013). [Changes of dynamic visual acuity after phacoemulsification combined with intraocular lens implantation]. *Zhonghua yan ke za zhi* 49, 405–409.
- Backhouse, S., Fox, S., Ibrahim, B., and Phillips, J. R. (2012). Peripheral refraction in myopia corrected with spectacles versus contact lenses. *Ophthalmic Physiol. Opt.* 32, 294–303.

Ethics statement

The studies involving human participants were reviewed and approved by the Peking University Third Hospital Medical Science Research Ethics Committee. The patients/participants provided their written informed consent to participate in this study.

Author contributions

YW contributed to the design and data collection. YG involved the data collection. YG and YL analyzed and interpreted the data and major contributors in writing the manuscript. YC and XL revised the manuscript. All authors read, commented, and approved the final manuscript.

Funding

This work was supported by the National Natural Science Foundation of China (82201243).

Conflict of interest

The authors declare that the research was conducted in the absence of any commercial or financial relationships that could be construed as a potential conflict of interest.

Publisher's note

All claims expressed in this article are solely those of the authors and do not necessarily represent those of their affiliated organizations, or those of the publisher, the editors and the reviewers. Any product that may be evaluated in this article, or claim that may be made by its manufacturer, is not guaranteed or endorsed by the publisher.

Supplementary material

The Supplementary Material for this article can be found online at: <https://www.frontiersin.org/articles/10.3389/fnins.2023.1142339/full#supplementary-material>

- Bakaraju, R. C., Ehrmann, K., Ho, A., and Papas, E. B. (2008). Pantoscopic tilt in spectacle-corrected myopia and its effect on peripheral refraction. *Ophthalmic Physiol. Opt.* 28, 538–549. doi: 10.1111/j.1475-1313.2008.00589.x
- Chansue, E., Tanheksakdi, M., Swasditutra, S., and McAlinden, C. (2015). Safety and efficacy of VisuMax[®] circle patterns for flap creation and enhancement following small incision lenticule extraction. *Eye Vis.* 2:21. doi: 10.1186/s40662-015-0031-5
- Dacey, D. M. (1994). Physiology, morphology and spatial densities of identified ganglion cell types in primate retina. *Ciba Found. Symp.* 184, 12–28.
- Geer, I., and Robertson, K. M. (1993). Measurement of central and peripheral dynamic visual acuity thresholds during ocular pursuit of a moving target. *Opt. Vis. Sci.* 70, 552–560. doi: 10.1097/00006324-199307000-00006
- Ghirlando, A., Gambato, C., and Midena, E. (1995). LASEK and photorefractive keratectomy for myopia: clinical and confocal microscopy comparison. *J. Refract. Surg.* 2007, 694–702. doi: 10.3928/1081-597X-20070901-08
- Hirano, M., Hutchings, N., Simpson, T., and Dalton, K. (2017). Validity and repeatability of a novel dynamic visual acuity system. *Opt. Vis. Sci.* 94, 616–625. doi: 10.1097/OPX.0000000000001065
- Kirwan, C., and O'Keefe, M. (2009). Comparative study of higher-order aberrations after conventional laser in situ keratomileusis and laser epithelial keratomileusis for myopia using the technolas 217z laser platform. *Am. J. Ophthalmol.* 147, 77–83. doi: 10.1016/j.ajo.2008.07.014
- Lacherez, P., Au, S., and Wood, J. M. (2014). Visual motion perception predicts driving hazard perception ability. *Acta Ophthalmol.* 92, 88–93. doi: 10.1111/j.1755-3768.2012.02575.x
- Lee, M. W., Nam, K. Y., Park, H. J., Lim, H. B., and Kim, J. Y. (2020). Longitudinal changes in the ganglion cell-inner plexiform layer thickness in high myopia: a prospective observational study. *Br. J. Ophthalmol.* 104, 604–609. doi: 10.1136/bjophthalmol-2019-314537
- Lewerenz, D., Blanco, D., Ratzlaff, C., and Zodrow, A. (2018). The effect of prism on preferred retinal locus. *Clin. Exp. Opt.* 101, 260–266.
- Lewis, P., Rosén, R., Unsbo, P., and Gustafsson, J. (2011). Resolution of static and dynamic stimuli in the peripheral visual field. *Vis. Res.* 51, 1829–1834.
- Lin, Z., Martinez, A., Chen, X., Li, L., Sankaridurg, P., Holden, B. A., et al. (2010). Peripheral defocus with single-vision spectacle lenses in myopic children. *Opt. Vis. Sci.* 87, 4–9.
- Liu, Z., Hou, Z., Ge, S., Pang, H., and Wang, W. (2020). Vision function of pseudophakic eyes with posterior capsular opacification under different speed and spatial frequency. *Int. Ophthalmol.* 40, 3491–3500. doi: 10.1007/s10792-020-01536-9
- Long, G. M., and Zavod, M. J. (2002). Contrast sensitivity in a dynamic environment: effects of target conditions and visual impairment. *Hum. Fact.* 44, 120–132. doi: 10.1518/0018720024494784
- Moharrer, M., Tang, X., and Luo, G. (2020). With motion perception, good visual acuity may not be necessary for driving hazard detection. *Trans. Vis. Sci. Technol.* 9:18. doi: 10.1167/tvst.9.13.18
- Mwanza, J. C., Durbin, M. K., Budenz, D. L., Girkin, C. A., Leung, C. K., Liebmann, J. M., et al. (2011). Profile and predictors of normal ganglion cell-inner plexiform layer thickness measured with frequency-domain optical coherence tomography. *Invest. Ophthalmol. Vis. Sci.* 52, 7872–7879. doi: 10.1167/iops.11-7896
- Reinstein, D. Z., Archer, T. J., and Gobbe, M. (2014). Small incision lenticule extraction (SMILE) history, fundamentals of a new refractive surgery technique and clinical outcomes. *Eye Vis.* 1:3. doi: 10.1186/s40662-014-0003-1
- Reinstein, D. Z., Archer, T. J., and Randleman, J. B. (1995). JRS standard for reporting astigmatism outcomes of refractive surgery. *J. Refract. Surg.* 2014, 654–659.
- Seo, S., Lee, C. E., Jeong, J. H., Park, K. H., Kim, D. M., and Jeoung, J. W. (2017). Ganglion cell-inner plexiform layer and retinal nerve fiber layer thickness according to myopia and optic disc area: a quantitative and three-dimensional analysis. *BMC Ophthalmol.* 17:22. doi: 10.1186/s12886-017-0419-1
- Skottun, B. C. (2016). A few words on differentiating magno- and parvocellular contributions to vision on the basis of temporal frequency. *Neurosci. Biobehav. Rev.* 71, 756–760. doi: 10.1016/j.neubiorev.2016.10.016
- Spring, M., and Montagnini, A. (2011). Do we track what we see? Common versus independent processing for motion perception and smooth pursuit eye movements: a review. *Vis. Res.* 51, 836–852. doi: 10.1016/j.visres.2010.10.017
- Stulting, R. D., Dupps, W. J. Jr., Kohnen, T., Mamalis, N., Rosen, E. S., Koch, D. D., et al. (2011). Standardized graphs and terms for refractive surgery results. *J. Cataract Refract. Surg.* 37, 1–3.
- Uchida, Y., Kudoh, D., Murakami, A., Honda, M., and Kitazawa, S. (2012). Origins of superior dynamic visual acuity in baseball players: superior eye movements or superior image processing. *PLoS One* 7:e31530. doi: 10.1371/journal.pone.0031530
- Wang, Y., Guo, Y., Wang, J., Liu, Z., and Li, X. (2021). Pupillary response to moving stimuli of different speeds. *J. Eye Mov. Res.* 14:10.16910/jemr.14.1.2.
- Wang, Y., Guo, Y., Wei, S., Yuan, Y., Wu, T., Zhang, Y., et al. (2022b). Binocular dynamic visual acuity in eyeglass-corrected myopic patients. *J. Vis. Exp.* 29. doi: 10.3791/63864
- Wang, Y., Guo, Y., Wei, S., Wu, T., Yuan, Y., Zhang, Y., et al. (2022a). Dynamic visual acuity after small incision lenticule extraction for myopia patients. *Percept. Mot. Skills* 1–16. doi: 10.1177/003151525221133434
- Wen, D., McAlinden, C., Flitcroft, I., Tu, R., Wang, Q., Alió, J., et al. (2017). Postoperative efficacy, predictability, safety, and visual quality of laser corneal refractive surgery: a network meta-analysis. *Am. J. Ophthalmol.* 178, 65–78. doi: 10.1016/j.ajo.2017.03.013
- Wilkins, L., Gray, R., Gaska, J., and Winterbottom, M. (2013). Motion perception and driving: predicting performance through testing and shortening braking reaction times through training. *Invest. Ophthalmol. Vis. Sci.* 54, 8364–8374. doi: 10.1167/iops.13-12774
- Wu, T., Wang, Y., Wei, S., Guo, Y., and Li, X. (2022). Developing dynamic defocus curve for evaluating dynamic vision accommodative function. *BMC Ophthalmol.* 22:106. doi: 10.1186/s12886-022-02335-9
- Wu, T. Y., Wang, Y. X., and Li, X. M. (2021). Applications of dynamic visual acuity test in clinical ophthalmology. *Int. J. Ophthalmol.* 14, 1771–1778. doi: 10.18240/ijo.2021.11.18
- Yıldırım, Y., Alagöz, C., Demir, A., Ölcü, O., Özveren, M., Ağca, A., et al. (2016). Long-term results of small-incision lenticule extraction in high myopia. *Turk J. Ophthalmol.* 46, 200–204.
- Yu, M., Chen, M., and Dai, J. (2019a). Comparison of the posterior corneal elevation and biomechanics after SMILE and LASEK for myopia: a short- and long-term observation. *Graefes Arch. Clin. Exp. Ophthalmol.* 257, 601–606. doi: 10.1007/s00417-018-04227-5
- Yu, M., Chen, M., Liu, W., and Dai, J. (2019b). Comparative study of wave-front aberration and corneal asphericity after SMILE and LASEK for myopia: a short and long term study. *BMC Ophthalmol.* 19:80. doi: 10.1186/s12886-019-1084-3



OPEN ACCESS

EDITED BY

Tina Yang,
Guangdong Provincial People's Hospital, China

REVIEWED BY

Masahiko Ayaki,
Keio University, Japan
Xiuming Jin,
Zhejiang University, China

*CORRESPONDENCE

Xuemin Li
✉ lxmxm66@sina.com

†These authors have contributed equally
to this work

SPECIALTY SECTION

This article was submitted to
Visual Neuroscience,
a section of the journal
Frontiers in Neuroscience

RECEIVED 26 November 2022

ACCEPTED 17 February 2023

PUBLISHED 08 March 2023

CITATION

Ren X, Wang Y, Wu T, Jing D and Li X (2023)
Binocular dynamic visual acuity in dry eye
disease patients.
Front. Neurosci. 17:1108549.
doi: 10.3389/fnins.2023.1108549

COPYRIGHT

© 2023 Ren, Wang, Wu, Jing and Li. This is an
open-access article distributed under the terms
of the [Creative Commons Attribution License
\(CC BY\)](https://creativecommons.org/licenses/by/4.0/). The use, distribution or reproduction
in other forums is permitted, provided the
original author(s) and the copyright owner(s)
are credited and that the original publication in
this journal is cited, in accordance with
accepted academic practice. No use,
distribution or reproduction is permitted which
does not comply with these terms.

Binocular dynamic visual acuity in dry eye disease patients

Xiaotong Ren[†], Yuexin Wang[†], Tingyi Wu[†], Dalan Jing[†] and
Xuemin Li^{*}

Department of Ophthalmology, Peking University Third Hospital, Beijing, China

Purpose: To investigate binocular dynamic visual acuity (DVA) for patients with dry eye disease (DED).

Methods: The prospective study included DED patients. The binocular DVA at 40 and 80 degrees per second (dps), Ocular Surface Disease Index (OSDI), tear meniscus height (TMH), tear film break-up time first (TBUTF), corneal fluorescein staining (CFS), eyelid margin abnormalities and meibomian gland (MG) abnormalities morphology and function were evaluated. A deep learning model was applied to quantify the MG area proportion. The correlation between DVA and DED parameters was analyzed.

Results: A total of 73 DED patients were enrolled. The age, OSDI, CFS, MG expressibility, secretion quality, and eyelid margin abnormalities were significantly positively correlated with the DVA for 40 and 80 dps (all $P < 0.05$). The MG area proportion in the upper eyelid was negatively correlated with DVA at 40 dps ($R = -0.293$, $P < 0.001$) and at 80 dps ($R = -0.304$, $P < 0.001$). Subgroup analysis by MG grade demonstrated that the DVA of patients with severe MG dropout ($<25\%$ of the total area) was significantly worse than other mild and moderate groups, both in 40 and 80 dps (all $P < 0.05$). The patients with CFS showed worse 40 ($P < 0.001$) and 80 dps ($P < 0.001$) DVA than the patients without CFS.

Conclusion: Binocular DVA is significantly associated with DED symptoms and signs. The DED patients with CFS and severe MG dropout and dysfunction have worse DVA.

KEYWORDS

dynamic visual acuity (DVA), dry eye disease (DED), meibomian gland area, meibomian gland dropout, artificial intelligence (AI)

1. Introduction

Dry eye disease (DED) is a multifactorial ocular surface disorder that affects millions worldwide (Craig et al., 2017; Stapleton et al., 2017). The Tear Film and Ocular Surface Society Dry Eye Workshop II (TFOS DEWS II) pointed out in 2017 that the central pathophysiological concept of DED is the loss of tear film homeostasis (Bron et al., 2017; Craig et al., 2017). The tear film plays an important role as the forefront refractive component of the eye (Craig et al., 2017; Wolffsohn et al., 2017). Decreased tear stability in DED patients causes ocular surface-related and vision-related symptoms, yet the routine static visual acuity might be normal (Benitez-Del-Castillo et al., 2017; Koh et al., 2018). The negative effect of

these symptoms may even lead to depression, and affect work productivity, personal success and the economy (Tong et al., 2010; Uchino et al., 2014; Nichols et al., 2016; Stapleton et al., 2017).

Increasing research evaluated the impact of DED on vision-related daily activities. Proceedings of the Osmoprotection in Dry Eye Disease–Expert Opinion (OCEAN) group meeting proposed that in DED patients with normal conventional visual acuity, the difficulties with driving, reading and computer use might be related to impaired visual function (Benitez-Del-Castillo et al., 2017). Thus, the effect of DED on visual function has been paid increasing attention (Tong et al., 2010; Uchino et al., 2014; Mathews et al., 2017; Karakus et al., 2018a,b). Previous studies demonstrated that the DED is associated with deteriorated contrast sensitivity, higher order aberration (HOA), objective scattering index (OSI), and surface asymmetric index (SAI) (Goto et al., 2006; Kaido, 2018; Koh, 2018; Ma et al., 2020). The current visual function assessment mainly focuses on static vision, and certain limitations exist as static vision disturbance could not sufficiently demonstrate functional disability (Karakus et al., 2018a). Most objects we see in real-life have relative motion, so a favorable dynamic vision function is required for daily tasks (Kaido, 2018; Wu et al., 2021; Wang et al., 2022a,b). Dynamic visual acuity (DVA) describes the ability to identify the details of an object as it moves (Nakatsuka et al., 2006; Palidis et al., 2017; Wu et al., 2021). It could better reflect real-life situations vision and is more sensitive to visual disturbance and improvement (Kaido, 2018; Wang et al., 2022a). There are several methods for DVA testing (DVAT), commonly classified into static- and moving-optotypes DVATs (Wu et al., 2021). The latter test with screen demonstration has the advantage of accessibility, standardization and a short learning curve that is generally used in ophthalmology (Palidis et al., 2017; Wu et al., 2021). To the best of our knowledge, no study has investigated the impact of DED on DVA.

This study aims to evaluate the DVA in DED patients and investigate the influential factors that might affect DVA, including objective and subjective clinical dry eye parameters. The present research provides insight into the application of the DVA test to evaluate the functional vision of DED patients. With further improvement, the DVA test might facilitate the assessment and treatment of DED in patients with high demand for dynamic vision, including athletes and drivers.

2. Materials and methods

2.1. Participants

The present research is a prospective cross-sectional study and the protocol is approved by the Human Research and Ethics Committee of Peking University Third Hospital (approval number M2020431). The research was conducted adhered to the tenets of the Declaration of Helsinki. Informed consent was obtained from each patient before enrollment.

Consecutive patients who were diagnosed with DED were enrolled from October 2021 to December 2021. DED was diagnosed according to TFOS DEWS II in 2017 (Craig et al., 2017). The inclusion criteria included: (a) age 18 to 45 years; (b) a monocular best-corrected visual acuity (BCVA) of 1.0

(decimal) or more. Exclusion criteria consisted of (a) severe ocular surface diseases, lens abnormalities, glaucoma, uveitis, and retinal diseases; (b) history of intraocular surgery; (c) diseases that affect the free movement of the globe, such as obvious extraocular muscle abnormalities, including Thyroid associated ophthalmopathy (TAO) and so on; (d) conjunctivochalasis; (e) dry eye related systemic diseases, such as Sjogren's syndrome, Stevens-Johnson syndrome, and rheumatism; (f) cognitive disorders; (g) other diseases or conditions unsuitable for this clinical trial judged by the researchers.

2.2. Evaluation index

All ophthalmologic examinations were performed under unchanged conditions by a single investigator (RXT) in the same examination room. To minimize the influence of the preceding test on the subsequent test, the clinical assessments of the enrolled patients were conducted in the following order: OSDI questionnaire, Ocular surface comprehensive analyzer, DVA and slit-lamp. An interval of 5 min was arranged between two different tests.

2.2.1. Ocular surface disease index

Patients' subjective symptoms were evaluated by the OSDI questionnaire, which included 12 questions and every item scored 0 to 4. OSDI = (sum of scores for all questions answered \times 100)/(total number of answered questions \times 4). It ranged from 0 to 100.

2.2.2. Oculus Keratograph–Ocular surface comprehensive analyzer

To evaluate the meibomian gland (MG) dropout and the tear film, including the tear meniscus height (TMH) and tear film break-up time first (TBUTF), a non-invasive, Placido ring-based, ocular surface comprehensive analyzer (Keratograph 5 M; OCULUS, Wetzlar, Germany) was used. To avoid errors, the examination was repeated three times in each patient. The analyzer captured infrared photographs of the anterior segment of the eyes, enabling assessments of TBUTF, inferior TMH and the extent MG dropout. The superior and inferior margin of the tear meniscus was manually labeled and then the TMH was calculated automatically by the machine.

The meibograph with the best quality from three repeated capture was chosen for quantitative analysis using a deep learning model. The model leverages a convolutional network based on U-Net to segment the tarsus and meibomian glands area from meibograph. The model achieved an accuracy of 0.985 for segmenting the tarsus area and 0.937 for the meibomian gland area tested on an external dataset. The representatives of the meibograph and segmentation results for the upper and lower lid tarsus and meibomian gland area are demonstrated in Figure 1. The meibomian gland area proportion (%) is calculated as the ratio of the meibomian gland and tarsus area.

2.2.3. Dynamic visual acuity test

We assessed binocular DVA (abbreviated simply as DVA) at 40 and 80 dps under the best-corrected visual acuity, and the steps have been described in detail in our previous research

(Wang et al., 2022a,b). The DVA test system included a self-developed program which ran on a laptop and demonstrated a 14-inch 120 Hz TN screen. The testing program was programmed with MATLAB 2017b (MathWorks, Natick, MA, United States) to display the moving letter E (standard logarithm visual chart) of a certain speed and size. During the test, the letter E moved horizontally from the middle of the screen's left side to its right side.

Before the test, we adjusted the seat to make the subject's sight at the screen's midpoint level and the test was performed at 4 m. Before the formal test, the subject was pre-trained sufficiently to understand the testing procedure and the motion pattern of the optotypes to avoid the learning effect. The test began with the optotypes three lines larger than the static visual acuity (SVA) result. Eight "letter E" optotypes with a random opening direction of the same size were presented once per 2 s. The subject was asked to identify the opening directions. If the accuracy reaches 5/8, we changed the optotypes to the smaller size until the size for which identified less than five optotypes. Recorded the minimum size (A, LogMAR) that subjects could recognize (five out of eight optotypes are identified correctly) and the number (b) of optotypes one size smaller that could be identified. The DVA calculation was as follows:

$$DVA = A - \frac{0.1}{8} * b$$

2.2.4. Slit lamp examination

A slit lamp examination was performed to assess the eyelid margin signs, expressibility and secretion quality of the MG, corneal fluorescein staining (CFS). First, eyelid margin abnormalities were evaluated, including rounding of the posterior margin, irregularity of the eyelid margin, hyperkeratosis, eyelid margin telangiectasia and neovascularization. For each abnormality, if it existed, it would be recorded as 1 point; otherwise, it would be recorded as 0 points. Then the doctor applied fixed pressure to the glands at three positions (nasal, central, and temporal) of the upper and lower eyelid to evaluate the MG expressibility. In each position, five MGs were evaluated. MG expressibility was scored as 0, all 5 glands expressible; 1, 3–4 glands expressible; 2, 1–2 glands expressible; 3, no glands expressible. And it was calculated as the sum of the three positions with a total score of 9. Observe the secretion quality of eight MGs in the middle 1/3 of the upper and lower eyelids. The scoring criteria are as follows: 0, clear; 1, cloudy; 2, cloudy with debris; or 3, inspissated like toothpaste. Next, the doctor applied a drop of fluorescein sodium and then viewed the cornea with a slit lamp using cobalt blue illumination to assess CFS. The cornea was divided into 4 quadrants. Staining was scored from 0 to 3 in each quadrant and then summed. All the evaluation indexes were recorded with both eyes separately.

2.3. Statistical analysis

Statistical product and service solutions (SPSS) software version 23 (SPSS Inc., Chicago, IL, USA) was used for statistical analysis. The Kolmogorov-Smirnov test was applied to check the normality of the data distribution. The continuous variable data were presented as the mean and standard deviation (SD), and the categorical variables were shown as numbers (and percentages).

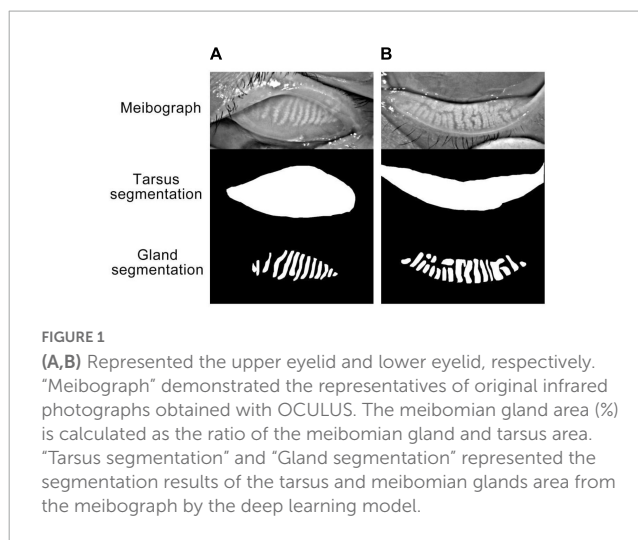


FIGURE 1

(A,B) Represented the upper eyelid and lower eyelid, respectively. "Meibograph" demonstrated the representatives of original infrared photographs obtained with OCULUS. The meibomian gland area (%) is calculated as the ratio of the meibomian gland and tarsus area. "Tarsus segmentation" and "Gland segmentation" represented the segmentation results of the tarsus and meibomian glands area from the meibograph by the deep learning model.

The mean BCVA and each DED parameter are calculated from two eyes for subsequent correlation analysis. Pearson's correlation was assessed to analyze the relationship between the DVA and age, BCVA, and each continuous evaluation index for DED. Otherwise, Spearman's correlation analysis was applied. A multivariate linear model was applied to analyze the potentially influential factors for DVA, including the above factors in one model. Collinearity analysis was performed, and we excluded the variables with a variance inflation factor of more than five based on the clinical significance.

To further reveal the effect of MG dropout and CFS on DVA, patients were grouped based on the upper meibomian gland dropout severity in the original meibograph or the existence of CFS in subgroup analysis. Three groups were created, including mild MG dropout (>50% of the total area), moderate MG dropout (25–50% of the total area) and severe MG dropout (<25% of the total area), respectively. One-way ANOVA was used to compare the differences of DVA in 40 and 80 dps among groups with different meibomian gland dropout severity, and Bonferroni correction was conducted for *post-hoc* analysis. An Independent sample *t*-test was performed to compare the DVA between the DED patient with and without CFS. *P*-values less than 0.05 were considered statistically significant.

3. Results

3.1. The characteristics of the patients

Seventy-three patients were included in the study. The characteristics of the patients are summarized in Table 1. The average age of the enrolled patients was 35.57 ± 10.16 years. Male accounted for 26% of the enrolled patients.

3.2. The correlation between DVA and associated factors

The results of the correlation analysis between the DVA and the associated parameters are summarized in Table 2. The age,

LogMAR BCVA, OSDI, and CFS were significantly positively correlated with the DVA for 40 dps and 80 dps ($P < 0.05$ for all the analyses). Except between hyperkeratosis of the eyelid margin and 40 dps DVA, there was a notable correlation between all the eyelid margin abnormalities and DVA, both 40 dps and 80 dps ($P < 0.05$ for all the analyses). A significant positive correlation was observed between the upper and lower meibomian gland expressibility, secretion quality and the DVA at 40 dps and 80 dps ($P < 0.05$ for all the analyses). The MG area proportion in the upper eyelid was significantly negatively correlated with the postoperative DVA at 40 dps ($R = -0.293$, $P < 0.001$) and at 80 dps ($R = -0.304$, $P < 0.001$).

3.3. Differences by MG grade and CFS

As shown in Table 3, there was no significant difference in age and BCVA among the three groups with different meibomian gland grades (all $P > 0.05$). The DVA at 40 dps of patients with severe meibomian gland dropout was significantly worse than that with mild ($P < 0.001$) and moderate ($P = 0.001$) meibomian gland dropout. There was no significant difference in 40 dps DVA between the mild and moderate meibomian gland group ($P = 0.401$). The result was similar for 80 dps DVA in that the severe

meibomian gland dropout group had the worst DVA compared with the mild ($P = 0.001$) and moderate ($P = 0.004$) groups.

The result of DVA at 40 and 80 dps in DED patients with and without CFS is shown in Table 4. The CFS group showed significantly worse DVA, both at 40 ($P < 0.001$) and 80 dps ($P < 0.001$), than that in the non-CFS group.

4. Discussion

This study aims to investigate the DVA in DED patients and investigate the associated influential factors. We found a significant correlation between DVA and DED severity in patients whose conventional static vision was normal. DVA serves as a linkage between DED parameters and dynamic visual ability, which could better reflect life scenes than static visual acuity. These observations indicate that it is necessary to test DVA in DED patients, especially for patients with high demand for dynamic vision. The present research innovatively proposes a simple and objective way to measure the dynamic vision in dry eye patients to better reflect daily life visual function.

Dry eye disease patients usually showed normal static visual acuity testing with a conventional visual chart. Therefore, although DED has been regarded as disturbing the quality of life, it has not been considered a serious visual disorder. Previous research found that the reading rate was lower in DED patients than in healthy

TABLE 1 Characteristic of patients.

Parameters	Mean \pm SD	Range
Age (years)	35.57 \pm 10.16	20, 45
Sex (male/female)	19/54	
LogMAR BCVA	-0.039 \pm 0.020	-0.1, 0
LogMAR DVA (40 dps)	0.109 \pm 0.047	0.375, 0
LogMAR DVA (80 dps)	0.194 \pm 0.079	0.425, 0.063
OSDI (scores)	43.28 \pm 19.31	21, 81
TMH (cm)	0.17 \pm 0.06	0.08, 0.30
TBUTF (s)	4.87 \pm 2.43	2.0, 11
CFS (scores)	2.49 \pm 2.38	0, 12
Eyelid margin abnormalities		
Rounding in posterior margin (number, %)	27 (37.0)	
Irregularity (number, %)	20 (27.4)	
Hyperkeratosis (number, %)	12 (16.4)	
Telangiectasia (number, %)	40 (54.8)	
Meibomian gland assessments		
Expressibility (upper, 0–9)	3.58 \pm 1.32	2, 8
Expressibility (lower, 0–9)	2.25 \pm 1.07	1, 6
Secretion quality (upper, 0–3)	1.63 \pm 0.55	1, 3
Secretion quality (lower, 0–3)	1.24 \pm 0.43	1, 3
MG area proportion (upper, %)	36.99 \pm 14.04	0.45–66.43
MG area proportion (lower, %)	33.32 \pm 12.36	2.18–65.98

BCVA, best-corrected visual acuity; CFS, corneal fluorescein staining; Dps, degree per second; DVA, dynamic visual acuity; MG, meibomian gland; OSDI, ocular surface disease index; TBUTF, tear film break-up time first; TMH, tear meniscus height.

TABLE 2 Correlation analysis between DVA and potential influencing factors.

Parameters	DVA at 40 dps	DVA at 80 dps
Age (years)	0.376**	0.294**
Sex	0.140	0.031
LogMAR BCVA	0.412**	0.259**
OSDI (scores)	0.382**	0.434**
TMH (cm)	0.020	0.003
TBUTF (s)	0.064	0.011
CFS (scores)	0.444**	0.428**
Eyelid margin abnormalities		
Rounding in posterior margin (0/1)	0.349**	0.500**
Irregularity (0/1)	0.393**	0.428**
Hyperkeratosis (0/1)	0.025	0.217**
Telangiectasia (0/1)	0.460**	0.457**
Meibomian gland assessments		
Expressibility (upper, 0–9)	0.361**	0.457**
Expressibility (lower, 0–9)	0.384**	0.473**
Secretion quality (upper, 0–3)	0.452**	0.553**
Secretion quality (lower, 0–3)	0.272**	0.297**
MGs area proportion (upper, %)	-0.293**	-0.304**
MGs area proportion (lower, %)	-0.161	-0.113

BCVA, best-corrected visual acuity; CFS, corneal fluorescein staining; Dps, degree per second; DVA, dynamic visual acuity; MG, meibomian gland; OSDI, ocular surface disease index; TBUTF, tear film break-up time first; TMH, tear meniscus height. P-values less than 0.05 were considered statistically significant. * $P < 0.05$, ** $P < 0.01$.

TABLE 3 Comparison of DVA among different Meibomian gland (MG) grades in the upper eyelid.

Parameters	Mild group	Moderate group	Severe group	P1	P2	P3
Number (patients)	25	26	22			
Sex (male/female)	6/19	8/18	5/17			
Age (years)	35.07 ± 7.60	36.51 ± 11.05	35.98 ± 10.89	0.300	0.069	0.291
LogMAR BCVA	0.024 ± 0.043	0.016 ± 0.039	0.013 ± 0.031	0.392	0.290	0.720
LogMAR DVA (40 dps)	0.088 ± 0.061	0.101 ± 0.057	0.155 ± 0.089	0.401	<0.001	0.001
LogMAR DVA (80 dps)	0.169 ± 0.063	0.187 ± 0.066	0.236 ± 0.095	0.292	0.001	0.004

Mild group: mild MG dropout (> 50% of the total area), Moderate group: moderate MG dropout (25–50% of the total area), Severe group: severe MG dropout (<25% of the total area). DVA, dynamic visual acuity; dps, degree per second; BCVA, best-corrected visual acuity. P1: Mild group vs. Moderate group; P2: Mild group vs. Severe group; P3: Moderate group vs. Severe group. *P*-values less than 0.05 were considered statistically significant.

control subjects (Ridder et al., 2013; Karakus et al., 2018b), and the reading rate decreased as the DED severity increased (Ridder et al., 2013; Ousler et al., 2015). The previous visual function evaluation on dry eye mainly focused on static vision assessment, including contrast sensitivity (CS), surface regularity index (SRI), surface asymmetry index (SAI), higher order aberrations (HOAs), objective scattering index (OSI), and potential visual acuity (PVA) (Huang et al., 2002; Goto et al., 2006; Puell et al., 2006; Ridder et al., 2009, 2013; Ousler et al., 2015; Benitez-Del-Castillo et al., 2017; Koh, 2018; Ma et al., 2020; Gao et al., 2021). These studies showed that tear film changes in DED patients might lead to irregularities on the corneal surfaces (Goto et al., 2006; Benitez-Del-Castillo et al., 2017; Koh et al., 2018; Ma et al., 2020) causing glare disability, irregular astigmatism, worse SRI, SAI, HOAs, PVA, and CS for the dry eye patients (Huang et al., 2002; Goto et al., 2006; Ridder et al., 2009). Irregular astigmatism, OSI and HOAs were correlated with the severity of DED (Goto et al., 2006; Benitez-Del-Castillo et al., 2017; Koh, 2018; Ma et al., 2020; Shimizu et al., 2020). And these optical quality indices in DED patients could improve after treatment (Huang et al., 2002; Qiu et al., 2012; Gao et al., 2021). However, considering the limitations of these static vision assessments, which could not sufficiently reflect life scenario visual function and these changes may be too subtle in mild dry eyes (Huang et al., 2002), the present study included dynamic vision assessment. Dynamic vision plays an important role in performing daily tasks (Ren et al., 2020) such as driving, speed reading, and identifying high-speed table tennis, and badminton. Deschamps et al. (2013) evaluated the impact of DED on visual performance while driving and pointed out that DED patients need more response time to identify target than healthy subjects and were more often missed targets appearing at a crossroad entrance. DVA represents visual acuity identifying the moving objects, and its special signaling pathway and influencing factors differ from static visual acuity (Rokszin et al., 2010; Skottun, 2016). Different eye movements were required for moving object detection. When we look at moving objects at a velocity of up to 50 degrees per second, smooth pursuits could stabilize it close to the fovea, but for higher velocity, saccades were needed to catch up with the gaze lag (de Brouwer et al., 2002; Palidis et al., 2017; Michel et al., 2020). Thus, we chose two velocities for the test, 40 and 80 degrees per second (dps) to better assess DVA for DED patients.

In the present study, we found that DVA was correlated with MG dropout and function, palpebral margin abnormalities, CFS and OSDI. There was a significant difference in DVA among

TABLE 4 Comparison of DVA between CFS and non-CFS groups.

	Non-CFS group	CFS group	<i>P</i>
Number (patients)	40	33	
Sex (male/female)	11/29	8/25	
Age (Years)	36.361 ± 10.332	37.317 ± 9.722	0.084
LogMAR BCVA	0.012 ± 0.022	0.008 ± 0.024	0.168
LogMAR DVA (40 dps)	0.089 ± 0.072	0.138 ± 0.069	<0.001
LogMAR DVA (80 dps)	0.174 ± 0.079	0.223 ± 0.070	<0.001

BCVA, best-corrected visual acuity; CFS, corneal fluorescein staining; CFS group: CFS scores > 0 for any eye; dps: degree per second; DVA, dynamic visual acuity; Non-CFS group: CFS scores were 0 for both eyes. *P*-values less than 0.05 were considered statistically significant.

patients with different degrees of meibomian gland dropout in the upper eyelid. The patients with severe MG dropout showed worse DVA than mild or moderate dropout in 40 and 80 dps. And DVA is correlated with the expressibility and secretion quality of MG. These results together indicated that meibomian gland morphology and function affect DVA. The obstruction of the meibomian gland and poor quality of secretion meibum contributes to the instability of the tear film and the rough optical surface (Mudgil and Millar, 2011), which might lead to a more prominent interface optical scatter (larger OSI). The obvious optical scatter of tear film might contribute to the greater artifact for moving object imaging, bringing worse DVA. In addition, the amount of meibum is significantly reduced due to severe dropout of the meibomian gland (Eom et al., 2013; Kim et al., 2018), and it also contributes to the instability of the tear film.

Similarly, corneal fluorescein staining (CFS) also posed a positive correlation with DVA. Past studies confirmed that CFS is related to visual quality (Kaido et al., 2011; Leonardi et al., 2019). Corneal staining shows corneal epithelial damage (Kaido et al., 2011), and the optical surface of the cornea becomes irregular, which might contribute to greater artifacts, and more inconsistent imaging when observing moving objects. In our research, eyelid margin abnormalities also showed relevance to DVA. The normal structural eyelid margin plays an important role in the distribution and formation of the normal tear film (Bai et al., 2021). The existence of eyelid margin abnormalities indicates more severe DED, the greater probability of tear film instability and higher CFS scores. Thus, the imaging of moving optotypes might be affected during the DVA test due to the rough optical surface.

Ocular Surface Disease Index sums up the subjective symptoms of DED and could reflect the severity of dry eye (Belmonte et al., 2017). The present study proved that worse DVA is associated with worse OSDI. The worse OSDI score, indicating uncomfortable DED-related visual experience, might cause shorter fixation time and more frequent blinking. An excellent DVA is closely related to reasonable eye tracking on moving objects. Problems such as non-persistence vision would affect the tracking of moving objects, including smooth pursuit and saccade, and reduce the prediction of moving object trajectory, leading to poor DVA.

The low TMH, indicating the quantitative deficiency of tear film, was associated with functional visual acuity and optical quality reduction (Goto et al., 2003; Kaido et al., 2006, 2011; Kaido, 2018). But no correlation was found between DVA and TMH in the present study. The quantity deficiency might not affect the stability and consistency of the tear film, which affects DVA. Short TBUT contributes to impaired visual function (Kaido, 2018; Koh et al., 2018) but no correlation was found between DVA and TBUT in our study. The individual data demonstrates that the shortest TBUT of the enrolled subjects was 2 s. It exceeded the time of the visual target moving from left to right. Therefore, the tear film might not break during the visual target movement.

Dynamic visual acuity could be recommended for evaluation for DED patients beyond conventional visual examinations and the evaluation of optical quality. The present research demonstrated that DVA is an excellent bridge linking visual function and dry eye symptoms and signs. Additionally, DVA is a sensitive indicator to detect the severity changes of dry eye. Severe MG dropout patients might be incompetent in some daily tasks for their poor DVA, including sports and driving. It is also helpful to determine the therapeutic effects of DED treatments, assessing the ability to return to normal visual function and performance of daily tasks. For the tasks with high demand for DVA, more attention should be paid to the DED. The DED in athletes might affect their sports level and the DED of drivers or pilot might affect their driving safety. The dynamic vision-based test could facilitate the comprehensive DED evaluation in these occupations. With further improvement and popularization, occupational-related DVA thresholds would establish and guide the DED treatment.

Certain limitations exist in the present study. The sample size is relatively small, and the research lacks a control group without DED for comparison. In addition, we did not classify DED types. Then, we only included subjects aged 18–45 in this study, whose disease severity might be mild. In the future, we will expand the age range of the subjects. Furthermore, the effect of dry eye treatment on DVA requires further exploration. Finally, the DVA test only involved one test distance and a single horizontal moving pattern. Improvements are planned to include different motor patterns for assessment. Future studies will include a larger sample, parameters for real-life tasks in more detail, and assessment before and after DED treatment.

5. Conclusion

In conclusion, binocular DVA is significantly associated with DED symptoms and signs. The DED patients with CFS and

severe MG dropout and dysfunction have worse DVA. The present research provides the basis for the DVA test in DED evaluation. With further improvement, the DVA test might guide the DED assessment and treatment, especially in patients with high demand for dynamic vision.

Data availability statement

The datasets generated and analyzed during the current study are not publicly available but are available from the corresponding author on reasonable request.

Ethics statement

The studies involving human participants were reviewed and approved by the Human Research and Ethics Committee of Peking University Third Hospital. The patients/participants provided their written informed consent to participate in this study.

Author contributions

XR: research design, data acquisition, and manuscript preparation. YW: research design, data analysis, and manuscript preparation. TW: data acquisition and data analysis. DJ: data acquisition and manuscript preparation. XL: research design. All authors read and approved the final version of this manuscript.

Funding

This work was supported by National Natural Science Foundation of China (82201243).

Conflict of interest

The authors declare that the research was conducted in the absence of any commercial or financial relationships that could be construed as a potential conflict of interest.

Publisher's note

All claims expressed in this article are solely those of the authors and do not necessarily represent those of their affiliated organizations, or those of the publisher, the editors and the reviewers. Any product that may be evaluated in this article, or claim that may be made by its manufacturer, is not guaranteed or endorsed by the publisher.

References

- Bai, Y., Ngo, W., Khanal, S., Nichols, K. K., and Nichols, J. J. (2021). Human precorneal tear film and lipid layer dynamics in meibomian gland dysfunction. *Ocul. Surf.* 21, 250–256. doi: 10.1016/j.jtos.2021.03.006
- Belmonte, C., Nichols, J. J., Cox, S. M., Brock, J. A., Begley, C. G., Bereiter, D. A., et al. (2017). TFOS DEWS II pain and sensation report. *Ocul. Surf.* 15, 404–437. doi: 10.1016/j.jtos.2017.05.002
- Benitez-Del-Castillo, J., Labetoulle, M., Baudouin, C., Rolando, M., Akova, Y. A., Aragona, P., et al. (2017). Visual acuity and quality of life in dry eye disease: Proceedings of the OCEAN group meeting. *Ocul. Surf.* 15, 169–178. doi: 10.1016/j.jtos.2016.11.003
- Bron, A. J., de Paiva, C. S., Chauhan, S. K., Bonini, S., Gabison, E. E., Jain, S., et al. (2017). TFOS DEWS II pathophysiology report. *Ocul. Surf.* 15, 438–510. doi: 10.1016/j.jtos.2017.05.011
- Craig, J. P., Nichols, K. K., Akpek, E. K., Caffery, B., Dua, H. S., Joo, C. K., et al. (2017). TFOS DEWS II definition and classification report. *Ocul. Surf.* 15, 276–283. doi: 10.1016/j.jtos.2017.05.008
- de Brouwer, S., Yuxsel, D., Blohm, G., Missal, M., and Lefevre, P. (2002). What triggers catch-up saccades during visual tracking? *J. Neurophysiol.* 87, 1646–1650. doi: 10.1152/jn.00432.2001
- Deschamps, N., Ricaud, X., Rabut, G., Labbe, A., Baudouin, C., and Denoyer, A. (2013). The impact of dry eye disease on visual performance while driving. *Am. J. Ophthalmol.* 156, 184–189.e3. doi: 10.1016/j.ajo.2013.02.019
- Eom, Y., Lee, J. S., Kang, S. Y., Kim, H. M., and Song, J. S. (2013). Correlation between quantitative measurements of tear film lipid layer thickness and meibomian gland loss in patients with obstructive meibomian gland dysfunction and normal controls. *Am. J. Ophthalmol.* 155, 1104–1110.e2. doi: 10.1016/j.ajo.2013.01.008
- Gao, Y., Liu, R., Liu, Y., Ma, B., Yang, T., Hu, C., et al. (2021). Optical quality in patients with dry eye before and after treatment. *Clin. Exp. Optom.* 104, 101–106. doi: 10.1111/coo.13111
- Goto, E., Ishida, R., Kaido, M., Dogru, M., Matsumoto, Y., Kojima, T., et al. (2006). Optical aberrations and visual disturbances associated with dry eye. *Ocul. Surf.* 4, 207–213. doi: 10.1016/S1542-0124(12)70167-2
- Goto, E., Yagi, Y., Kaido, M., Matsumoto, Y., Konomi, K., and Tsubota, K. (2003). Improved functional visual acuity after punctal occlusion in dry eye patients. *Am. J. Ophthalmol.* 135, 704–705. doi: 10.1016/S0002-9394(02)02147-5
- Huang, F. C., Tseng, S. H., Shih, M. H., and Chen, F. K. (2002). Effect of artificial tears on corneal surface regularity, contrast sensitivity, and glare disability in dry eyes. *Ophthalmology* 109, 1934–1940. doi: 10.1016/S0161-6420(02)01136-3
- Kaido, M. (2018). Functional visual acuity. *Invest. Ophthalmol. Vis. Sci.* 59, DES29–DES35. doi: 10.1167/iops.17-23721
- Kaido, M., Dogru, M., Yamada, M., Sotozono, C., Kinoshita, S., Shimazaki, J., et al. (2006). Functional visual acuity in Stevens-Johnson syndrome. *Am. J. Ophthalmol.* 142, 917–922. doi: 10.1016/j.ajo.2006.07.055
- Kaido, M., Matsumoto, Y., Shigeno, Y., Ishida, R., Dogru, M., and Tsubota, K. (2011). Corneal fluorescein staining correlates with visual function in dry eye patients. *Invest. Ophthalmol. Vis. Sci.* 52, 9516–9522. doi: 10.1167/iops.11-8412
- Karakus, S., Agrawal, D., Hindman, H. B., Henrich, C., Ramulu, P. Y., and Akpek, E. K. (2018a). Effects of prolonged reading on dry eye. *Ophthalmology* 125, 1500–1505. doi: 10.1016/j.optha.2018.03.039
- Karakus, S., Mathews, P. M., Agrawal, D., Henrich, C., Ramulu, P. Y., and Akpek, E. K. (2018b). Impact of dry eye on prolonged reading. *Optom. Vis. Sci.* 95, 1105–1113. doi: 10.1097/OPX.0000000000001303
- Kim, H. M., Eom, Y., and Song, J. S. (2018). The relationship between morphology and function of the meibomian glands. *Eye Contact Lens* 44, 1–5. doi: 10.1097/ICL.0000000000000336
- Koh, S. (2018). Irregular astigmatism and higher-order aberrations in eyes with dry eye disease. *Invest. Ophthalmol. Vis. Sci.* 59, DES36–DES40. doi: 10.1167/iops.17-23500
- Koh, S., Tung, C. I., Inoue, Y., and Jhanji, V. (2018). Effects of tear film dynamics on quality of vision. *Br. J. Ophthalmol.* 102, 1615–1620. doi: 10.1136/bjophthalmol-2018-312333
- Leonardi, A., Doan, S., Amrane, M., Ismail, D., Montero, J., Nemeth, J., et al. (2019). Controlled trial of cyclosporine a cationic emulsion in pediatric vernal keratoconjunctivitis: The VEKTIS study. *Ophthalmology* 126, 671–681. doi: 10.1016/j.optha.2018.12.027
- Ma, J., Wei, S., Jiang, X., Chou, Y., Wang, Y., Hao, R., et al. (2020). Evaluation of objective visual quality in dry eye disease and corneal nerve changes. *Int. Ophthalmol.* 40, 2995–3004. doi: 10.1007/s10792-020-01483-5
- Mathews, P. M., Ramulu, P. Y., Swenor, B. S., Utine, C. A., Rubin, G. S., and Akpek, E. K. (2017). Functional impairment of reading in patients with dry eye. *Br. J. Ophthalmol.* 101, 481–486. doi: 10.1136/bjophthalmol-2015-308237
- Michel, L., Laurent, T., and Alain, T. (2020). Rehabilitation of dynamic visual acuity in patients with unilateral vestibular hypofunction: Earlier is better. *Eur. Arch. Otorhinolaryngol.* 277, 103–113. doi: 10.1007/s00405-019-05690-4
- Mudgil, P., and Millar, T. J. (2011). Surfactant properties of human meibomian lipids. *Invest. Ophthalmol. Vis. Sci.* 52, 1661–1670. doi: 10.1167/iops.10-5445
- Nakatsuka, M., Ueda, T., Nawa, Y., Yukawa, E., Hara, T., and Hara, Y. (2006). Effect of static visual acuity on dynamic visual acuity: A pilot study. *Percept. Mot. Skills* 103, 160–164. doi: 10.2466/pms.103.1.160-164
- Nichols, K. K., Bacharach, J., Holland, E., Kislan, T., Shettle, L., Lunacsek, O., et al. (2016). Impact of dry eye disease on work productivity, and patients' Satisfaction with over-the-counter dry eye treatments. *Invest. Ophthalmol. Vis. Sci.* 57, 2975–2982. doi: 10.1167/iops.16-19419
- Ousler, G. R., Rodriguez, J. D., Smith, L. M., Lane, K. J., Heckley, C., Angjeli, E., et al. (2015). Optimizing reading tests for dry eye disease. *Cornea* 34, 917–921. doi: 10.1097/ICO.0000000000000490
- Palidis, D. J., Wyder-Hodge, P. A., Fookan, J., and Sperling, M. (2017). Distinct eye movement patterns enhance dynamic visual acuity. *PLoS One* 12:e0172061. doi: 10.1371/journal.pone.0172061
- Puell, M. C., Benitez-del-Castillo, J. M., Martinez-de-la-Casa, J., Sanchez-Ramos, C., Vico, E., Perez-Carrasco, M. J., et al. (2006). Contrast sensitivity and disability glare in patients with dry eye. *Acta Ophthalmol. Scand.* 84, 527–531. doi: 10.1111/j.1600-0420.2006.00671.x
- Qiu, W., Liu, Z., Zhang, Z., Ao, M., Li, X., and Wang, W. (2012). Punctal plugs versus artificial tears for treating dry eye: A comparative observation of their effects on contrast sensitivity. *J. Ocul. Biol. Dis. Infor.* 5, 19–24. doi: 10.1007/s12177-012-9094-x
- Ren, X., Wang, Y., Wang, D., Wu, B., Wu, L., Xu, Y., et al. (2020). A novel standardized test system to evaluate dynamic visual acuity post trifocal or monofocal intraocular lens implantation: A multicenter study. *Eye (Lond)* 34, 2235–2241. doi: 10.1038/s41433-020-0780-9
- Ridder, W. R., LaMotte, J., Hall, J. J., Sinn, R., Nguyen, A. L., and Abufarje, L. (2009). Contrast sensitivity and tear layer aberrometry in dry eye patients. *Optom. Vis. Sci.* 86, E1059–E1068. doi: 10.1097/OPX.0b013e3181b599bf
- Ridder, W. R., Zhang, Y., and Huang, J. F. (2013). Evaluation of reading speed and contrast sensitivity in dry eye disease. *Optom. Vis. Sci.* 90, 37–44. doi: 10.1097/OPX.0b013e3182780dbb
- Rokszin, A., Markus, Z., Braunitzer, G., Berenyi, A., Benedek, G., and Nagy, A. (2010). Visual pathways serving motion detection in the mammalian brain. *Sensors (Basel)* 10, 3218–3242. doi: 10.3390/s100403218
- Shimizu, E., Aketa, N., Yazu, H., Uchino, M., Kamoi, M., Sato, Y., et al. (2020). Corneal higher-order aberrations in eyes with chronic ocular graft-versus-host disease. *Ocul. Surf.* 18, 98–107. doi: 10.1016/j.jtos.2019.10.005
- Skottun, B. C. (2016). A few words on differentiating magno- and parvocellular contributions to vision on the basis of temporal frequency. *Neurosci. Biobehav. Rev.* 71, 756–760. doi: 10.1016/j.neubiorev.2016.10.016
- Stapleton, F., Alves, M., Bunya, V. Y., Jalbert, I., Lekhanont, K., Malet, F., et al. (2017). TFOS DEWS II epidemiology report. *Ocul. Surf.* 15, 334–365. doi: 10.1016/j.jtos.2017.05.003
- Tong, L., Waduthantri, S., Wong, T. Y., Saw, S. M., Wang, J. J., Rosman, M., et al. (2010). Impact of symptomatic dry eye on vision-related daily activities: The Singapore Malay eye study. *Eye (Lond)* 24, 1486–1491. doi: 10.1038/eye.2010.67
- Uchino, M., Uchino, Y., Dogru, M., Kawashima, M., Yokoi, N., Komuro, A., et al. (2014). Dry eye disease and work productivity loss in visual display users: The Osaka study. *Am. J. Ophthalmol.* 157, 294–300. doi: 10.1016/j.ajo.2013.10.014
- Wang, Y., Guo, Y., Wei, S., Yuan, Y., Wu, T., Zhang, Y., et al. (2022b). Binocular dynamic visual acuity in eyeglass-corrected myopic patients. *J. Vis. Exp.* 181. doi: 10.3791/63864
- Wang, Y., Guo, Y., Wei, S., Wu, T., Yuan, Y., Zhang, Y., et al. (2022a). Dynamic visual acuity after small incision lenticule extraction for myopia patients. *Percept. Mot. Skills* 315125221133434. doi: 10.1177/00315125221133434 [Epub ahead of print].
- Wolffsohn, J. S., Arita, R., Chalmers, R., Djalilian, A., Dogru, M., Dumbleton, K., et al. (2017). TFOS DEWS II diagnostic methodology report. *Ocul. Surf.* 15, 539–574. doi: 10.1016/j.jtos.2017.05.001
- Wu, T. Y., Wang, Y. X., and Li, X. M. (2021). Applications of dynamic visual acuity test in clinical ophthalmology. *Int. J. Ophthalmol.* 14, 1771–1778. doi: 10.18240/ijo.2021.11.18



OPEN ACCESS

EDITED BY

Jiawei Zhou,
Wenzhou Medical University, China

REVIEWED BY

Rong Song,
Sun Yat-sen University, China
Yuexin Wang,
Peking University Third Hospital, China

*CORRESPONDENCE

Xiaoyu Liu
✉ x.y.liu@buaa.edu.cn
Yubo Fan
✉ yubofan@buaa.edu.cn

SPECIALTY SECTION

This article was submitted to
Visual Neuroscience,
a section of the journal
Frontiers in Neuroscience

RECEIVED 12 January 2023

ACCEPTED 13 March 2023

PUBLISHED 27 March 2023

CITATION

Tang Z, Liu X, Huo H, Tang M, Qiao X, Chen D,
Dong Y, Fan L, Wang J, Du X, Guo J, Tian S
and Fan Y (2023) Eye movement
characteristics in a mental rotation task
presented in virtual reality.
Front. Neurosci. 17:1143006.
doi: 10.3389/fnins.2023.1143006

COPYRIGHT

© 2023 Tang, Liu, Huo, Tang, Qiao, Chen,
Dong, Fan, Wang, Du, Guo, Tian and Fan. This
is an open-access article distributed under the
terms of the [Creative Commons Attribution
License \(CC BY\)](#). The use, distribution or
reproduction in other forums is permitted,
provided the original author(s) and the
copyright owner(s) are credited and that the
original publication in this journal is cited, in
accordance with accepted academic practice.
No use, distribution or reproduction is
permitted which does not comply with
these terms.

Eye movement characteristics in a mental rotation task presented in virtual reality

Zhili Tang¹, Xiaoyu Liu^{1,2*}, Hongqiang Huo¹, Min Tang¹,
Xiaofeng Qiao¹, Duo Chen¹, Ying Dong¹, Linyuan Fan¹,
Jinghui Wang¹, Xin Du¹, Jieyi Guo¹, Shan Tian¹ and Yubo Fan^{1,2*}

¹Key Laboratory for Biomechanics and Mechanobiology of Ministry of Education, Beijing Advanced Innovation Center for Biomedical Engineering, School of Biological Science and Medical Engineering and School of Engineering Medicine, Beihang University, Beijing, China, ²State Key Laboratory of Virtual Reality Technology and Systems, Beihang University, Beijing, China

Introduction: Eye-tracking technology provides a reliable and cost-effective approach to characterize mental representation according to specific patterns. Mental rotation tasks, referring to the mental representation and transformation of visual information, have been widely used to examine visuospatial ability. In these tasks, participants visually perceive three-dimensional (3D) objects and mentally rotate them until they identify whether the paired objects are identical or mirrored. In most studies, 3D objects are presented using two-dimensional (2D) images on a computer screen. Currently, visual neuroscience tends to investigate visual behavior responding to naturalistic stimuli rather than image stimuli. Virtual reality (VR) is an emerging technology used to provide naturalistic stimuli, allowing the investigation of behavioral features in an immersive environment similar to the real world. However, mental rotation tasks using 3D objects in immersive VR have been rarely reported.

Methods: Here, we designed a VR mental rotation task using 3D stimuli presented in a head-mounted display (HMD). An eye tracker incorporated into the HMD was used to examine eye movement characteristics during the task synchronically. The stimuli were virtual paired objects oriented at specific angular disparities (0, 60, 120, and 180°). We recruited thirty-three participants who were required to determine whether the paired 3D objects were identical or mirrored.

Results: Behavioral results demonstrated that the response times when comparing mirrored objects were longer than identical objects. Eye-movement results showed that the percent fixation time, the number of within-object fixations, and the number of saccades for the mirrored objects were significantly lower than that for the identical objects, providing further explanations for the behavioral results.

Discussion: In the present work, we examined behavioral and eye movement characteristics during a VR mental rotation task using 3D stimuli. Significant differences were observed in response times and eye movement metrics between identical and mirrored objects. The eye movement data provided further explanation for the behavioral results in the VR mental rotation task.

KEYWORDS

eye movements, virtual reality, naturalistic stimuli, mental rotation, three-dimensional stimuli, visual perception

1. Introduction

Mental rotation is the ability to mentally represent and rotate two-dimensional (2D) images or three-dimensional (3D) objects (Shepard and Metzler, 1971) and has been widely used to examine visuospatial ability (Pletzer et al., 2019; Ito et al., 2022). In classical mental rotation tasks, participants visually perceive 3D objects and mentally rotate them until the objects are identified. It is generally accepted that the mental rotation process includes five cognitive stages (Desrocher et al., 1995): (i) processing of visual information and creating mental images of the presented objects (imagining and evaluating the presented objects from different angles); (ii) mentally rotating the objects or images; (iii) comparing the presented objects; (iv) determining whether the presented objects are identical; (v) making a decision (indicated by a button). Response times and accuracy rates are widely employed in examining a mental rotation effect and mental rotation performance (Shepard and Metzler, 1971; Berneiser et al., 2018), but these behavioral indices are not sufficient to fully understand the related complex cognitive processes. Recent studies have provided evidence that eye movement characteristics are promising for examining these mental processes (Xue et al., 2017; Toth and Campbell, 2019; Tiwari et al., 2021).

Eye-tracking technology is an effective tool for examining cognitive processes required for complex cognitive tasks (Lancry-Dayan et al., 2023). Eye movements captured by eye tracking systems can provide comprehensive information on mental processes in mental rotation tasks and have been effective in revealing brain activity (Toth and Campbell, 2019). It has been suggested that eye movement parameters could characterize mental representation according to specific patterns (Nazareth et al., 2019). Eye movement metrics, including fixations and saccades, have been used in studies using mental rotation tasks (Suzuki et al., 2018). Identifying fixations allows researchers to examine objects of interest (Mast and Kosslyn, 2002); fixations are mainly responsible for the acquisition of visual information in mental rotation tasks (Yarbus, 1967). A recent study indicated that fixation metrics could illustrate mental rotation strategies, and that fixation patterns were related to mental rotation performance (Nazareth et al., 2019). Saccades are the rapid eye movements between fixations (Kowler et al., 1995). Saccades serve to rapidly shift the fovea to a new target to integrate visual information from fixations. The integration allows a brain to compare the visual information obtained from fixations with the remembered image of the object (Ibbotson and Kregelberg, 2011). In addition, eye tracking data can be used to characterize different mental rotation strategies. Holistic and piecemeal strategies have been extensively investigated in previous studies on mental rotation (Khooshabeh et al., 2013; Hsing et al., 2023). The holistic strategy refers to mentally rotating one of two 3D objects as a whole and encoding the spatial information of the object. For instance, when comparing two objects, one object is holistically rotated along a vertical axis for comparison with the other object. The piecemeal strategy refers to segmenting an object into several pieces and encoding only part of its spatial information. For instance, one of the two objects would be segmented into several independent pieces, and participants may mentally rotate one piece of both objects and see if the two pieces match. Strategy ratio was commonly used to reflect which strategies are performed

during mental rotation (Khooshabeh and Hegarty, 2010). The strategy ratio refers to the ratio of the number of fixations within an object to the number of saccades between the two objects. In a holistic strategy, the ratio would be 1; in a piecemeal strategy, the ratio would be greater than one. Although previous studies have provided insights into eye movement characteristics in mental rotation tasks, these findings have mainly used 2D images presented on computer screens (Xue et al., 2017; Campbell et al., 2018). Previously, the use of visual stimuli has relied heavily on simplified image stimuli (Snow and Culham, 2021), which are distinctly different from naturalistic stimuli.

Recently, visual neuroscience studies have focused on visual behavior in response to naturalistic stimuli rather than simplified images (Haxby et al., 2020; Jaaskelainen et al., 2021; Musz et al., 2022). Visual behavior and brain activity evoked by planar images are different from those evoked by natural 3D objects (Marini et al., 2019; Chiquet et al., 2020). Natural 3D objects are rich in depth cues and visual input from the surrounding environment (e.g., edges) (Chiquet et al., 2020). For example, a recent study showed that 3D objects triggered more stronger brain responses than 2D images do (Marini et al., 2019; Tang et al., 2022).

Virtual Reality (VR) is an emerging technology used to provide naturalistic stimuli, allowing us to understand behavioral characteristics in an immersive environment similar to real world (Hofmann et al., 2021). This technology serves to fill the gap between traditional presentations based on 2D computer screen and naturalistic visual presentations close to real world (Wenk et al., 2022). Virtual environments can simulate real-world visual inputs (Robertson et al., 1993; Minderer and Harvey, 2016), allowing more naturalistic 3D objects with depth cues (El Jamiy and Marsh, 2019). Comparing with the mental rotation tasks using 2D images, the VR version of mental rotation task using 3D objects provides new opportunities to quantify visuospatial ability in environments similar to the real world. For example, a recent work has shown the impact of virtual environments on mental rotation performance. They assessed the differences in mental rotation ability based on dimensionality and the complexity of virtual environments, which provided new insights into the impact of stereo 3D objects on mental rotation performance (Lochhead et al., 2022). Their results suggested that the performance advantage of 3D objects could be greater than that of conventional 2D mediums. In addition, the previous work of our lab demonstrated the behavioral performance and neural oscillations in the mental rotation task using 2D images and using stereoscopic 3D objects (Tang et al., 2022). These studies inspired some expanded studies related to the VR version of mental rotation task, such as exploration of eye movement characteristics. Eye-tracking technology was incorporated into a head-mounted display (HMD), allowing to provide a new opportunity to understand human visual behavior in VR (Clay et al., 2019; Chiquet et al., 2020). Eye movement characteristics based on 3D objects help to understand visual behavior in a natural context close to real world (Chiquet et al., 2020). However, the eye movement characteristics in mental rotation tasks using naturalistic 3D objects with depth cues have been rarely reported.

Here, we designed a VR mental rotation task using 3D stimuli presented in a HMD with an eye tracker to examine the eye movements during the task synchronically. We first used behavioral performance to validate a mental rotation effect presented in

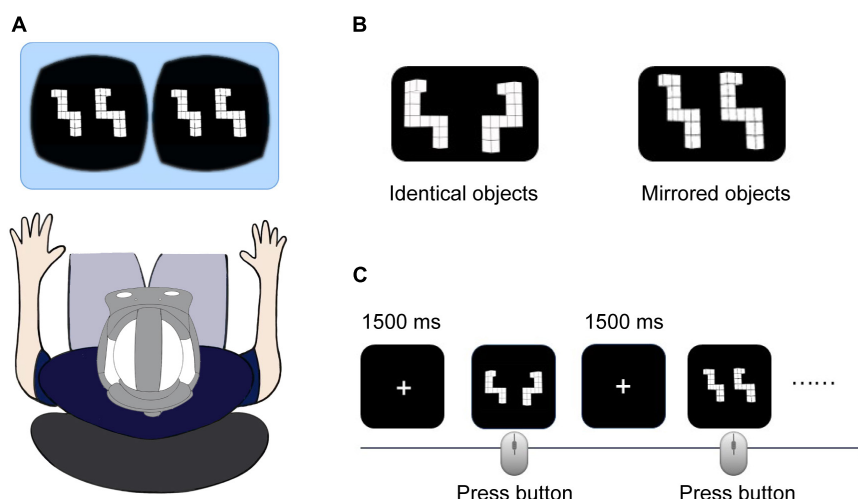


FIGURE 1

(A) Rendered 3D visual stimuli presented by a head-mounted display (HMD). (B) Sample of three-dimensional (3D) identical and mirrored stimuli. (C) Schematic diagram of the mental rotation task. The participants were asked to judge whether the paired objects were identical or mirrored and respond by pressing a mouse button (left: identical and right: mirrored) as quickly and accurately as possible.

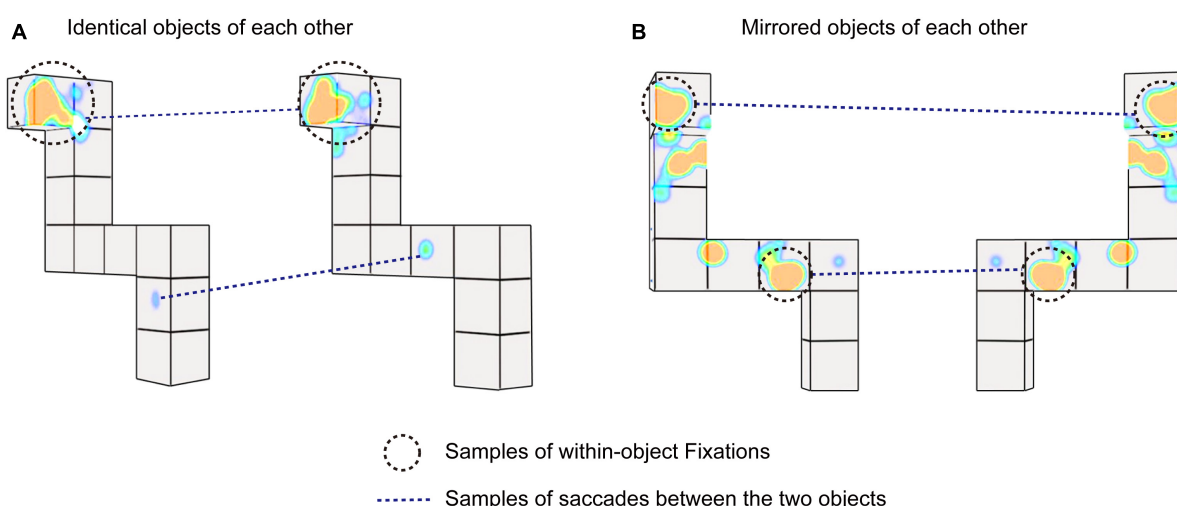


FIGURE 2

Examples of eye movements during the virtual reality (VR) mental rotation. (A) Sample three-dimensional (3D) identical stimuli. (B) Sample 3D mirrored stimuli. Black circles with dotted lines indicate samples of fixations within one object. Dotted lines indicate samples of saccades between the two objects.

a VR environment. Further, we highlighted the eye movement characteristics in this task. As we expected, our results indicated that the VR task also evoke a mental rotation effect, suggesting that the virtual task was effective and available. We analyzed the eye movement data to explain the behavioral results observed in the VR mental rotation task.

2. Materials and methods

2.1. Participants

Thirty-three participants were enrolled [17 females and 16 males; mean age = 28.59 years, standard deviation (SD) = 2.41].

All participants were recruited from university, were right-handed, and had normal or corrected-to normal vision. Written informed consent was obtained from all participants, and ethical approval was granted by the local ethical committee in accordance with the Declaration of Helsinki. Data from one participant was excluded because of low eye tracking data quality. Thus, data from 32 participants were included in the analysis.

2.2. Construction of 3D visual stimuli

We constructed 120 pairs of 3D objects based on original stimuli from the mental-rotation stimulus library (the 4th prototype) (Peters and Battista, 2008). The 3D paired objects were

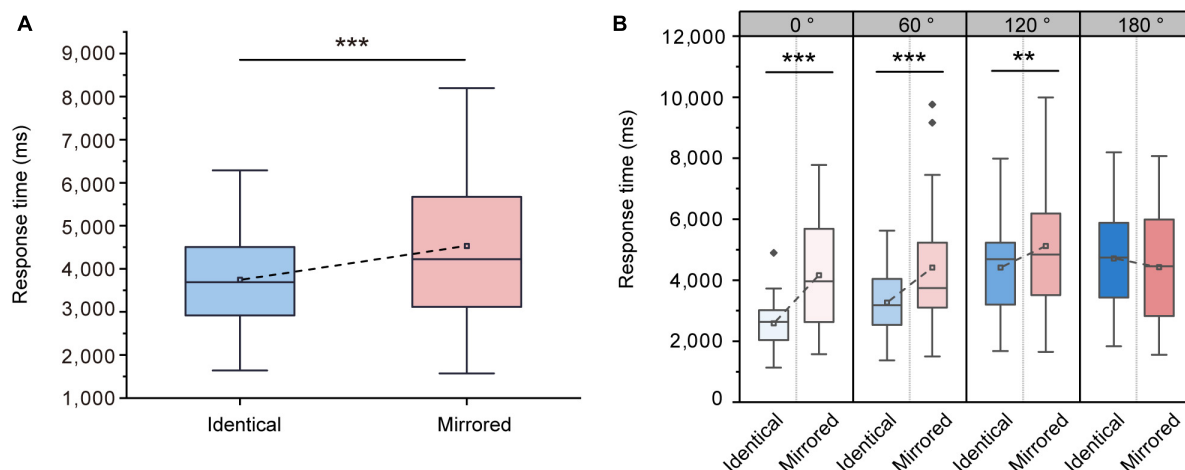


FIGURE 3

Changes in response times during the virtual reality (VR) mental rotation task. (A) Boxplots present response times for identical and mirrored objects. (B) Grouped boxplots present response times for identical and mirrored objects at 0, 60, 120 and 180°. The boxplots illustrate the first quartile, median, and third quartile and 1.5 times the interquartile range for both the upper and lower ends of the box. Black horizontal lines and asterisks denote significant differences (** $p < 0.01$, *** $p < 0.001$).

TABLE 1 Overview of response times (mean \pm standard error) for identical and mirrored objects at four angular disparities.

	Identical (ms)	Mirrored (ms)	Statistics
0°	2586.57 \pm 139.26	4166.23 \pm 328.10	$F(1, 31) = 40.307, p < 0.001, \eta_p^2 = 0.565$
60°	3268.35 \pm 186.32	4415.54 \pm 363.68	$F(1, 31) = 18.313, p < 0.001, \eta_p^2 = 0.371$
120°	4416.90 \pm 269.35	5122.03 \pm 378.53	$F(1, 31) = 8.235, p < 0.01, \eta_p^2 = 0.210$
180°	4714.69 \pm 313.53	4425.12 \pm 333.83	$F(1, 31) = 3.345, p = 0.077, \eta_p^2 = 0.097$

oriented at specific angular disparities (0, 60, 120, and 180°). For each pair, the two stimuli were identical or mirrored objects (Figure 1B). The 120 stimuli consisted of pairs of objects (identical, mirrored) in four angular disparities (0, 60, 120, and 180°).

Each 3D object was constructed using 3D Studio Max (Autodesk Inc., San Rafael, CA, USA) and stored as .obj files. We used the Unity game engine (Unity Software, Inc., San Francisco, CA, USA) to render the 3D objects. The rendered 3D visual stimuli were presented in a HMD (VIVE Pro Eye; HTC Corporation, Taipei, Taiwan) in randomized sequences [generated using MATLAB (The MathWorks, Natick, MA, USA)].

2.3. Experiment procedure

All participants completed the VR mental rotation task with 3D stimuli presented in the HMD in a quiet room (Figure 1A). Participants' information, including demographic data and VR experience, were collected before the experiment. During the experiment, participants were seated comfortably in a chair. The experimenter put a VR headset on the participants' head, and a five-point calibration of the eye tracker was performed before the experiment. We started the experiment when the calibrations were successful.

The VR mental rotation task consisted of 120 trials separated into two blocks of 60 trials. Short breaks of approximate 5 min were assigned between blocks to prevent participant fatigue. For each trial, a white fixation cross was displayed in the center of the HMD for 1,500 ms, followed by the presentation of a pair of 3D visual stimuli. The participants were asked to judge whether the paired objects were identical or mirrored and to respond by pressing a mouse button (left button for identical and right button for mirrored) as quickly and accurately as possible. The trial ended once the participants indicated their decision by pressing a button (Figure 1C).

2.4. Behavioral data acquisition and analysis

We used a customized script in the Unity 3D platform to record behavioral data including response times and accuracy rates. Stimulus onsets and trial completion times were marked by the script. The response time was defined as the duration from stimulus onset to trial completion. The accuracy rate was defined as the ratio of trials correctly judged out of the total number of trials.

2.5. Eye movement data acquisition and analysis

The eye tracker was incorporated into the HMD. Eye movement data were collected using an eye tracking SDK (SRanipal), with a maximum frequency of 120 Hz. A collider (i.e., a Unity object) was added to the surface of each 3D object presented in the HMD. The eye tracker in the HMD could capture all the possible gazes on the surface of the collider.

Eye movement events, including fixations and saccades, were identified to represent the eye movement characteristics in the VR

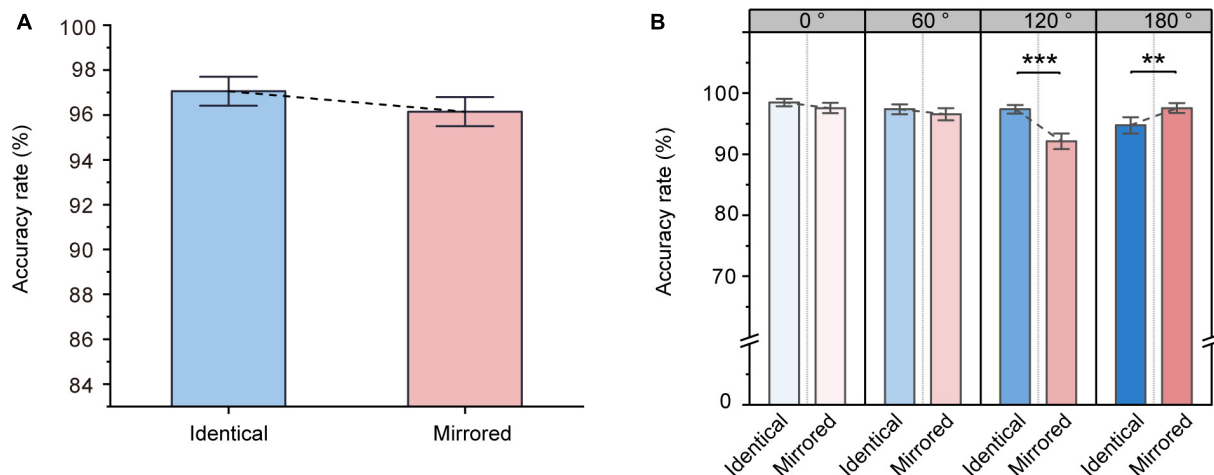


FIGURE 4

Changes in accuracy rates during the virtual reality (VR) mental rotation task. (A) Bar graphs present average accuracy rates for identical and mirrored objects. (B) Grouped bar graphs present accuracy rates for identical and mirrored objects at 0, 60, 120 and 180°. Error bars denote standard errors. Black lines and asterisks denote significant differences (** $p < 0.01$, *** $p < 0.001$).

mental rotation task. For each trial, we applied an identification by dispersion threshold (IDT) algorithm to group the collected gaze data into fixations (Salvucci and Goldberg, 2000; Llanes-Jurado et al., 2020). The end of each fixation was marked as a saccade event. The IDT algorithm requires two parameters: the dispersion threshold and the minimum fixation duration (Blignaut, 2009). This algorithm has been found to be the most similar to manual detection from human experts (Andersson et al., 2017). In the present study, fixations were marked using a 1° spatial dispersion threshold (Blignaut, 2009; Arthur et al., 2021) and a minimum duration of 60 ms (Komogortsev et al., 2010). To test the reliability of the results presented in our study, we used the eye movement metrics to compare the eye movement results obtained from the IDT algorithm with the three dispersion thresholds (1, 1.2, and 1.4°). Further analyses showed that the eye movement results obtained from the dispersion threshold of 1° were consistent with that from the dispersion thresholds of 1.2 and 1.4°, respectively (Supplementary Figures 1–4). Detailed statistical results are listed in Supplementary Tables 1–4. These results justify the dispersion threshold of 1° in our study.

Four eye movement metrics were used based on prior studies. The percent fixation time, the number of within-object fixations, the number of saccades, and the strategy ratio were used to quantify visual behavior (Khooshabeh and Hegarty, 2010; Khooshabeh et al., 2013; Lavoie et al., 2018; Nazareth et al., 2019; Hsing et al., 2023). Examples of the eye movement metrics (e.g., fixations and saccades) are presented in Figure 2. The eye movement metrics were defined as follows.

2.5.1. Percent fixation time

The amount of time fixated on the two objects during the mental rotation task divided by the total duration of the task (i.e., response time), multiplied by 100.

2.5.2. Number of within-object fixations

The number of fixations per second made on either of the two objects.

TABLE 2 Accuracy rates (mean \pm standard error) for identical and mirrored objects at four angular disparities.

	Identical (%)	Mirrored (%)	Statistics
0°	98.43 \pm 0.61	98.13 \pm 0.68	F (1, 31) = 0.129, p = 0.721, η_p^2 = 0.004
60°	97.29 \pm 0.84	96.46 \pm 1.04	F (1, 31) = 0.392, p = 0.536, η_p^2 = 0.012
120°	97.71 \pm 0.64	92.08 \pm 1.32	F (1, 31) = 29.160, p < 0.001, η_p^2 = 0.485
180°	94.79 \pm 1.36	97.91 \pm 0.75	F (1, 31) = 9.992, p < 0.01, η_p^2 = 0.242

2.5.3. Number of saccades

The number of saccades that a participant made from one 3D object to another within 1 s.

2.5.4. Strategy ratio

The ratio of the number of fixations within an object to the number of saccades made between the two objects. The strategy ratio was used to reflect holistic or piecemeal strategies. A strategy ratio close to one indicates a holistic strategy, and a strategy ratio greater than one suggests a piecemeal strategy.

2.6. Statistical analysis

All statistical analyses were conducted using SPSS software (IBM Corp., Armonk, NY, USA). Two-way repeated-measures analysis of variance (ANOVA) was used to analyze behavioral metrics (response time and accuracy rate) and eye movement metrics (fixations and saccades). Stimulus Type (identical and mirrored) and Angular Disparity (0, 60, 120, and 180°) served as within-subject factors. Sphericity was examined using Mauchly's test of sphericity; if the assumption of sphericity had been violated, Greenhouse-Geisser correction were reported. Bonferroni correction was used to account for multiple comparisons. The effect size was evaluated using partial eta squared (η_p^2). All data are presented as mean \pm standard error of the mean (SE). The detailed

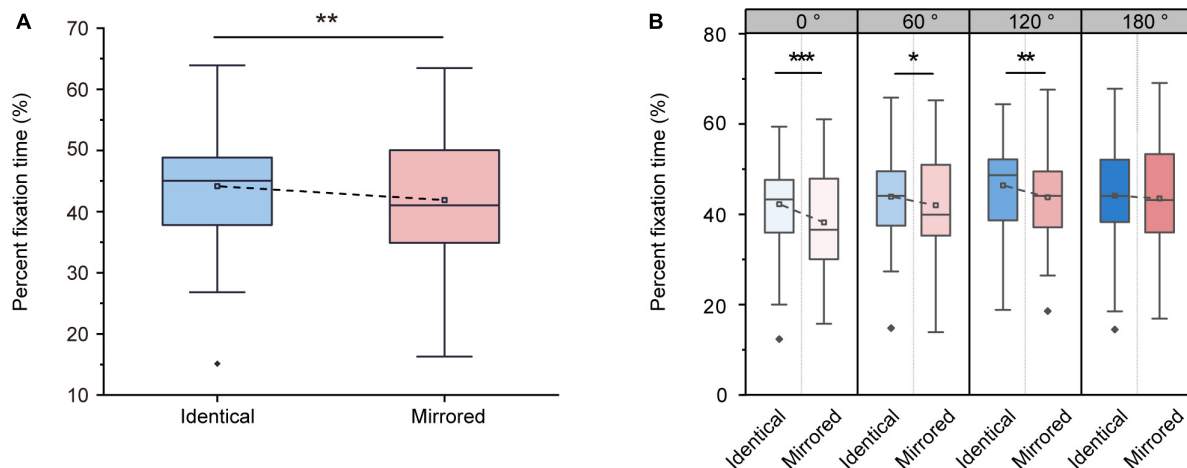


FIGURE 5

Changes in percent fixation time during the virtual reality (VR) mental rotation task. (A) Boxplots present percent fixation times for identical and mirrored objects. (B) Grouped boxplots present percent fixation times for identical and mirrored objects at 0, 60, 120 and 180°. The boxplots illustrate the first quartile, median, and third quartile and 1.5 times the interquartile range for both the upper and lower ends of the box. Black horizontal lines and asterisks denote significant differences (* $p < 0.05$, ** $p < 0.01$, *** $p < 0.001$).

TABLE 3 Overview of percent fixation time (mean \pm standard error) for identical and mirrored objects at four angular disparities.

	Identical (%)	Mirrored (%)	Statistics
0°	42.24 \pm 1.87	38.20 \pm 2.24	$F(1, 31) = 11.919, p < 0.01, \eta_p^2 = 0.278$
60°	43.90 \pm 1.97	41.99 \pm 2.19	$F(1, 31) = 4.558, p < 0.05, \eta_p^2 = 0.128$
120°	46.39 \pm 1.86	43.78 \pm 1.99	$F(1, 31) = 9.134, p < 0.01, \eta_p^2 = 0.228$
180°	44.16 \pm 2.07	43.51 \pm 2.28	$F(1, 31) = 0.402, p = 0.531, \eta_p^2 = 0.013$

statistical results about ANOVA were listed in [Supplementary Table 5](#).

3. Results

3.1. Behavioral results

3.1.1. Response time

Response times were used to examine whether there is a mental rotation effect during the VR task. The ANOVA on the response times showed significant main effects of Stimulus Type [$F(1, 31) = 22.147, p < 0.001, \eta_p^2 = 0.417$] and Angular Disparity [$F(3, 93) = 39.530, p < 0.001, \eta_p^2 = 0.560$]. The significant main effect of Stimulus Type was caused by lower response times when presented with identical objects (3746.63 ± 207.94 ms, mean \pm SE) compared to mirrored objects (4532.23 ± 327.65 ms, mean \pm SE; [Figure 3A](#)). The interaction between Stimulus Type and Angular Disparity was also significant [$F(3, 93) = 17.854, p < 0.001, \eta_p^2 = 0.365$]. Pairwise comparisons revealed significant differences in response times between identical and mirrored objects at 0, 60 and 120° (all $p < 0.01$; [Table 1](#) and [Figure 3B](#)). There was no significant difference in response times between identical and mirrored objects at 180° ($p = 0.077$; [Table 1](#) and [Figure 3B](#)).

3.1.2. Accuracy rate

The ANOVA on the accuracy rates showed no significant main effect of Stimulus Type [$F(1, 31) = 2.519, p = 0.123, \eta_p^2 = 0.075$]. The accuracy rates for identical objects (97.05 ± 0.64 %, mean \pm SE) were not significantly higher than that for mirrored objects (96.14 ± 0.65 %, mean \pm SE; [Figure 4A](#)). There was a significant main effect of Angular Disparity [$F(3, 93) = 5.255, p = 0.002, \eta_p^2 = 0.145$] and a significant interaction between Angular Disparity and Stimulus Type [$F(3, 93) = 11.873, p < 0.001, \eta_p^2 = 0.277$]. The differences in different angular disparity between identical and mirrored objects were further revealed. Pairwise comparisons revealed significant differences in accuracy rates between identical and mirrored objects at 120 and 180° (all $p < 0.01$; [Table 2](#) and [Figure 4B](#)). There was no difference (all $p > 0.05$; [Table 2](#) and [Figure 4B](#)) in accuracy rates between identical and mirrored objects at 0 and 60°.

3.2. Eye movement results

3.2.1. Percent fixation time

The ANOVA on the percent fixation time revealed significant main effects of Stimulus Type [$F(1, 31) = 11.658, p = 0.002, \eta_p^2 = 0.273$] and Angular Disparity [$F(3, 93) = 14.334, p < 0.001, \eta_p^2 = 0.316$]. The significant main effect of Stimulus Type demonstrated that the percent fixation time was significantly higher for identical objects (44.18 ± 1.84 %, mean \pm SE) than for mirrored objects (41.87 ± 2.11 %, mean \pm SE; [Figure 5A](#)). Moreover, there was also a significant interaction between Angular Disparity and Stimulus Type [$F(3, 93) = 2.789, p = 0.045, \eta_p^2 = 0.083$]. Pairwise comparisons revealed significant differences between identical and mirrored objects at 0, 60 and 120° (all $p < 0.05$; [Table 3](#) and [Figure 5B](#)). There was no difference in the percent fixation time ($p = 0.531$; [Table 3](#) and [Figure 5B](#)) between identical and mirrored objects at 180°.

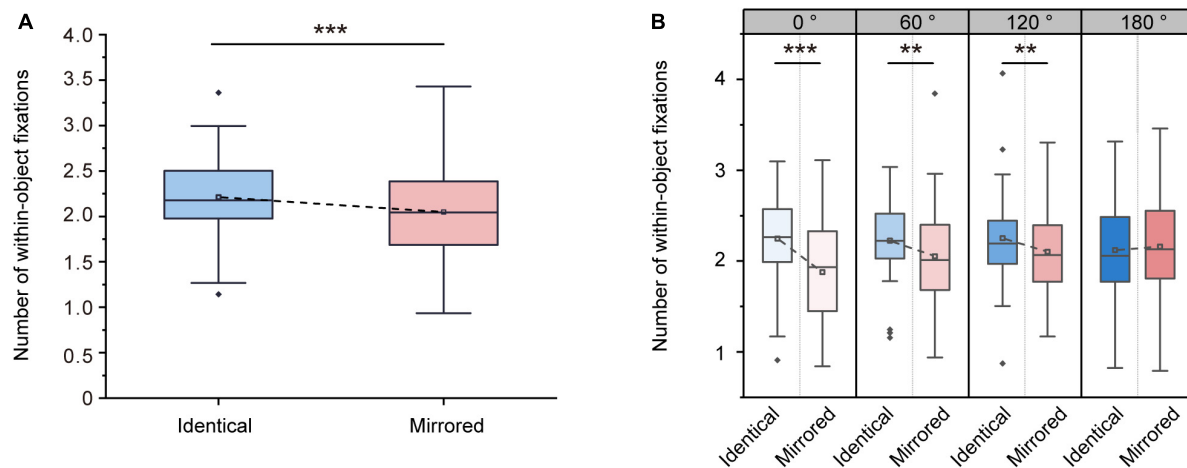


FIGURE 6

Changes in number of within-object fixations during the virtual reality (VR) mental rotation task. (A) Boxplots present the number of within-object fixations for identical and mirrored objects. (B) Grouped boxplots present the number of within-object fixations for identical and mirrored objects at 0, 60, 120 and 180°. The boxplots illustrate the first quartile, median, and third quartile and 1.5 times the interquartile range for both the upper and lower ends of the box. Black horizontal lines and asterisks denote significant differences (** $p < 0.01$, *** $p < 0.001$).

TABLE 4 Overview of number of within-object fixations (mean \pm standard error) for identical and mirrored objects at four angular disparities.

	Identical	Mirrored	Statistics
0°	2.25 \pm 0.08	1.88 \pm 0.10	F (1, 31) = 37.476, $p < 0.001$, $\eta_p^2 = 0.547$
60°	2.22 \pm 0.07	2.05 \pm 0.10	F (1, 31) = 12.646, $p < 0.01$, $\eta_p^2 = 0.290$
120°	2.25 \pm 0.09	2.10 \pm 0.09	F (1, 31) = 9.907, $p < 0.01$, $\eta_p^2 = 0.242$
180°	2.12 \pm 0.09	2.15 \pm 0.10	F (1, 31) = 0.746, $p = 0.394$, $\eta_p^2 = 0.024$

3.2.2. Number of within-object fixations

Repeated-measures ANOVA on the number of within-object fixations revealed a significant main effect of Stimulus Type [F (1, 31) = 32.853, $p < 0.001$, $\eta_p^2 = 0.515$]. The number of within-object fixations was significantly higher for identical objects (2.21 \pm 0.08, mean \pm SE) than for mirrored objects (2.05 \pm 0.09, mean \pm SE; Figure 6A), suggesting that the participants might make multiple comparisons within an object when comparing identical objects. This was akin to a piecemeal strategy (Khooshabeh et al., 2013), in which the participants might break the objects into pieces and encode partial spatial information. We also observed a significant main effect of Angular Disparity [F (3, 93) = 3.225, $p = 0.026$, $\eta_p^2 = 0.094$] and a significant interaction between Angular Disparity and Stimulus Type [F (3, 93) = 11.929, $p < 0.001$, $\eta_p^2 = 0.278$]. Pairwise comparisons revealed significant differences in the number of within-object fixations between identical and mirrored objects at 0, 60 and 120° (all $p < 0.01$; Table 4 and Figure 6B). However, there was no difference ($p = 0.394$; Table 4 and Figure 6B) in the number of within-object fixations between identical and mirrored objects at 180°.

3.2.3. Number of saccades

Repeated-measures ANOVA revealed significant main effects of Stimulus Type [F (1, 31) = 20.299, $p < 0.001$, $\eta_p^2 = 0.396$] and Angular Disparity [F (3, 93) = 11.343, $p < 0.001$, $\eta_p^2 = 0.268$].

The significant main effect of Stimulus Type was due to a higher number of saccades for identical objects (0.61 \pm 0.03, mean \pm SE) compared to for mirrored objects (0.54 \pm 0.04, mean \pm SE; Figure 7A). A significant interaction between Angular Disparity and Stimulus Type was also observed [F (3, 93) = 6.760, $p < 0.001$, $\eta_p^2 = 0.179$]. Pairwise comparisons revealed significant differences in the number of saccades between identical and mirrored objects at 0, 60 and 120° (all $p < 0.01$; Table 5 and Figure 7B). However, there was no difference in the number of saccades ($p = 0.595$; Table 5 and Figure 7B) between identical and mirrored objects at 180°.

3.2.4. Strategy ratio

Repeated-measures ANOVA on strategy ratios revealed significant main effects of Stimulus Type [F (1, 31) = 17.008, $p < 0.001$, $\eta_p^2 = 0.354$] and Angular Disparity [F (3, 93) = 9.987, $p < 0.001$, $\eta_p^2 = 0.244$]. The significant main effect of Stimulus Type demonstrated that the strategy ratio for identical objects (2.04 \pm 0.08, mean \pm SE) was significantly lower than that for mirrored objects (2.17 \pm 0.12, mean \pm SE; Figure 8A). Moreover, there was a significant interaction between Angular Disparity and Stimulus Type [F (3, 93) = 23.035, $p < 0.001$, $\eta_p^2 = 0.426$]. Pairwise comparisons revealed significant differences in strategy ratios between identical and mirrored objects at 120° ($p < 0.001$; Table 6 and Figure 8B). There was no difference in strategy ratios ($p > 0.05$; Table 6 and Figure 8B) between identical and mirrored objects at 0, 60 and 180°.

4. Discussion

In the present study, we presented behavioral and eye movement characteristics during a VR mental rotation task using 3D objects. We found that the VR mental rotation task also evoked a mental rotation effect. Significant differences were observed in response times and eye movement metrics between identical and mirrored objects. The eye movement data further explained the

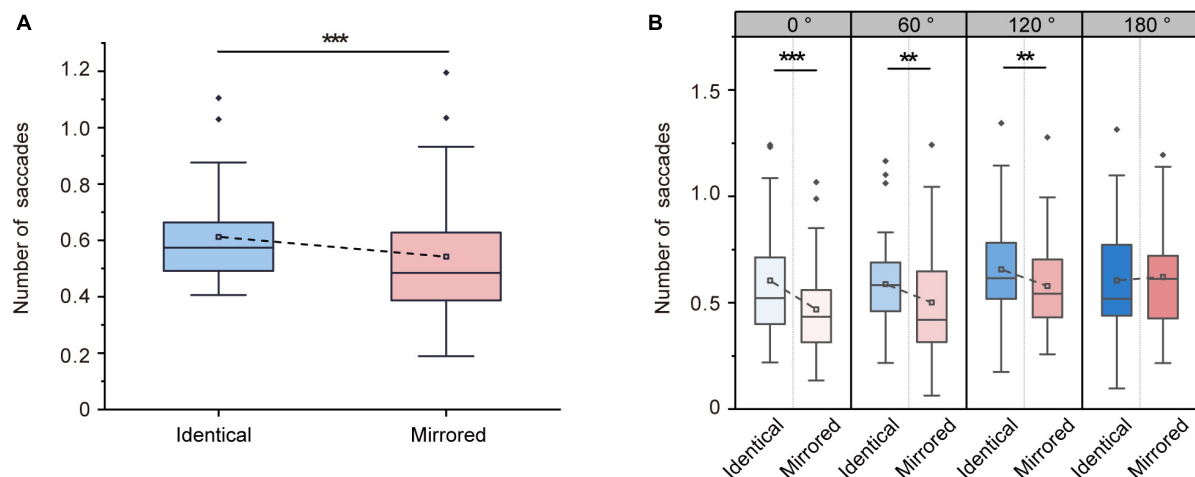


FIGURE 7

Changes in number of saccades during the virtual reality (VR) mental rotation task. (A) Boxplots present the number of saccades for identical and mirrored objects. (B) Grouped boxplots present the number of saccades for identical and mirrored objects at 0, 60, 120 and 180°. The boxplots illustrate the first quartile, median, and third quartile and 1.5 times the interquartile range for both the upper and lower ends of the box. Black horizontal lines and asterisks denote significant differences (** $p < 0.01$, *** $p < 0.001$).

TABLE 5 Overview of number of saccades (mean \pm standard error) for identical and mirrored stimuli at four angular disparities.

	Identical	Mirrored	Statistics
0°	0.60 \pm 0.04	0.46 \pm 0.04	$F(1, 31) = 25.221, p < 0.001, \eta_p^2 = 0.449$
60°	0.58 \pm 0.04	0.50 \pm 0.04	$F(1, 31) = 10.733, p < 0.01, \eta_p^2 = 0.257$
120°	0.65 \pm 0.04	0.57 \pm 0.03	$F(1, 31) = 12.330, p < 0.01, \eta_p^2 = 0.285$
180°	0.60 \pm 0.04	0.62 \pm 0.04	$F(1, 31) = 0.288, p = 0.595, \eta_p^2 = 0.009$

reasons for that response times were longer when comparing mirrored objects than when comparing identical objects.

Based on mental rotation task using 2D images, we conducted a VR mental rotation task using 3D objects. The 2D images presented via a computer screen provide an illusion of depth (Snow and Culham, 2021). Compared to 2D images of the 3D objects (Griksiene et al., 2019; Toth and Campbell, 2019), 3D objects presented in VR can provide real depth cues, enhancing the realness of visual stimuli (Tang et al., 2022). VR allows balances between experimental control and ecological validity (Snow and Culham, 2021). The stereo 3D objects presented in VR in the current task are more ecologically valid than simple 2D images, which can improve our understanding of the neural mechanisms associated with naturalistic visual stimuli. Previously, some studies have compared the mental rotation performance of 2D and stereo 3D forms (Neubauer et al., 2010; Price and Lee, 2010; Lochhead et al., 2022; Tang et al., 2022). Although some factors (i.e., experimental paradigm, sample size, and experimental environment) may affect the experimental results of comparisons between conventional 2D and stereo 3D forms, these studies may provide support for the VR mental rotation task with eye tracking.

As expected, we observed a significant mental rotation effect (Shepard and Metzler, 1971), indicating that the VR mental rotation task is effective and available. Interestingly, the identical and mirrored stimuli are different in behavioral performance, which was consistent with literatures (Hamm et al., 2004; Paschke

et al., 2012; Chen et al., 2014). Our results demonstrated that the accuracy rate for identical objects decreased at 180° and the accuracy rate for mirrored objects increased at 180°, which were line with the findings of a prior study (Chen et al., 2014). The differences in accuracy rate between identical and mirrored objects might be associated with the differences in cognitive processing and a decrease of the task difficulty at higher angular disparities for mirrored objects (Paschke et al., 2012). Due to opposite arm positions, the paired mirrored stimulus at 180° could be directly perceived as mirrored object without any rotation manipulation. That is, the participants probably determined the mirrored objects by only comparing the arm positions of objects, which might increase correct responses. By contrast, rotation operation is required at 120°. Response-preparation theory (Cooper and Shepard, 1973) suggested that motor response during mental rotation was planned on the basis of the expectancy of the paired objects being identical. For mirrored objects, the expectancy may result in that an already planned motor response would have to be inhibited and re-planned. Moreover, the expectancy would contribute to a lower accuracy rate because the planned motor responses were probably difficult to inhibit. Therefore, the accuracy rates for identical objects are higher than that for mirrored objects at 120°. Response times were higher when comparing mirrored objects than when comparing identical objects, which might be attributed to additional cognitive processing. In the 3D mental rotation task, participants were asked to decide whether the paired objects were identical or mirrored. The participants mentally represented the paired objects and rotated them and simultaneously made a direct match between their internal mental representation and the external visual stimuli. A decision of “mirrored” would be made if the participants discovered that some parts of the paired objects were different. When the participants identified differences between objects, more response time was required to choose the “mirrored” response. This was possibly associated with the strategy of visual processing during mental

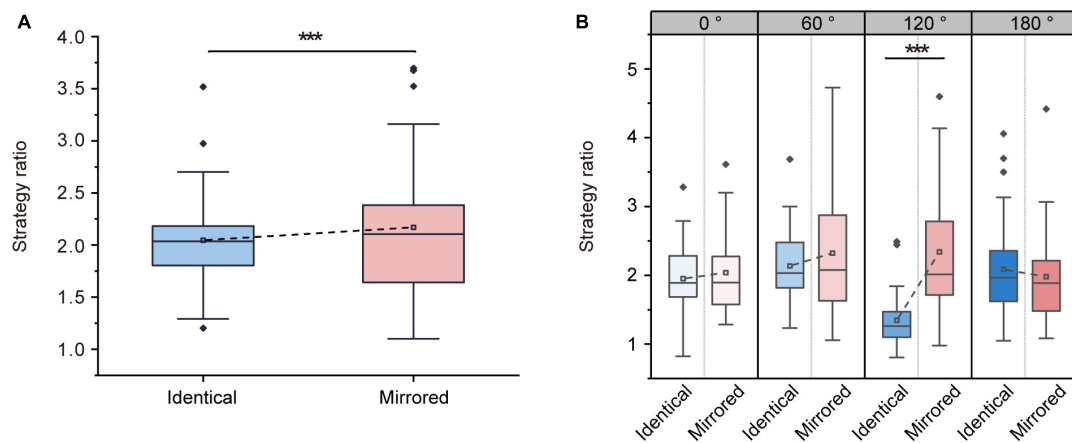


FIGURE 8

Changes in strategy ratio during the virtual reality (VR) mental rotation task. (A) Boxplots present average strategy ratio for identical and mirrored objects. (B) Grouped boxplots present strategy ratio for identical and mirrored objects at 0, 60, 120 and 180°. The boxplots illustrate the first quartile, median, and third quartile and 1.5 times the interquartile range for both the upper and lower ends of the box. Black horizontal lines and asterisks denote significant differences (***) $p < 0.001$.

rotation (Toth and Campbell, 2019), which was further supported by the eye tracking data.

Eye movements allow us to scan the visual field with high resolution (Mast and Kosslyn, 2002), and can provide insights into visual behavior in mental rotation task using 2D images (Nazareth et al., 2019). However, few studies have reported eye movements in mental rotation tasks involving naturalistic 3D stimuli. In the present work, we analyzed eye movement parameters, including fixations and saccades, to quantify the processes of visual processing of 3D objects. We found that percent fixation time was higher when participants compared identical objects than mirrored objects. Eye fixations provide information on active processing of information (Mast and Kosslyn, 2002) and are associated with visual attention (Verghese et al., 2019; Skaramagkas et al., 2023). The 3D objects were encoded at each fixation and was then reconstructed in the brain based on input from multiple fixations. Effective visual information can be extracted around these fixations (Ikeda and Takeuchi, 1975). The higher percent fixation times for identical objects suggested that the participants spent more time fixating on the objects, indicating that the participants might allocate more attention to the objects during the completion of the mental rotation task when comparing the identical objects. The increased attention suggested that more visual information was obtained when the participants compared identical 3D objects. In addition, the number of fixations made on 3D objects per second was higher for identical objects than for mirrored objects, suggesting that the participants might make more fixations per second when comparing identical objects. Because visual information was obtained from each fixation, the participants dealt with more visual information per second when comparing the identical objects. This may indicate that the efficiency of visual information acquisition was higher for identical objects than for mirrored objects. These results further illustrated that faster response times for identical objects could be attributed to increased attention and higher efficiency of visual information acquisition.

Visual strategies during mental rotation have been associated with behavioral performance (Heil and Jansen-Osmann, 2008).

TABLE 6 Overview of strategy ratio (mean \pm standard error) for identical and mirrored objects at four angular disparities.

	Identical	Mirrored	Statistics
0°	1.95 \pm 0.09	2.03 \pm 0.11	F (1, 31) = 0.643, p = 0.429, η_p^2 = 0.020
60°	2.13 \pm 0.09	2.32 \pm 0.14	F (1, 31) = 2.083, p = 0.159, η_p^2 = 0.063
120°	1.34 \pm 0.06	2.34 \pm 0.15	F (1, 31) = 70.104, p < 0.001, η_p^2 = 0.693
180°	2.08 \pm 0.13	1.97 \pm 0.12	F (1, 31) = 1.145, p = 0.243, η_p^2 = 0.044

Strategy dichotomies, including holistic and piecemeal strategies, have been extensively discussed in previous studies (Heil and Jansen-Osmann, 2008; Khooshabeh et al., 2013). The piecemeal strategy generally results in longer response times compared with the holistic strategy. These different visual strategies can be reflected by the strategy ratio, which is the ratio of the number of within-object fixations to the number of between-object saccades. The present study showed a difference in strategy ratios between mirrored objects and identical objects. Previous studies demonstrated that a strategy ratio close to 1 indicated a holistic strategy and a strategy ratio greater than one indicated a piecemeal strategy (Khooshabeh and Hegarty, 2010). Thus, the participants in the present study preferred a piecemeal strategy for mirrored objects compared with identical objects. For mirrored objects, participants performed multiple fixations within one object to compare different parts of the object before they switched to the other. Fixation switches were more frequently observed when comparing mirrored objects than when comparing identical objects. Fixation switches between the two 3D objects could be regarded as constant updates, which is necessary to maintain the object perception (Hyun and Luck, 2007). These constant updates may be more difficult during the mental rotation of mirrored objects. These findings provided further explanation for the behavioral results observed in the VR mental rotation task.

This study presents the behavioral and eye movement characteristics in a VR mental rotation task with eye tracking, but it still has some limitations. Although the present VR mental rotation task elicits a mental rotation effect, comparing the characteristics of VR to 2D mental rotation task is also important. The comparisons could provide compelling evidence that whether the VR mental rotation task is a better alternative. Future studies could add a conventional 2D mental rotation task with eye tracking and compare the differences in behavioral and eye movement characteristics between 2D and VR mental rotation tasks.

5. Conclusion

In the present work, we examined behavioral and eye movement characteristics during a VR mental rotation task using 3D stimuli. Significant differences were obtained in behavioral performance and eye movement metrics in the rotation and comparison of identical and mirrored objects. Eye movement metrics, including the percent fixation time, the number of within-object fixations, and the number of saccades, were significantly lower when comparing mirrored objects than identical objects. The eye movement data provided further explanation for the behavioral results in the VR mental rotation task.

Data availability statement

The original contributions presented in this study are included in the article/**Supplementary material**, further inquiries can be directed to the corresponding authors.

Ethics statement

The studies involving human participants were reviewed and approved by the current study adhered to the tenets of the Declaration of Helsinki, and the ethical approval was approved by Beihang University (BM20200183). All of the participants provided written informed consents in advance of the study. A signed informed consent statement was received from each participant. The patients/participants provided their written informed consent to participate in this study.

References

- Andersson, R., Larsson, L., Holmqvist, K., Stridh, M., and Nystrom, M. (2017). One algorithm to rule them all? An evaluation and discussion of ten eye movement event-detection algorithms. *Behav. Res. Methods* 49, 616–637. doi: 10.3758/s13428-016-0738-9
- Arthur, T., Harris, D. J., Allen, K., Naylor, C. E., Wood, G., Vine, S., et al. (2021). Visuo-motor attention during object interaction in children with developmental coordination disorder. *Cortex* 138, 318–328. doi: 10.1016/j.cortex.2021.02.013
- Berneiser, J., Jahn, G., Grothe, M., and Lotze, M. (2018). From visual to motor strategies: Training in mental rotation of hands. *Neuroimage* 167, 247–255. doi: 10.1016/j.neuroimage.2016.06.014
- Blignaut, P. (2009). Fixation identification: The optimum threshold for a dispersion algorithm. *Atten. Percept. Psychophys.* 71, 881–895. doi: 10.3758/APP.71.4.881
- Campbell, M. J., Toth, A. J., and Brady, N. (2018). Illuminating sex differences in mental rotation using pupillometry. *Biol. Psychol.* 138, 19–26. doi: 10.1016/j.biopsycho.2018.08.003
- Chen, H., Guo, X., Lv, Y., Sun, J., and Tong, S. (2014). “Mental rotation process for mirrored and identical stimuli: A beta-band ERD study,” in *Proceedings of the 2014 36th annual international conference of the IEEE engineering in medicine and biology society, EMBC 2014*, (Piscataway, NJ: Institute of Electrical and Electronics Engineers Inc), 4948–4951. doi: 10.1109/EMBC.2014.6944734

Author contributions

ZT: formal analysis, writing—original draft, and visualization. XL: conceptualization, funding acquisition, project administration, and writing—review and editing. HH and XD: formal analysis. MT and LF: software. XQ, DC, JW, and JG: visualization. YD: writing—original draft. ST: writing—review and editing. YF: conceptualization, funding acquisition, project administration, supervision, and writing—review and editing. All authors contributed to the article and approved the submitted version.

Funding

This work was supported by the National Key Research and Development Plan of China (2020YFC2005902) and the National Natural Science Foundation of China (T2288101, U20A20390, and 11827803).

Conflict of interest

The authors declare that the research was conducted in the absence of any commercial or financial relationships that could be construed as a potential conflict of interest.

Publisher's note

All claims expressed in this article are solely those of the authors and do not necessarily represent those of their affiliated organizations, or those of the publisher, the editors and the reviewers. Any product that may be evaluated in this article, or claim that may be made by its manufacturer, is not guaranteed or endorsed by the publisher.

Supplementary material

The Supplementary Material for this article can be found online at: <https://www.frontiersin.org/articles/10.3389/fnins.2023.1143006/full#supplementary-material>

- Chiquet, S., Martarelli, C. S., and Mast, F. W. (2020). Eye movements to absent objects during mental imagery and visual memory in immersive virtual reality. *Virtual Real.* 25, 655–667. doi: 10.1007/s10055-020-00478-y
- Clay, V., König, P., and König, S. (2019). Eye tracking in virtual reality. *J. Eye Mov. Res.* 12, 1–8. doi: 10.16910/jemr.12.1.3
- Cooper, L. A., and Shepard, R. N. (1973). “Chronometric studies of the rotation of mental images,” in *Visual information processing*, ed. W. G. Chase (Amsterdam: Elsevier), 75–176.
- Desrocher, M. E., Smith, M. L., and Taylor, M. J. (1995). Stimulus and sex-differences in performance of mental rotation—evidence from event-related potentials. *Brain Cogn.* 28, 14–38. doi: 10.1006/brcg.1995.1031
- El Jamiy, F., and Marsh, R. (2019). Survey on depth perception in head mounted displays: Distance estimation in virtual reality, augmented reality, and mixed reality. *IET Image Proc.* 13, 707–712. doi: 10.1049/iet-ipr.2018.5920
- Griksiene, R., Arnatkeviciute, A., Monciunskaitė, R., Koenig, T., and Ruksenas, O. (2019). Mental rotation of sequentially presented 3D figures: Sex and sex hormones related differences in behavioural and ERP measures. *Sci. Rep.* 9:18843. doi: 10.1038/s41598-019-55433-y
- Hamm, J. P., Johnson, B. W., and Corballis, M. C. (2004). One good turn deserves another: An event-related brain potential study of rotated mirror-normal letter discriminations. *Neuropsychologia* 42, 810–820. doi: 10.1016/j.neuropsychologia.2003.11.009
- Haxby, J. V., Gobbini, M. I., and Nastase, S. A. (2020). Naturalistic stimuli reveal a dominant role for agentic action in visual representation. *Neuroimage* 216:116561. doi: 10.1016/j.neuroimage.2020.116561
- Heil, M., and Jansen-Osmann, P. (2008). Sex differences in mental rotation with polygons of different complexity: Do men utilize holistic processes whereas women prefer piecemeal ones? *Q. J. Exp. Psychol.* 61, 683–689. doi: 10.1080/17470210701822967
- Hofmann, S. M., Klotzsche, F., Mariola, A., Nikulin, V. V., Villringer, A., and Gaebler, M. (2021). Decoding subjective emotional arousal from EEG during an immersive virtual reality experience. *Elife* 10:e64812. doi: 10.7554/eLife.64812
- Hsing, H. W., Bairaktarova, D., and Lau, N. (2023). Using eye gaze to reveal cognitive processes and strategies of engineering students when solving spatial rotation and mental cutting tasks. *J. Eng. Educ.* 112, 125–146. doi: 10.1002/jee.20495
- Hyun, J. S., and Luck, S. J. (2007). Visual working memory as the substrate for mental rotation. *Psychonom. Bull. Rev.* 14, 154–158. doi: 10.3758/BF03194043
- Ibbotson, M., and Kregelberg, B. (2011). Visual perception and saccadic eye movements. *Curr. Opin. Neurobiol.* 21, 553–558. doi: 10.1016/j.conb.2011.05.012
- Ikeda, M., and Takeuchi, T. (1975). Influence of foveal load on the functional visual field. *Percept. Psychophys.* 18, 255–260. doi: 10.3758/BF03199371
- Ito, T., Kamiue, M., Hosokawa, T., Kimura, D., and Tsubahara, A. (2022). Individual differences in processing ability to transform visual stimuli during the mental rotation task are closely related to individual motor adaptation ability. *Front. Neurosci.* 16:941942. doi: 10.3389/fnins.2022.941942
- Jaaskelainen, I. P., Sams, M., Glerean, E., and Ahveninen, J. (2021). Movies and narratives as naturalistic stimuli in neuroimaging. *Neuroimage* 224:117445. doi: 10.1016/j.neuroimage.2020.117445
- Khooshabeh, P., and Hegarty, M. (2010). “Representations of shape during mental rotation,” in *Proceedings of the 2010 AAAI spring symposium*, (San Francisco, CA: AI Access Foundation), 15–20.
- Khooshabeh, P., Hegarty, M., and Shipley, T. F. (2013). Individual differences in mental rotation: Piecemeal versus holistic processing. *Exp. Psychol.* 60, 164–171. doi: 10.1027/1618-3169/a000184
- Komogortsev, O. V., Gobert, D. V., Jayarathna, S., Koh, D. H., and Gowda, S. M. (2010). Standardization of automated analyses of oculomotor fixation and saccadic behaviors. *IEEE Trans. Biomed. Eng.* 57, 2635–2645. doi: 10.1109/tbme.2010.2057429
- Kowler, E., Anderson, E., Doshier, B., and Blaser, E. (1995). The role of attention in the programming of saccades. *Vis. Res.* 35, 1897–1916. doi: 10.1016/0042-6989(94)00279-U
- Lancry-Dayana, O. C., Ben-Shakhar, G., and Pertzov, Y. (2023). The promise of eye-tracking in the detection of concealed memories. *Trends Cogn. Sci.* 27, 13–16. doi: 10.1016/j.tics.2022.08.019
- Lavoie, E. B., Valevicius, A. M., Boser, Q. A., Kovic, O., Vette, A. H., Pilarski, P. M., et al. (2018). Using synchronized eye and motion tracking to determine high-precision eye-movement patterns during object-interaction tasks. *J. Vis.* 18:18. doi: 10.1167/18.6.18
- Llanes-Jurado, J., Marin-Morales, J., Guixeres, J., and Alcaniz, M. (2020). Development and calibration of an eye-tracking fixation identification algorithm for immersive virtual reality. *Sensors* 20:4956. doi: 10.3390/s20174956
- Lochhead, I., Hedley, N., Çöltekin, A., and Fisher, B. (2022). The immersive mental rotations test: Evaluating spatial ability in virtual reality. *Front. Virtual. Real.* 3:820237. doi: 10.3389/fvrvr.2022.820237
- Marini, F., Breeding, K. A., and Snow, J. C. (2019). Distinct visuo-motor brain dynamics for real-world objects versus planar images. *Neuroimage* 195, 232–242. doi: 10.1016/j.neuroimage.2019.02.026
- Mast, F. W., and Kosslyn, S. M. (2002). Eye movements during visual mental imagery. *Trends Cogn. Sci.* 6, 271–272. doi: 10.1016/s1364-6613(02)01931-9
- Minderer, M., and Harvey, C. D. (2016). Forum neuroscience virtual reality explored. *Nature* 533, 324–324. doi: 10.1038/nature17899
- Musz, E., Loiotile, R., Chen, J., and Bedny, M. (2022). Naturalistic audio-movies reveal common spatial organization across “visual” cortices of different blind individuals. *Cereb. Cortex* 33, 1–10. doi: 10.1093/cercor/bhac048
- Nazareth, A., Killick, R., Dick, A. S., and Pruden, S. M. (2019). Strategy selection versus flexibility: Using eye-trackers to investigate strategy use during mental rotation. *J. Exp. Psychol. Learn. Mem. Cogn.* 45, 232–245. doi: 10.1037/xlm0000574
- Neubauer, A. C., Bergner, S., and Schatz, M. (2010). Two- vs. Three-dimensional presentation of mental rotation tasks: Sex differences and effects of training on performance and brain activation. *Intelligence* 38, 529–539. doi: 10.1016/j.intell.2010.06.001
- Paschke, K., Jordan, K., Wüstenberg, T., Baudewig, J., and Leo Müller, J. (2012). Mirrored or identical—is the role of visual perception underestimated in the mental rotation process of 3D-objects? A combined fMRI-eye tracking-study. *Neuropsychologia* 50, 1844–1851. doi: 10.1016/j.neuropsychologia.2012.04.010
- Peters, M., and Battista, C. (2008). Applications of mental rotation figures of the Shepard and Metzler type and description of a mental rotation stimulus library. *Brain Cogn.* 66, 260–264. doi: 10.1016/j.bandc.2007.09.003
- Pletzer, B., Steinbeisser, J., Van Laak, L., and Harris, T. (2019). Beyond biological sex: Interactive effects of gender role and sex hormones on spatial abilities. *Front. Neurosci.* 13:675. doi: 10.3389/fnins.2019.00675
- Price, A., and Lee, H. S. (2010). The effect of two-dimensional and stereoscopic presentation on middle school students’ performance of spatial cognition tasks. *J. Sci. Educ. Technol.* 19, 90–103. doi: 10.1007/s10956-009-9182-2
- Robertson, G. G., Card, S. K., and Mackinlay, J. D. (1993). Three views of virtual reality: Nonimmersive virtual reality. *Computer* 26:81. doi: 10.1109/2.192002
- Salvucci, D. D., and Goldberg, J. H. (2000). “Identifying fixations and saccades in eye-tracking protocols,” in *Proceedings of the eye tracking research and applications symposium 2000*, ed. S. N. Spencer (New York, NY: Association for Computing Machinery (ACM)), 71–78.
- Shepard, R. N., and Metzler, J. (1971). Mental rotation of 3-dimensional objects. *Science* 171, 701–703. doi: 10.1126/science.171.3972.701
- Skaramagkas, V., Giannakakis, G., Ktistakis, E., Manousos, D., Karatzanis, I., Tachos, N. S., et al. (2023). Review of eye tracking metrics involved in emotional and cognitive processes. *IEEE Rev. Biomed. Eng.* 16, 260–277. doi: 10.1109/RBME.2021.3066072
- Snow, J. C., and Culham, J. C. (2021). The treachery of images: How realism influences brain and behavior. *Trends Cogn. Sci.* 25, 506–519. doi: 10.1016/j.tics.2021.02.008
- Suzuki, A., Shinozaki, J., Yazawa, S., Ueki, Y., Matsukawa, N., Shimohama, S., et al. (2018). Establishing a new screening system for mild cognitive impairment and Alzheimer’s disease with mental rotation tasks that evaluate visuospatial function. *J. Alzheimers Dis.* 61, 1653–1665. doi: 10.3233/jad-170801
- Tang, Z. L., Liu, X. Y., Huo, H. Q., Tang, M., Liu, T., Wu, Z. X., et al. (2022). The role of low-frequency oscillations in three-dimensional perception with depth cues in virtual reality. *Neuroimage* 257:119328. doi: 10.1016/j.neuroimage.2022.119328
- Tiwari, A., Pachori, R. B., and Sanjram, P. K. (2021). Isomorphic 2D/3D objects and saccadic characteristics in mental rotation. *Comput. Mater. Continua* 70, 433–450. doi: 10.32604/cmc.2022.019256
- Toth, A. J., and Campbell, M. J. (2019). Investigating sex differences, cognitive effort, strategy, and performance on a computerised version of the mental rotations test via eye tracking. *Sci. Rep.* 9:19430. doi: 10.1038/s41598-019-56041-6
- Verghese, P., McKee, S. P., and Levi, D. M. (2019). Attention deficits in amblyopia. *Curr. Opin. Psychol.* 29, 199–204. doi: 10.1016/j.copsyc.2019.03.011
- Wenk, N., Buettler, K. A., Penálver-Andrés, J., Müri, R. M., and Marchal-Crespo, L. (2022). Naturalistic visualization of reaching movements using head-mounted displays improves movement quality compared to conventional computer screens and proves high usability. *J. Neuroeng. Rehabil.* 19:137. doi: 10.1186/s12984-022-01101-8
- Xue, J., Li, C., Quan, C., Lu, Y., Yue, J., and Zhang, C. (2017). Uncovering the cognitive processes underlying mental rotation: An eye-movement study. *Sci. Rep.* 7:10076. doi: 10.1038/s41598-017-10683-6
- Yarbus, A. L. (1967). “Eye movements during fixation on stationary objects,” in *Eye movements and vision*, ed. A. L. Yarbus (Boston, MA: Springer), 103–127.



OPEN ACCESS

EDITED BY

Xuemin Li,
Peking University Third Hospital,
Haidian,
China

REVIEWED BY

ZhiPeng Gao,
Taiyuan University of Technology,
China
Shaoying Tan,
Hong Kong Polytechnic University,
Hong Kong SAR,
China

*CORRESPONDENCE

Fangjun Bao

✉ baofjmd@wmu.edu.cn

Xiaofei Wang

✉ xiaofei.wang@buaa.edu.cn

[†]These authors have contributed equally to this work

SPECIALTY SECTION

This article was submitted to
Visual Neuroscience,
a section of the journal
Frontiers in Neuroscience

RECEIVED 24 February 2023

ACCEPTED 13 March 2023

PUBLISHED 31 March 2023

CITATION

Fan L, Wang J, Li Q, Song Z, Dong J, Bao F and Wang X (2023) Eye movement characteristics and visual fatigue assessment of virtual reality games with different interaction modes. *Front. Neurosci.* 17:1173127. doi: 10.3389/fnins.2023.1173127

COPYRIGHT

© 2023 Fan, Wang, Li, Song, Dong, Bao and Wang. This is an open-access article distributed under the terms of the [Creative Commons Attribution License \(CC BY\)](https://creativecommons.org/licenses/by/4.0/). The use, distribution or reproduction in other forums is permitted, provided the original author(s) and the copyright owner(s) are credited and that the original publication in this journal is cited, in accordance with accepted academic practice. No use, distribution or reproduction is permitted which does not comply with these terms.

Eye movement characteristics and visual fatigue assessment of virtual reality games with different interaction modes

Lei Fan^{1,2,3†}, Junjie Wang^{1,2†}, Qi Li³, Zhenhao Song³, Jinhui Dong³, Fangjun Bao^{1,2*} and Xiaofei Wang^{2,3*}

¹National Engineering Research Center of Ophthalmology and Optometry, Eye Hospital, Wenzhou Medical University, Wenzhou, China, ²School of Ophthalmology and Optometry and School of Biomedical Engineering, Wenzhou Medical University, Wenzhou, China, ³Key Laboratory for Biomechanics and Mechanobiology of Ministry of Education, Beijing Advanced Innovation Center for Biomedical Engineering, School of Biological Science and Medical Engineering, Beihang University, Beijing, China

This study aimed to investigate the eye movement characteristics and visual fatigue of virtual reality games with different interaction modes. Eye movement data were recorded using the built-in eye tracker of the VR device and eye movement parameters were calculated from the recorded raw data. The Visual Fatigue Scales and Simulator Sickness Questionnaire were used to subjectively assess visual fatigue and overall discomfort of the VR experience. Sixteen male and 17 female students were recruited for this study. Results showed that both the primary and 360 mode of VR could cause visual fatigue after 30min of gameplay, with significant differences observed in eye movement behavior between the two modes. The primary mode was more likely to cause visual fatigue, as shown by objective measurements of blinking and pupil diameter. Fixation and saccade parameters also showed significant differences between the two modes, possibly due to the different interaction modes employed in the 360 mode. Further research is required to examine the effects of different content and interactive modes of VR on visual fatigue, as well as to develop more objective measures for assessing it.

KEYWORDS

virtual reality, eye movements, visual fatigue, video games, interaction mode

Introduction

Virtual reality (VR) is a technology that enables users to experience immersive, computer-generated environments. In recent years, VR has gained widespread popularity with a range of applications, including entertainment (DJSCOE, Vile – Parle (W), Mumbai et al., 2014), education (Ruan, 2022), and healthcare (Mirelman et al., 2011; Maples-Keller et al., 2017). The concept of the “metaverse,” a virtual shared space that is accessible through the internet, has also contributed to the promotion of VR. Additionally, the development of VR games has contributed to the growth of this technology, as gamers can experience a level of immersion that is impossible with traditional gaming platforms. As the application of VR continues to grow rapidly, it is crucial to understand its potential impact on eye health and explore quantitative measures for monitoring its effects.

Visual fatigue is a condition where the eyes become uncomfortable due to prolonged and intense focus on certain tasks. It can be caused by activities such as reading or staring at a digital screen for an extended period. It was defined as a decrease in the performance of the human visual system in specific conditions (Lynch and Hockey, 1984). VR can lead to uncomfortable symptoms such as eyestrain, dizziness, and other visual fatigue (Hua, 2017). The vergence-accommodation conflict (VAC) is the leading cause of visual fatigue in the VR (Iskander et al., 2019). The effects of VR on visual fatigue have been studied extensively using questionnaires. Previous studies have also demonstrated a strong correlation between eye movement and visual fatigue. Changes in eye movement speed, fixation duration, and blinking frequency reflect fatigue status and mental load (Kim et al., 2011a; Bang et al., 2014). Characteristics associated with blinking and eye movements can be used to assess visual fatigue. Wang and colleagues developed two machine learning models for assessing eye fatigue using features related to blinking and eye movements (Wang et al., 2019). By analyzing the relationship between VAC and variability in convergence angle, Iskander and colleagues proposed a visual fatigue likelihood metric based on biomechanical analysis of the oculomotor system (Iskander et al., 2019; Iskander and Hossny, 2021). Oculomotor behavior is also closely linked to the mechanical load on the eye and optic nerve tissues. Eye movement has been shown to cause a transient increase in intraocular pressure and deformation of the posterior eye globe (Wang et al., 2017). Excessive or abnormal eye movement may be a risk factor for glaucoma and myopia.

Most studies on the effects of VR on visual fatigue have focused on comparing the pre- and post-exposure state of the eye or comparing eye movement differences when viewing different video content (Mohamed Elias et al., 2019; Yoon et al., 2020). However, there has been limited research on the differences in visual fatigue and eye movement behaviors in different interactive modes within VR. Therefore, this study aims to investigate the visual fatigue differences and eye movement behaviors in different interaction modes of a VR game.

Methods

Subject recruitment and clinical examinations

In this study, 16 male and 17 female students were recruited from Beihang University. The mean age was 23.85 (standard deviation: 2.12) years. Exclusion criteria include abnormal stereo vision, strabismus, retinal disease, visual field defects or other eye diseases, limitations in body movement and balance, inability to understand and follow the instructions provided by the researchers, and inability to participate in the entire experimental process. Written informed consent was obtained from all participants. The study was reviewed and approved by the Biomedical Ethics Committee of Beihang University and was conducted in accordance with the guidelines of the Declaration of Helsinki.

Virtual reality game and eye tracking

In the study, Virtual Reality games are used as visual stimuli, because games are considered to be the most attractive and immersive experience for users. It can enhance users' reactions after games (Pallavicini et al., 2018). The game used in this study was Beat Saber (Beat Games). Beat Saber involves a substantial number of objects

(fixation targets) that move toward the player's eyes from a distance, necessitating continuous accommodation and convergence by the player's eyes as the objects approach. These eye responses are closely linked to the development of visual fatigue. Furthermore, this game is widely popular and has been used in several studies as an experimental task to study symptoms of visual fatigue (Szpak et al., 2020; Banstola et al., 2022). Additionally, the game offers both primary and 360 modes, which perfectly aligns with the requirements of our study. This game simulates two controllers as lightsabers and objects (notes, bombs, obstacles, etc.) fly toward the player from a distance. Then the player must swing the lightsaber in their hands to slash the notes according to the music beat. Subjects were asked to play the game for 30 min in two interactive modes: primary mode and 360 mode. In the primary mode, the objects came from straight ahead of the player's eyes, and the subject did not need to turn their head or body (Figure 1A). In the 360 mode, objects could come from around the player, requiring the player to turn their heads and bodies to look in different directions (Figure 1B).

The VR device used in this study was the HTC VIVE Pro Eye (HTC Corporation Inc.). It has a built-in eye tracker provided by Tobii (Tobii AB, Stockholm, Sweden). The eye tracker has a data output frequency of up to 120 Hz and an accuracy range of 0.5°–1.1°. In this study, the frequency of the eye tracker data was reduced to 30 Hz to minimize the computational load. A reliability study showed that 30 Hz was sufficient to accurately capture all the eye movement parameters used in this study, as compared to the 120 Hz data. We recorded the gaze direction at each time point, enabling us to capture eye movements in all directions within the raw data. Furthermore, the data for both eyes were simultaneously recorded, ensuring that all monocular information was included in the raw data. Raw data provided by the eye tracker includes the origin of the gaze, gaze vectors, eye openness, pupil diameter, and data validity. Raw data from the eye tracker was obtained using the HTC SRanipal SDK as .csv files, and custom Python code was used to calculate all the eye movement parameters.

Subjective assessment of visual fatigue

Visual fatigue was subjectively assessed using the Visual Fatigue Scales consisted of 11 symptoms, each containing 5 identical symptom levels (0 = none, 1 = mild, 2 = moderate, 4 = severe; Wang and Cui, 2014). The scale is developed using the Delphi method, which is suitable for screening of visual fatigue in the general population, and each item is independent of others.

The overall discomfort of the VR experience was also assessed using a Simulator Sickness Questionnaire (SSQ). It includes 16 symptoms related to simulator disorders, which are divided into three subscales: nausea symptoms (N) such as hiccups, sweating, and increased salivation, etc.; oculomotor symptoms (O) such as eye strain, eye focus, blurred vision, etc.; disorientation problems (D) such as dizziness. Each symptom has 4 different levels of severity (0 = no symptoms, 1 = mild symptoms, 2 = moderate symptoms, 3 = severe symptoms). The total score is calculated by summing the weighted score of each item, with higher scores indicating more severe sickness symptoms.

Experimental procedure

Before the experiment, general information such as gender and age was collected from the subject. All subjects had normal or

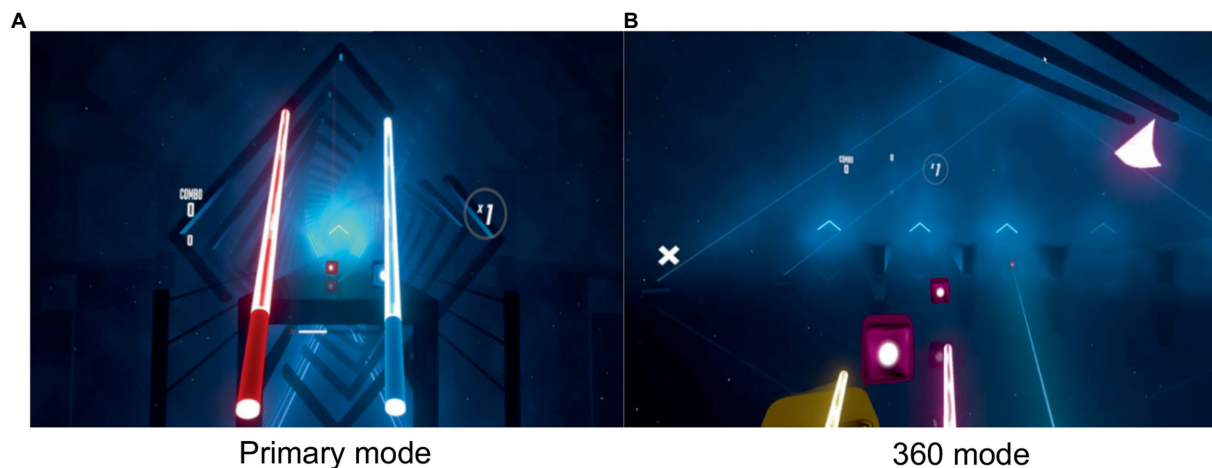


FIGURE 1

(A) In Beat Saber's primary mode, a series of blocks is thrown at the player from directly ahead. It's simple and straightforward, but can be very challenging at high levels. (B) In the 360 mode, notes can come from all around the player and making the game considerably more complex.

best-corrected visual acuity of ≤ 0 LogMAR. All subjects were asked to observe a distance of more than 6 m for at least 30 min before the experiment to allow for eye relaxation. SSQ was then administered to assess the subjects' condition before performing VR. Next, the subjects were randomly assigned to play the VR game in either the primary mode or the 360 mode. The SSQ was administered again after the game to assess the subjects' condition. The second half of the experiment followed the same procedure as the first half, including observation at a distance of more than 6 m for at least 30 min, administering the SSQ, and playing the VR game in the other interactive mode. The SSQ was administered again after the game.

Luminance of the VR game

Screen recordings of the VR game scene were obtained for all VR sessions. The luminance of the scene was calculated using the RGB intensity of all the pixels in each video frame, using the following formula: $\text{Luminance} = 0.2126 \times \text{Red} + 0.7152 \times \text{Green} + 0.0722 \times \text{Blue}$ (Nguyen and Brown, 2017). This method of calculating luminance is based on how the human eye perceives light and considers the different sensitivity of the three cone types in the retina to different wavelengths of light. The luminance values were used to evaluate the brightness of the VR game at each time point during the experiment.

Data processing to obtain eye movement parameters

All data processing was conducted in Python (version 3.7.4, python.org). The fixation of the eye was determined using the I-DT algorithm (Blignaut, 2009). This algorithm requires the setting of two parameters: a dispersion threshold and a temporal threshold. In this study, these parameters were set to 0.02269 and 150 ms, respectively. After identifying fixations, several eye movement parameters were calculated: fixation duration, fixation angle, saccade duration, and saccade magnitude. Fixation duration was the

time spent on a single fixation, and total fixation was the sum of all fixation durations. The average fixation duration was the mean of all fixation durations. Similarly, saccade duration and average saccade duration were calculated. The fixation angle was defined as the angle between the direction of a fixation point and the primary gaze direction. The saccade magnitude was defined as the angle between the vectors of two consecutive fixation points. The average and maximum saccade were also calculated. The average rotation angle of the eye was defined as the mean angle between all gaze vectors and the primary gaze direction. The blinking frequency and average blinking duration were then determined using the continuity and validity of the eye openness data. The device sampling rate is 30 Hz. Each row of data differs by about 33.3 ms. Judging invalid data of more than three consecutive rows as a single blink behavior. The average blink duration was ~ 100 ms.

Statistical analysis

Statistical analyses were performed using Python (version 3.7.4, python.org). Data were expressed as mean \pm standard deviation. The Kolmogorov–Smirnov test was used to assess the normality of the variables. Paired *t*-tests were used to compare differences in eye movement behavior between the two interactive modes of the VR game. Wilcoxon signed-rank tests were used to compare differences in subjective symptoms before and after VR in the two interactive modes. Pearson's coefficient was used to analyze the correlation between scene luminance and pupil diameter. A *p*-value of < 0.05 was considered statistically significant.

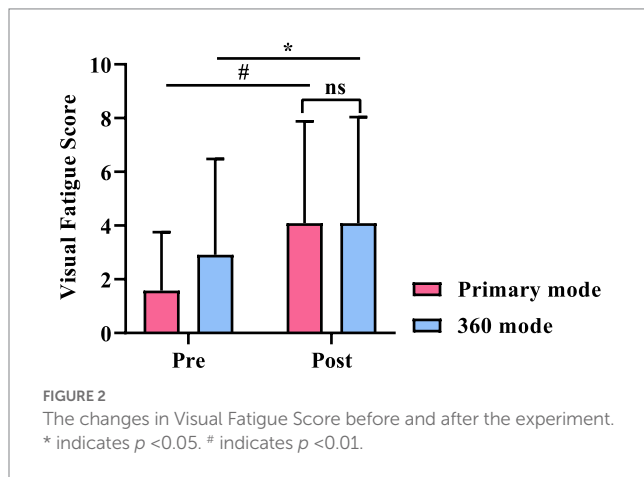
Results

Subjective assessment results

The 360 mode and the primary mode showed a deepening of visual fatigue symptoms when compared before and after the

experimental task ($p < 0.05$), but there was no difference between the visual fatigue scores when comparing the two scenes after the experiment ($p = 0.712$; Figure 2).

SSQ also showed a significant increase in all subscale scores when comparing the two scenes before and after the experiment ($p < 0.01$). As seen in Figure 3, the 360 mode produced greater discomfort symptoms than the primary mode, but there was no difference between the discomfort symptoms caused by the two ($p > 0.05$; Figure 3).



Eye movement parameters

Table 1 shows the eye movement parameters in the primary mode and the 360 mode. The primary mode had higher fixation frequency, total fixation duration, and average fixation duration compared to the 360 mode ($p < 0.05$). There was no significant difference between the average fixation angle of both eyes. The 360 mode had higher total saccade duration, average saccade duration, average saccade magnitude of both eyes, and maximum saccade magnitude compared to the primary mode ($p < 0.05$). The 360 mode had a higher average blinking duration than primary mode ($p < 0.05$), but the blinking frequency was lower ($p < 0.05$). There was no significant difference between the average rotation angle of both eyes.

Luminance of the VR game and pupil diameter

The pupil diameter in the 360 mode was larger than in the primary mode (Figure 4A). However, the luminance in the 360 mode was higher than in the primary mode (Figure 4B). Correlation analysis found no correlation between luminance and pupil diameter in either the 360 mode or the primary mode.

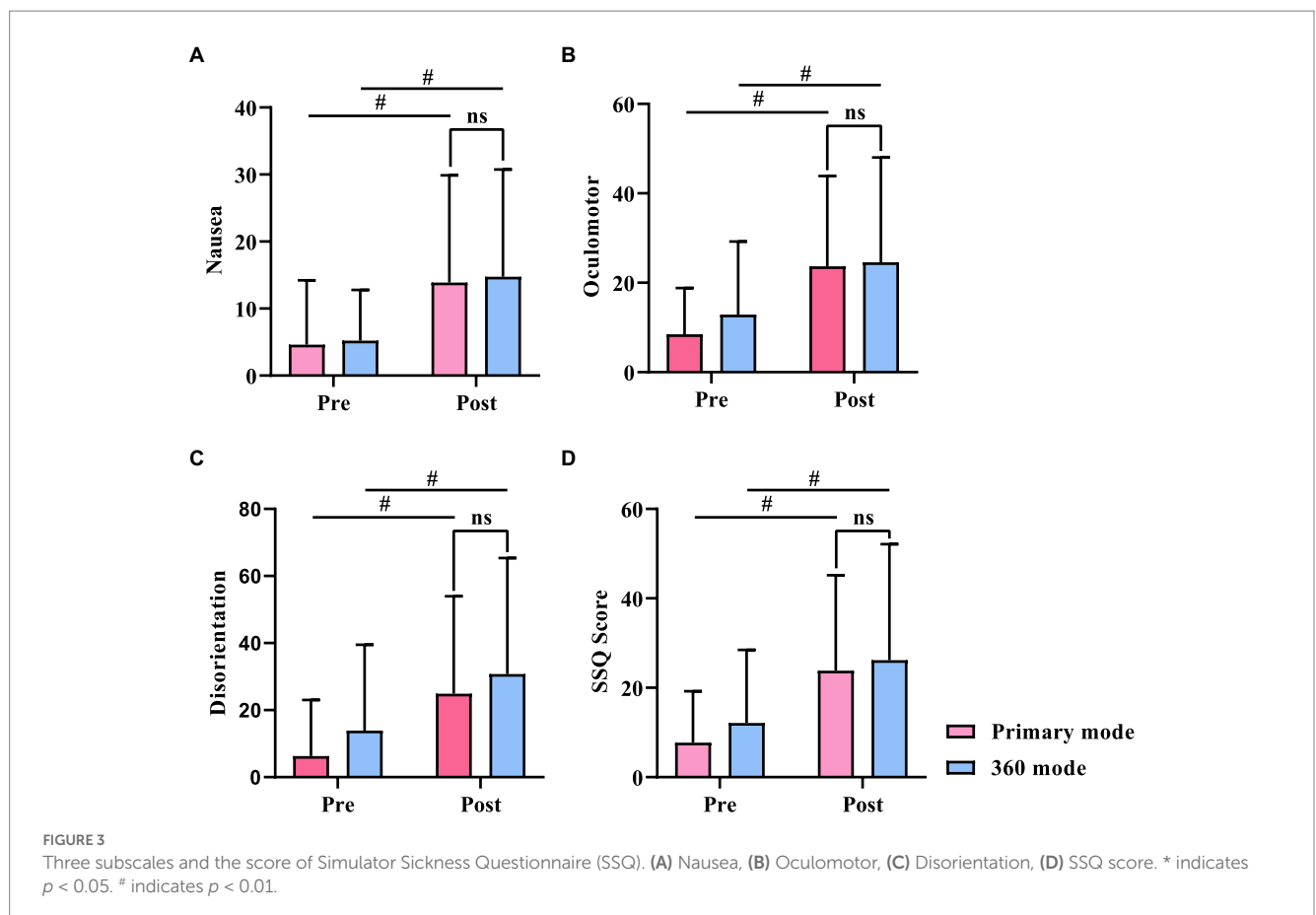
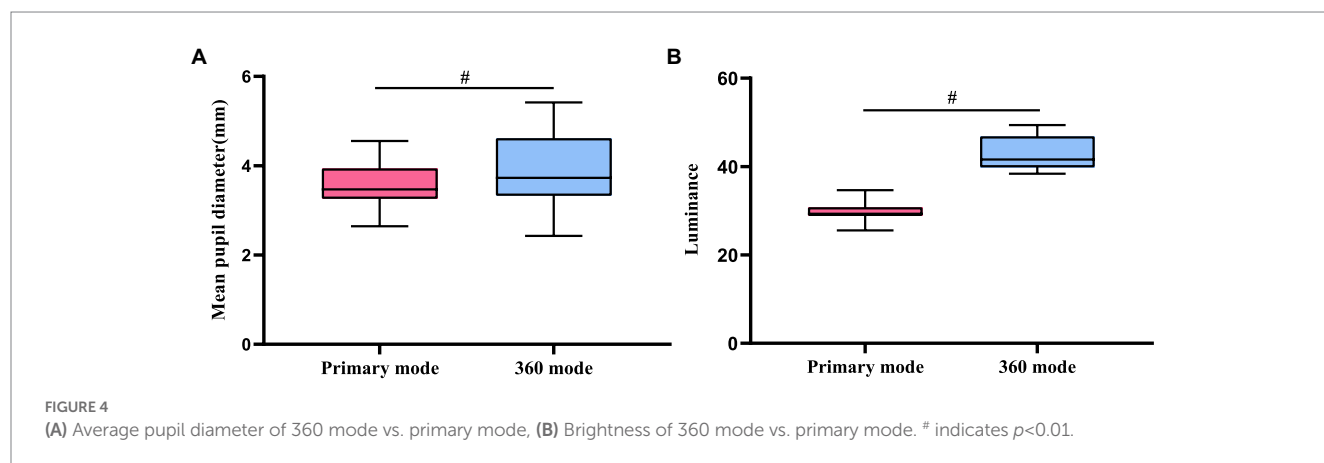


TABLE 1 Primary mode and 360 mode eye movement features analysis.

Eye movement parameters	Primary mode	360 mode	Value of <i>p</i>
Fixation frequency	110.60 ± 7.21	108.00 ± 6.26	0.049
Total fixation duration (s)	1003.59 ± 163.92	747.12 ± 110.74	<0.001
Average fixation duration (s)	305.48 ± 63.32	231.59 ± 38.58	<0.001
Average fixation angle: left eye (°)	12.70 ± 3.53	11.69 ± 3.10	0.074
Average fixation angle: right eye (°)	12.83 ± 3.59	11.92 ± 3.25	0.102
Total saccade duration (s)	788.13 ± 167.65	1049.09 ± 110.77	<0.001
Average saccade duration (s)	236.67 ± 43.68	324.67 ± 37.75	<0.001
Average saccade magnitude: left eye (°)	2.45 ± 0.48	3.07 ± 0.51	<0.001
Average saccade magnitude: right eye (°)	2.40 ± 0.42	3.02 ± 0.49	<0.001
Maximum saccade magnitude: left eye (°)	27.48 ± 4.32	30.35 ± 3.99	0.004
Maximum saccade magnitude: right eye (°)	27.46 ± 3.50	29.99 ± 3.57	0.002
Blinking frequency	20.05 ± 7.71	17.52 ± 7.26	0.029
Average blinking duration (s)	0.48 ± 0.34	0.67 ± 0.68	0.035
Average rotation angle: left eye (°)	12.70 ± 3.44	12.23 ± 2.95	0.396
Average rotation angle: right eye (°)	12.63 ± 3.53	12.30 ± 3.07	0.547

Values of indicators were shown as mean ± standard deviation (SD). The bold values indicate $p < 0.05$.



Discussion

Eye movement behavior is closely related to visual fatigue and eye health. This study investigated the differences in eye movement behavior during different interaction modes in a virtual reality environment and assessed their impact on visual fatigue using subjective questionnaires. Results showed that both interaction modes of the VR experience could lead to visual fatigue, and there were significant differences in eye movement behavior between the primary mode and the 360 mode.

We used two questionnaires to evaluate the different symptoms induced by VR usage. The first questionnaire was the Visual Fatigue Questionnaire, which was used to assess only visual fatigue symptoms. The second questionnaire was SSQ, which was used to assess a range of physical discomfort symptoms induced by VR. Utilizing a combination of these two questionnaires could greatly enhance the strength of our study. The results showed that there were significant differences in visual fatigue scores (Figure 2) and SSQ

scores (Figure 3) before and after the VR experience ($p < 0.05$). These findings suggest that subjects experienced a significant increase in visual fatigue and discomfort after playing VR games for 30 min in both primary and 360 modes. However, there were no significant differences in the scores of the questionnaires between the two modes in terms of visual fatigue or discomfort symptoms, including the three SSQ subscales of nausea, oculomotor, and disorientation symptoms.

It is important to acknowledge that using questionnaires to assess visual fatigue may have limitations due to varying perceptions and definitions of visual fatigue among individuals, as well as their applicability in certain contexts. Additionally, questionnaires may require a certain threshold of visual fatigue to be reached before they can detect it. Therefore, objective methods that can capture the physiological responses of the eye may increase the accuracy and sensitivity of the assessment. In this study, we incorporated eye movement parameters, including blinking and pupil size changes, to evaluate the state of the eye during VR gameplay. Numerous studies

have investigated the relationship between eye movement parameters and visual fatigue (Kim et al., 2011a,b, 2018; Fournassi et al., 2017; Wang et al., 2018, 2019; Parisay et al., 2020). Our findings indicated that there were notable differences in eye movement behavior between the primary mode and the 360 modes.

The measurement of blink parameters is a commonly used objective method for assessing visual fatigue (Heo et al., 2014), with a higher blinking frequency indicating a greater level of visual fatigue. Our results indicate that the blinking frequency is greater in the primary mode than in the 360 mode, whereas the average blinking duration is longer in the 360 mode than in the primary mode. These results suggest that the primary mode causes more visual fatigue than the 360 mode. In the primary mode, the fixation target is only presented from a fixed direction in front of the eyes, and participants are required to experience the virtual scene for 30 min, potentially resulting in boredom and fatigue. The increase in blinking frequency and decrease in blinking duration observed in this study may be a way of mitigating visual fatigue. Zhang and colleagues studied blink characteristics when viewing 3D and 2D videos and found that blinking frequency increased during 3D viewing and decreased during 2D viewing, with no significant differences in blinking duration between the two viewing modes (Zhang et al., 2013). Although our study is not directly comparable to theirs, both studies demonstrated differences in blink parameters when viewing the same content with different modes.

Pupil diameter is another common way of assessing visual fatigue. Previous studies have shown that a decreased pupil diameter is correlated with a more severe level of visual fatigue (Lee et al., 2013; Naeeri et al., 2021). In this study, the pupil diameter was significantly smaller in the primary mode than in the 360 mode (Figure 4A). It is important to note that differences in pupil diameter may also be affected by factors such as scene brightness (Cheng et al., 2006; Lee and Park, 2009) and mental load (Hess and Polt, 1964). However, in our study, the scene brightness was greater in the 360 mode than that in the primary mode (Figure 4B), and further correlation analysis revealed no significant correlation between luminance and pupil diameter in either mode. Thus, we can conclude that differences in pupil diameter between the two modes were not due to differences in scene brightness. The difference in pupil diameter between the two modes may be attributed to differences in task patterns. In the 360 mode, the areas of interest were distributed all around the subject, making the task more complex, exciting, and active, leading to a larger pupil diameter. Conversely, in the primary mode, the objects only come from the front of the subject, and participants may have experienced boredom, resulting in a smaller pupil diameter. These findings also align with our results for blink parameters, suggesting that the primary mode may be more likely to induce visual fatigue than the 360 mode.

Our results showed that the fixation frequency, average fixation duration and total fixation duration were greater in the primary mode than in the 360 mode (Table 1). However, there was no difference in the average fixation angle between the two modes. An increased fixation duration and decreased fixation frequency are a reflection of visual fatigue, as prolonged fixation time may indicate a need for more time to focus and process the information of interest (Naeeri et al., 2021). Feng et al. used fixation frequency and saccade amplitude to assess the effect of far-infrared therapy in relieving visual fatigue and demonstrated

the effectiveness of these parameters in assessing visual fatigue (Feng et al., 2019). While there was no similar study performed before, previous studies can be used to interpret our results. Chapman and Underwood studied the driver's eye movements while watching different scenes (Chapman and Underwood, 1998). They showed that, in rural areas with low visual complexity, eye movements showed longer fixation durations and shorter saccade distances, whereas in urban areas with high visual complexity, eye movements showed shorter fixation durations. In our experiments, the target in the primary mode comes only from a fixed direction in front of the eyes, allowing the participant to spend more time gazing at the target and processing the relevant information. In contrast, in the 360 mode, objects appeared from multiple directions, with a larger environmental area and more visual search required, resulting in shorter fixation durations. Taken together, our findings suggest that the fixation parameters indicate that the primary mode is more likely to cause visual fatigue than the 360 mode, which is consistent with the other parameters examined in our study.

Our study demonstrated a significant difference in saccade parameters between the primary mode and the 360 mode. Specifically, the total saccade duration, average saccade duration, saccade amplitude and maximum saccade amplitude of each eye were greater in the 360 mode than in the primary mode. These differences may be attributed to the interaction modes employed in the 360 mode, which has a larger play area and visual stimulus targets from all around the subjects. This finding is similar to a study on driving on different roads, which found that saccade lengths were longer for urban clips than rural clips (Chapman and Underwood, 1998). Urban roads are generally more complex and hazardous, resulting in greater eye movement behavior, with the human eye requiring constant reception and processing of information.

Our study has several limitations that warrant further study. Subjective measures of visual fatigue are not always accurate, especially when conducting brief virtual reality immersion experiments. During our experiment, participants were standing for the entire 30-min duration. However, in VR, subjects are often more excited and the resulting visual fatigue may be less pronounced and more difficult to assess subjectively. For future studies, it is recommended to extend the experimental time and identify more suitable experimental tasks for assessing visual fatigue in VR environments.

Conclusion

Our study found that both the primary and 360 modes of VR could cause visual fatigue after 30 min of gameplay, with significant differences observed in eye movement behavior between the two modes. Results from objective measurements of blinking and pupil diameter suggest that the primary mode is more likely to cause visual fatigue. Fixation parameters and saccade parameters also showed significant differences between the two modes, possibly due to the different interaction modes employed in the 360 mode. Further study is needed to fully understand the effects of VR on visual fatigue and develop strategies for mitigating any negative effects. This includes researching the impact of various VR content and interactive modes on visual fatigue and developing more objective methods for assessing it.

Data availability statement

The data analyzed in this study is subject to the following licenses/restrictions: The data that support the findings of this study are available at reasonable request from the corresponding author. The data are not publicly available as it is part of an ongoing larger study. Requests to access these datasets should be directed to XW, xiaofei.wang@buaa.edu.cn.

Ethics statement

The studies involving human participants were reviewed and approved by Biomedical Ethics Committee of Beihang University. The patients/participants provided their written informed consent to participate in this study.

Author contributions

LF and JW contributed equally to this work and both are first authors. LF, JW, and XW contributed to the conception of the manuscript, as well as to its writing and revision. LF, ZS, JD, and QL were responsible for collecting and analyzing the data. JW, FB, and XW provided research guidance and supervision throughout the

project. All authors contributed to reading and approving the submitted version.

Funding

This research was supported by National Natural Science Foundation of China (12272030), the 111 Project (B13003) and the Fundamental Research Funds for the Central Universities.

Conflict of interest

The authors declare that the research was conducted in the absence of any commercial or financial relationships that could be construed as a potential conflict of interest.

Publisher's note

All claims expressed in this article are solely those of the authors and do not necessarily represent those of their affiliated organizations, or those of the publisher, the editors and the reviewers. Any product that may be evaluated in this article, or claim that may be made by its manufacturer, is not guaranteed or endorsed by the publisher.

References

- Bang, J., Heo, H., Choi, J. S., and Park, K. (2014). Assessment of eye fatigue caused by 3D displays based on multimodal measurements. *Sensors* 14, 16467–16485. doi: 10.3390/s140916467
- Banstola, S., Hanna, K., and O'Connor, A. (2022). Changes to visual parameters following virtual reality gameplay. *Br. Ir. Orthopt. J.* 18, 57–64. doi: 10.22599/bioj.257
- Blignaut, P. (2009). Fixation identification: the optimum threshold for a dispersion algorithm. *Atten. Percept. Psychophys.* 71, 881–895. doi: 10.3758/APP.71.4.881
- Chapman, P. R., and Underwood, G. (1998). Visual search of driving situations: danger and experience. *Perception* 27, 951–964. doi: 10.1068/p270951
- Cheng, A. C. K., Rao, S. K., Cheng, L. L., and Lam, D. S. C. (2006). Assessment of pupil size under different light intensities using the Procyon pupillometer. *J. Cataract Refract Surg* 32, 1015–1017. doi: 10.1016/j.jcrs.2006.02.033
- DJSCOE, Vile – Parle (W), MumbaiRajesh Desai, P., Nikhil Desai, P., Deepak Ajmera, K., Mehta, K., Deepak Ajmera, K., et al. (2014). A review paper on oculus rift-a virtual reality headset. *Int. J. Eng. Trends Technol.* 13, 175–179. doi: 10.14445/22315381/IJETT-V13P237
- Feng, Y., Wang, L., and Chen, F. (2019). An eye-tracking based evaluation on the effect of far-infrared therapy for relieving visual fatigue, 2019 41st annual international conference of the IEEE engineering in medicine and biology society (EMBC). Presented at the 2019 41st annual international conference of the IEEE engineering in Medicine & Biology Society (EMBC), IEEE, Berlin, Germany, pp. 313–316.
- Fourtassi, M., Rode, G., and Pisella, L. (2017). Using eye movements to explore mental representations of space. *Ann. Phys. Rehabil. Med.* 60, 160–163. doi: 10.1016/j.rehab.2016.03.001
- Heo, H., Lee, W. O., Shin, K. Y., and Park, K. R. (2014). Quantitative measurement of eyestrain on 3D stereoscopic display considering the eye Foveation model and edge information. *Sensors* 14, 8577–8604. doi: 10.3390/s140508577
- Hess, E. H., and Polt, J. M. (1964). Pupil size in relation to mental activity during simple problem-solving. *Science* 143, 1190–1192. doi: 10.1126/science.143.3611.1190
- Hua, H. (2017). Enabling focus cues in head-mounted displays. *Proc. IEEE* 105, 805–824. doi: 10.1109/JPROC.2017.2648796
- Iskander, J., and Hossny, M. (2021). Measuring the likelihood of VR visual fatigue through ocular biomechanics. *Displays* 70:102105. doi: 10.1016/j.displa.2021.102105
- Iskander, J., Hossny, M., and Nahavandi, S. (2019). Using biomechanics to investigate the effect of VR on eye vergence system. *Appl. Ergon.* 81:102883. doi: 10.1016/j.apergo.2019.102883
- Kim, D., Choi, S., Choi, J., Shin, H., and Sohn, K. (2011a). Visual fatigue monitoring system based on eye-movement and eye-blink detection, in: A. J. Woods, N. S. Holliman and N. A. Dodgson (Eds.), Presented at the IS&T/SPIE electronic imaging, San Francisco Airport, California, USA, 786303.
- Kim, D., Choi, S., Park, S., and Sohn, K. (2011b). Stereoscopic visual fatigue measurement based on fusional response curve and eye-blinks, 2011 17th international conference on digital signal processing (DSP). Presented at the 2011 17th international conference on digital signal processing (DSP), IEEE, Corfu, Greece, 1–6.
- Kim, J., Sunil Kumar, Y., Yoo, J., and Kwon, S. (2018). Change of blink rate in viewing virtual reality with HMD. *Symmetry* 10:400. doi: 10.3390/sym10090400
- Lee, W. O., Heo, H., Lee, E. C., and Park, K. R. (2013). Minimizing eyestrain on a liquid crystal display considering gaze direction and visual field of view. *Opt. Eng.* 52:073104. doi: 10.1117/1.OE.52.7.073104
- Lee, E., and Park, K. (2009). Measuring eyestrain from LCD TV according to adjustment factors of image. *IEEE Trans. Consum. Electron.* 55, 1447–1452. doi: 10.1109/TCE.2009.5278012
- Lynch, M. J., and Hockey, R. (1984). Stress and fatigue in human performance. *Am. J. Psychol.* 97:630. doi: 10.2307/1422181
- Maples-Keller, J. L., Bunnell, B. E., Kim, S.-J., and Rothbaum, B. O. (2017). The use of virtual reality Technology in the Treatment of anxiety and other psychiatric disorders. *Harv. Rev. Psychiatry* 25, 103–113. doi: 10.1097/HRP.0000000000000138
- Mirelman, A., Maidan, I., Herman, T., Deutsch, J. E., Giladi, N., and Hausdorff, J. M. (2011). Virtual reality for gait training: can it induce motor learning to enhance complex walking and reduce fall risk in patients with Parkinson's disease? *J. Gerontol. A Biol. Sci. Med. Sci.* 66A, 234–240. doi: 10.1093/gerona/gdq201
- Mohamed Elias, Z., Batumalai, U. M., and Azmi, A. N. H. (2019). Virtual reality games on accommodation and convergence. *Appl. Ergon.* 81:102879. doi: 10.1016/j.apergo.2019.102879
- Naeeri, S., Kang, Z., Mandal, S., and Kim, K. (2021). Multimodal analysis of eye movements and fatigue in a simulated glass cockpit environment. *Aerospace* 8:283. doi: 10.3390/aerospace8100283
- Nguyen, R. M. H., and Brown, M. S. (2017). Why you should forget luminance conversion and do something better, 2017 IEEE conference on computer vision and pattern recognition (CVPR). Presented at the 2017 IEEE conference on computer vision and pattern recognition (CVPR), IEEE, Honolulu, HI, pp. 5920–5928.
- Pallavicini, F., Ferrari, A., Zini, A., Garcea, G., Zancacchi, A., Barone, G., et al. (2018). "What distinguishes a traditional gaming experience from one in virtual reality? An

exploratory study” in *Advances in human factors in wearable technologies and game design*, eds. T. Ahram and C. Falcão, vol. 608 (Cham: Springer International Publishing), 225–231.

Parisay, M., Poullis, C., and Kersten-Oertel, M., (2020). FELiX: fixation-based eye fatigue load index a multi-factor measure for gaze-based interactions, 2020 13th international conference on human system interaction (HSI). Presented at the 2020 13th international conference on human system interaction (HSI), IEEE, Tokyo, Japan, 74–81.

Ruan, B. (2022). VR-assisted environmental education for undergraduates. *Adv. Multimed.* 2022, 1–8. doi: 10.1155/2022/3721301

Szpak, A., Michalski, S. C., and Loetscher, T. (2020). Exergaming with beat saber: an investigation of virtual reality aftereffects. *J. Med. Internet Res.* 22:e19840. doi: 10.2196/19840

Wang, G., and Cui, H., (2014). *Binocular Vision*. Beijing: People's Medical Publishing House 608.

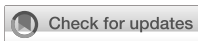
Wang, X., Fisher, L. K., Milea, D., Jonas, J. B., and Girard, M. J. A. (2017). Predictions of optic nerve traction forces and Peripapillary tissue stresses following horizontal eye movements. *Invest. Ophthalmol. Vis. Sci.* 58, 2044–2053. doi: 10.1167/iovs.16-21319

Wang, Y., Zhai, G., Chen, S., Min, X., Gao, Z., and Song, X. (2019). Assessment of eye fatigue caused by head-mounted displays using eye-tracking. *Biomed. Eng. Online* 18:111. doi: 10.1186/s12938-019-0731-5

Wang, Y., Zhai, G., Zhou, S., Chen, S., Min, X., Gao, Z., et al. (2018). Eye fatigue assessment using unobtrusive eye tracker. *IEEE Access* 6, 55948–55962. doi: 10.1109/ACCESS.2018.2869624

Yoon, H. J., Kim, J., Park, S. W., and Heo, H. (2020). Influence of virtual reality on visual parameters: immersive versus non-immersive mode. *BMC Ophthalmol.* 20:200. doi: 10.1186/s12886-020-01471-4

Zhang, L., Ren, J., Xu, L., Qiu, X. J., and Jonas, J. B. (2013). Visual comfort and fatigue when watching three-dimensional displays as measured by eye movement analysis. *Br. J. Ophthalmol.* 97, 941–942. doi: 10.1136/bjophthalmol-2012-303001



OPEN ACCESS

EDITED BY

Pan Long,
Western Theater General Hospital, China

REVIEWED BY

Narendra Kumar Sharma,
Banasthali University, India
Kai Jin,
Zhejiang University, China

*CORRESPONDENCE

Xuemin Li
✉ lxmxm66@sina.com

RECEIVED 22 January 2023

ACCEPTED 04 April 2023

PUBLISHED 09 May 2023

CITATION

Wang Y, Yu X, Liu Z, Lv Z, Xia H, Wang Y,
Li J and Li X (2023) Influence of hypobaric
hypoxic conditions on ocular structure and
biological function at high attitudes: a narrative
review.
Front. Neurosci. 17:1149664.
doi: 10.3389/fnins.2023.1149664

COPYRIGHT

© 2023 Wang, Yu, Liu, Lv, Xia, Wang, Li and Li.
This is an open-access article distributed under
the terms of the [Creative Commons Attribution
License \(CC BY\)](https://creativecommons.org/licenses/by/4.0/). The use, distribution or
reproduction in other forums is permitted,
provided the original author(s) and the
copyright owner(s) are credited and that the
original publication in this journal is cited, in
accordance with accepted academic practice.
No use, distribution or reproduction is
permitted which does not comply with these
terms.

Influence of hypobaric hypoxic conditions on ocular structure and biological function at high attitudes: a narrative review

Yuchen Wang^{1,2}, Xinli Yu³, Ziyuan Liu^{1,2}, Zhongsheng Lv^{1,2},
Huaqin Xia^{1,2}, Yiren Wang^{1,2}, Jiayi Li^{1,2} and Xuemin Li^{1,2*}

¹Department of Ophthalmology, Peking University Third Hospital, Beijing, China, ²Beijing Key Laboratory of Restoration of Damaged Ocular Nerve, Peking University Third Hospital, Beijing, China, ³School of Biological Science and Medical Engineering, Beihang University, Beijing, China

Background: With the development of science and technology, high-altitude environments, involving aviation, aerospace, and mountainous regions, have become the main areas for human exploration, while such complex environments can lead to rapid decreases in air and oxygen pressure. Although modern aircrafts have pressurized cabins and support equipment that allow passengers and crew to breathe normally, flight crew still face repeated exposure to hypobaric and hypoxic conditions. The eye is a sensory organ of the visual system that responds to light and oxygen plays a key role in the maintenance of normal visual function. Acute hypoxia changes ocular structure and function, such as the blood flow rate, and can cause retinal ischemia.

Methods: We reviewed researches, and summarized them briefly in a review.

Results: The acute hypobaric hypoxia affects corneal, anterior chamber angle and depth, pupils, crystal lens, vitreous body, and retina in structure; moreover, the acute hypoxia does obvious effect on visual function; for example, vision, intraocular pressure, oculometric features and dynamic visual performance, visual field, contrast sensitivity, and color perception.

Conclusion: We summarized the changes in the physiological structure and function of the eye in hypoxic conditions and to provide a biological basis for the response of the human eye at high-altitude.

KEYWORDS

hypobaric hypoxia, ocular structure, biological function, high attitude, dynamic visual performance

1. Introduction

With the development of science and technology, high-altitude environments, involving aviation, aerospace, and mountainous regions, have become the main areas for human exploration. However, such complex environments can lead to rapid decreases in air and oxygen pressure, for example, when the flight height changes significantly. Although modern aircrafts have pressurized cabins and support equipment that allow

passengers and crew to breathe normally, flight crew still face repeated exposure to hypobaric and hypoxic conditions. Moreover, helicopters do not normally carry oxygen supply equipment. Thus, hypobarism and hypoxia can become an issue when flying over the plateau.

Human beings struggle to adapt to the hypobaric hypoxia caused by the high-altitude environment, and low-oxygen saturation can be harmful (Burtscher et al., 2021). For example, chronic hypobaric hypoxia can cause brain or lung edema, dyspnea, and emotional and consciousness disorders, while acute hypobaric hypoxia can lead to shock, myocardial infarction, and other adverse events (Petrassi et al., 2012).

The eye is a sensory organ of the visual system that responds to light and oxygen plays a key role in the maintenance of normal visual function. Acute hypobaric hypoxia changes ocular structure and function, such as the blood flow rate, and can cause retinal ischemia (Kaur et al., 2009), while chronic hypobaric hypoxia causes retinal neovascularization. Hypobaric hypoxia also has an impact on human color recognition, dark vision, and contrast sensitivity.

Flying an aircraft has a high visual demand and not only requires precise and timely visual acquisition, but also requires the ability to make accurate judgments based on the surrounding environment. During hypobaric hypoxia, these systems may be compromised, thus affecting the ability of pilots to perform tasks in civil and military situations and posing a potential threat to safety.

Therefore, the purpose of this literature review is to clarify the changes in the physiological structure and function of the eye in hypoxic conditions and to provide a biological basis for the response of the human eye at high-altitude (Figure 1).

2. The influence of hypobaric hypoxia on ocular structure

2.1. Influence on the cornea

Studies have shown that the eyes are one of the most hypoxia-sensitive organs (Akberova et al., 2016). High-altitude exposure affects the normal function of the optical pathway, especially the cornea (Nebbioso et al., 2014), and causes structural changes at different levels of hypobaric hypoxia. Willmann et al. (2013) studied the changes of ocular surface caused by chronic hypobaric hypoxia at high altitudes in 14 healthy adults, who ascended from 1,635 m to 4,559 m within 6 h on a mountain, and stayed at 4,559 m for 4 days. On the day 1 of rapid elevation, the thickness of tear film and the corneal epithelium significantly decreased, while the thickness of the corneal endothelium and corneal stroma significantly increased. Corneal thickness continued to increase until day 4, but rapidly decreased to the baseline level when the group returned to sea level. Thus, staying at 4,559 m for 4 days induced moderate chronic hypobaric hypoxia. Chronic hypobaric hypoxia causes anaerobic glycolysis in corneal epithelial cells and lactic acid accumulation. Eventually, the lactic acid diffuses through the corneal stroma and endothelium and metabolizes in the aqueous humor, leading to osmotic pressure-dependent aqueous humor reflux. This reduces corneal endothelial pump activity and leads to corneal edema and increased corneal thickness (O'Leary et al., 1981). In the lack of oxygen, corneal edema happens, claim Pang et al. (2021). This finding further indicates that corneal edema caused by ATP deficiency and pH changes as a result of lactate/CO₂ accumulation and increased glycolysis are the causes of hypoxia-induced edema.

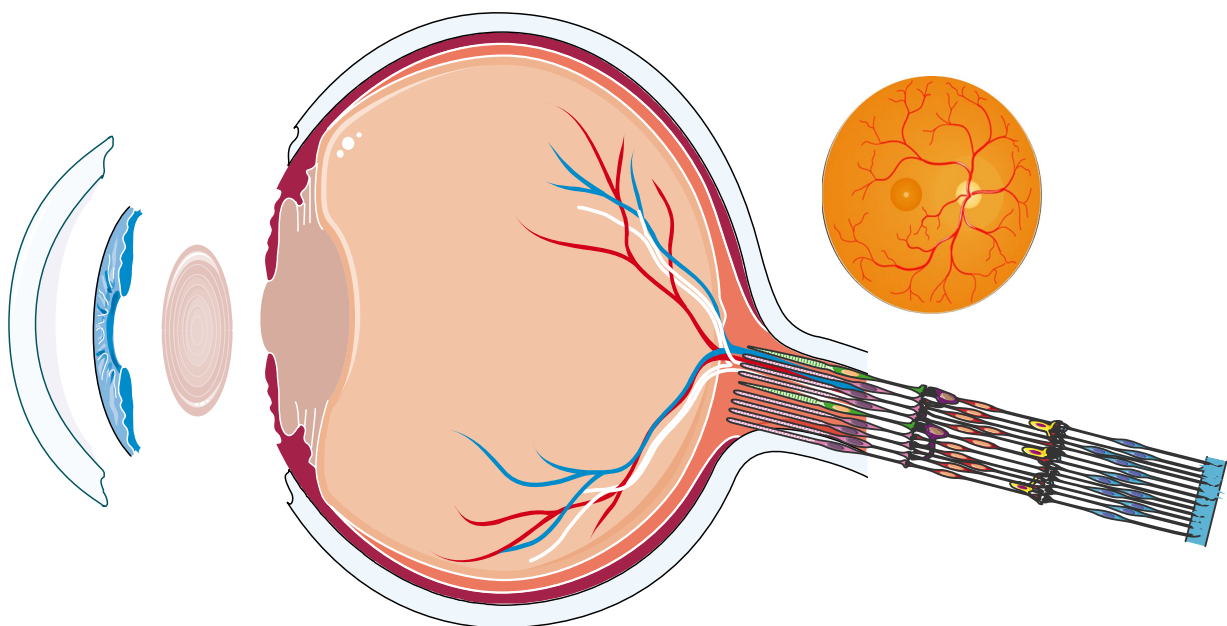


FIGURE 1
The overall structure of the ocular.

Akberova et al. (2016) identified the effects of acute hypobaric hypoxia on conjunctival and corneal epithelium. *In vitro* experiments, whereby mice were placed in an acute hypoxic environment with a pressure of 180 mmHg for 3 min, revealed intracellular DNA breakage and apoptosis in conjunctival and corneal epithelial cells, but not corneal stromal cells. Therefore, it was proposed that conjunctival and corneal epithelial cells initially respond to environmental changes, and activate a protective mechanism to prevent the corneal stroma from being affected by substance metabolism during acute hypobaric hypoxia. As a result, when the cells undergo apoptosis, the normal tear film is damaged, the ocular surface environmental homeostasis is disrupted, and ocular surface diseases such as dry eyes occur.

Therefore, regardless of acute or chronic hypobaric hypoxia, we can predict that high altitudes lead to a disorder in corneal collagen arrangement, a decrease in the stability of the corneal epithelium and tear film layer, an increase in functional irregularity, and the occurrence of clinical symptoms such as dry eye symptoms, decreased vision, and astigmatism. These symptoms can subsequently affect the judgment of flight personnel using the complex instrument panels on aircrafts during flights at high-altitude, posing a threat safety.

2.2. Influence on anterior chamber angle and depth

Acute or chronic angle-closure glaucoma can occur following drastic changes in chamber angle and depth, resulting in vision loss, visual field defects, and serious harm to the optic nerves. Hence, it is important to study the influence of hypobaric hypoxia on the anterior chamber angle (ACA) and anterior opening distance (AOD). Interestingly, in the previous study, the AOD and ACA decreased during the elevation from 1,635 to 4,559 m, and showed a downward trend during the stay at 4,559 m. However, no significant changes in AOD or ACA during exposure to high altitude were noted (Willmann et al., 2013). Similarly, Jatinder et al. demonstrated that there was no statistical difference in AOD long-term follow-up data between residents living at an altitude of 3,300 m and residents living at an altitude of 1,700 m (Bali et al., 2005). Thus, long- and short-term stays in a high-altitude environment may not affect the AOD.

2.3. Influence on pupils

The pupil is an indicator that reflects the effect of hypobaric hypoxia on the central nervous system (CNS). Cymerman et al. (2005) investigated oculomotor reflexes, including pupil diameter (PD), constriction amplitude (CA), constriction latency (CL), and saccadic velocity (SV) during acute hypobaric hypoxia over a period of 2 weeks at 4,300 m with measurements taken every 2 days. They found that PD, CA, and CL were significantly lower than baseline levels and remained up to 14 days (Krusche et al., 2020). Additionally, under different light intensities of 12 cd/m², 1 cd/m², and 0.1 cd/m², the corresponding PDs were 0.55 mm, 0.46 mm, and 0.29 mm, respectively. These values then decreased by 14, 11, and 8% when exposed to hypobaric hypoxia and increased by 9, 5, and 1% under normal oxygen concentration conditions. Thus, exposure to high altitude causes hypoxic myosis, which promotes pupil sphincter activity in the Edinger–Westphal nucleus of the oculomotor nerve in the mesencephalon, leading to

pupil constriction. The retinal afferent light stimulation and supranuclear inhibitory pathways are crucial factors in regulating pupil size. When light is reduced, the supranuclear inhibitory pathway is relatively activated, and hypobaric hypoxia inhibits the activation of the central and parasympathetic nervous systems; thus, constricting the pupil.

2.4. Influence on crystal lens

The influence of acute or chronic hypobaric hypoxia on the lens has not yet been studied in the human eye. The lens naturally exists in a hypoxic environment due to the lack of blood supply, resulting in a decrease in the oxygen concentration from the lens surface to the core. According to a study by Shui et al. (2006), oxygen is distributed differently in various rabbit eye tissues. Under hyperoxic conditions (21% O₂), oxygen concentration was the lowest at the posterior surface of the lens, and decreased more obviously as oxygen levels decreased. Hypobaric hypoxia did not cause changes in the lens structure. Shui and Beebe (2008) subsequently measured the proliferation rate of lens epithelial cells under high- and low-oxygen concentrations *in vitro* and found that the proliferative activity of the cells did not increase when the oxygen level was below normal. In contrast, hypobaric hypoxia has been shown to cause lens maturation through the activation of hypoxia-inducing factor (HIF1a) (Brennan et al., 2020), which regulates hypoxia-responsive genes and promotes the elimination of organelles in epithelial cells, enabling them to differentiate into lens fibrocytes and achieve regular arrangement. In addition, hyperoxia is associated with age-related cataracts. Zhang et al. (2010) studied the rat lens and revealed that oxygen depletion did not induce reactive oxygen species (ROS). Moreover, there was no effect on the gene expression of mitochondrial DNA (mtDNA) and mtDNA base excision repair enzyme (mtBER) in the lens following hypobaric hypoxia, and the nucleus remained transparent. However, ROS were induced when the oxygen concentration increased to 60%, and following a significant increase in oxygen consumption in the lens, the lens fibers became irregular. Consequently, normal age-related lens growth required relatively low-oxygen levels. Overall, hypobaric hypoxia has no effect on the lens.

2.5. Influence on vitreous body

The retina has two major systems that supply oxygen. The outer plexus, where photoreceptor cells are located, receives nutrients through choroid blood circulation, while the inner retina is mainly supplied by the shallow and deep capillary plexuses of the central retinal artery branch. As such, the inner retina is more sensitive to hypobaric hypoxia. Under hypoxic conditions, a large number of soluble factors such as cytokines, chemokines, and growth factors are secreted into the vitreous cavity (dell'Omo et al., 2013). Cytokines are involved in cell proliferation, inflammation, immunity, tissue repair, and other biological processes. They can enhance immune responses by directing the recruitment of leukocytes to sites of inflammation. Growth factors are involved in diabetic retinopathy. During hypobaric hypoxia, macrophages collect in low-oxygen areas, express monocyte chemoattractant protein-1, and release tumor necrosis factor α (TNF- α), which causes the release of interleukin 8 (IL-8) and vascular

endothelial growth factor (VEGF) and eventually results in retinal vasculopathy. Hence, although there is currently no relevant study on the vitreous in acute or chronic hypobaric hypoxia, we cannot underestimate the effect of hypobaric hypoxia on the vitreous body. Further studies are needed to determine whether hypobaric hypoxia affects vitreous composition, liquefaction, and early post-detachment.

2.6. Influence on retina

The retina is a highly differentiated neural structure with poor hypobaric hypoxia tolerance, which causes retinal artery spasm, blood stasis, and an increase in venous pressure and tortuous filling. These can then lead to retinal hemorrhage, macular edema, and even acute retinal artery occlusion following extreme or transient vision loss. Therefore, it is very important for pilots to understand the influence of hypobaric hypoxia on the retina when they encounter emergencies at high altitudes.

Kaur et al. (2009) studied a rat model exposed to 5% oxygen and 95% nitrogen for 2 h and found that hypobaric hypoxia led to damage of the retinal cell structure, increased VEGF concentration and NO production, increased vessel permeability (such that Müller cells became swollen), and neural cell degeneration (Shinojima et al., 2021). Additionally, in rat models exposed to 10% oxygen for 48 h (Mesentier-Louro et al., 2020), hypobaric hypoxia increased expression of proapoptotic transcriptional regulator CCAAT-enhancer-binding protein homologous protein (CHOP) in glial cells in the retina and optic nerve. Histological, immunofluorescence, and morphometric analyses revealed a significant increase in CHOP immunoreactivity in astrocytes in all layers of retinal neurons and in intra-retinal, retro-bulbar, and anterior myelinated optic nerves. As CHOP is a marker of endoplasmic reticulum (ER) stress, we can conclude that hypobaric hypoxia leads to severe retinal stress injury. In addition, hypobaric hypoxia induced an obvious increase in glial fibrillary acidic protein (GFAP), which is associated with the reactive activity of astrocytes, especially in the retina and myelinated nerve fibers. Oligodendrocytes are particularly vulnerable to hypoxic ischemia and it was found that the number of oligodendrocytes obviously decreased during hypobaric hypoxia, indicating that glial function can be impeded in the early stages of hypobaric hypoxia.

In chronic hypobaric hypoxia, the metabolism and survival function of the pigment epithelium and photoreceptors in the outer layer are affected. A longitudinal study by Ebner et al. (2021) conducted over 11 weeks in hypobaric hypoxia at 3,450 m revealed a shortening of photoreceptor segment length, which may indicate that longer durations of hypobaric hypoxia exposure gradually decreases the color discrimination ability and sensitivity of the human eye. However, this has yet to be observed in human studies.

Hypobaric hypoxia can also cause capillary overperfusion (Neumann et al., 2016), resulting in vasogenic cerebral edema. The retina is the only part of the CNS that can observe and measure capillary blood flow. Therefore, it is very important to identify the regulatory properties of the retina and choroid during hypobaric hypoxia. Bosch et al. (2009) observed changes in retinal blood vessels in 27 individuals at different altitudes over 2 weeks and found that the diameter of retinal blood vessels increased significantly, especially arteries, at a height of 4,497 and 5,533 m, but returned to baseline levels when the altitude dropped. Therefore, high altitudes triggered retinal blood vessel dilation. Moreover,

retinal blood flow velocity steadily increased as altitude increased, and peaked at 6,265 m. Afterward, the velocity decreased despite further ascent. This may be related to the vessel diameter, perfusion pressure, blood viscosity, or significantly increased hematocrit. Nevertheless, this showed that retinal blood is sensitive to changes in oxygen concentration and adapts quickly (Baertschi et al., 2016). In contrast, the choroidal capillary flow velocity around the macular fovea did not increase at 4,497 and 5,533 m, but did increase and remained stable after ascending to 6,265 m. The choroid oxygen transport capacity was also relatively high whereas oxygen levels were highly reserved, such that the choroidal blood flow extracted low oxygen, yet remained relatively stable. Frayser et al. (1974) also found that retinal blood flow increased by 89% after 2 weeks of high-altitude exposure at 7,456 m. Following an increase in the duration and altitude of exposure to the plateau environment, blood flow increased by 128% after 1 week and 174% after 7 weeks. Thus, the mechanism of adaption ensured oxygen delivery to the retina. However, there was a steady decline in retinal blood flow velocity after an initial increase, which was associated with increased blood viscosity and hematocrit. Moreover, a case of high-altitude retinopathy with vitreous hemorrhage in 4,760 m high, was reported by Shrestha et al. (2021), the vascular bed or capillaries of tiny arterial collateral leaks are what cause retinal hemorrhage. Due to the increased blood flow and flow velocity, these capillaries may become more brittle. Increased cerebral blood flow and raised cerebral venous pressure are the results of changes in the circulatory and respiratory physiology brought on by changes and abnormalities in retinal hemodynamics and hypobaric hypoxia. These impacts reduce the uptake of cerebrospinal fluid, which causes hypobaric hypoxia to increase cerebrospinal fluid and cause papilledema.

In summary, we found that hypobaric hypoxia led to increased retinal vascular permeability *in vitro*, VEGF and NO metabolite release, ER stress, and ultimately apoptosis and degradation of retinal glial cells and neurons. Hypoxia-induced vascular dilation and increased blood flow velocity have also been observed in humans. Schatz et al. (2013) assessed the functional integrity of retinal layers at 341 and 4,559 m using electroretinography (ERG). The data showed a change in retinal function in the inner, outer, and ganglion cell layers, with the cone-rod response (phototransduction and visual processing) being the most vulnerable, suggesting that cone and rod function may be affected by high-altitude exposure. Furthermore, hypobaric hypoxia may contribute to adverse events such as retinal blood vessel bleeding and loss of photoreceptor cell function.

As such above, hypoxia has a significant effect on the structure of all parts of the human eye, thus affecting visual function.

3. Influences on visual function

Clarifying the influence of acute and chronic hypobaric hypoxia on ocular structure is conducive to our study of the influence of hypobaric hypoxia on visual function.

3.1. Influence on vision

Vision is the most intuitive indicator of the effect of hypobaric hypoxia on the human eye. Gekeler et al. (2019) explored changes in vision in the plateau environment (4,559 m) after 3 days. The average best-corrected visual acuity (BCVA) of participants was -0.19

logMAR at ground level. The average BCVA was 0.01 logMAR on day 2 at 4,559 m, and 0.05 logMAR on day 3 of 4,559 m. A gradual decline in visual acuity was observed, but this was not statistically significant. Winkle et al. (1998) evaluated the effects of hypobaric hypoxia on participants who previously underwent radial keratotomy (RK) surgery, whereby participants were subjected to ocular surface hypobaric hypoxia for 2 h, and found a significant tendency of hyperopic shift and corneal flattening. However, in an experiment conducted by Nelson et al. (2001), the opposite result was found following exposure to hypoxic conditions on the ocular surface in 20 participants who previously underwent laser *in situ* keratomileusis (LASIK) surgery, who experienced obvious myopia drift occurred and corneal steepening. Until now, there has been no literature on specific changes in visual acuity following hypobaric hypoxia exposure; thus, further verification is needed.

3.2. Influence on intraocular pressure

The high-altitude hypobaric hypoxia environment clearly effects intraocular pressure (IOP) (Albis-Donado et al., 2018; Najmanova et al., 2018). Yang et al. (2019) and Bruttini et al. (2020) illustrated that within the moderate altitude range of 1,300 m (19°C) to 3,466 m (−1.4°C), the average IOP at 3,466 m was statistically lower than that at sea level, and altitude significantly correlated with IOP. Subsequently, Willmann et al. (2017) studied IOP at 4,559 m after 3 days and found no significant change compared with baseline levels. However, IOP after corneal thickness correction was measured and was significantly lower than baseline.

Conversely, Wu et al. (2020) measured the IOP of 20 participants after 7 days at 3,658 m (Beijing to Tibet) and found the mean IOP was statistically higher than baseline. In addition, Najmanova et al. (2018) studied IOP at 6,200 m for 4 and 10 min and found that the mean IOP increased by 1.2 mmHg and 0.9 mmHg, respectively, but returned to the baseline level when oxygen was restored. This indicates an upward trend in IOP as altitude increases.

Overall, the studies relating altitude and IOP were mixed; therefore, it was necessary to summarize the relevant results. Yang et al. (2019) conducted a meta-analysis on IOP changes at different altitudes. The data showed that IOP significantly decreased with the increase in altitude between 3,000 and 5,500 m, whereas IOP increased at extreme altitudes of over 5,000 m. They also found that a duration of exposure of more than 72 h was likely to induce a decrease in IOP. A potential reason for this is that the decrease in blood oxygen saturation (Yang and Wang, 2022) at higher altitude inhibits carbonic anhydrase activity and affects the formation of aqueous humor. Alternatively, inhibition of pigmentation-free epithelial cells of the ciliary body may result in decreased aqueous humor production and IOP. The temperature in the plateau environment was significantly lower than the baseline level, causing the local microarteries contracted after exposure and resulting in a decrease in superficial scleral vein pressure; thus, reducing the outflow resistance of the aqueous humor and IOP. Moreover, corneal metabolism switches to anaerobic metabolism in an anoxic environment. This leads to the accumulation of extracellular metabolites and increased extracellular osmotic pressure, which causes corneal edema and increases central corneal thickness and IOP. In summary, many factors affect IOP, but these variations are not obvious. Therefore, we hypothesize that the

high-altitude environment has little influence on IOP, is relatively safe, but needs to be further clarified.

3.3. Influence on oculometric features and dynamic visual performance

During high-altitude flight, pilots need to obtain timely information from the display control interface under motion; therefore, it is important to identify the effect of hypobaric hypoxia on dynamic vision and oculometric features. Data related to ocular movement are direct indicators of biological cognitive activity. Stepanek et al. (2014) assessed oculometric features such as blink metrics, PD, fixations, and saccades under different hypoxic conditions [hypoxic hypoxia (HH) with 8% O₂ and isocapnic hypoxia (IH) with 7% O₂ + 5% CO₂ + balance N₂]. They found that in HH and IH, the blink rate increased by a factor of 1 compared to the baseline level, and the blink rate was faster in HH than in IH. In addition, the blink interval and duration decreased with an increase in blink frequency. Faster recovery of the blink rate occurred when transitioning to normoxia. As for pupil movement, the proportion of PD that significantly increased under HH conditions was significantly higher than that which occurred under IH conditions. PD returned to baseline levels when the oxygen content returned to normal. This may be partly because hypobaric hypoxia activates the sympathetic nervous system, leading to increased dopamine release and blink rate (Panjwani et al., 2006).

Additionally, the time of pupil fixation increased by 8% under HH and 0.4% under IH, but pupil saccade function, such as average saccade length, total saccade times, saccade amplitude, and saccade velocity were not significantly different under different hypoxic conditions. Ocular fixation and micro-saccades are considered as indicators of attention and cognition. Micro-saccades can help counteract visual adaptation by shifting retinal images during movement to maintain visibility during fixation. We found that increased fixation time is required in anoxic environments, suggesting that hypobaric hypoxia may lead to impaired fixation stability. Therefore, oculometric features and access to information may be affected when hypobaric hypoxia occurs during flight.

As dynamic visual performance is an important factor in ensuring the safety of high-altitude flight, Krusche et al. (2020) studied the changes in dynamic visual performance of healthy individuals at 3,647 and 4,554 m. Under the condition that the brightness of the display and the distance from human eyes were stable and consistent, they detected four different motion contrasts: 100, 50, 30, and 20%. The results showed that for 30 and 20% contrast, the dynamic vision performance gradually decreased as the altitude increased, while under 20% contrast, the dynamic vision above the fovea of the macula decreased significantly. Therefore, we believe that hypobaric hypoxia affects the dynamic vision and increases the risk of in-flight accidents.

3.4. Influence on visual field

Through our literature review, we learned that hypobaric hypoxia effects eye movement and dynamic vision. According to the study of Krusche et al. (2020), dynamic vision above the macula fovea significantly changes during hypobaric hypoxia, which suggests that

the visual field may also change. Therefore, it is necessary to review the effects of hypobaric hypoxia on the visual field. [Hornig et al. \(2008\)](#) studied 15 healthy young male pilots with a mean arterial oxygen saturation (SaO₂) of 99% and a mean visual field sensitivity of 43.9 dB at ground level. When the altitude increased to 7,620 m, SaO₂ dropped to 64% within 3 min and the mean visual sensitivity was significantly reduced by 7.2 dB. In the range of 0°–10°, the visual sensitivity decreased by 6.1 dB on average. In the range of 10°–20°, the visual sensitivity decreased by 7.0 dB. In the range of 20°–30°, the peripheral visual sensitivity decreased by 8.3 dB. Therefore, peripheral visual sensitivity diminished more than central sensitivity. Furthermore, [Feigl et al. \(2011\)](#) analyzed absolute sensitivities (in dB) at 1°, 3°, 6°, 10°, 15°, 22°, and 30° eccentricities, and the mean defect (MD) and pattern defect (PD) were calculated by static and flicker visual perimetry. Under photopic illumination, flicker and static visual field sensitivities at all eccentricities, or MD and PD, were not significantly different between hypoxic and normoxic conditions. However, the static field was more sensitive than the flicker field in detecting low-sensitivity areas under hypoxic and normal oxygen conditions.

These findings are consistent with previous studies that have shown that the retina is unable to perform its normal physiological functions under hypobaric hypoxia, ER stress, or photoreceptor cell damage.

The decrease in the peripheral visual field was more obvious than that in the central visual field during hypobaric hypoxia. This may be related to the accumulation of rods in the peripheral visual field and distribution of cones in the central part of the retina. Hypobaric hypoxia leads to an increased threshold of rods and cones in the visual field, and a decreased response to light stimulation. Thus, visual field sensitivity decreased with a decrease in oxygen concentration.

3.5. Influence on contrast sensitivity

Contrast sensitivity (CS) is a very important function for pilots to observe their surroundings during night flights. [Connolly and Hosking \(2009\)](#) preliminarily explored the CS threshold under hypoxic conditions at 3,048 m and found that the sensitivity threshold significantly correlated with oxygen at ~1 cd/m² and that contrast acuity obviously decreased and increased after 100% oxygen inhalation. Therefore, oxygen supply can enhance dynamic CS during flight, which is conducive to flight safety.

[Gekeler et al. \(2019\)](#) also investigated the change in CS during hypobaric hypoxia. The average CS at ground level was 1.28 logCS, while the average CS at 4,559 m was 1.03 logCS on day 1, −0.10 logCS on day 2, and −0.12 logCS on day 3. Therefore, the CS significantly decreased at 4,559 m, which positively correlated with oxygen saturation.

Hypobaric hypoxia also affects night vision, which includes light sensitivity in the peripheral and central parts of the retina. [Gekeler et al. \(2019\)](#) confirmed that night vision gradually decreased under hypobaric hypoxia conditions as altitude increased, and that the dark adaptation threshold increased and delayed the dark adaptation peak. Under mesopic conditions at dusk, the oxygen consumption of photoreceptors, especially rods, is enhanced compared to bright light conditions, making the outer retina more sensitive to low oxygen at light levels associated with night flight. [Connolly and Barbur \(2009\)](#) examined the oxygenation state on the contrast thresholds required to

maintain visual acuity at low photopic (12 cd/m²), upper mesopic (1 cd/m²), and mid-mesopic (0.1 cd/m²) luminance. They found that the contrast threshold increased at all light levels, particularly at 1 cd/m² to 0.1 cd/m², relative to normoxia. Hypobaric hypoxia increases contrast thresholds; thus, visual performance between ~10 cd/m² and 0.1 cd/m² is oxygen-dependent.

Under dim conditions, contrast sensitivity decreases due to low photopic vision, glare, and shadows. However, hypobaric hypoxia has a more significant effect on contrast sensitivity. According to a previous study, hypobaric hypoxia led to dysfunction of photoreceptor cells under dim conditions. Contrast sensitivity may be further decreased as dark adaptation is prolonged. Consequently, changes in pupil size under dim light may also affect the appearance of ocular problems, such as high-order aberrations. Thus, as the influence of the pupil was not excluded in the above experiments, this should be clarified further.

3.6. Influence on color perception

[Connolly and Barbur \(2009\)](#) showed that hypobaric hypoxia impacted the ratio of red to green in the color scope test in individuals with normal color vision (NCV), such that the ratio of green fluorescence in NCV individuals was lower than that under normal oxygen concentrations.

[Hovis et al. \(2012\)](#) revealed that color assessment and diagnosis (CAD) test results at 3,780 m above sea level suggested that the red-green thresholds of NCV patients relatively increased, while the yellow-blue thresholds did not notably change. Conversely, [Connolly et al. \(2008\)](#) found that hypobaric hypoxia significantly impaired color sensitivity at the lowest light level, in which red-green and yellow-blue thresholds were noticeably impaired, with the latter most affected. Yellow-blue threshold asymmetry obvious at the lowest light level, such that the yellow threshold corresponded to an increase in the short-wave sensitive cone signal, which was more damaged than the complementary blue threshold, indicating that the increase and decrease in the short-wave sensitive cone signal were asymmetrical at low light levels.

[Connolly and Serle \(2014\)](#) investigated the ability to recognize information using night-vision equipment and dim dashboards under hypoxic conditions, and noted the changes in recognition thresholds after inhaling oxygen. They hypothesized that mild breathing disorders may lead to a decrease in color sensitivity. When the background color of the night-vision instrument was green, the brightness was 1.0 cd/m² and 3.0 cd/m², while the dim instrument panel was 1.0 cd/m² and 0.1 cd/m². Color threshold discrimination was detected under normal (air), hyperoxic (100% O₂), and hypoxic (13.7% O₂) environments. They found that oxygen was an important factor when discriminating color, as the red-green and rod-related color thresholds were enhanced by 20–25% during hypobaric hypoxia and enhanced by 50% when using the night-vision device. Hypobaric hypoxia leads to increased metabolic demand and slowed signal conduction; hence, hypobaric hypoxia at high altitudes has a certain impact on the recognition ability of human color vision.

[Hovis et al. \(2012\)](#) revealed the relationship between altitude and color sensitivity in individuals with NCV and red-green vision deficits. The color threshold was measured using the Cambridge color test (CCT), the color assessment and diagnosis (CAD) test, and the cone

TABLE 1 Effects of hypoxia on ocular structure and function.

Subjects	Age (number)	Hypoxia conditions	Main results	Citation	Duration of hypoxia
Rats	3 months (20)	Hypoxia was created by pumping air from the pressure chamber for 1 min before reaching a pressure of 180 mm Hg	The DNA were damaged and apoptosis in the anterior epithelium of the cornea and conjunctiva	Akberova et al. (2016)	1 min
Rats	1-day-old	Hypoxia was created by a chamber filled with a gas mixture of 5% oxygen/95% nitrogen	Muller cell processes were swollen in the inner nuclear layer, ganglion cells were swollen and mitochondria were disrupted	Kaur et al. (2009)	2 h
Rats	6–8 weeks	Hypoxia was created by a chamber filled with 20.9–10% oxygen	Hypoxia induced thinning of the retina on OCT but little cell loss on histology. Hypoxia led to significant reduction of total number of oligodendroglia in the optic nerve	Mesentier-Louro et al. (2020)	48 h
Rats	9 weeks (6)	Mice were exposed to short-term hypobaric hypoxia at 3,450 m above sea level	Rod segment length showed a significant shortening	Ebner et al. (2021)	48 h
Healthy humans	Not specific (6)	5,334 m	The circulated retinal blood flow of $367 \text{ mL} \cdot 100 \text{ g}^{-1} \cdot \text{min}^{-1}$ was significantly greater than the flow of $331 \text{ mL} \cdot 100 \text{ g}^{-1} \cdot \text{min}^{-1}$	Frayser et al. (1974)	5 days
Radial keratotomy (RK) humans	26–58 years (20)	Humidified compressed air (20% oxygen) was filtered on one side and humidified 100% nitrogen (0% oxygen) on the other side. (sealed goggle-type microenvironment chamber)	A significant hyperopic shift and corneal flattening occurred in all subjects with RK compared with those of control subjects	Winkle et al. (1998)	2 h
Healthy humans	26–58 years (20)	Humidified compressed air (20% oxygen) was filtered on one side and humidified 100% nitrogen (0% oxygen) on the other side. (sealed goggle-type microenvironment chamber)	A significant increase in corneal thickening occurred	Winkle et al. (1998)	2 h
Laser <i>in situ</i> keratomileusis (LASIK) humans	38.8 years (20)	Humidified nitrogen (airtight goggle system)	A significant myopic shift occurred in LASIK corneas exposed to hypoxia compared with myopic control subjects. A significant increase in corneal thickening occurred	Nelson et al. (2001)	2 h
Healthy humans	38.8 years (20)	Humidified nitrogen (airtight goggle system)	A significant increase in corneal thickening occurred	Nelson et al. (2001)	2 h
Healthy humans	Not specific	4,300 m (transport)	The pupil diameter and constriction latency decreased. The constriction amplitude decreased. The saccadic velocity increased	Cymerman et al. (2005)	48 h
Healthy humans	31.4 (15)	7,620 m (simulated)	Mean visual sensitivity was significantly reduced. Peripheral sensitivity was slightly but significantly more diminished than central sensitivity	Horng et al. (2008)	3 min

(Continued)

TABLE 1 (Continued)

Subjects	Age (number)	Hypoxia conditions	Main results	Citation	Duration of hypoxia
Healthy humans	30	3,048 m (mask)	At mesopic luminance (1 cd/m ²), sensitivity was consistently poorest with hypoxia and greatest with supplementary oxygen at all eccentricities and in all field quadrants, suggesting oxygen-dependent performance. Hypoxia significantly impaired color sensitivity at the lowest light level, in which red-green and yellow-blue thresholds were noticeably impaired	Connolly and Barbur (2009)	1 h
Healthy humans	43 years (27)	4,497 m (hike) 5,533 m (hike) 6,265 m (hike) 7,546 m (hike)	The initial increase in macular retinal blood velocity was followed by a decrease at higher altitudes despite further ascent, whereas choroidal flow increase occurred later, at even higher altitudes	Bosch et al. (2009)	4,497 m–3 d 5,533 m–3 d 6,265 m–6 d 7,546 m–3 d
Healthy humans	20.9 ± 0.5 (14)	Breathing 12% oxygen (hypoxia)	Under photopic illumination, flicker and static visual field sensitivities at all eccentricities were not significantly different between hypoxia and normoxia conditions	Feigl et al. (2011)	3 min
Healthy humans	37.6 ± 12.6 (13)	3,780 m (stimulated)	The red-green thresholds of NCV patients relatively increased, while the yellow-blue thresholds did not notably change	Hovis et al. (2012a)	4.5 h
Healthy humans	25–54 years (13)	4,559 m (cable car)	The maximum response of the scotopic sensitivity function, the implicit times of the a- and b-wave of the combined rod-cone responses, and the implicit times of the photopic negative responses (PhNR) were significantly altered. The most affected ERG parameters are related to combined rod-cone responses, which indicate that phototransduction and visual processing, especially under conditions of rod-cone interaction, are primarily affected at high altitude	Schatz et al. (2013)	48 h
Healthy humans	36 ± 9 years (14)	4,559 m (trekking)	A significant increase of CCT during altitude exposure due to stromal edema were shown. This change was completely reversible upon descent	Willmann et al. (2013)	48 h
Healthy humans	32 ± 5 (20)	5,486 m (hypobaric chamber with 10% oxygen mask)	Pachymetry values related to corneal thickness in conditions of hypobarism revealed a statistically significant increase	Nebbioso et al. (2014)	Not specific
Healthy humans	32.4 ± 9.8 (25)	7,894 m (mask)	Blink rates were significantly increased under hypoxic conditions. The percentage change in pupil size fluctuation was increased. Total saccadic times under hypoxic conditions were significantly increased compared with normoxia	Stepanek et al. (2014)	3 min
Healthy humans	32.8 ± 5.8 (12)	Breathing 13.7% oxygen, balance nitrogen	Contrast acuity thresholds were elevated consistently under hypoxia by up to 25% relative to breathing oxygen	Connolly and Serle (2014)	1 h

(Continued)

TABLE 1 (Continued)

Subjects	Age (number)	Hypoxia conditions	Main results	Citation	Duration of hypoxia
Healthy humans	46.6 ± 7.8 years (33)	6,000 m (trekking)	Retinal venous pressure and ocular perfusion pressure changed significantly at both high altitude of 4,200 and 6,000 m	Baertschi et al. (2016)	Not specified
Healthy humans	36.7 ± 10.8 (17)	3,000 m (funicular)	Retinal arterial and venous diameter increased, arterial and venous response to flicker light decreased	Neumann et al. (2016)	48 h
Healthy humans	34.9 (26)	Breathing 12% oxygen 87% nitrogen (diluting tanked)	Under mesopic hypoxia conditions, the known high-oxygen demand of rods may reduce the retinal oxygen available for cones thereby diminishing color sensitivity as well as other cone functions	Temme et al. (2017)	15 min
Healthy humans	41.7 ± 9.4 (41)	2,234 m (sea level)	Mean IOP with Dynamic contour tonometry showed not a significant difference. Mean Goldmann applanation tonometry IOP at the two altitudes was statistically significant difference	Albis-Donado et al. (2018)	24 h
Healthy humans	25.2 ± 3.8 (38)	6,200 m (simulated)	The hypoxia induced changes in intraocular pressure were significantly correlated with the arterial oxygen saturation changes, whereas the relationship with intraocular pressure baseline and initial heart rate were insignificant	Najmanova et al. (2018)	10 min
Healthy humans	35 ± 8 years (14)	4,559 m (cable car)	A significant decrease in contrast sensitivity (CS) was found for Weber CS at high altitude compared with baseline. Visual acuity remained unchanged	Gekeler et al. (2019)	48 h
Healthy humans	24 ± 2.5 year (11)	4,554 m (hike)	A significant reduction in dynamic visual performance in the superior parafoveal retinal subfield, partly representing the lower visual field	Krusche et al. (2020)	48 h
Healthy humans	24.0 ± 2.5 (11)	4,223 m (hike)	A significant reduction in dynamic visual performance in the superior parafoveal retinal subfield, partly representing the lower visual field	Krusche et al. (2020)	6 days

specific contrast test (CSCT) at the ground and at 3,780 m. CAD showed that the red-green threshold slightly increased by 10% for trichromatic individuals, while the yellow-blue threshold did not significantly change. For dichroic individuals (i.e., the red-green-deficient population), the blue-yellow threshold slightly increased. Meanwhile, the red-green threshold did not notably increase and no significant changes were observed in the other colors. CCT and CSCT did not reveal any significant changes in chromatic thresholds. The oxygen concentration at which color perception begins to be impaired corresponds to ~2,400 m above sea level. As the altitude increased to 3,000 m, the range of impaired color discrimination began to involve visible light, and the loss of color discrimination became more pronounced above 4,000 m. In conclusion (Temme et al., 2017), the color sensitivity of human eyes at low light levels changes, especially the asymmetric change in the yellow-blue threshold during hypobaric hypoxia. Rod density increases and cone density decreases further away from the fovea, and the color sensitivity is more susceptible to the influence of hypobaric hypoxia. However, the mechanism remains unclear (Table 1).

4. Discussion

In summary, visual perception activities in high-altitude flights are more complex and involves not only static vision but also dynamic vision, which encompasses the observer's ability to recognize dynamic target details. High-altitude hypoxic environments cause changes in the physiological structure of the eye, such as corneal thickness and rod and cone cell density, and in biological optics, such as diopter state changes. These changes affect the overall visual function of the human eye, such as color discrimination, color sensitivity, the resolution of external objects under different light intensities, such as contrast sensitivity, and the recognition of moving objects from different aspects. However, much is still unknown, especially with regard to color sensitivity as changes in red-green and yellow-blue perception thresholds can lead to serious visual difficulties for pilots when flying at the plateau. Therefore, further research on the changes in visual color perception caused by the plateau environment is required.

References

- Akberova, S. I., Markitantova, Y. V., Ryabtseva, A. A., and Stroeve, O. G. (2016). Hypoxia as pathogenic factor affecting the eye tissues: the selective apoptotic damage of the conjunctiva and anterior epithelium of the cornea. *Dokl. Biochem. Biophys.* 467, 150–152. doi: 10.1134/S1607672916020198
- Albis-Donado, O., Bhartiya, S., Gil-Reyes, M., Casale-Vargas, G., Arreguin-Rebollar, N., and Kahook, M. Y. (2018). Citius, Altius, Fortius: agreement between Perkins and dynamic contour tonometry (Pascal) and the impact of altitude. *J. Curr. Glaucoma Pract.* 12, 40–44. doi: 10.5005/jp-journals-10028-1242
- Baertschi, M., Dayhaw-Barker, P., and Flammer, J. (2016). The effect of hypoxia on intra-ocular, mean arterial, retinal venous and ocular perfusion pressures. *Clin. Hemorheol. Microcirc.* 63, 293–303. doi: 10.3233/CH-152025
- Bali, J., Chaudhary, K. P., and Thakur, R. (2005). High altitude and the eye: a case controlled study in clinical ocular anthropometry of changes in the eye. *High Alt. Med. Biol.* 6, 327–338. doi: 10.1089/ham.2005.6.327
- Bosch, M. M., Merz, T. M., Barthelmes, D., Petrig, B. L., Truffer, F., Bloch, K. E., et al. (2009). New insights into ocular blood flow at very high altitudes. *J. Appl. Physiol.* 106, 454–460. doi: 10.1152/japphysiol.90904.2008
- Brennan, L., Disatham, J., and Kantorow, M. (2020). Hypoxia regulates the degradation of non-nuclear organelles during lens differentiation through activation of HIF1a. *Exp. Eye Res.* 198:108129. doi: 10.1016/j.exer.2020.108129
- Bruttini, C., Verticchio Vercellin, A., Klersy, C., de Silvestri, A., Tinelli, C., Riva, I., et al. (2020). The Mont Blanc study: the effect of altitude on intra ocular pressure

Author contributions

YuW reviewed the literatures and drafted the manuscript. XY, HX, JL, ZhL, and YiW participated in the translation of articles. ZiL reviewed the manuscript. XL gave final approval of the version to be submitted and any revised version. All authors contributed to the article and approved the submitted version.

Funding

This study was supported by Beijing Natural Science Foundation, grant number 7202229.

Acknowledgments

Thanks to SMART SERVICE MEDICAL ART for providing us with the original images. We thank XL and their team at the Peking university third hospital in reviewing the articles. The content of the manuscript has not been previously appeared online.

Conflict of interest

The authors declare that the research was conducted in the absence of any commercial or financial relationships that could be construed as a potential conflict of interest.

Publisher's note

All claims expressed in this article are solely those of the authors and do not necessarily represent those of their affiliated organizations, or those of the publisher, the editors and the reviewers. Any product that may be evaluated in this article, or claim that may be made by its manufacturer, is not guaranteed or endorsed by the publisher.

and central corneal thickness. *PLoS One* 15:e0237343. doi: 10.1371/journal.pone.0237343

Burtscher, J., Mallet, R. T., Burtscher, M., and Millet, G. P. (2021). Hypoxia and brain aging: neurodegeneration or neuroprotection? *Ageing Res. Rev.* 68:101343. doi: 10.1016/j.arr.2021.101343

Connolly, D. M., and Barbur, J. L. (2009). Low contrast acuity at photopic and mesopic luminance under mild hypoxia, normoxia, and hyperoxia. *Aviat. Space Environ. Med.* 80, 933–940. doi: 10.3357/asm.2535.2009

Connolly, D. M., Barbur, J. L., Hosking, S. L., and Moorhead, I. R. (2008). Mild hypoxia impairs chromatic sensitivity in the mesopic range. *Invest. Ophthalmol. Vis. Sci.* 49, 820–827. doi: 10.1167/iops.07-1004

Connolly, D. M., and Hosking, S. L. (2009). Oxygenation state and mesopic sensitivity to dynamic contrast stimuli. *Optom. Vis. Sci.* 86, 1368–1375. doi: 10.1097/OPX.0b013e3181be9d89

Connolly, D. M., and Serle, W. P. (2014). Assisted night vision and oxygenation state: 'steady adapted gaze'. *Aviat. Space Environ. Med.* 85, 120–129. doi: 10.3357/asm.3764.2014

Cymerman, A., Muza, S. R., Friedlander, A. L., Fulco, C. S., and Rock, P. B. (2005). Saccadic velocity and pupillary reflexes during acclimatization to altitude (4300 m). *Aviat. Space Environ. Med.* 76, 627–634.

- dell'Omo, R., Semeraro, F., Bamonte, G., Cifariello, F., Romano, M. R., and Costagliola, C. (2013). Vitreous mediators in retinal hypoxic diseases. *Mediat. Inflamm.* 2013:935301. doi: 10.1155/2013/935301
- Ebner, L. J. A., Samardzija, M., Storti, F., Todorova, V., Karademir, D., Behr, J., et al. (2021). Transcriptomic analysis of the mouse retina after acute and chronic normobaric and hypobaric hypoxia. *Sci. Rep.* 11:16666. doi: 10.1038/s41598-021-96150-9
- Feigl, B., Zele, A. J., and Stewart, I. B. (2011). Mild systemic hypoxia and photopic visual field sensitivity. *Acta Ophthalmol.* 89, e199–e204. doi: 10.1111/j.1755-3768.2010.01959.x
- Frayser, R., Gray, G. W., and Houston, C. S. (1974). Control of the retinal circulation at altitude. *J. Appl. Physiol.* (1985) 37, 302–304. doi: 10.1152/jappl.1974.37.3.302
- Gekeler, K., Schatz, A., Fischer, M. D., Schommer, K., Boden, K., Bartz-Schmidt, K. U., et al. (2019). Decreased contrast sensitivity at high altitude. *Br. J. Ophthalmol.* 103, 1815–1819. doi: 10.1136/bjophthalmol-2018-313260
- Horng, C. T., Liu, C. C., Wu, D. M., Wu, Y. C., Chen, J. T., Chang, C. J., et al. (2008). Visual fields during acute exposure to a simulated altitude of 7620 m. *Aviat. Space Environ. Med.* 79, 666–669. doi: 10.3357/ASEM.2160.2008
- Hovis, J. K., Milburn, N. J., and Nesthus, T. E. (2012). Hypoxia, color vision deficiencies, and blood oxygen saturation. *J. Opt. Soc. Am. A Opt. Image Sci. Vis.* 29, A268–A274. doi: 10.1364/JOSAA.29.00A268
- Kaur, C., Sivakumar, V., Foulds, W. S., Luu, C. D., and Ling, E. A. (2009). Cellular and vascular changes in the retina of neonatal rats after an acute exposure to hypoxia. *Invest. Ophthalmol. Vis. Sci.* 50, 5364–5374. doi: 10.1167/iops.09-3552
- Krusche, T., Limmer, M., Jendrusch, G., and Platen, P. (2020). Influence of natural hypobaric hypoxic conditions on dynamic visual performance. *High Alt. Med. Biol.* 21, 1–11. doi: 10.1089/ham.2019.0033
- Mesentier-Louro, L. A., Shariati, M. A., Dalal, R., Camargo, A., Kumar, V., Shamskhou, E. A., et al. (2020). Systemic hypoxia led to little retinal neuronal loss and dramatic optic nerve glial response. *Exp. Eye Res.* 193:107957. doi: 10.1016/j.exer.2020.107957
- Najmanova, E., Pluhacek, F., Botek, M., Krejci, J., and Jarosova, J. (2018). Intraocular pressure response to short-term extreme Normobaric hypoxia exposure. *Front. Endocrinol. (Lausanne)* 9:785. doi: 10.3389/fendo.2018.00785
- Nebbioso, M., Fazio, S., Di Blasio, D., and Pescosolido, N. (2014). Hypobaric hypoxia: effects on intraocular pressure and corneal thickness. *ScientificWorldJournal* 2014:585218. doi: 10.1155/2014/585218
- Nelson, M. L., Brady, S., Mader, T. H., White, L. J., Parmley, V. C., and Winkle, R. K. (2001). Refractive changes caused by hypoxia after laser in situ keratomileusis surgery. *Ophthalmology* 108, 542–544. doi: 10.1016/s0161-6420(00)00592-3
- Neumann, T., Baertschi, M., Vilser, W., Drinda, S., Franz, M., Brückmann, A., et al. (2016). Retinal vessel regulation at high altitudes. *Clin. Hemorheol. Microcirc.* 63, 281–292. doi: 10.3233/CH-162041
- O'Leary, D. J., Wilson, G., and Henson, D. B. (1981). The effect of anoxia on the human corneal epithelium. *Am. J. Optom. Physiol. Optic* 58, 472–476.
- Pang, K., Lennikov, A., and Yang, M. (2021). Hypoxia adaptation in the cornea: current animal models and underlying mechanisms. *Animal Model Exp. Med.* 4, 300–310. doi: 10.1002/ame2.12192
- Panjwani, U., Thakur, L., Anand, J. P., Malhotra, A. S., and Banerjee, P. K. (2006). Effect of simulated ascent to 3500 meter on neuro-endocrine functions. *Indian J. Physiol. Pharmacol.* 50, 250–256.
- Petrassi, F. A., Hodkinson, P. D., Walters, P. L., and Gaydos, S. J. (2012). Hypoxic hypoxia at moderate altitudes: review of the state of the science. *Aviat. Space Environ. Med.* 83, 975–984. doi: 10.3357/ASEM.3315.2012
- Schatz, A., Willmann, G., Fischer, M. D., Schommer, K., Messias, A., Zrenner, E., et al. (2013). Electroretinographic assessment of retinal function at high altitude. *J. Appl. Physiol.* (1985) 115, 365–372. doi: 10.1152/japplphysiol.00245.2013
- Shinojima, A., Lee, D., Tsubota, K., Negishi, K., and Kurihara, T. (2021). Retinal diseases regulated by hypoxia-basic and clinical perspectives: a comprehensive review. *J. Clin. Med.* 10:5496. doi: 10.3390/jcm10235496
- Shrestha, A., Suwal, R., and Shrestha, B. (2021). Vitreous hemorrhage following high-altitude retinopathy. *Case Rep. Ophthalmol. Med.* 2021, 7076190–7076193. doi: 10.1155/2021/7076190
- Shui, Y. B., and Beebe, D. C. (2008). Age-dependent control of lens growth by hypoxia. *Invest. Ophthalmol. Vis. Sci.* 49, 1023–1029. doi: 10.1167/iops.07-1164
- Shui, Y. B., Fu, J. J., Garcia, C., Dattilo, L. K., Rajagopal, R., McMillan, S., et al. (2006). Oxygen distribution in the rabbit eye and oxygen consumption by the lens. *Invest. Ophthalmol. Vis. Sci.* 47, 1571–1580. doi: 10.1167/iops.05-1475
- Stepanek, J., Pradhan, G. N., Cocco, D., Smith, B. E., Bartlett, J., Studer, M., et al. (2014). Acute hypoxic hypoxia and isocapnic hypoxia effects on oculometric features. *Aviat. Space Environ. Med.* 85, 700–707. doi: 10.3357/ASEM.3645.2014
- Temme, L. A., St. Onge, P., and O'Brien, K. (2017). "Color vision in the twilight zone: an unsolved problem," in *Proc. SPIE 10197, Degraded Environments: Sensing, Processing, and Display*.
- Willmann, G., Schatz, A., Zhou, A., Schommer, K., Zrenner, E., Bartz-Schmidt, K. U., et al. (2013). Impact of acute exposure to high altitude on anterior chamber geometry. *Invest. Ophthalmol. Vis. Sci.* 54, 4241–4248. doi: 10.1167/iops.13-12158
- Willmann, G., Schommer, K., Schultheiss, M., Fischer, M. D., Bartz-Schmidt, K. U., Gekeler, F., et al. (2017). Effect of high altitude exposure on intraocular pressure using Goldmann Applanation tonometry. *High Alt. Med. Biol.* 18, 114–120. doi: 10.1089/ham.2016.0115
- Winkle, R. K., Mader, T. H., Parmley, V. C., White, L. J., and Polse, K. A. (1998). The etiology of refractive changes at high altitude after radial keratotomy. Hypoxia versus hypobaria. *Ophthalmology* 105, 282–286. doi: 10.1016/s0161-6420(98)93094-9
- Wu, Y., Qiong Da, C. R., Liu, J., and Yan, X. (2020). Intraocular pressure and axial length changes during altitude acclimatization from Beijing to Lhasa. *PLoS One* 15:e0228267. doi: 10.1371/journal.pone.0228267
- Yang, Y. Q., and Wang, N. L. (2022). Effects of special natural environments and mechanisms on intraocular pressure. *Zhonghua Yan Ke Za Zhi* 58, 949–953. doi: 10.3760/cma.j.cn112142-20220525-00264
- Yang, Y., Xie, Y., Sun, Y., Cao, K., Li, S., Fan, S., et al. (2019). Intraocular pressure changes of healthy lowlanders at different altitude levels: a systematic review and meta-analysis. *Front. Physiol.* 10:1366. doi: 10.3389/fphys.2019.01366
- Zhang, Y., Ouyang, S., Zhang, L., Tang, X., Song, Z., and Liu, P. (2010). Oxygen-induced changes in mitochondrial DNA and DNA repair enzymes in aging rat lens. *Mech. Ageing Dev.* 131, 666–673. doi: 10.1016/j.mad.2010.09.003



OPEN ACCESS

EDITED BY

Xuemin Li,
Peking University Third Hospital, China

REVIEWED BY

Ioannis Liampas,
University of Thessaly, Greece
Mark Ettenhofer,
University of California, San Diego,
United States
Trevor Jeremy Crawford,
Lancaster University, United Kingdom

*CORRESPONDENCE

Joong Il Kim
✉ jikim@kiom.re.kr
Jaeuk U. Kim
✉ jaeukkim@kiom.re.kr

RECEIVED 22 February 2023

ACCEPTED 23 May 2023

PUBLISHED 15 June 2023

CITATION

Opwonya J, Ku B, Lee KH, Kim JI and
Kim JU (2023) Eye movement changes as an
indicator of mild cognitive impairment.
Front. Neurosci. 17:1171417.
doi: 10.3389/fnins.2023.1171417

COPYRIGHT

© 2023 Opwonya, Ku, Lee, Kim and Kim. This is
an open-access article distributed under the
terms of the [Creative Commons Attribution
License \(CC BY\)](#). The use, distribution or
reproduction in other forums is permitted,
provided the original author(s) and the
copyright owner(s) are credited and that the
original publication in this journal is cited, in
accordance with accepted academic practice.
No use, distribution or reproduction is
permitted which does not comply with these
terms.

Eye movement changes as an indicator of mild cognitive impairment

Julius Opwonya^{1,2}, Boncho Ku¹, Kun Ho Lee^{3,4,5}, Joong Il Kim^{1*}
and Jaeuk U. Kim^{1,2*}

¹Digital Health Research Division, Korea Institute of Oriental Medicine, Daejeon, South Korea, ²KM Convergence Science, University of Science and Technology, Daejeon, South Korea, ³Gwangju Alzheimer's Disease and Related Dementias (GARD) Cohort Research Center, Chosun University, Gwangju, South Korea, ⁴Department of Biomedical Science, Chosun University, Gwangju, South Korea, ⁵Dementia Research Group, Korea Brain Research Institute, Daegu, South Korea

Background: Early identification of patients at risk of dementia, alongside timely medical intervention, can prevent disease progression. Despite their potential clinical utility, the application of diagnostic tools, such as neuropsychological assessments and neuroimaging biomarkers, is hindered by their high cost and time-consuming administration, rendering them impractical for widespread implementation in the general population. We aimed to develop non-invasive and cost-effective classification models for predicting mild cognitive impairment (MCI) using eye movement (EM) data.

Methods: We collected eye-tracking (ET) data from 594 subjects, 428 cognitively normal controls, and 166 patients with MCI while they performed prosaccade/antisaccade and go/no-go tasks. Logistic regression (LR) was used to calculate the EM metrics' odds ratios (ORs). We then used machine learning models to construct classification models using EM metrics, demographic characteristics, and brief cognitive screening test scores. Model performance was evaluated based on the area under the receiver operating characteristic curve (AUROC).

Results: LR models revealed that several EM metrics are significantly associated with increased odds of MCI, with odds ratios ranging from 1.213 to 1.621. The AUROC scores for models utilizing demographic information and either EM metrics or MMSE were 0.752 and 0.767, respectively. Combining all features, including demographic, MMSE, and EM, notably resulted in the best-performing model, which achieved an AUROC of 0.840.

Conclusion: Changes in EM metrics linked with MCI are associated with attentional and executive function deficits. EM metrics combined with demographics and cognitive test scores enhance MCI prediction, making it a non-invasive, cost-effective method to identify early stages of cognitive decline.

KEYWORDS

Alzheimer's disease, mild cognitive impairment, eye movement analysis and synthesis, machine learning (ML), saccades

1. Introduction

Alzheimer's disease (AD) is a progressive neurodegenerative disorder characterized by the accumulation of amyloid beta ($A\beta$) plaques and neurofibrillary tau-based tangles, beginning decades before symptoms appear and lead to cognitive decline, with individuals progressing from normal cognitive abilities to prodromal AD and ultimately AD dementia (Jack et al., 2018). While treatment can ameliorate some symptoms of dementia, there is no currently available cure, and the disease inevitably progresses (Alzheimer's Association, 2022). Early diagnosis and intervention during the mild cognitive impairment (MCI) stage are essential to preventing the progression to dementia and improving the quality of life for those with preclinical or prodromal AD (Gauthier et al., 2006).

Validated biomarkers that are proxies for AD neuropathologic changes exist but are underutilized due to their invasive, high cost, and limited availability (Jack et al., 2018). A neuropsychological evaluation is the most widespread method used in clinical settings to screen for cognitive impairment and obtain a global index of cognitive functioning (Nasreddine et al., 2005; McKhann et al., 2011; Bradfield, 2021). Evaluations range from simple bedside tests and brief screening tools to detailed neuropsychological batteries. Brief cognitive screening tests have been used and refined throughout the years, including the Mini-Mental State Examination (MMSE), Mini Cognitive Assessment Instrument (Mini-Cog), and Montreal Cognitive Assessment (MoCA) (Bradfield, 2021). Brief cognitive measures, such as the MMSE that can be easily administered with minimal training are optimal for fast-paced, high-patient-volume screening settings that often encounter older adult patients with cognitive problems. Although an array of brief cognitive screening tools that are sensitive to AD exist, most depend on intact linguistic function, which is highly influenced by demographic variables, and they may not be sensitive to the early stages of cognitive impairment (Nasreddine et al., 2005).

Furthermore, several cognitive tests entail writing and drawing, and motor dysfunction is highly prevalent in dementia patients, which can impact the results. Therefore, the utility of these brief cognitive tests, especially in patients with late-stage AD, can be limited. The gold standard for cognitive examination is a neuropsychological assessment battery, which requires in-depth training to ensure standardized administration and accurate interpretation of the findings (McKhann et al., 2011). Neuropsychological battery testing is not typically feasible in fast-paced clinical settings, such as primary care facilities. A rapid and easy-to-administer, non-invasive screening tool that is accurate and sensitive to the detection of MCI and AD dementia could accelerate new therapeutics for AD by selecting good trial candidates in the preclinical or prodromal stages and also screen healthy individuals in primary care facilities (Cummings et al., 2021).

Machine learning models built using non-invasive patient data are obvious candidates for use as screening tools. Previous research has demonstrated the use of machine learning in classifying MCI/AD dementia patients and cognitively normal controls and the potential of speech and language-based tools for non-invasive AD risk stratification (de la Fuente Garcia et al., 2020; Pulido et al., 2020; Tanveer et al., 2020). A major challenge in implementing a large-scale language tool is the presence of linguistic differences among speakers of different languages and dialects, which can result in variations in expression, speaking speed, and word usage. For these reasons, there

are gaps between the clinical potential, research contexts, and actual clinical implementations of these tools.

Another modality gaining momentum is eye movement (EM) analysis; in recent years, eye-tracking (ET) devices have provided adequate temporal resolution, accuracy, and precision for measuring EM and detecting changes in pupil diameter (Klingner et al., 2008; Tobii Technology AB, 2012). The ET technique provides a non-invasive, quantitative, and objective evaluation of EM, which researchers can apply to assess cognitive function. Recent research suggests that impaired EM may be an early indicator of AD (Anderson and MacAskill, 2013), evident even in the prodromal stage and worsening as the disease progresses (Albers et al., 2015; Kusne et al., 2017); EM metrics may be used as biomarkers of both disease status and progression. Promising findings have emerged recently on the predictive value of EM data collected during reading tasks alone or combined with language data during reading activities (Biondi et al., 2018; de la Fuente Garcia et al., 2020).

The present study aimed to investigate the potential utility of EM data collected during an interleaved paradigm in differentiating individuals with MCI from CN controls. Specifically, we aimed to investigate the potential of EM data, either independently or in combination with neuropsychological scores, to improve the accuracy of distinguishing between individuals with MCI and CN controls. We collected demographic information, cognitive scores, and EM metrics from participants who completed the PS/AS and Go/No-go tasks. We explored the potential benefits of combining these datasets with MMSE scores. This study sheds light on the potential of EM data as a novel biomarker for MCI and examines the advantages of using a multimodal approach for improving prediction accuracy.

2. Methods

2.1. Participants

In total, 679 individuals participated in the study between October 2019 and December 2020. We divided the participants into MCI patient and age-matched CN control groups. MCI patients and CN controls were recruited at the Gwangju Alzheimer's Disease and Related Dementia (GARD) center (Gwangju City, South Korea) (Doan et al., 2022).

We examined all the participants through detailed clinical consultations, incorporating a neuropsychological battery and the Clinical Dementia Rating (CDR) scale. CN controls were identified clinically as those who had a CDR score of zero and no sign of cognitive impairment; those with a CDR score of 0.5 and evidence of cognitive decline in one or more domains were considered MCI (Albert et al., 2011). MCI patients had a Seoul Neuropsychological Screening Battery-Second Edition (SNSB-II) *z* score of less than -1.5 in at least one of the domains. The SNSB-II is a widely used tool in South Korea for evaluating cognitive function in patients with MCI and dementia (Kang et al., 2003). In our study, all participants were assessed using the Korean version of the MMSE, which was included in the SNSB-II (Park, 1989).

Potential study participants underwent magnetic resonance imaging (MRI) scans to screen for evidence of brain atrophy or other focal brain lesions. Exclusion criteria for the study were as follows: the presence of focal brain lesions on MRI, including lacunes and white

TABLE 1 Participants' demographic information and neuropsychological test scores.

Characteristic	All ¹ (N=594)	MCI ¹ (N=166)	CN ¹ (N=428)	<i>p</i> value ²
Sex (female)	321 (54%)	83 (50%)	238 (56%)	0.2
Age	71.80 (6.42)	73.45 (6.63)	71.17 (6.22)	<0.001
Education level	13.0 (4.4)	12.9 (4.5)	13.1 (4.4)	0.8
MMSE score	27.32 (2.16)	26.16 (2.64)	27.77 (1.75)	<0.001

¹The values represent the mean (SD) for continuous variables and *n* (%) for categorical variables. The *p* values for the continuous variables were obtained using the Wilcoxon rank sum test. For the categorical variables, the *p* values were derived from the Chi-squared test statistics.

²Pearson's Chi-squared test; Wilcoxon rank sum test. The bold fonts indicate a *p* value lower than 0.05.

matter hyperintensity lesions of grade 2 or more (Fazekas et al., 1987; Kim et al., 2008); less than 3 years of education; and medical conditions that could interfere with the study design, such as mental health instability or a history of excessive alcohol consumption. A total of 85 participants were excluded based on these criteria. Specifically, we excluded 25 individuals diagnosed with AD dementia, 60 participants with visual impairments, and those who failed calibration and the preliminary trials that were conducted to familiarize participants with the task requirements before the actual trial. A total of 594 participants were included in the final analysis, including 428 CN controls and 166 MCI patients, as shown in Table 1. The CN group included 428 subjects (190 males, 238 females), with a mean age of 71.2 ± 6.2 years; the MCI group included 166 subjects (83 males, 83 females), with a mean age of 73.5 ± 6.6 years (see Table 1). We obtained written informed consent from all participants or their legal guardians after providing a detailed description of the study, which was approved by the Chonnam National University Hospital Institutional Review Board (IRB no CNUH-2019-279).

2.2. Eye-tracking recordings and the experimental paradigm

The standardized pipeline used to preprocess the gaze data collected for each participant has been described in detail elsewhere (Opwonya et al., 2022). We recorded SEM data on the Tobii Pro spectrum system (Tobii Pro AB, Danderyd, Sweden), sampled at 300 Hz, and processed with Tobii Pro Lab version 1.118. Visual stimuli were presented on a monitor approximately 65 centimeters from the participants. Furthermore, we used a desk with adjustable chin and forehead rests to maintain a suitable angle between each participant's gaze and the ET monitor.

Our experimental design involved two interleaved sessions: the PS/AS (PA) and the Go/No-go (GN). Each session consisted of 30 blocks, each consisting of 3 trials, with two standard (PS and Go) trials and one deviant trial (AS and No-go), as shown in Figure 1. The condition (PS, AS, Go, and No-go) and the peripheral target, projected at $\pm 10^\circ$ in the horizontal plane (left/right), were randomly interleaved with an equal frequency throughout each block.

This study classified six EM-related responses, including fixation duration, correct responses, anticipations, omissions, corrected inhibition errors, and uncorrected inhibition errors. We classified all errors as the summation of anticipatory errors, omissions, and

inhibition errors in the PS/AS and Go trials and all errors as the summation of inhibition errors in the No-go trials. Criteria were established to determine the PS/AS and Go/No-go responses.

Correct responses for PS and Go trials were defined as the first saccade directed toward the target location, followed by a sustained fixation within the area of interest (AOI). For AS trials, correct responses were defined as the first saccade in the opposite direction of the target location, followed by sustained fixation within the AOI. In No-go trials, correct responses were identified as a maintained fixation at the center of the screen despite the appearance of any directional targets, indicating successful inhibition.

Anticipatory errors were defined as the first saccade that occurred less than 80 ms following target stimulus onset, while omission errors were defined as the absence of eye movement within 500 ms of target presentation. Inhibition errors were further subcategorized into corrected and uncorrected errors. Uncorrected inhibition errors were trials where the target stimuli inappropriately captured the gaze, but no corrective saccade was made. Corrected inhibition errors were defined as errors in which the gaze was redirected from an incorrect to a correct direction within 400 ms, with a gaze variation $\leq 1^\circ$.

2.3. Statistical analysis

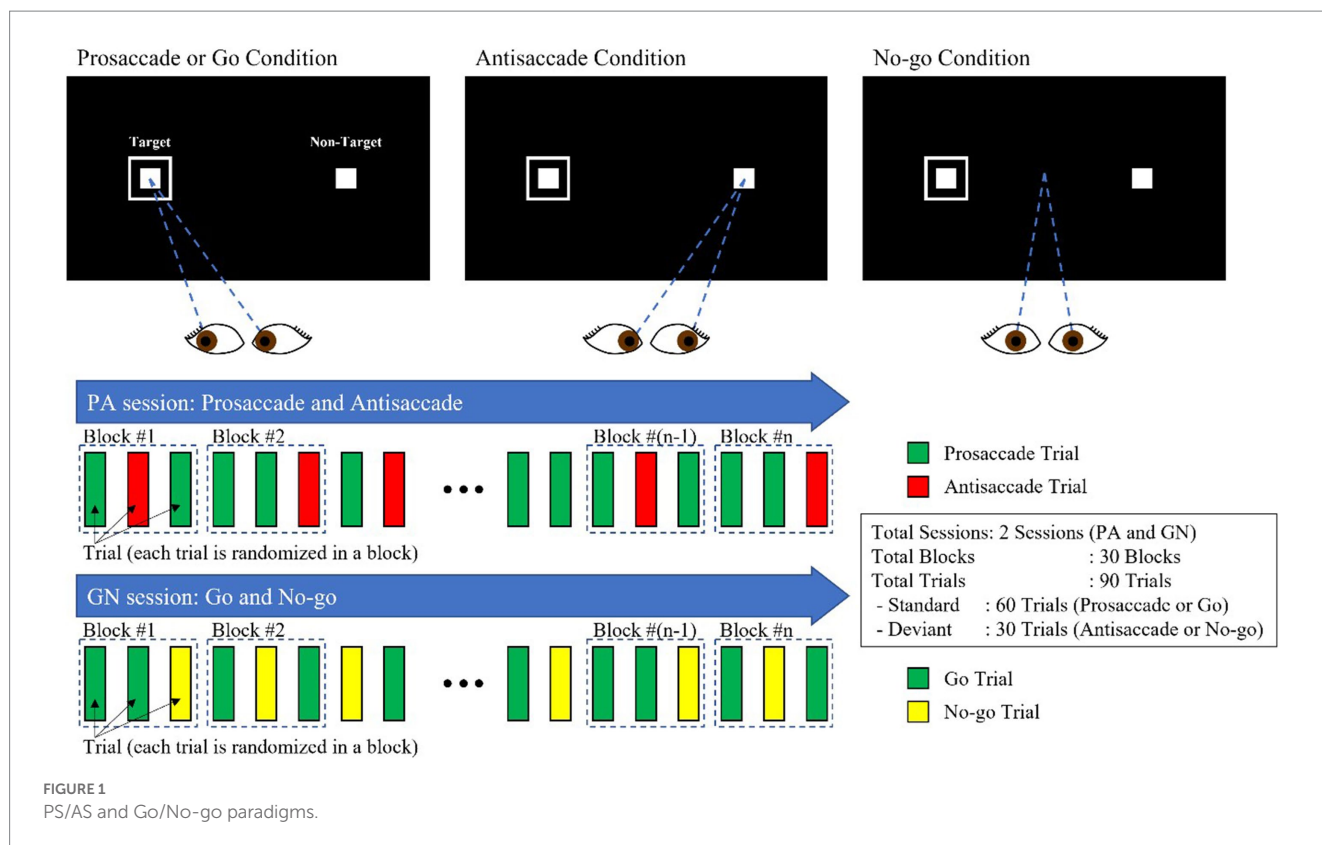
R version 4.2.2, including the *gtsummary* (v.1.6.2) and *tidyverse* packages (v.1.3.2), was used for statistical analysis (Wickham, 2017; Sjoberg et al., 2021; R Core Team, 2022). We performed binomial logistic regression analyses to examine the ability of EM metrics to distinguish between CN controls and MCI patients. We estimated ORs from two logistic regression models (crude and adjusted), which included adjustments for age, sex, and education level.

2.4. Machine learning and model selection

We used the *mikropml* package (v.1.4.0) to train and evaluate models to predict cognitive status from the EM metrics obtained from PS/AS and Go/No-go tasks. Demographics, cognitive scores, and ET metric data were used to generate logistic regression (LR), random forest (RF), support vector machine (SVM), and extreme gradient boosting (XGB) classification models to predict cognitive status.

We aimed to classify patients with MCI (vs. CN controls) using each feature set (see below); we built classifiers using demographic characteristics, MMSE scores, and EM metric data. We performed LR on all feature sets using a modified version of the machine learning pipeline presented in the study by Topcuoglu et al. (2021) and caret version 6.0-93 in R version 4.2.2. Furthermore, we performed RF, SVM with a radial basis kernel, and XGB classification for the feature sets using the same method implemented in *mikropml* (Topcuoglu et al., 2021). We randomly split the data into 80/20 train/test splits, and the train/test splits were identical across models generated with different feature sets for a valid comparison.

Given that the data were imbalanced, we applied the synthetic minority oversampling technique (SMOTE) during cross-validation, which allowed for proper evaluation of the model's capability to generalize from the training data and avoided biases or overly optimistic estimates (Santos et al., 2018). Hyperparameters were selected via cross-validation on the training set to maximize the



average area under the receiver operating characteristics curve (AUROC) across cross-validation folds.

2.5. Feature sets

We studied the relationship between cognitive status and six feature sets: (i) demographic characteristics—sex, age, and years of education; (ii) MMSE scores; (iii) demographic characteristics and MMSE scores; (iv) EM features—variables derived from the PS/AS and Go/No-go tasks; (v) demographic characteristics and EM features; and (vi) demographic characteristics, MMSE scores, and EM features. Demographic features (particularly age, sex, and years of education) can be obtained noninvasively and are predictive of dementia in previous studies (Calvin et al., 2019).

2.6. Feature set preprocessing

We preprocessed all six datasets by mapping categorical features to binary variables, centering and scaling the continuous features, and removing features present in only one sample or all but one sample.

2.7. Baseline classifier

We selected the best available classification method using demographic information (age, sex, and education level) as the baseline for our algorithm development (see Table 1).

2.8. Model performance

To characterize the accuracy of the MMSE scores and EM metrics, we performed receiver operating characteristic (ROC) curve analyses to calculate the AUROC and the deviance across all train/test splits. We selected the optimal model based on the highest AUROC and lowest binomial deviance in each combination of learning algorithms and six feature sets. Subsequently, we evaluated the predictive performance of this model on the test set. Feature importance was calculated using a permutation test, which breaks the relationship between the feature and the true outcome in the test data and measures the change in model performance.

3. Results

3.1. Participant characteristics

The participants' baseline demographic characteristics and cognitive scores are shown in Table 1. Patients with MCI were significantly older ($p < 0.001$) and had significantly lower MMSE total scores ($p < 0.001$) than CN controls. There was no difference in sex or years of education between the groups.

3.2. Eye-movement tasks

Several EM variables were significantly predictive of MCI on all tasks, even after being adjusted for demographics.

3.3. Prosaccade tasks

Univariate logistic regression models adjusted for demographics showed increased odds of MCI for individuals with wider latency variability (OR 1.532, 95% CI 1.262–1.868, $p < 0.001$), more errors (OR 1.348, 95% CI 1.106–1.645, $p = 0.003$), and more anticipations (OR 1.213, 95% CI 1.006–1.461, $p = 0.043$) (see Table 2).

3.4. Antisaccade tasks

Univariate logistic regression models adjusted for demographics revealed increased odds of MCI for individuals with more errors (OR 1.604; 95% CI 1.295–2.002; $p < 0.001$), more uncorrected errors (OR 1.394; 95% CI 1.171–1.665; $p < 0.001$), and more anticipations (OR 1.041; 95% CI 1.041–1.517; $p = 0.018$) (see Table 2).

3.5. Go tasks

Univariate logistic regression models adjusted for demographics showed increased odds of MCI for individuals with a wider latency variability (OR, 1.216; 95% CI, 1.003–1.477; $p = 0.047$), more errors

(OR, 1.555; 95% CI 1.274–1.906; $p < 0.001$), more anticipations (OR, 1.307; 95% CI 1.086–1.554; $p = 0.0053$), and more omissions (OR, 1.295; 95% CI 1.084–1.554; $p = 0.0053$) (see Table 3).

3.6. No-go tasks

Univariate logistic regression models adjusted for demographics showed increased odds of MCI for individuals with a wider fixation variability (OR, 1.454; 95% CI, 1.198–1.788; $p < 0.001$), more errors (OR, 1.598; 95% CI 1.324–1.933; $p < 0.001$), and more uncorrected errors (OR, 1.621; 95% CI 1.343–1.961; $p < 0.001$) (see Table 3).

3.7. Diagnostic performance of the feature sets

3.7.1. Baseline demographic characteristics

Table 4 shows the performance of the four classification algorithms (LR, RF, SVM, and XGB) and summarizes the diagnostic performance of the six feature sets. The LR algorithm exhibited the highest AUROC of 0.656 with deviance of 161.409; hence, we used it as the baseline for all subsequent experiments.

TABLE 2 Estimated odds ratios and 95% confidence intervals of Pro/antisaccade EM variables derived from the two logistic regression models.

Variables	Crude model			Adjusted model		
	OR ¹	95% CI ²	<i>p</i> value	OR ¹	95% CI ²	<i>p</i> value ³
Prosaccade						
Correct	0.717	0.597, 0.858	<0.001	0.736	0.601, 0.899	0.003
Latency	1.171	0.98, 1.400	0.082	1.137	0.945, 1.367	0.173
Latency SD	1.564	1.305, 1.883	<0.001	1.532	1.262, 1.868	<0.001
All errors	1.399	1.170, 1.677	<0.001	1.348	1.106, 1.645	0.003
Uncorrected error	1.115	0.936, 1.319	0.219	1.082	0.904, 1.286	0.381
Self-corrected	1.017	0.848, 1.214	0.857	0.998	0.829, 1.197	0.986
Anticipations	1.245	1.047, 1.480	0.014	1.213	1.006, 1.461	0.043
Omissions	1.195	1.008, 1.414	0.041	1.137	0.95, 1.353	0.151
Antisaccade						
Correct	0.614	0.501, 0.745	<0.001	0.621	0.495, 0.771	<0.001
Latency	0.878	0.732, 1.051	0.158	0.867	0.719, 1.043	0.131
Latency SD	0.97	0.807, 1.158	0.725	0.929	0.774, 1.112	0.426
All errors	1.642	1.353, 2.009	<0.001	1.604	1.295, 2.002	<0.001
Uncorrected error	1.447	1.221, 1.722	<0.001	1.394	1.171, 1.665	<0.001
Corrected error	0.702	0.574, 0.852	<0.001	0.713	0.581, 0.868	<0.001
Anticipations	1.297	1.088, 1.545	0.004	1.257	1.041, 1.517	0.018
Omissions	1.224	1.033, 1.448	0.020	1.178	0.99, 1.400	0.066

¹OR, odds ratio.

²CI, confidence interval; SD, standard deviation.

³*p* value obtained from the Wald test. The models were adjusted for age, sex, and years of education. The bold font indicates a *p* value lower than 0.05.

TABLE 3 Estimated odds ratios and 95% confidence intervals of Go/No-go EM variables derived from the two logistic regression models.

Variables	Crude model			Adjusted model		
	OR ¹	95% CI ²	<i>p</i> value	OR ¹	95% CI ²	<i>p</i> value ³
Go						
Correct	0.610	0.507, 0.732	<0.001	0.616	0.501, 0.753	<0.001
Latency	1.227	1.028, 1.467	0.024	1.174	0.98, 1.413	0.090
Latency SD	1.269	1.061, 1.522	0.009	1.216	1.003, 1.477	0.047
All errors	1.596	1.332, 1.919	<0.001	1.555	1.274, 1.906	<0.001
Uncorrected error	1.177	0.99, 1.393	0.061	1.141	0.96, 1.355	0.135
Self-corrected	0.948	0.788, 1.134	0.564	0.935	0.775, 1.122	0.473
Anticipations	1.334	1.123, 1.585	0.001	1.307	1.086, 1.572	0.005
Omissions	1.365	1.152, 1.626	<0.001	1.295	1.084, 1.554	0.004
No-go						
Correct	0.604	0.505, 0.721	<0.001	0.604	0.497, 0.731	<0.001
Fixation duration	0.692	0.581, 0.822	<0.001	0.712	0.592, 0.854	<0.001
Fixation duration SD	1.503	1.240, 1.837	<0.001	1.458	1.198, 1.788	<0.001
All errors	1.603	1.346, 1.912	<0.001	1.598	1.324, 1.933	<0.001
Uncorrected error	1.621	1.362, 1.935	<0.001	1.621	1.343, 1.961	<0.001
Corrected error	0.996	0.823, 1.184	0.964	0.949	0.779, 1.135	0.579

¹OR, odds ratio.²CI, confidence interval; SD, standard deviation.³*p* value obtained from the Wald test. The models were adjusted for age, sex, and years of education. The bold font indicates a *p* value lower than 0.05.

TABLE 4 AUROC results of prediction models according to feature set and classification model.

	Logistic regression		Random forest		Support vector machine		Extreme gradient boosting	
	AUROC	Deviance	AUROC	Deviance	AUROC	Deviance	AUROC	Deviance
Demo	0.656	161.409	0.552	–	0.610	–	0.613	158.382
MMSE	0.742	161.418	0.593	–	0.743	–	0.671	161.908
EM	0.702	149.244	0.715	–	0.643	–	0.707	148.732
Demo + MMSE	0.767	135.817	0.610	–	0.764	–	0.717	139.122
Demo + EM	0.700	149.333	0.752	–	0.718	–	0.726	137.378
Demo + MMSE + EM	0.773	138.866	0.831	–	0.769	–	0.840	121.671

Values in bold in each column represent the highest performance.

3.7.2. Classification performance

In this study, we compared different models to determine the best predictors of cognitive impairment. Specifically, we examined the performance of a baseline model against two other models: one that included demographics and EM and another that included demographics and MMSE total score. The model incorporating EM as a predictor showed superior performance with an AUROC of 0.715, surpassing the baseline model that used only demographic information. However, the MMSE total score had a slightly higher AUROC than the EM features alone with AUROC of 0.743. Furthermore, we observed that adding demographics to either the EM or MMSE features independently resulted in further performance improvements, with AUROCs of 0.752 and 0.767, respectively. Finally, we evaluated the performance of a combined model that included all

features, namely demographics, MMSE total score, and EM. Our analysis demonstrated that this model had the best overall performance, with an AUROC of 0.840 and lowest deviance of 121.671, as shown in Figure 2 and Table 4. Incorporating EM into predictive models may improve their accuracy in identifying cognitive impairment, and a combination of demographics, MMSE total score, and EM can effectively predict cognitive impairment, suggesting the importance of using multiple features in clinical assessments. Additional performance metrics, such as sensitivity and specificity, are provided in Supplementary Appendix Table A1.

To determine each feature set's contribution to the classification model's performance, we calculated the feature importance using a permutation test, identifying the five most important features, as shown in Figure 3.

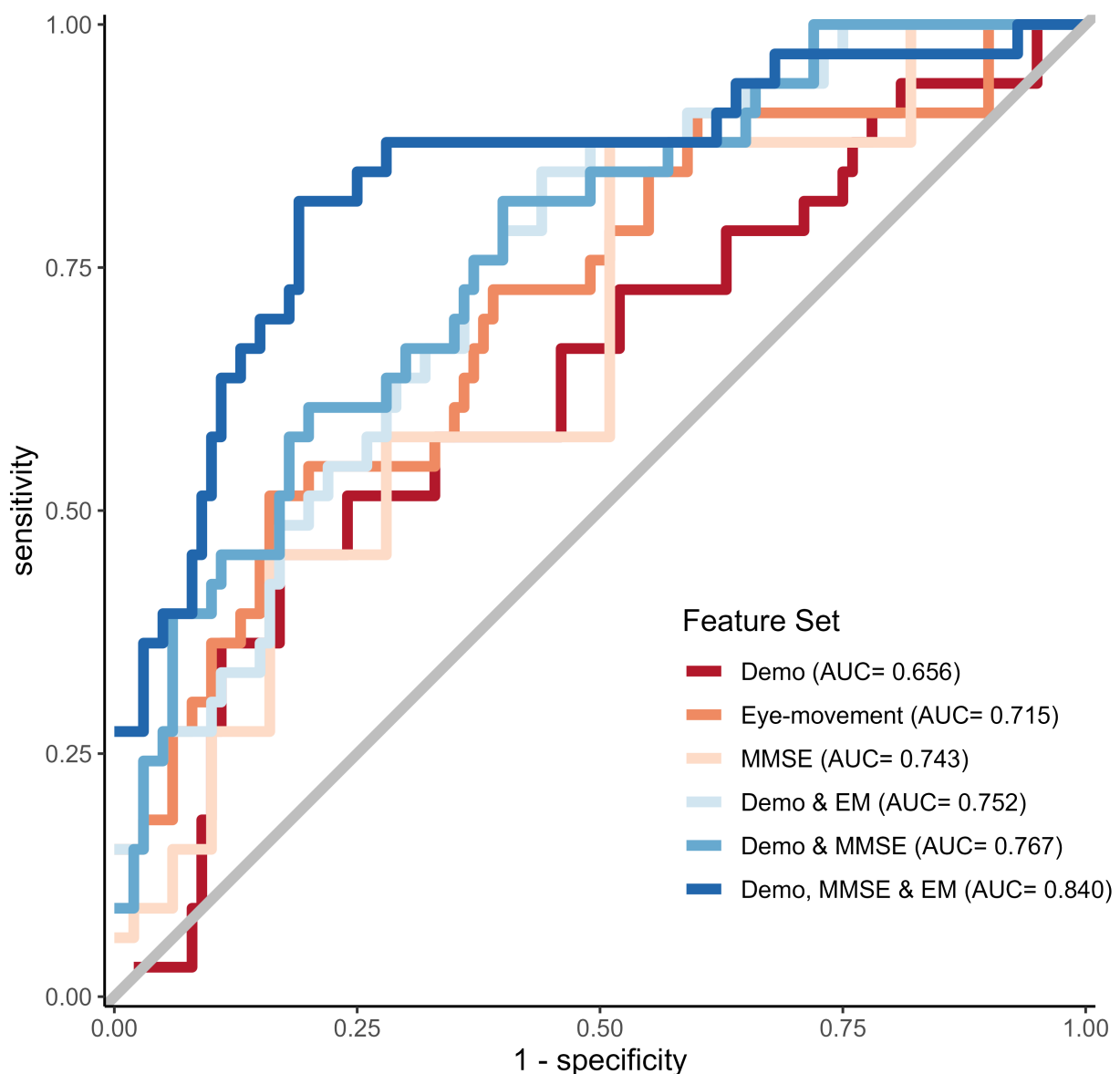


FIGURE 2
ROC curves for the best-performing prediction models per feature set.

4. Discussion

This study evaluated the efficacy of EM metrics for screening MCI patients from CN controls, comparing these metrics individually or jointly with other easily accessible and cost-effective measures such as demographic information and MMSE scores. Specifically, we developed and validated prediction models with the ability to identify individuals with MCI using an ET paradigm comprising PS/AS and Go/No-go tasks and examining the contributions of demographic information, MMSE scores, and EM data.

The cohort EM variables that were consistently associated with MCI were latency variability, fixation duration variability, the number of errors, anticipations, and omissions (Opwonya et al., 2022). Kapoula et al. (2010) suggested that a wide latency distribution is a good index of attentional fluctuation when participants perform SEM tasks. Therefore,

the greater latency variability in the MCI group suggests more extended moments of inattention where their focus drifted from the task to other irrelevant things. Fixation duration, which represents the relative focus on an object, with a greater average fixation time indicating a greater degree of attention (Tullis and Albert, 2013), was shorter and had more variability in the MCI group, indicating a disengagement of attention. Participants with difficulties in sustained attention or working memory, such as the MCI group in our study, showed increased odds of omissions in Go and AS tasks, further supporting the suggestion that they have attention deficiencies (Crawford et al., 2013). Our results suggested that the MCI group had poorer sustained attention than the CN group, as indicated by the greater saccade latency variability, shorter fixation duration, and more frequent omissions.

When a participant preempts the onset signal of a task with an anticipatory EM in advance of the target, anticipation errors are generated (Crawford et al., 2013). The MCI group showed

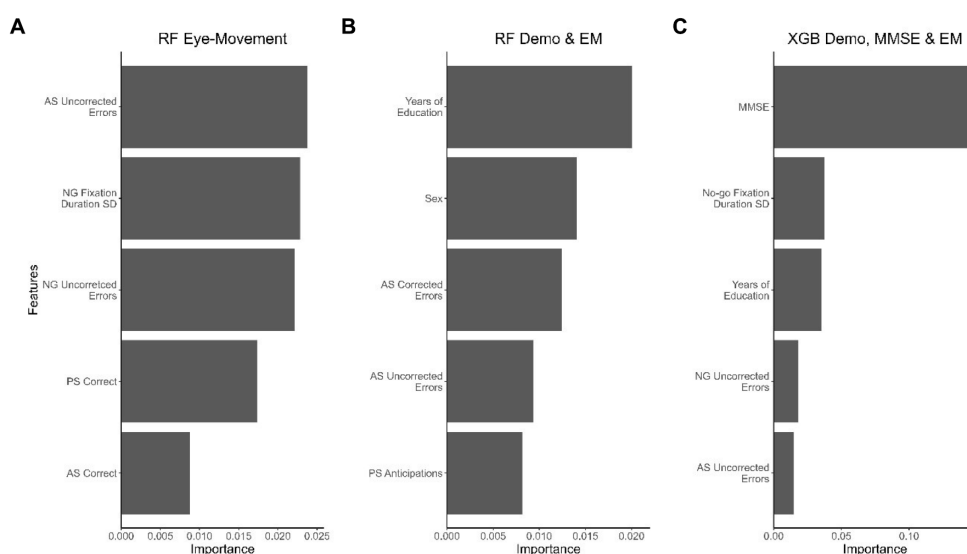


FIGURE 3

The top 5 features that contributed the most to the best-performing model in each dataset. (A) RF model with the EM dataset, (B) RF model with demographic and EM data, and (C) XGB model with demographic data, MMSE scores, and EM data. Important features for the LR and SVM models were selected according to decreasing importance to the AUROC value when the feature was permuted.

increased odds of making anticipatory saccades. The higher frequency of anticipatory errors in the MCI group sheds light on the inhibitory dysfunction in these patients. Furthermore, we evaluated corrected and uncorrected inhibition errors to assess specific inhibitory processes. We found that the MCI group had increased odds of not correcting errors, consistent with an impairment in error monitoring. These findings are consistent with previous results, which showed that PS/AS and Go/No-go tasks could demonstrate specific deficits in inhibitory control, latency, and self-monitoring in patients with MCI compared to CN controls (Opwonya et al., 2022). Previous studies have linked variables such as latency variability, fixation duration variability, errors, anticipations, and omissions with increased odds of MCI or AD dementia (Crawford et al., 2013; Noiret et al., 2018; Opwonya et al., 2021, 2022) and likely contribute to cognitive function deficits in this patient group.

Next, we employed machine learning models to evaluate the predictive performance of EM features from the PS/AS and Go/No-go tasks, demographic information, and MMSE scores in a cohort of individuals with and without cognitive impairment. Upon comparing the EM feature performance to the baseline model, we found the EM metrics reliable for distinguishing MCI patients from CN. The results showed that the models using EM features alone outperformed those using demographic characteristics alone. Specifically, the discriminative ability of the ET model was superior in this dataset, with a peak AUROC of 0.715, compared to the demographic characteristics model, with an AUROC of 0.656. However, the MMSE alone had a higher performance with an AUROC of 0.743 than EM features. Incorporating demographic characteristics, MMSE scores, and EM data in the prediction model further improved the detection of MCI, yielding the highest AUROC of 0.840 and lowest

deviance of 121.671. These findings suggest that EM metrics captured during PS/AS and Go/No-go tasks can help detect subtle cognitive impairment and have additive clinical utility when combined with demographic characteristics and MMSE scores.

Previous research has shown that the MMSE and Montreal cognitive assessment (MoCA) are effective diagnostic tools for dementia (Roalf et al., 2013). The MoCA is more sensitive and accurate in differentiating MCI patients from CN individuals than the MMSE (Nasreddine et al., 2005; Roalf et al., 2013). Longitudinal assessments are essential for determining the progression from MCI to AD dementia or other forms of dementia in clinical and research settings. Additionally, these assessments assist in differential diagnosis and the measurement of the treatment effectiveness. However, conducting serial assessments can be challenging due to practice effects, particularly when using brief cognitive tests like MMSE and MoCA. Utilizing eye-tracking technology can reduce potential confounding associated with repeated task exposure, although it does not eliminate carryover effects from the test-retest method. Compared to high-cost or invasive techniques, non-invasive tools such as eye trackers provide data that may not require expert interpretation in the clinical context and pose no risk to patients. The ability of non-experts to interpret EM metrics will rely on establishing consistent performance by simple or automated classification algorithms, irrespective of potential confounding factors such as age and educational level. Dementia pathology causes progressive neurodegeneration, resulting in altered oculomotor performance and a decline in cognitive functions (Molitor et al., 2015; Barral et al., 2020). Previous studies have demonstrated a considerable impact of aging on saccadic reaction times, as younger adults exhibit notably quicker mean reaction times than their older

counterparts (Polden et al., 2020). Our study revealed weak to moderate correlations between demographics, specifically age and level of education, and EM variables. The correlation coefficients for these relationships are provided in [Supplementary Appendix Figures A1, A2](#).

Furthermore, aging effects have been observed in oculomotor function, specifically in processing speed, spatial memory, and inhibitory control (Salthouse, 1996; Peltsch et al., 2011; Crawford et al., 2017). Eye movement changes in psychiatric disorders have been extensively studied, with schizophrenia being one of the most researched conditions in this regard. In individuals with schizophrenia, the most prominent saccadic abnormalities are inhibition errors and decreased spatial accuracy during volitional saccades (Broerse et al., 2001). However, it is essential to note that neither deficits are exclusive to individuals with schizophrenia. Our experimental results show promise for developing a non-invasive risk stratification tool, as we could accurately distinguish MCI patients from CN controls using EM behavior assessed during PS/AS and Go/No-go tasks.

The study has limitations, as EM changes can occur with several neurological conditions and MCI subtypes (e.g., amnesic vs. nonamnesic conditions) (Garbutt et al., 2008; Molitor et al., 2015). Eye-tracking can be used in multiple neurological disorders, but more research with diverse samples is needed to test this possibility. Additionally, eye-tracking depends on good visual function in subjects and requires high-performance devices, which can limit its availability despite minimal staff training needs.

In summary, during the trials, patients with MCI had difficulty maintaining fixation, suppressing saccades, or making saccades toward or away from the target. The results show that EM metrics may reveal impaired sustained attention, working memory, and executive control function in patients with MCI performing EM tasks. This study shows that machine learning can aid in automatically detecting cognitive impairment using eye-tracking data. The classification model with EM metrics performed better than the model with demographic characteristics, indicating the usefulness of EM feature analysis for early-stage cognitive decline detection. Combining EM metrics, demographic characteristics, and MMSE scores resulted in the best classification performance. Combining these modalities improves model performance and demonstrates that EM metrics, demographic characteristics, and MMSE data are complementary in detecting cognitive impairment. Our study, which had a sample size of approximately 600 participants, the largest sample size of a clinical trial in this area to date, provides strong evidence for the effectiveness of EM metrics in screening patients with MCI and has significant implications for clinical practice.

The following are our primary contributions: first, we built a dataset that includes EM data collected during interleaved EM tasks, brief cognitive test scores, and demographic information. Then, we used this dataset to study the contribution of the EM data to the classification of patients with MCI vs. CN controls, showing that EM data collected noninvasively could discriminate between patients with MCI and CN controls. Finally, we showed that EM data collected during an interleaved EM task complemented demographic and MMSE score data in detecting subtle cognitive impairment.

Data availability statement

The raw data supporting the conclusions of this article will be made available by the authors, without undue reservation.

Ethics statement

The studies involving human participants were reviewed and approved by Chonnam National University Hospital Institutional Review Board (IRB no CNUH-2019-279). The patients/participants provided their written informed consent to participate in this study.

Author contributions

JO, BK, JIK, and JUK conceived the manuscript. Data verification was carried out by JO and JIK. JO and BK performed the statistical analyses and generated the figures. Drafting of the manuscript was done by JO, BK, JIK, and JUK. Methodology and administration of the trial were overseen by JIK, KHL, and JUK. All authors contributed to the article and approved the submitted version.

Funding

The Korean Government funded this study under a grant (KSN1823130) to the Korea Institute of Oriental Medicine.

Acknowledgments

The authors gratefully acknowledge the staff of Gwangju Alzheimer's Disease and Related Dementia (GARD) center for their assistance with data acquisition and participant recruitment.

Conflict of interest

The authors declare that the research was conducted in the absence of any commercial or financial relationships that could be construed as a potential conflict of interest.

Publisher's note

All claims expressed in this article are solely those of the authors and do not necessarily represent those of their affiliated organizations, or those of the publisher, the editors and the reviewers. Any product that may be evaluated in this article, or claim that may be made by its manufacturer, is not guaranteed or endorsed by the publisher.

Supplementary material

The Supplementary material for this article can be found online at: <https://www.frontiersin.org/articles/10.3389/fnins.2023.1171417/full#supplementary-material>

References

- Albers, M. W., Gilmore, G. C., Kaye, J., Murphy, C., Wingfield, A., Bennett, D. A., et al. (2015). At the interface of sensory and motor dysfunctions and Alzheimer's disease. *Alzheimers Dement.* 11, 70–98. doi: 10.1016/j.jalz.2014.04.514
- Albert, M. S., DeKosky, S. T., Dickson, D., Dubois, B., Feldman, H. H., Fox, N. C., et al. (2011). The diagnosis of mild cognitive impairment due to Alzheimer's disease: recommendations from the National Institute on Aging-Alzheimer's Association workgroups on diagnostic guidelines for Alzheimer's disease. *Alzheimers Dement.* 7, 270–279. doi: 10.1016/j.jalz.2011.03.008
- Alzheimer's Association (2022). "2022 Alzheimer's disease facts and figures" in *Alzheimer's and Dementia* (John Wiley & Sons, Ltd)
- Anderson, T. J., and MacAskill, M. R. (2013). Eye movements in patients with neurodegenerative disorders. *Nat. Rev. Neurol.* 9, 74–85. doi: 10.1038/nrneuro.2012.273
- Barral, O., Jang, H., Newton-Mason, S., Shajan, S., Soroski, T., Carenini, G., et al. (2020). "Non-invasive classification of Alzheimer's disease using eye tracking and language" in *Proceedings of the 5th machine learning for healthcare conference*. eds. D.-V. Finale, F. Jim, J. Ken, K. David, R. Rajesh and W. Byron et al. (Proceedings of Machine Learning Research: PMLR). Available at: <https://proceedings.mlr.press/v126/barral20a.html>
- Biondi, J., Fernandez, G., Castro, S., and Agamennoni, O. (2018). Eye movement behavior identification for Alzheimer's disease diagnosis. *J. Integr. Neurosci.* 17, 349–354. doi: 10.31083/j.jin.2018.04.0416
- Bradfield, N. I. (2021). Mild cognitive impairment: diagnosis and subtypes. *Clin. EEG Neurosci.* 54, 4–11. doi: 10.1177/15500594211042708
- Broerse, A., Crawford, T. J., and den Boer, J. A. (2001). Parsing cognition in schizophrenia using saccadic eye movements: a selective overview. *Neuropsychologia* 39, 742–756. doi: 10.1016/S0028-3932(00)00155-X
- Calvin, C. M., Wilkinson, T., Starr, J. M., Sudlow, C., Hagenaars, S. P., Harris, S. E., et al. (2019). Predicting incident dementia 3–8 years after brief cognitive tests in the UK biobank prospective study of 500,000 people. *Alzheimers Dement.* 15, 1546–1557. doi: 10.1016/j.jalz.2019.07.014
- Crawford, T. J., Higham, S., Mayes, J., Dale, M., Shaunak, S., and Lekwuwa, G. (2013). The role of working memory and attentional disengagement on inhibitory control: effects of aging and Alzheimer's disease. *Age (Dordr.)* 35, 1637–1650. doi: 10.1007/s11357-012-9466-y
- Crawford, T. J., Smith, E. S., and Berry, D. M. (2017). Eye gaze and aging: selective and combined effects of working memory and inhibitory control. *Front. Hum. Neurosci.* 11:563. doi: 10.3389/fnhum.2017.00563
- Cummings, J., Lee, G., Zhong, K., Fonseca, J., and Taghva, K. (2021). Alzheimer's disease drug development pipeline: 2021. *Alzheimers Dement. (NY)* 7:e12179. doi: 10.1002/trc2.12179
- de la Fuente Garcia, S., Ritchie, C. W., and Luz, S. (2020). Artificial intelligence, speech, and language processing approaches to monitoring Alzheimer's disease: a systematic review. *J. Alzheimers Dis.* 78, 1547–1574. doi: 10.3233/JAD-200888
- Doan, D. N. T., Ku, B., Kim, K., Jun, M., Choi, K. Y., Lee, K. H., et al. (2022). Segmental bioimpedance variables in association with mild cognitive impairment. *Front. Nutr.* 9:873623. doi: 10.3389/fnut.2022.873623
- Fazekas, F., Chawluk, J. B., Alavi, A., Hurtig, H. I., and Zimmerman, R. A. (1987). MR signal abnormalities at 1.5 T in Alzheimer's dementia and normal aging. *AJR Am. J. Roentgenol.* 149, 351–356. doi: 10.2214/ajr.149.2.351
- Garbutt, S., Matlin, A., Hellmuth, J., Schenk, A. K., Johnson, J. K., Rosen, H., et al. (2008). Oculomotor function in frontotemporal lobar degeneration, related disorders and Alzheimer's disease. *Brain* 131, 1268–1281. doi: 10.1093/brain/awn047
- Gauthier, S., Reisberg, B., Zaudig, M., Petersen, R. C., Ritchie, K., Broich, K., et al. (2006). Mild cognitive impairment. *Lancet* 367, 1262–1270. doi: 10.1016/S0140-6736(06)68542-5
- Jack, C. R. Jr., Bennett, D. A., Blennow, K., Carrillo, M. C., Dunn, B., Haeberlein, S. B., et al. (2018). NIA-AA research framework: toward a biological definition of Alzheimer's disease. *Alzheimers Dement.* 14, 535–562. doi: 10.1016/j.jalz.2018.02.018
- Kang, Y., Na, D. L., and Hahn, S. (2003). Seoul neuropsychological screening battery. *Incheon: Human Brain Research and Consulting Co*
- Kapoula, Z., Yang, Q., Vernet, M., Dieudonne, B., Greffard, S., and Verny, M. (2010). Spread deficits in initiation, speed and accuracy of horizontal and vertical automatic saccades in dementia with lewy bodies. *Front. Neurol.* 1:138. doi: 10.3389/fneur.2010.00138
- Kim, K. W., MacFall, J. R., and Payne, M. E. (2008). Classification of white matter lesions on magnetic resonance imaging in elderly persons. *Biol. Psychiatry* 64, 273–280. doi: 10.1016/j.biopsych.2008.03.024
- Klingner, J., Kumar, R., and Hanrahan, P. (2008). Measuring the task-evoked pupillary response with a remote eye tracker. in: *Proceedings of the 2008 symposium on Eye tracking research and applications*, 69–72.
- Kusne, Y., Wolf, A. B., Townley, K., Conway, M., and Peyman, G. A. (2017). Visual system manifestations of Alzheimer's disease. *Acta Ophthalmol.* 95, e668–e676. doi: 10.1111/aos.13319
- McKhann, G. M., Knopman, D. S., Chertkow, H., Hyman, B. T., Jack, C. R. Jr., Kawas, C. H., et al. (2011). The diagnosis of dementia due to Alzheimer's disease: recommendations from the National Institute on Aging-Alzheimer's Association workgroups on diagnostic guidelines for Alzheimer's disease. *Alzheimers Dement.* 7, 263–269. doi: 10.1016/j.jalz.2011.03.005
- Molitor, R. J., Ko, P. C., and Ally, B. A. (2015). Eye movements in Alzheimer's disease. *J. Alzheimers Dis.* 44, 1–12. doi: 10.3233/JAD-141173
- Nasreddine, Z. S., Phillips, N. A., Bedirian, V., Charbonneau, S., Whitehead, V., Collin, I., et al. (2005). The Montreal cognitive assessment, MoCA: a brief screening tool for mild cognitive impairment. *J. Am. Geriatr. Soc.* 53, 695–699. doi: 10.1111/j.1532-5415.2005.53221.x
- Noiret, N., Carvalho, N., Laurent, E., Chopard, G., Binetruy, M., Nicolier, M., et al. (2018). Saccadic eye movements and Attentional control in Alzheimer's disease. *Arch. Clin. Neuropsychol.* 33, 1–13. doi: 10.1093/arclin/acx044
- Opwonya, J., Doan, D. N. T., Kim, S. G., Kim, J. I., Ku, B., Kim, S., et al. (2021). Saccadic eye movement in mild cognitive impairment and Alzheimer's disease: a systematic review and Meta-analysis. *Neuropsychol. Rev.* 32, 193–227. doi: 10.1007/s11065-021-09495-3
- Opwonya, J., Wang, C., Jang, K. M., Lee, K., Kim, J. I., and Kim, J. U. (2022). Inhibitory control of saccadic eye movements and cognitive impairment in mild cognitive impairment. *Front. Aging Neurosci.* 14:871432. doi: 10.3389/fnagi.2022.871432
- Park, J.-H. (1989). Standardization of Korean version of the Mini-mental state examination (MMSE-K) for use in the elderly. Part II. Diagnostic validity. *J. Korean Neuropsychiatr. Assoc.* 28, 508–513.
- Peltesch, A., Hemraj, A., Garcia, A., and Munoz, D. (2011). Age-related trends in saccade characteristics among the elderly. *Neurobiol. Aging* 32, 669–679. doi: 10.1016/j.neurobiolaging.2009.04.001
- Polden, M., Wilcockson, T. D. W., and Crawford, T. J. (2020). The disengagement of visual attention: an eye-tracking study of cognitive impairment, ethnicity and age. *Brain Sci.* 10:461. doi: 10.3390/brainsci10070461
- Pulido, M. L. B., Hernandez, J. B. A., Ballester, M. A. F., Gonzalez, C. M. T., Mekyska, J., and Smekal, Z. (2020). Alzheimer's disease and automatic speech analysis: a review. *Expert Syst. Appl.* 150:113213. doi: 10.1016/j.eswa.2020.113213
- R Core Team (2022). R: A language and environment for statistical computing. R Foundation for Statistical Computing, Vienna, Austria. Available at: <https://www.R-project.org/>
- Roalf, D. R., Moberg, P. J., Xie, S. X., Wolk, D. A., Moelter, S. T., and Arnold, S. E. (2013). Comparative accuracies of two common screening instruments for classification of Alzheimer's disease, mild cognitive impairment, and healthy aging. *Alzheimers Dement.* 9, 529–537. doi: 10.1016/j.jalz.2012.10.001
- Salthouse, T. A. (1996). The processing-speed theory of adult age differences in cognition. *Psychol. Rev.* 103, 403–428. doi: 10.1037/0033-295X.103.3.403
- Santos, M. S., Soares, J. P., Abreu, P. H., Araujo, H., and Santos, J. (2018). Cross-validation for imbalanced datasets: avoiding overoptimistic and Overfitting approaches [research frontier]. *IEEE Comput. Intell. Mag.* 13, 59–76. doi: 10.1109/mci.2018.2866730
- Sjoberg, D. D., Whiting, K., Curry, M., Lavery, J. A., and Larmarange, J. (2021). Reproducible summary tables with the gtsummary package. *R Journal* 13, 570–594. doi: 10.32614/RJ-2021-053
- Tanveer, M., Richhariya, B., Khan, R. U., Rashid, A. H., Khanna, P., Prasad, M., et al. (2020). Machine learning techniques for the diagnosis of Alzheimer's disease: a review. *ACM Trans. Multimedia Comput. Commun. Appl.* 16, 1–35. doi: 10.1145/3344998
- Tobii Technology AB (2012). Tobii® Technology accuracy and precision test method for remote eye trackers. Tobii Pro, Danderyd, Sweden. Available at: <http://www.tobiipro.com/>
- Topcuoglu, B. D., Lapp, Z., Sovacool, K. L., Snitkin, E., Wiens, J., and Schloss, P. D. (2021). Mikropml: user-friendly R package for supervised machine learning pipelines. *J. Open Source Softw.* 6, 2–3. doi: 10.21105/joss.03073
- Tullis, T., and Albert, B. (2013). *Measuring the user experience: Collecting, analyzing, and presenting usability metrics*. Amsterdam, Heidelberg: Morgan Kaufmann, Elsevier.
- Wickham, H. (2017). The tidyverse. *R package ver 1.1*.



OPEN ACCESS

EDITED BY

Xuemin Li,
Peking University Third Hospital, China

REVIEWED BY

Sukru Demiral,
Clinical Center (NIH), United States
Alessio Fracasso,
University of Glasgow, United Kingdom

*CORRESPONDENCE

Olivia G. Calancie
✉ olivia.calancie@queensu.ca

RECEIVED 04 March 2023

ACCEPTED 30 May 2023

PUBLISHED 22 June 2023

CITATION

Calancie OG, Parr AC, Brien DC, Huang J, Pitigoi IC, Coe BC, Booij L, Khalid-Khan S and Munoz DP (2023) Motor synchronization and impulsivity in pediatric borderline personality disorder with and without attention-deficit hyperactivity disorder: an eye-tracking study of saccade, blink and pupil behavior. *Front. Neurosci.* 17:1179765. doi: 10.3389/fnins.2023.1179765

COPYRIGHT

© 2023 Calancie, Parr, Brien, Huang, Pitigoi, Coe, Booij, Khalid-Khan and Munoz. This is an open-access article distributed under the terms of the [Creative Commons Attribution License \(CC BY\)](https://creativecommons.org/licenses/by/4.0/). The use, distribution or reproduction in other forums is permitted, provided the original author(s) and the copyright owner(s) are credited and that the original publication in this journal is cited, in accordance with accepted academic practice. No use, distribution or reproduction is permitted which does not comply with these terms.

Motor synchronization and impulsivity in pediatric borderline personality disorder with and without attention-deficit hyperactivity disorder: an eye-tracking study of saccade, blink and pupil behavior

Olivia G. Calancie^{1*}, Ashley C. Parr², Don C. Brien¹, Jeff Huang¹, Isabell C. Pitigoi¹, Brian C. Coe¹, Linda Booij^{3,4}, Sarosh Khalid-Khan^{1,5} and Douglas P. Munoz¹

¹Queen's Eye Movement Lab, Centre for Neuroscience Studies, Queen's University, Kingston, ON, Canada, ²Department of Psychiatry, University of Pittsburgh, Pittsburgh, PA, United States, ³Department of Psychiatry, McGill University, Montreal, QC, Canada, ⁴Research Centre and Eating Disorders Continuum, Douglas Mental Health University Institute, Montreal, QC, Canada, ⁵Division of Child and Youth Psychiatry, Department of Psychiatry, School of Medicine, Queen's University, Kingston, ON, Canada

Shifting motor actions from reflexively reacting to an environmental stimulus to predicting it allows for smooth synchronization of behavior with the outside world. This shift relies on the identification of patterns within the stimulus – knowing when a stimulus is predictable and when it is not – and launching motor actions accordingly. Failure to identify predictable stimuli results in movement delays whereas failure to recognize unpredictable stimuli results in early movements with incomplete information that can result in errors. Here we used a metronome task, combined with video-based eye-tracking, to quantify temporal predictive learning and performance to regularly paced visual targets at 5 different interstimulus intervals (ISIs). We compared these results to the random task where the timing of the target was randomized at each target step. We completed these tasks in female pediatric psychiatry patients (age range: 11–18 years) with borderline personality disorder (BPD) symptoms, with ($n=22$) and without ($n=23$) a comorbid attention-deficit hyperactivity disorder (ADHD) diagnosis, against controls ($n=35$). Compared to controls, BPD and ADHD/BPD cohorts showed no differences in their predictive saccade performance to metronome targets, however, when targets were random ADHD/BPD participants made significantly more anticipatory saccades (i.e., guesses of target arrival). The ADHD/BPD group also significantly increased their blink rate and pupil size when initiating movements to predictable versus unpredictable targets, likely a reflection of increased neural effort for motor synchronization. BPD and ADHD/BPD groups showed increased sympathetic tone evidenced by larger pupil sizes than controls. Together, these results support normal temporal motor prediction in BPD with and without ADHD, reduced response inhibition in BPD with comorbid ADHD, and increased pupil sizes in BPD patients. Further these results emphasize the importance of controlling for comorbid ADHD when querying BPD pathology.

KEYWORDS

predict saccade, response inhibition, eye movement, metronome, psychotropic medication, arousal, psychiatric disease

1. Introduction

Borderline personality disorder (BPD) affects 1–2% of the population and represents a significant portion (15–30%) of patients in psychiatric clinics and inpatient hospitals (Gunderson et al., 2018). Individuals with BPD are highly susceptible to addiction, disability, incarceration, and death by suicide (Leichsenring et al., 2011). The Diagnostic and Statistical Manual of Mental Disorders (DSM-V) defines BPD based on nine distinct traits, requiring individuals to exhibit at least five of these traits for a diagnosis (American Psychiatric Association, 2022). These traits encompass emotional instability, efforts to avoid abandonment, identity disturbance, chronic feelings of emptiness, difficulty controlling anger, patterns of interpersonal conflict, recurrent suicidal behavior, stress-related paranoid ideation or dissociation, and impulsive behavior. As BPD symptoms typically emerge during adolescence (Wright et al., 2016), it is crucial to characterize the biology of the disease during this stage to facilitate early identification and therapeutic intervention.

Among the various techniques available for investigating brain-based behavior, video-based eye-tracking has emerged as a powerful non-invasive tool that can assess different levels of the nervous system (McDowell et al., 2008; Eckstein et al., 2017). Firstly, vision provides valuable insights into the integrity of various structures such as the retina, optic nerves, brainstem, thalamic lateral geniculate nuclei, and visual cortex. Secondly, the coordination of rapid eye movements, known as saccades, for visual scene exploration involves neural signaling from widespread areas of the brain, including the cortex, subcortical nuclei, brainstem, and cerebellum (Liversedge et al., 2011). In fact, more than 50% of cortical surface is dedicated to visual processing. Thirdly, blinks, in addition to maintaining the health of the anterior surface of the eye, have been found to vary with cognitive demand and are sensitive to disruptions in dopaminergic neurotransmitter signaling, as seen in conditions like Parkinson's disease and Schizophrenia (Basso et al., 1996; Swartrauber and Fujikawa, 1998; Taylor et al., 1999; Schmahmann, 2000; Agostino et al., 2008; Cruz et al., 2011). Fourthly, the constriction and dilation of pupils, regulated by the sphincter and dilator muscles respectively, reflect the tone of the parasympathetic and sympathetic nervous systems (Kandel et al., 2000). By precisely quantifying eye behavior in terms of saccades, blinks, and pupil responses, it is possible to gain insights into the underlying function of the nervous system, ranging from neurotransmitter levels to neural circuitry. Indeed, the extensive body of eye-tracking literature demonstrates how eye behavior changes during human development (Luna et al., 2008; Calancie et al., 2022; Yep et al., 2022), aging (Peltsch et al., 2011; Yep et al., 2022), psychiatric pathology (Hutton and Ettinger, 2006; Gooding and Basso, 2008; Rommelse et al., 2008; Thakkar et al., 2011; Huang et al., 2022), and neurologic disease (Brien et al., 2023; Riek et al., 2023).

Previous eye-tracking studies have provided valuable insights into the eye behavior of individuals with borderline personality disorder (Grootens et al., 2008; Rentrop et al., 2008; Jacob et al., 2010; Bertsch

et al., 2017; Kaiser et al., 2019; Bortolla et al., 2020; Seitz et al., 2021; Parr et al., 2022), with all but one (Parr et al., 2022) describing BPD in adults. These eye-tracking studies have reported an increased incidence of anticipatory saccades in BPD (Grootens et al., 2008; Parr et al., 2022), which are characterized by initiating eye movements before the minimum required time for visual target processing and subsequent saccade execution. Anticipatory saccades can be viewed as indicators of irregular waiting impulsivity, reflecting the ability to withhold actions to gather sufficient information for making accurate choices (Dalley and Robbins, 2017). This behavior has been associated with diminished prefrontal cortex activity and has been observed in other psychiatric pathologies (Pierrot-deseilligny et al., 1991; Gaymard et al., 1998; Ross et al., 1998; Walker et al., 1998; Carr et al., 2006; Yep et al., 2018). However, the extent to which this finding in BPD is influenced by presence of comorbid psychopathology, such as ADHD, remains unclear. Furthermore, studies have shown that individuals with BPD exhibit faster saccade reaction times to emotionally valent stimuli compared to controls, suggesting an attentional bias toward negative emotional stimuli in particular, consistent with the reliable findings of limbic system hyperactivity (Schulze et al., 2016; Bertsch et al., 2017; Bortolla et al., 2020; Seitz et al., 2021).

Despite these studies, there is limited understanding of other basic saccade parameters, such as peak velocity and amplitude, in individuals with BPD, as most previous eye-tracking studies have focused solely on saccade reaction time. Consequently, the functioning of the reflexive saccade system in BPD remains poorly understood. Similarly, blink behaviors in BPD have received a paucity of research attention. Although two previous studies using startle response paradigms found no differences in induced blink responses between non-medicated BPD patients and controls (Herpertz and Koetting, 2005; Limberg et al., 2011), there is a dearth of studies examining baseline blink rate or the modulation of blink rate by different task sets in BPD. Considering that antipsychotic medication is commonly prescribed for managing BPD and affects dopaminergic and other signaling pathways (Jongkees and Colzato, 2016), it is plausible that blink rates may be altered in individuals with BPD.

Pupillary analysis has been explored in one study of BPD, which revealed increased pupillary dilation magnitude in adolescent females with BPD when exposed to maternal criticism (Scott et al., 2017). However, it remains unknown whether pupil size is larger than that of matched controls under emotionally neutral conditions. Given the heightened incidences of aggression, self-harm, and impulsivity in individuals with BPD (Stepp et al., 2012; Gunderson et al., 2018), characteristic of the fight or flight response, it is hypothesized that sympathetic nervous system tone is elevated in BPD patients, leading to increased pupil diameters compared to controls at rest.

To further investigate eye behavior in BPD, the present study collected video-based eye-tracking data from adolescent patients with BPD and age-matched controls. Two oculomotor tasks were performed, involving the movement of eyes toward visual targets with different temporal predictabilities. In the metronome task, participants

were instructed to move their eyes in time with a target that alternated between two fixed locations at a fixed interstimulus interval (ISI; 5 ISIs were tested ranging from 500–1,500 ms). The random task was identical to the metronome task except the timing of the target was randomized at each step, making the target's location predictable but its timing unpredictable. In the metronome task, successful prediction of targets requires maintenance of the ISI and the production of voluntary saccades that match the timing of target arrival. In the random task, however, participants need to only reflexively react to targets given that their timing was unknown. The tasks aimed to evaluate variations in blink and pupil responses associated with different task difficulties. As BPD is frequently comorbid with ADHD (with an incidence of approximately 50%) (Philipsen et al., 2008; Fossati et al., 2014), and previous research has shown distinct behaviors in individuals with comorbid ADHD and BPD, the data of individuals with BPD and comorbid ADHD (referred to as 'ADHD/BPD') were analyzed separately. Additionally, considering that most pediatric BPD patients receiving medical care at our tertiary care hospital were female, and previous BPD studies have supported gender-based differences in BPD behavior, we specifically recruited female participants for this study (McCormick et al., 2007; Herpertz et al., 2017).

2. Materials and methods

2.1. Participants and study recruitment

The research protocol was reviewed and approved by Queen's University Faculty of Health Sciences (protocol ID: PHYS-007-97). We recruited females aged 11–18 years (*Mean age* = $15.8 \pm \text{Standard Deviation}$ = 1.6 years), inclusive for study participation. Child and adolescent psychiatrist co-author SKK recruited pediatric psychiatry participants from Hotel Dieu Hospital Child and Youth Mental Health's Dialectical Behavioral Therapy outpatient clinic which provides psychiatric care for pediatric patients with signs of BPD. Patients attending this clinic have high health care utilization (e.g., multiple emergency room visits for suicide attempts and frequent resulting hospitalizations). Those who were interested in study participation completed an in-person interview for BPD symptomology, known as the Structured Clinical Interview for DSM-5 Diagnosis for Borderline Personality Disorder (SCID-PD-5). The interview was delivered by a graduate student who received SCID-PD-5 training and supervision by SKK. Patients who met criteria for BPD on the SCID-PD-5 (i.e., >5 responses with a score of 2) were invited to participate in the research study and are referred to the 'BPD' participant group moving forward. Members of the BPD participant group who had a pre-existing comorbid diagnosis of ADHD diagnosed by a child and adolescent psychiatrist were analyzed separately as the 'ADHD/BPD' group. Participants in the BPD and ADHD/BPD groups were not asked to interrupt their medication regimen on the day of testing and any medications that the patients were taking were documented. Participants had normal or corrected-to-normal vision and were free of ocular conditions. Control participants were recruited via study flyers advertised in the local newspaper and university campuses. Control participants were required to meet the following criteria for study inclusion: (1) absence of neurological, ocular, or psychiatric diagnoses; (2) not taking

psychotropic medications; and (3) normal or corrected-to-normal vision.

Participants aged ≥ 17 years old provided written consent. Participants aged 11–16 years provided their oral assent and written consent was obtained by a legal guardian. Participants were compensated for their time at a rate of \$20/h. Clinical participants filled out self-report scales to provide measures of BPD and ADHD symptomology. Based on previous eye-tracking studies in BPD and ADHD cohorts (Gould et al., 2001; Grootens et al., 2008; Hakvoort-Schwerdtfeger et al., 2013; Parr et al., 2022), sample sizes for adequate statistical power was estimated with the following parameters: ANOVA design (3 groups: BPD, ADHD/BPD, and control), 0.05 alpha level, 0.8 power, and 0.5 medium effect size. It was determined that a sample size of 64 resulted in a statistical test power of 0.805, resulting in 21.3 participants per group.

2.2. Eye-tracking set-up and task paradigms

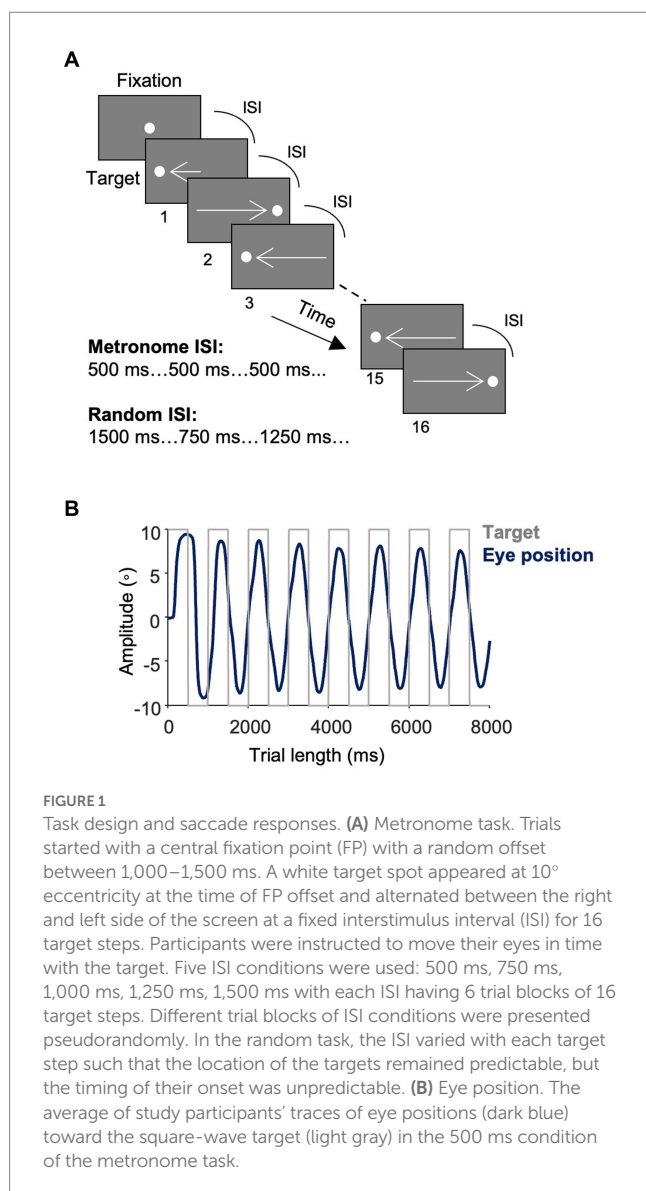
2.2.1. Eye-tracking set-up

Eye-tracking was completed in a black-out room with participants seated and their head position stabilized by a fixed head mount and chin rest. Participants were seated 60 cm away from a 17-inch LCD iiYama Prolite monitor with a viewing angle of 32×26 degrees. The LCD monitor has a refresh rate of 60-Hz with a screen resolution of $1,280 \times 1,024$ pixels. Monocular eye position was recorded at a sampling rate of 500 Hz with an infrared video-based eye-tracker (Eyelink 1000 Plus, SR Research Ltd., ON, Canada). Prior to completing the experimental tasks, participants performed a 9-point calibration and validation procedure. Accuracy of eye position from target was required to be within 1.5° for collection of eye-tracking data.

2.2.2. Experimental task paradigms

Two eye-tracking tasks (Figure 1A) were completed by each participant, the *metronome task* and *random task*. In the metronome task, participants were cued with a central fixation point (FP; 0.5° in diameter and 44 cd/m^2 in luminance) with a random offset between 1,000–1,500 ms. A target then appeared on the right-side of the screen, 10 degrees away from central FP. The target proceeded to step between the right and left side of the screen for 16-target steps. Thereby the first target step was 10 degrees away from the central FP, with the following target steps were 20 degrees in the opposite direction from the previous target step (Figure 1B). The timing of the ISI was held constant for each of the 16 target steps – with 5 different ISI durations tested: 500 ms (i.e., 2 target steps per second), 750 ms, 1,000 ms, 1,250 ms and 1,500 ms. Thus, the location and timing of target appearance was predictable. Participants completed 6 blocks of each ISI, yielding 96 total target steps per ISI. ISI conditions were arranged with pseudorandom order so that all participants were exposed to the same order of ISI blocks. Participants were instructed to try and match the timing of their saccade with the appearance of the target.

The random task was identical to the metronome task except that the ISI changed with each target step, such that the direction of the target remained predictable, however, the timing of its appearance was random. The same 5 ISIs were used for target steps and a pseudorandom order was used, such that participants were never cued with more than two identical ISIs back-to-back. Like the metronome



task, participants completed a total of 30 experimental blocks of 16 target steps. In both tasks, participants performed a re-calibration and validation procedure every 5 blocks to ensure accurate eye-tracking during the duration of the recording. The order of tasks was randomized so that some participants completed the metronome task first and others did the random task first. Together, the metronome and random tasks took about 25 min to complete.

2.2.3. Self-report clinical questionnaires

Self-report measures of impulsivity, BPD symptoms and suicidality were obtained by clinical participants prior to eye-tracking. Impulsivity was assessed using the Barratt Impulsivity Scale (BIS), a well-validated tool that provides a measure of impulsivity as a total score and domains of impulsivity as subscale scores (Barratt, 1959; Moeller et al., 2001). Subscales include Attention, Motor, Cognitive Instability, Perseverance, Self-control, and Cognitive Complexity. BPD symptom severity was measured with the Borderline Symptom List 23 (BSL) which asks over the last week how often individuals felt statements such as, 'I did not trust other people', 'My mood rapidly

cycled in terms of anxiety, anger, and depression', and 'Criticism has a devastating effect on me' (Bohus et al., 2009). Suicidality was assessed with the Suicide Behaviors Questionnaire – Revised (SBQ), which asks statements such as, 'Have you ever thought about or attempted to kill yourself?' and 'How often have you thought about killing yourself in the past year?' (Osman et al., 2001). A cut-off score of ≥ 7 has a sensitivity of 93% and specificity of 95% of detecting individuals at suicide risk.

2.3. Behavior detection and analysis

2.3.1. Saccade detection

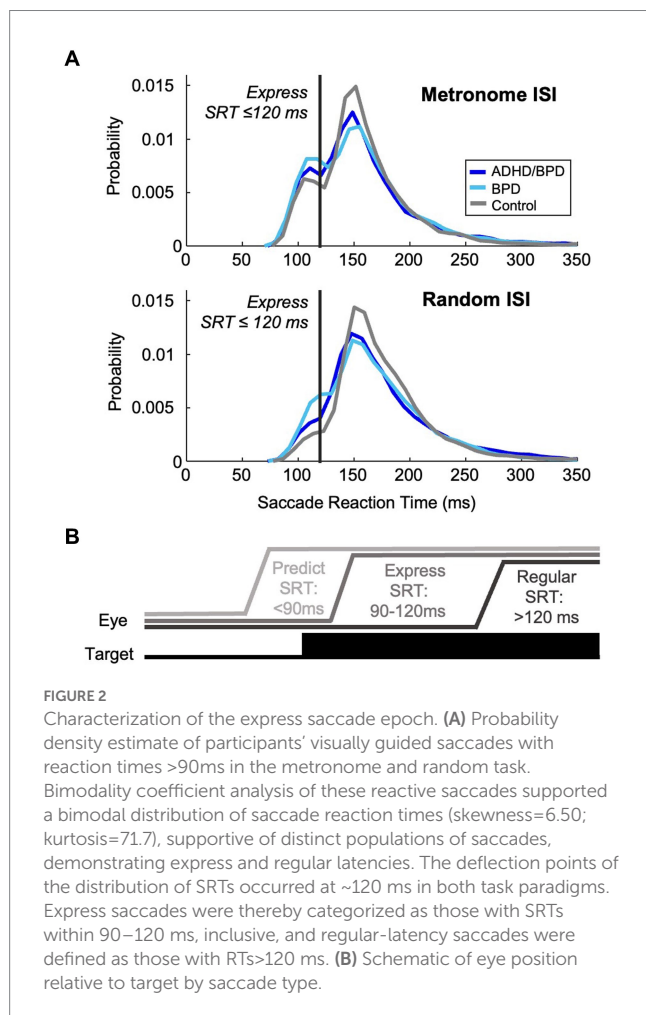
Data from Eyelink 1,000 Plus were analyzed offline using Matlab version R2022 (MathWorks). Saccades were labeled when the instantaneous velocity of eye position in the x and y plane was greater than 2 standard deviations above the mean fixation velocity (defined as $<50^\circ/\text{s}$) for at least five continuous data points.

2.3.2. Eye-tracking parameters

2.3.2.1. Saccade

Metrics of saccade data included saccade reaction time (SRT), amplitude ($^\circ$), and peak velocity ($^\circ/\text{s}$). SRT was calculated by subtracting the time of the start of a saccade from target appearance. Saccades were defined as *predict*, *express* or *regular* according to SRT. Predict saccades are generated before the minimum amount of time needed for neural signaling of the visual target has elapsed and a saccade motor command to said target is generated. Previous work showed that when generating a saccade to one of two potential target locations, saccades with RTs > 90 ms had an accuracy above 95%, whereas those initiated with RTs < 90 ms had a chance accuracy of 50%, indicating the lower limit for SRTs to visual stimuli as 90 ms (Munoz et al., 1998). Saccades made before 90 ms are considered a *guess* to a potential target location and are internally generated. Express saccades occur when the incoming visual transient signal combines with a saccade motor command, causing ultra-fast saccades to targets. The upper epoch of the express saccade window has been shown to vary with experimental conditions (i.e., target luminance, presence of a fixation gap, and target eccentricity) (Weber et al., 1992; Paré and Munoz, 1996; Dorris and Munoz, 1998; Marino and Munoz, 2009; Marino et al., 2015). We thus quantified the express epoch according to the distribution of SRTs in the metronome and random tasks. Bimodal coefficient testing was performed to identify the change in SRT distribution between express and regular saccade latencies (when the visual transient signal does not combine with a saccade motor command). For both metronome and random tasks, the deflection in SRT distribution between the two saccade populations was observed at ~ 120 ms (Figure 2A). Accordingly, the express saccade epoch for this paper was defined as 90–120 ms, inclusive (Figure 2B), in agreement with a previous study with the same experimental tasks (Calancie et al., 2022). Regular latency saccades were defined as those with SRTs > 120 ms. Percentage of trials with predict, express and regular saccades to targets was calculated per subject in the 5 metronome ISI conditions and in the random task and averaged within groups to allow for group comparison.

Saccade amplitude to target was measured in degrees with a maximum eye position error of $\pm 1.5^\circ$ away from target location. Peak saccade velocity was calculated for each saccade with its maximum set



to 1,000°/s, as saccades made above this threshold are due to signal noise and do not reflect true saccades. The main sequence of saccades was calculated for individual subjects using square root models of amplitude and peak velocity, which has been shown to be a robust model for main sequence characterization of saccades with amplitudes between 5–20° (Gibaldi and Sabatini, 2021). Individual main sequence models were then averaged for each group and model coefficients and 95% CIs are reported.

2.3.2.2. Blink

During eye-tracking there are periods when the eye position signal is absent, known as eye loss – some of which are caused by blinks. To separate eye loss due to blinks from eye loss due to poor video-based tracking or not following the instructions of the experimental task, we plotted the durations of eye loss. As supported by previous blink literature (Caffier et al., 2003; Betke and Chau, 2005), we observed a consistent profile of eye loss durations between 50–300 ms characteristic of blinks and therefore used this duration limit for blink classification and subsequent analysis. Blink rates and blink reaction times relative to target appearance were computed for the experimental paradigms.

In the metronome task, blink probability was analyzed for each individual subject from –1,000 ms to +1,000 ms relative to target appearance. A logical array was computed for individual subjects at

each data collection point across the trial length (i.e., 500 Hz sampling rate aka every 2 ms). The 2 ms timeslot was represented with a 0 when the participant was not currently in a blink or a 1 when they were blinking. Individuals' logical arrays were then averaged across the 480 metronome trials to create an average of blink probability per subject. Re-sampling via bootstrapping with replacement was performed to generate blink probability means and confidence intervals (CIs). Difference scores were then calculated between groups to allow for statistical comparison (i.e., re-sampled mean of ADHD/BPD blink probability – re-sampled mean of BPD blink probability). 95% CIs were computed for each difference score. If the 95% CI for the difference score did not include 0, the difference scores were considered significantly different from one another, supporting that blink probability varied by group at that time. We report periods of significant difference scores across the trial epoch for each group comparison as well as the corresponding standardized Cohen d effect sizes. Smoothing splines were fit to the blink probability and Cohen d effect size data using a fraction of the total number of data points approach (fraction = 0.05; the smoothed value reflected 100 ms of trial duration).

2.3.2.3. Pupil

Pupil size was recorded throughout the duration of the eye-tracking tasks to determine eye position. To provide a measure of average pupil size, indicative of autonomic tone, recordings were averaged over 200 ms following a saccade to target. This epoch was selected to avoid the pupillary light reflex triggered by target luminance which is known to take into effect >200 ms after stimulus appearance (Ellis, 1981; Wang et al., 2018). By analyzing pupil size post-saccade on a trial-by-trial level, its size could be subsequently compared by saccade type (i.e., predict, express, regular) as well as participant group. Pupil traces were included for analysis if they met the following criteria: (1) fixation occurred for a minimum of 200 ms; (2) the timing of fixation onset exceeded 100 ms between fixation and the next target appearance; (3) pupil velocity was within –5,000°/s to 5,000°/s; and (4) the pupil trace was free of any blinks or eye loss.

2.4. Statistical testing and reporting

Eye behavior data analyzed were saccade metrics (i.e., SRT, velocity, amplitude, main sequence), % predict, express, and regular saccades to metronome and random ISI targets, blinks (i.e., blink rate, blink reaction time to target, blink probability across trial length) and pupil size. Independent variables were group membership (ADHD/BPD, BPD, and control), task (metronome; random), and ISI (5 different ISIs were tested in the metronome task). Before group comparison analysis, data were tested for normalcy using the Shapiro–Wilk test. If eye-tracking data did not meet the Shapiro–Wilk's test for normality, non-parametric tests were performed, and mean ranks were reported. Group differences in eye behavior and task performance were assessed using the Kruskal–Wallis test for non-parametric data or ANOVA for parametric data. Analysis of group differences are based on the group mean of individual means of eye behavior variables. Correlation analyses were performed for clinical questionnaire data and eye behaviors using Spearman rank test or Pearson correlation depending on the data skewness. Main effects were followed-up with *post-hoc* *t*-tests using the Bonferroni

TABLE 1 Summary of demographic features and psychotropic medication prescriptions to clinical participants.

	ADHD/BPD mean (SD)	BPD mean (SD)	Control mean (SD)
Sample size (N)	22 F	23 F	35 F
Age (range = 11–18 years)	16.32 (1.55)	16.42 (1.48)	15.26 (1.43)
Medication Classes			
Stimulants (% of participants)	9 (40.9%)	4 (17.4%)	0
SSRIs (% of participants)	12 (54.5%)	17 (73.9%)	0
Second-generation antipsychotics (% of participants)	9 (40.9%)	9 (39.1%)	0

Clinical participants stayed on their medication regimen on the day of eye-tracking testing and reported the psychotropic agents that they were prescribed. Psychotropic drugs were classified according to whether they were among the stimulant, SSRI, or SGA medication class. Medication data are reported as the number (percentage) of participants within the given clinical group on that class of medication. Three psychiatric participants were not taking psychotropic medication, 22 were taking a drug from 1 psychotropic class, 15 from 2 classes, and 4 from 3 classes. Medication data was unavailable for 1 participant. No controls reported taking psychotropic medications on the day of testing. F, Female; SSRI, Selective Serotonin Reuptake Inhibitors.

correction to protect against type I errors (i.e., 0.05/number of eye behavior variables = corrected alpha) and effect sizes are reported as an eta-squared or Cohen's d. Based on previous papers that performed the metronome and random tasks in neuropsychiatric patients, we expected to observe a small to medium effect size for differences in % predict saccades to alternating targets between groups (Thakkar and Rolfs, 2019; Vaca-Palomares et al., 2019; Deravet et al., 2021). Due to the novel nature of blink and pupil analysis in BPD and ADHD/BPD participants during a saccade task, we did not have a prior expectation of the magnitude of effect sizes for blink and pupil variables.

3. Results

3.1. Participants

Table 1 shows the demographic data of study participants. 23 BPD, 22 ADHD/BPD and 35 control participants completed the research study and were included for analysis. Participants were on average 15–16 years of age and all participants were Female. Clinical participants were not asked to interrupt their medication regimen and their prescribed psychotropic drugs are reported in Table 1. Clinical participants filled out self-report questionnaires on BPD and ADHD symptomology in addition to eye-tracking testing (Table 2). Scores of psychiatric symptomology did not differ among BPD and ADHD/BPD participants.

3.2. Saccade behavior

3.2.1. Saccade main sequence and reaction time

The saccade main sequence was estimated per subject in the metronome task using saccade data from the 5 ISI conditions pooled together and then averaged for participant groups (Supplementary Figure S1). As expected, there was a significant effect of saccade type on the main sequence ($F[2,234] = 28.5$; $p = 8.38 \times 10^{-12}$, $\eta^2 = 0.196$), with a significantly lower main sequence observed for predict saccades (Mean model coefficient = 96.6, $SD = 1.80$) versus express ($M = 112.3$, $SD = 17.2$; $p < 5.117 \times 10^{-10}$) and regular ($M = 111.5$, $SD = 16.6$; $p < 2.75 \times 10^{-9}$). Main sequence fits for express and regular saccades did not differ. Main sequence model coefficients did not vary by participant group ($p = 0.332$); see Supplementary Figure S1 for model coefficients and 95% CIs. Average SRTs are plotted for each

TABLE 2 Self-report scores of impulsive and borderline personality disorder symptoms among clinical participants.

	ADHD/BPD mean (SD)	BPD mean (SD)	T-statistic	p
Impulsivity (BIS)				
Total	81.81 (10.56)	75.36 (8.29)	3.24	0.08
Motor	19.00 (4.02)	16.45 (3.42)	0.36	0.55
Cognitive instability	8.71 (1.71)	8.45 (2.02)	0.64	0.43
Attention	14.76 (2.98)	13.00 (2.12)	0.84	0.37
Self-control	17.14 (3.98)	15.91 (3.50)	0.55	0.46
Cognitive complexity	13.05 (2.80)	12.95 (2.03)	1.88	0.18
Perseverance	9.14 (2.01)	8.59 (2.20)	0.92	0.34
BPD Symptoms (BSL)	44.43 (25.09)	53.05 (23.98)	-1.15	0.26
Suicidality (SBQ)	13.63 (2.91)	13.85 (3.22)	0.22	0.83

ADHD/BPD and BPD patients did not significantly differ in their self-report scores in the BIS (Barratt Impulsivity Scale), BSL (Borderline Symptom List-23), or SBQ (Suicidal Behaviors Questionnaire).

target step in Supplementary Figure S2 in the random and metronome task. In the metronome task, participants generally made saccades with RTs < 90 ms (marked by a horizontal gray line) by target steps 3–4. SRTs to randomized targets were on average predictive in ADHD/BPD participants compared to reactive in BPD and control groups.

3.2.2. Temporal prediction

The percentage of predict, express or regular saccades did not differ among groups in the metronome task (see Table 3). In general, study participants produced 50–70% of saccades in anticipation of the target appearance, with fewer predict saccades observed in the slower pacing conditions (i.e., 1,250 ms and 1,500 ms ISI conditions). The percentage of predict saccades was consistently higher in the BPD group compared to ADHD/BPD and controls, however, this effect was non-significant. In the random task, the percentage of predict saccades significantly varied by group [$\chi^2(2) = 11.13$; $p = 0.004$; $\eta^2 = 0.148$; with a Mean rank of 49.64 for ADHD/BPD, 43.93 for BPD and 30.07 for controls]. Post-hoc tests revealed that ADHD/BPD participants made significantly more predict saccades than controls ($p = 0.005$; no other groups differed). Express saccades varied by group in the random task [$\chi^2(2) = 9.93$; $p = 0.007$; Mean rank of 42.34 for ADHD/BPD, 49.95 for BPD and 30.90 for controls],

TABLE 3 Percentage of predictive saccades toward randomized and predictable ISI targets.

	ADHD/BPD mean \pm SD	BPD mean \pm SD	Control mean \pm SD	Chi-square	<i>p</i>
% of Predict saccades					
Random ISI	25.12 \pm 16.78%	18.48 \pm 10.69%	12.68 \pm 10.55%	11.13	0.004
500 ms ISI	59.61 \pm 20.62%	68.23 \pm 17.19%	65.20 \pm 18.86%	2.75	0.25
750 ms ISI	61.82 \pm 17.94%	69.59 \pm 17.06%	67.59 \pm 19.45%	3.33	0.19
1,000 ms ISI	56.18 \pm 19.64%	60.12 \pm 19.14%	56.42 \pm 18.95%	0.66	0.72
1,250 ms ISI	49.71 \pm 18.34%	50.56 \pm 19.50%	45.12 \pm 19.62%	1.44	0.49
1,500 ms ISI	41.12 \pm 19.51%	43.78 \pm 18.63%	39.50 \pm 19.30%	1.0	0.58

A main effect of participant group \times % of predictive saccades was observed in the random task. Post-hoc *t*-tests showed that the ADHD/BPD group made significantly more predictive saccades compared to controls. Participant groups did not significantly differ in their percentage of predictive saccades toward metronome targets in any of the ISI conditions. As the ISI lengthened, % of predictive saccades decreased for all groups.

with BPD subjects generating more express saccades than controls ($p=0.006$). Additionally, a main effect of group on the percentage of regular saccades was found in the random task, $\chi^2(2)=14.86$; $p=0.001$; Mean rank of 30.14 for ADHD/BPD, 31.50 for BPD and 50.74 for controls. Both psychiatric cohorts, ADHD/BPD ($p=0.003$) and BPD ($p=0.006$), made significantly fewer regular saccades in the random task versus controls.

The target step for when individuals made their first predict saccade to regularly paced targets was analyzed to estimate speed of temporal predictive learning among groups. Kruskal-Wallis tests were performed with a Bonferroni correction applied for multiple comparisons ($0.05/5=0.01$ corrected alpha). Results found no group effect for four of the five ISIs. A significant effect was noted for the 1,000 ms ISI condition (KW test statistic=9.917, $p=0.007$) with a *post-hoc* significant difference between controls (Median = 4.00 \pm Standard Deviation = 2.17) and BPD (3.00 \pm 1.82; $p=0.002$). On average, BPD participants launched their first predict saccade one target step earlier than controls (i.e., target step 3 versus 4). Accuracy of temporal prediction to periodic targets was calculated based on the time gap between the end of the saccade and target appearance in milliseconds. There was no effect of group or ISI on temporal prediction accuracy ($F=2.604$, $p=0.075$; $F=1.675$, $p=0.155$, respectively). On average, participants ended their saccade ~ 100 – 200 ms prior to target appearance (Supplementary Figure S3).

3.3. Blink behavior

3.3.1. Blink duration

Durations of lost eye-tracking were plotted as histograms to identify signal loss that was characteristic of blinks (Figure 3). In agreement with previous literature, our data supported increased periods of eye loss between 50–300 ms, characteristic of blink durations (Caffier et al., 2003; Betke and Chau, 2005). Eye loss within this range was labeled as blinks for subsequent analyses, see dotted vertical lines denoting this range in Figure 3. A main effect of group on blink duration was observed ($F(2,75)=5.64$; $p=0.0052$), with *post-hoc* statistics revealing that individuals with ADHD/BPD made on average significantly longer blink durations (Mean = 167.3 ms \pm SD = 28.3) compared to controls (139.9 ms \pm 32.0; $p=0.0054$) but not compared to BPD (142.925 ms \pm 30.914; $p=0.0277$; failed Bonferroni correction for multiple comparisons).

3.3.2. Blink rate by diagnosis and psychotropic medication

A two-way ANOVA tested the effect of group \times ISI on blink rate. A main effect of participant group \times blink rate was found ($p<0.001$; Figure 4), however, there was no effect of ISI condition ($p=0.053$). Tukey post-hoc tests confirmed that ADHD/BPD participants had significantly higher blink rates than BPD ($p=0.002$) and controls ($p<0.001$). Blink rate did not vary among subjects when the timing of target appearance was random ($p=0.288$). Given the main effect of blink rate in ADHD/BPD participants, we tested if blink rate in the metronome task interacted with impulsivity measures, which are related to ADHD symptomology. Indeed, blink rate positively correlated with ADHD/BPD participants' total scores on the Barratt Impulsivity Scale (Rho correlation coefficient = 0.499; $p=0.021$). Barratt Impulsivity subscale measures demonstrated positive trends with blink rate, such as Perseverance (Rho = 0.514; $p=0.017$), Cognitive Complexity (Rho = 0.506; $p=0.019$) and Attention (Rho = 0.436; $p=0.048$), however, none of these results passed the Bonferroni correction for multiple comparisons ($0.05/6$ BIS subscales = 0.0083 corrected alpha).

To understand if increased ADHD/BPD blink rates were in part driven by medication effects, one-tailed independent *t*-tests were performed according to whether clinical participants were taking any medications from three common psychotropic drug classes (SSRIs; psychostimulants; second-generation antipsychotics) for the metronome and random task, respectively. Blink rates were averaged across the 5 ISI conditions for metronome analysis, however, mean blink rates for each ISI are plotted in Figure 5. No main effect of medication classes on blink rates was observed in the metronome task: stimulant ($t[42]=-0.89$, $p=0.81$), SSRI ($t[42]=1.48$, $p=0.07$), and SGA ($t[42]=0.99$, $p=0.16$). Nor was there a main effect of medication class on mean blink rates in the random task: stimulant ($t[42]=-0.71$, $p=0.76$), SSRI ($t[42]=1.61$, $p=0.057$), and SGA ($t[42]=0.17$, $p=0.43$). Despite the lack of main effects of medication class on blink rate, Figure 5 reveals that there was a trend of increased blink rate for SSRIs versus no SSRIs and this was also observed in the random task as well ($p=0.07$ and $p=0.05$, respectively). It is possible that this trend may prove significant in a larger sample size or in experimental designs that apply ON versus OFF within-subject analysis. Based on these results, psychotropic medication prescriptions do not appear to be a significant contributor for the blink-related differences observed between ADHD/BPD participants versus BPD and controls.

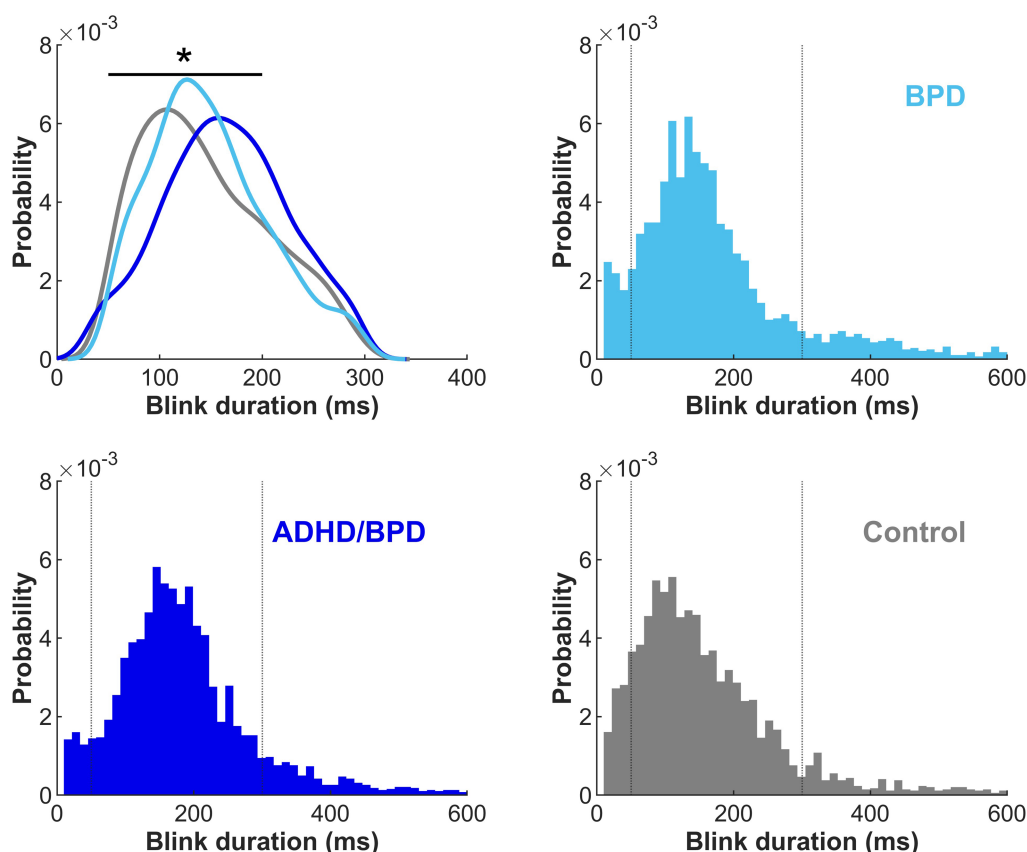


FIGURE 3

Duration of blinks by participant group in the metronome and random tasks combined. Kernel density estimate for eye loss durations between 50–300 ms are plotted by participant group in the upper left panel. The remaining three panels show eye loss durations with a range of 10–600 ms and a bin width of 50 ms. Dotted vertical lines represent the eye loss duration cut-off (50–300 ms) for blink analysis inclusion. Duration of blinks significantly varied by participant group, with ADHD/BPD participants making significantly longer blinks than control participants ($p < 0.01$).

3.3.3. Blink timing relative to target appearance

To understand when blinks occurred, we evaluated the ‘reaction time’ of blinks relative to target appearance when targets were predictable (i.e., metronome task). A main effect of ISI on blink reaction time was found ($F [4,331] = 82.908$; $p < 0.01$) and this effect did not vary with group ($p = 0.770$). Blink reaction times steadily climbed with longer ISI durations (bottom panel of Figure 4), showing that participants blinked at the half-way point of the ISI. For example, in the 500 ms interval, average participants’ blink reaction time was 275 ms and in the 750 ms interval, average blink RT was 404 ms.

Next, blink probabilities were analyzed on a trial-by-trial basis in the metronome task to determine if blink timing varied by saccade type. We sought to understand if the timing of blinks changed based on whether participants anticipated pacing targets or reflexively reacted to them. Mean blink probability and its 95% CI (shaded region) is plotted in Figure 6 for ADHD/BPD and control groups for the 1,000 ms before and after metronome target appearance. Periods where blink probabilities significantly differed by group are shown via significance lines at the top of panel B of Figure 6 with the color indicating which group had higher blink probabilities at that time. Standard Cohen d effect sizes for between-group differences at those time periods support large effect sizes between 0.6–0.8, with ADHD/BPD having higher blink probabilities than controls for all three saccade conditions.

The probability of blinks varied with saccade type relative to target onset at 0 ms (see vertical line). For both predict and express saccades,

blink probability was near 0 at target onset for all three comparisons (see Supplementary Figure S4 for BPD versus controls and ADHD/BPD versus BPD), whereas it is about 0.02–0.04 for regular saccades. In the 200 ms epoch prior to target appearance, blink probability is near 0 for predict saccades, 0.02 for express saccades, and 0.04 for regular saccades, demonstrating a systemic change in likelihood of participants blinking relative to SRT. These data demonstrate that blink probabilities for 200 ms prior to target appearance, irrespective of group membership, can reasonably predict the type of saccade a participant is going to make to target. There was a main effect of group on blink probability ($F [2,234] = 6.778$; $p = 0.01$). In general, ADHD/BPD participants had the highest blink probabilities compared to BPD and controls. In sum, these data suggest that the timing of when a blink occurs is tightly coupled with saccade onset, which does not change with psychopathology, likely reflective of low-level midbrain-brainstem coordination, whereas the probability of blinks on a given trial indeed varies with psychopathology.

3.4. Pupil behavior

3.4.1. Pupil size was elevated in BPD and ADHD/BPD

A main effect of pupil size by group was observed in the metronome task ($F [2,76] = 9.78$, $p = 1.66e-04$), with *post-hoc* t -tests revealing that

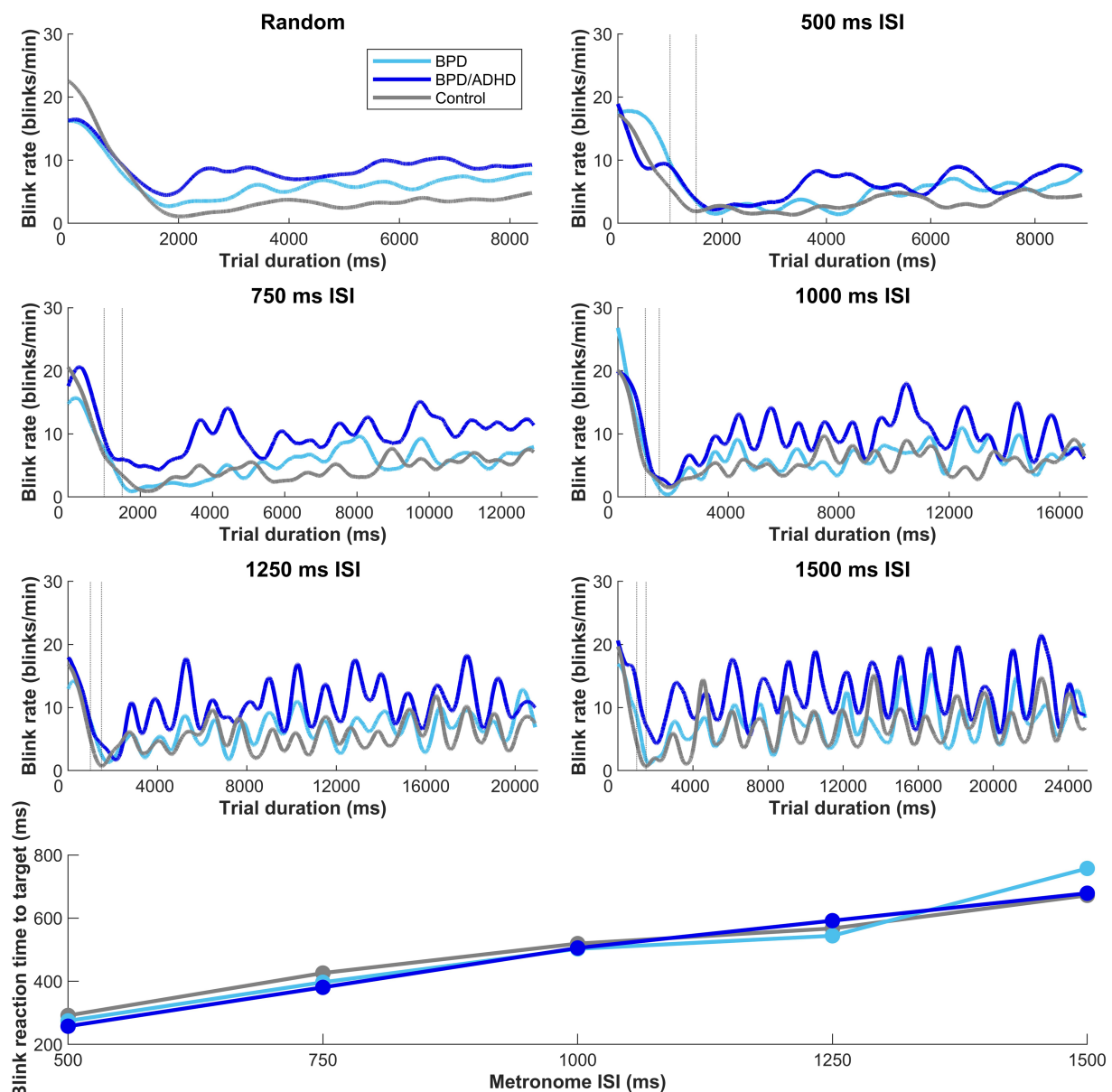


FIGURE 4

Moving average of blink rate in the metronome and random task across trial duration. Dashed vertical lines represent the random offset between 1,000–1,500 ms when the central fixation point at the start of trial disappeared. A main effect of blink rate by participant group was observed in the metronome task, with *t*-tests revealing higher blink rates in ADHD/BPD than BPD ($p=0.002$) and controls ($p<0.001$). Mean blink rates displayed a sinusoidal structure after the first 1–3 target steps, with the subsequent number of peaks corresponding to the number of target steps. No main effect of blink rate \times group was observed when the ISI of targets was randomized (top left panel). In the bottom panel of the figure, participant mean blink reaction times to target are plotted by target ISI. Blink reaction times roughly approximated the half-way point of the ISI, with a participant mean of $275.2\text{ms} \pm \text{standard deviation} = 101.0$ for 500 ms ISI, $404.4\text{ms} \pm 120.2$ [750 ms ISI], $510.7\text{ms} \pm 136.7$ [1,000 ms ISI], $567.5\text{ms} \pm 142.4$ [1,250 ms ISI], and $698.5\text{ms} \pm 198.7$ [1,500 ms ISI].

pupil sizes of ADHD/BPD ($\text{Mean} = 3,775.9 \pm \text{SD} = 1,206$) and BPD participants ($3,696.2 \pm 1,018$) were significantly larger than controls ($2,630.7 \pm 1,083$), $p = 6.75\text{e-}04$ and $p < 6.21\text{e-}04$, respectively (Figure 7). No difference in pupil size was found between ADHD/BPD and BPD participants ($p = 0.997$). A significant pupil size \times group effect was also observed in the random task ($F[2,75] = 5.2$, $p = 0.008$), with significant *post-hoc* differences among ADHD/BPD and controls ($p = 6.75\text{e-}04$) and BPD and controls ($p = 6.21\text{e-}04$) (Figure 7). Further, there was a

significant effect of task type (metronome versus random) on pupil size in ADHD/BPD participants, with a Mean of $3,775.91 \pm \text{SD} = 1,205.97$ in the metronome task and $3,473.61 \pm \text{SD} = 1,433.00$ in the random task ($Z = -2.06$, $p = 0.039$). No task-based effect was found on pupil size in BPD ($p = 0.833$) or controls ($p = 0.293$). There was no effect of pupil size \times saccade type ($p = 0.950$), ISI of alternating targets ($p = 0.998$), or psychotropic medication class (stimulants [$p = 0.122$]; SSRIs [$p = 0.542$]; and SGAs [$p = 0.339$]) (Figure 8).

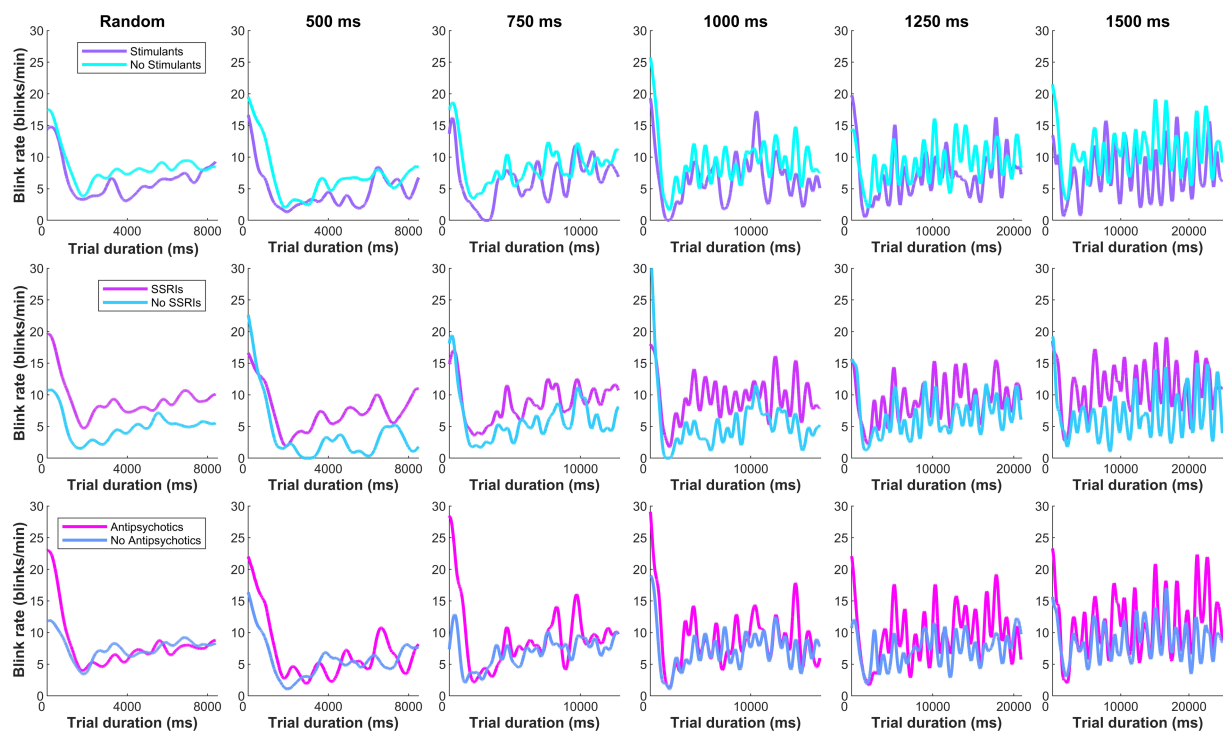


FIGURE 5

Moving average of clinical participants' blink rate according to their psychotropic medication class prescription. No main effect of medication classes were observed on blink rates in the metronome task (averaged across the 5 ISI conditions): stimulant ($t[42]=-0.89$, $p=0.81$), SSRI ($t[42]=1.48$, $p=0.07$), and second-generation antipsychotic ($t[42]=0.99$, $p=0.16$).

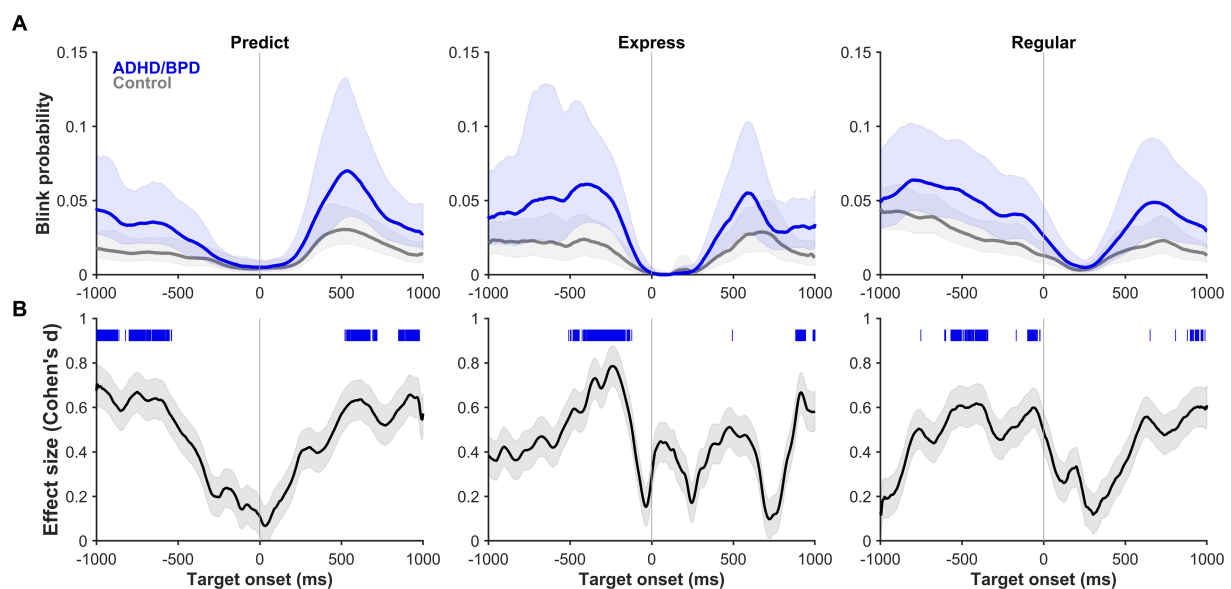


FIGURE 6

(A) Blink probability relative to target onset (vertical line at 0 ms) on metronome trials when ADHD/BPD participants (dark blue) and controls (gray) made a *predict* saccade (left panel), *express* saccade (middle panel), or *regular* saccade (right panel) to target. Shaded regions represent the 95% CIs of the individual mean blink probability averaged across subjects. (B) Effect sizes of the mean difference score of blink probabilities between ADHD/BPD and control groups relative to target onset. The absolute values of the Cohen's d effect sizes are plotted with the shaded regions representing the 95% CI. Regions of statistically significant differences in blink probabilities between ADHD/BPD and control groups are highlighted as tick marks with the color corresponding to which group had a higher blink probability at that timepoint. As seen by the blue tick marks, ADHD/BPD participants had periods of significantly higher blink probabilities versus controls in predict, express and regular saccade trials.

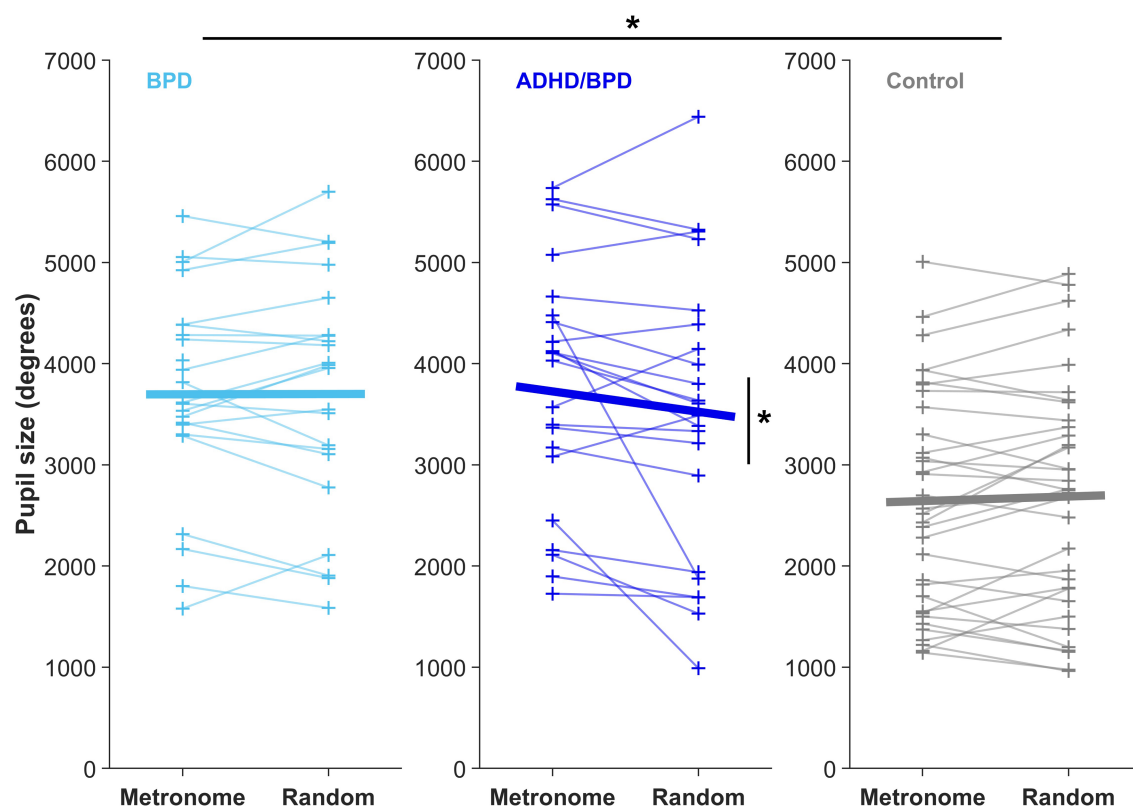


FIGURE 7

Mean pupil size from the time of saccade completion to 200-ms post-saccade in both experimental paradigms. Each + represents the mean pupil size of a subject. Horizontal bars display the group mean in the metronome and random tasks. There was a main effect of pupil size \times participant group in both experimental tasks, $*p < 0.05$. Only ADHD/BPD participants showed a task-based pupil size effect, with an increased pupil size in the metronome versus random task ($Z = -2.06$, $p = 0.039$).

4. Discussion

In this study, we tested *temporal motor prediction and response inhibition* in pediatric patients with BPD and ADHD/BPD versus age- and gender-matched healthy controls by manipulating the predictability of the external environment and observing how this shaped motor action. When visual targets were predictable, BPD cohorts could successfully launch predictive saccades to anticipate the upcoming target and showed similar acquisition of learning to controls. However, when target appearances were random, the BPD with comorbid ADHD group launched significantly more anticipatory saccades than BPD and control groups, demonstrating a failure to wait for the cued target before initiating motor action. Compared to controls, participants with BPD and ADHD/BPD had larger pupil sizes in all task paradigms, evidence of increased sympathetic arousal. ADHD/BPD subjects were the only group to show a task-based modulation (i.e., metronome task versus random task) of blink and pupil parameters. When synchronizing movements to periodic targets, ADHD/BPD participants significantly increased their blink rate and pupil size, likely a reflection of increased neural effort. We discuss our findings in relation to previous work on temporal motor prediction and response inhibition in BPD and ADHD and their associated neural circuits.

4.1. Temporal prediction is normal in BPD with and without comorbid ADHD

Saccade main sequence did not differ among groups, supporting neurotypical saccade-related brainstem firing that produces the tight coupling between saccade amplitude and velocity. A previous eye-tracking study in ADHD also noted a normal saccade main sequence compared to control participants (Fried et al., 2014). Individuals with BPD or ADHD/BPD did not demonstrate an impairment in their ability to identify the rhythmicity of an alternating target and generate predictive saccades to match its arrival. On average, participants produced their first predictive saccade by the third target step (Supplementary Figure S2). In the 1,000 ms ISI condition, BPD participants outperformed control subjects by generating their first predictive saccade by the third target step instead of the fourth. Furthermore, no differences in the accuracy of predictive saccade timing with target appearance were observed among the three groups (Supplementary Figure S3). Generally, participants landed their saccades 100–200 ms before the stimulus arrival, allowing sufficient time for sensory processing of the visual stimulus (with a minimum afferent delay of approximately 50 ms) and endogenous initiation of the subsequent saccade (with a minimum efferent delay of approximately 20 ms) (Sparks, 1978; Fischer and Boch,

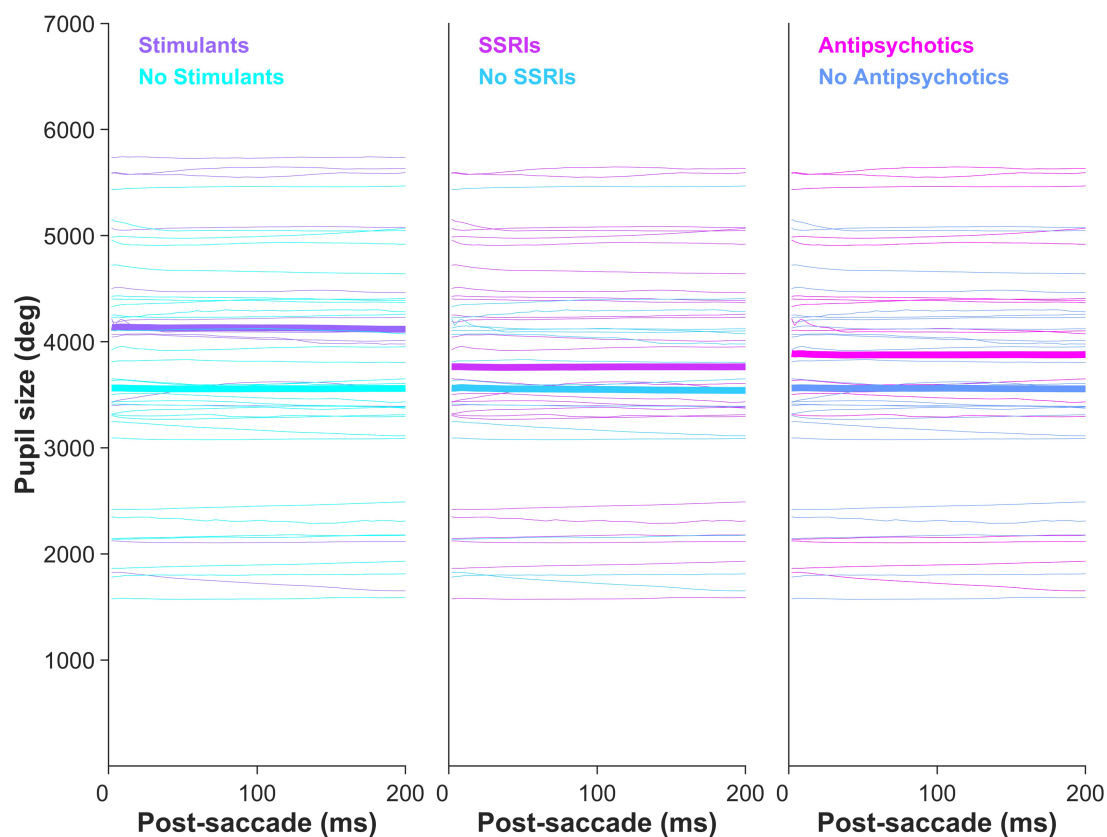


FIGURE 8

Clinical participants' mean pupil size by psychotropic medication class prescription. Pupil size did not vary by psychotropic medication: stimulants ($p=0.122$), SSRIs ($p=0.542$), and second-generation antipsychotics ($p=0.339$).

1983; Fischer and Ramsperger, 1984; Munoz and Wurtz, 1995; Schmolesky et al., 1998; White et al., 2017).

As expected, self-report measures of impulsivity in our study (Table 2) indicated significantly higher scores for individuals with BPD and ADHD/BPD compared to previously reported scores in neurotypical populations (Spinella, 2007). Despite the heightened impulsivity in the BPD and ADHD/BPD groups, their performance in temporal prediction was within the normal range. The predictability of visual targets and the allowance of fast motor actions may be well-suited for conditions favoring endogenous action instead of exogenous reaction. For instance, studies involving finger tapping to rhythmic visual stimuli in individuals with ADHD have shown no differences in mean synchronization times compared to controls (Rubia et al., 1999, 2001, 2003).

4.2. Increased anticipatory action in BPD with comorbid ADHD

We observed a main effect of participant group on the percentage of anticipatory saccades to unpredictable targets. Specifically, individuals with ADHD/BPD made twice as many anticipatory saccades as controls (Table 3), supporting a heightened waiting impulsivity. This finding is consistent with previous studies on cognitive control in ADHD, which reported

increased anticipatory responses (Castellanos et al., 2000; Nigg et al., 2002; Feifel et al., 2004; Carr et al., 2006; Yep et al., 2018). This form of behavioral inhibition does not result from an automatic response to an uninhibited stimulus but rather represents a *disinhibition* of a motor response to an internal cue (Grootens et al., 2008).

The production of anticipatory saccades to targets has been largely attributed to dampened prefrontal cortex (PFC) signaling, which provides inhibitory input to saccade-related neurons in the superior colliculus to prevent a saccade motor command until information is present (Pierrot-deseilligny et al., 1991; Gaymard et al., 1998). The PFC sends various signals, including executive control over eye movements, one of which is motor suppression. In tasks requiring temporal delays before making a saccade to a specific spatial location, a subset of PFC neurons (e.g., frontal eye field and caudal PFC) has been shown to exhibit increased activity in non-human primates during the gap period, conveying 'do not look' signals (Hasegawa et al., 2004). Temporarily silencing these neurons resulted in monkeys making a saccade before the end of the gap period. Structural abnormalities and lesions of the PFC in humans have also been associated with reduced saccade suppression (Guitton et al., 1985; Walker et al., 1998; Pierrot-Deseilligny et al., 2003). Importantly, functional neuroimaging studies combined with motor suppression tasks consistently demonstrate abnormal PFC signaling in individuals with ADHD compared to controls (Feifel et al., 2004;

Schneider et al., 2010; Hakvoort Schwerdtfeger et al., 2013). Therefore, we anticipate that the increased anticipatory saccades to random targets observed in individuals with BPD and ADHD correspond to abnormalities in PFC signaling.

Contrary to our results, two studies have reported increased anticipatory responses in individuals with BPD (Grootens et al., 2008; Parr et al., 2022). It remains unclear if this finding in BPD was partly driven by comorbid ADHD, as Grootens et al. (2008) did not exclude BPD participants with a comorbid ADHD diagnosis from study participation, nor did they report any potential differences in anticipatory responses between individuals with BPD and those with ADHD/BPD. Parr et al. (2022) in a study comparing anticipatory responses between pediatric participants with BPD and ADHD/BPD in a competitive mixed-strategy decision-making task, found no difference. However, the number of BPD participants with comorbid ADHD was limited ($n=12$), and anticipatory responses were rare (i.e., 6.7% of trials in BPD), leading to statistical constraints in the BPD versus ADHD/BPD analysis (Parr et al., 2022). Previous associations between response inhibition and BPD symptomology have been explained by comorbid ADHD diagnoses (Nigg et al., 2005; Lampe et al., 2007). Based on our findings and previous data, we postulate that impaired response inhibition previously observed in performance tasks utilizing emotionally neutral stimuli in BPD could be partially explained by comorbid ADHD. Importantly, while self-report measures of impulsivity assessed by the Barratt Impulsivity Scale did not differ between individuals with BPD and those with ADHD/BPD (Table 2), we observed differences in behavior among BPD cohorts. These findings suggest an improved sensitivity in detecting impulsive behavior when using motor tasks rather than relying solely on self-report measures of symptomatology.

4.3. Blink modulation by group and temporal predictability

Blink rates did not differ among groups in the random task when participants were asked to reflexively react to upcoming targets or in the fixation epoch prior to metronome task start when participants were instructed to look straight ahead (dashed vertical lines in Figure 4). These task periods likely reflect baseline blink rate when behavior is untaxed by cognitive demands. This result is in keeping with previous results of no difference in blink parameters among children with ADHD and controls during rest (Daugherty et al., 1993; Groen et al., 2017). However, when participants synchronized their saccades in time with the alternating target, a main effect of group on blink rate was observed. ADHD/BPD participants had higher blink rates than BPD and control groups in the metronome task, perhaps due to the added attentional demand to maintain the interstimulus interval. This interpretation is consistent with our finding of an increased pupil size in ADHD/BPD participants in the metronome versus random task.

Further, this result is in agreement with a previous study showing differences in blink rate in ADHD versus controls during cognitive tasks (Fried et al., 2014). Fried et al. (2014) found that unmedicated adults with ADHD had higher blink rates than controls during a saccade task and failed to suppress blinks during

periods of stimulus presentation. After administering their prescribed methylphenidate, the same participants underwent re-testing, revealing a decrease in their blink rate; however, it remained significantly higher than that of the control group. Moreover, medicated participants with ADHD exhibited greater suppression of blinks during intervals relevant to task performance. Unlike Fried et al.'s results, we did not observe differences in the timing of when blinks occurred relative to target onset in our ADHD/BPD group compared to BPD and controls (see Figure 6; Supplementary Figure S4), rather an increased frequency of blinks throughout the trial.

4.4. Blink rate and psychotropic medications

A limitation of our study is the absence of two data acquisition time points for comparing blink rates under medication ON and OFF conditions within the same subjects. However, it is worth noting that BPD patients are often treated with polypharmacy (Riffer et al., 2019), and we observed this pattern in our participants. Among our clinical participants, twenty-two were prescribed a medication from one psychotropic class, fifteen from two classes, four from three classes, and only three were not taking any psychotropic drugs. Therefore the opportunity for straightforward medication ON versus OFF analysis was limited. To examine whether the main effects of blink rates by group were influenced by medication classes, we compared the mean blink rates of clinical subjects based on their prescribed medication class. We found no significant difference in blink rate across medication classes, although there was a trend toward increased blink rates among those prescribed SSRIs (Figure 5). Previous research has shown that the administration of a strong centrally acting anticholinergic (promethazine hydrochloride) to controls can lead to an increased blink rate during a cognitive task paradigm, but this effect was not observed at rest (Naicker et al., 2016). Notably, metabolic modulation of the median raphe nucleus, which gives rise to most ascending serotonergic 5-HT projections to the cortex, has been shown to precede blinks in humans (Demiral et al., 2023). Within the ascending arousal network, modulation of BOLD activity in the median raphe nucleus prior to an eyeblink was second only to the substantia nigra, a site of dopamine synthesis (Demiral et al., 2023). Dopamine has been proposed to influence spontaneous blink rate through the inhibition of the spinal trigeminal complex via the basal ganglia's inputs to nucleus raphe magnus and superior colliculus, causing increased frequency of spontaneous blinking (Kaminer et al., 2011). Serotonin has been previously implicated in the production of blinks through its innervation of the orbicularis oculi muscle (LeDoux et al., 1998) and its role within the sleep-wake cycle (Monti, 2011). Future research is encouraged to investigate whether SSRI drugs, known to induce adverse eye-related side effects (e.g., dry eye) (Koçer et al., 2015), also increase blink rates in users.

Our failure to observe a difference in mean blink rate among participants taking stimulant or antipsychotic medications is not surprising given the heterogeneity of the literature. Among the three studies that investigated blink rate in individuals with ADHD ON and OFF methylphenidate, only one reported a decrease in blink rate during a cognitive task in the ON condition, and the blink rate

remained significantly higher than that of the control group (Daugherty et al., 1993; Fried et al., 2014; Groen et al., 2017). In another study, no relationship was found between PET measures of striatal dopaminergic receptor 1 and 2 availability and spontaneous blink rate in healthy adults (Demiral et al., 2022). Only under conditions of enhanced dopamine signaling, through the administration of a high dose of methylphenidate, was a relationship observed between putamen's D1R availability and blink rate (Demiral et al., 2022). The authors attributed these results to a reserve of dopamine receptors at baseline (Nielsen and Andersen, 1992; Tadori et al., 2009; Covey et al., 2013), requiring either large-scale damage to dopaminergic structures (e.g., substantia nigra in Parkinson's disease) or excessive receptor blockade (e.g., >80% D2R blockade for antipsychotic efficacy) for significant changes in blink rate. The dopamine receptor reserve theory postulates that low levels of dopamine signals can maintain normal function while excessive signaling can trigger pathological responses. Based on our findings of increased blink rates solely in the comorbid ADHD/BPD group, it is possible that the dopamine system is particularly stimulated in ADHD.

4.5. Increased pupil size in BPD

Pupil size is modulated by multiple processes, including global luminance (i.e., pupillary light reflex), orienting responses, cognition, stimulus salience, and autonomic tone through sympathetic and parasympathetic innervation (Loewenfeld, 1999; Alnæs et al., 2014; Wang et al., 2014). In our study paradigm, we controlled for global luminance and stimulus salience, with the only difference between tasks being the temporal properties of target arrival. Therefore, we interpret differences in pupillary behavior in terms of cognitive effort and autonomic tone. Pupil sizes following a saccade to the target significantly differed between groups in both the metronome and random tasks. The BPD and ADHD/BPD groups exhibited significantly larger pupil sizes than the control group in both tasks (Figure 8). Given that these results were observed across task sets with varying levels of difficulty, we propose that BPD patients exhibit elevated sympathetic tone compared to controls. Replication of these findings in future studies is needed due to its novelty. Interestingly, previous studies that examined pupil responses in ADHD participants during eye-tracking tasks reported either normal pupil sizes (Fried et al., 2014) or diminished sizes (Wainstein et al., 2017). Therefore, the finding of increased pupil sizes in our clinical participants may be specific to BPD pathology.

Like the blink rate findings, the ADHD/BPD group was the only group that showed a main effect of task condition on pupil size. Pupil sizes significantly increased in the metronome task compared to the random task for ADHD/BPD participants, likely indicating the increased cognitive load of the metronome task. In the pro- and anti-saccade task, pupil size increases during preparation to complete an anti-saccade and pupil size can reliably distinguish between correct and erroneous anti-saccade trials (Karatekin et al., 2010; Wang et al., 2015). In a visuo-spatial working memory task, pupil size corresponded with better task performance in ADHD and correlated with reaction time variability (Wainstein et al., 2017). Among clinical participants prescribed psychotropic medications, we observed that

pupil size did not significantly differ based on medication class (Supplementary Figure S8). However, there was a trend toward increased pupil sizes in individuals prescribed stimulant medications, consistent with the findings of Wainstein et al. (2017).

4.6. Limitations

Our study has several limitations. Firstly, we did not ask pediatric psychiatry participants to interrupt their psychotropic medication schedule. Considering that some of the medications taken by our participants require extended washout periods and cannot be easily paused and resumed without the risk of complications, we made a deliberate decision to prioritize the well-being of our participants and refrain from interrupting their medication regimen. Nonetheless, it is important to acknowledge that medication effects may have potentially masked certain behavioral differences among the groups. To address this concern, we examined whether the prescribed medications accounted for the variability observed in the participants' behavior. Our findings revealed that medications did not have a significant impact on the results of both blink and pupil parameters. However, further investigation involving testing under ON versus OFF medication conditions is recommended.

A second limitation is that we exclusively recruited female participants, so it is unknown whether males with BPD and ADHD/BPD would exhibit similar predictive saccade performance and eye-tracking metrics. Previous research supports gender-based differences in symptom presentation and brain circuitry in BPD, supporting the separate analysis of male and female BPD participants (McCormick et al., 2007; Herpertz et al., 2017). Furthermore, blink rate is known to differ between males and females (Bentivoglio et al., 1997; Sforza et al., 2008; Coors et al., 2021), highlighting the importance of analyzing blink parameters according to gender. However, based on large-scale eye-tracking studies, we do not expect saccade or pupil parameters to differ between females and males with BPD, as gender differences in these parameters have not been consistently reported across the lifespan (Hess and Polt, 1960; Luna et al., 2008; Tekin et al., 2018; Cascone et al., 2020; Yep et al., 2022).

Furthermore, we did not include an ADHD-only cohort to help determine whether the behaviors observed in BPD participants with comorbid ADHD were specifically related to ADHD or shared with BPD pathology. Future research in pediatric ADHD samples is needed to test whether our results of increased blink rate and pupil size in ADHD/BPD during tasks that tax cognitive demand is replicated.

Data availability statement

The original contributions presented in the study are included in the article/Supplementary material, further inquiries can be directed to the corresponding author.

Ethics statement

The studies involving human participants were reviewed and approved by Queen's University Faculty of Health Sciences. Written

informed consent to participate in this study was provided by participants aged ≥ 17 years old. Participants aged 16 years or below provided their oral assent and written consent was obtained by participants' legal guardian/next of kin.

Author contributions

OC, DB, LB, SK-K, and DM designed the experimental protocol. OC, AP, and SK-K recruited clinical participants. OC and AP recruited control participants, performed research and eye-tracking data collection. OC, DB, JH, IP, and BC wrote custom code and analyzed eye-tracking data. OC, AP, and DM wrote the manuscript. All authors provided manuscript edits and approved the submitted version.

Funding

This work was supported by the Southeastern Ontario Academic Medical Organization AFP Innovation Fund Award SEA-17-004 to OC, LB, DM, and SK-K and the Canadian Institutes of Health Research Grant MOP-FDN-148418 to DM. OC is supported by an Ontario Graduate Scholarship. DM is supported by the Canada Research Chair Program.

Conflict of interest

The authors declare that the research was conducted in the absence of any commercial or financial relationships that could be construed as a potential conflict of interest.

Publisher's note

All claims expressed in this article are solely those of the authors and do not necessarily represent those of their affiliated organizations, or those of the publisher, the editors and the reviewers. Any product that may be evaluated in this article, or claim that may be made by its manufacturer, is not guaranteed or endorsed by the publisher.

References

- Agostino, R., Bologna, M., Dinapoli, L., Gregori, B., Fabbrini, G., Accornero, N., et al. (2008). Voluntary, spontaneous, and reflex blinking in Parkinson's disease. *Mov. Disord.* 23, 669–675. doi: 10.1002/mds.21887
- Alnæs, D., Sneve, M. H., Espeseth, T., Endestad, T., van de Pavert, S. H. P., and Laeng, B. (2014). Pupil size signals mental effort deployed during multiple object tracking and predicts brain activity in the dorsal attention network and the locus coeruleus. *J. Vis.* 14, 1–20. doi: 10.1167/14.4.1
- American Psychiatric Association (2022). *Diagnostic and statistical manual of mental disorders* (5th ed., text rev.).
- Barratt, E. (1959). Anxiety and impulsiveness related to psychomotor efficiency. *Percept. Mot. Skills* 9, 191–198. doi: 10.2466/pms.1959.9.3.191
- Basso, M. A., Powers, A. S., and Evinger, C. (1996). An explanation for reflex blink hyperexcitability in Parkinson's disease. I. Superior colliculus. *J. Neurosci.* 16, 7308–7317. doi: 10.1523/jneurosci.16-22-07308.1996
- Bentivoglio, A. R., Bressman, S. B., Cassetta, E., Carretta, D., Tonali, P., and Albanese, A. (1997). Analysis of blink rate patterns in normal subjects. *Mov. Disord.* 12, 1028–1034. doi: 10.1002/mds.870120629
- Bertsch, K., Krauch, M., Stopfer, K., Haeussler, K., Herpertz, S. C., and Gamer, M. (2017). Interpersonal threat sensitivity in borderline personality disorder: an eye-tracking study. *J. Personal. Disord.* 31, 647–670. doi: 10.1521/pedi_2017_31_273
- Betke, M., and Chau, M. (2005). Real time eye tracking and blink detection with USB cameras. *Bost. Univ. Comput. Sci.* 2215, 1–10.
- Bohus, M., Kleindienst, N., Limberger, M. F., Stieglitz, R. D., Domsalla, M., Chapman, A. L., et al. (2009). The short version of the borderline symptom list (BSL-23): development and initial data on psychometric properties. *Psychopathology* 42, 32–39. doi: 10.1159/000173701
- Bortolla, R., Galli, M., Ramella, P., Sirtori, F., Visintini, R., and Maffei, C. (2020). Negative bias and reduced visual information processing of socio-emotional context in borderline personality disorder: a support for the hypersensitivity hypothesis. *J. Behav. Ther. Exp. Psychiatry* 69:101589. doi: 10.1016/j.jbtep.2020.101589
- Brien, D. C., Riek, H. C., Yep, R., Huang, J., Coe, B., Areshenkoff, C., et al. (2023). Classification and staging of Parkinson's disease using video-based eye tracking. *Park. Relat. Disord.* 110:105316. doi: 10.1016/j.parkreldis.2023.105316

Supplementary material

The Supplementary material for this article can be found online at: <https://www.frontiersin.org/articles/10.3389/fnins.2023.1179765/full#supplementary-material>

SUPPLEMENTARY FIGURE 1

Main sequence of predict, express, and regular saccades to metronome targets by subject group. Square root model fits for peak saccade velocity \times amplitude were computed for each individual participant and averaged across participants. Model coefficients are reported with 95% CI values listed in parenthesis. The increased frequency of regular saccades with 10° amplitudes represent saccades to the first step 10° away from central fixation point, whereas target steps 2–16 were 20° in separation. Main sequence model fits did not vary by participant group in any of the three saccade types.

SUPPLEMENTARY FIGURE 2

Averaged saccade reaction times to metronome targets at 5 different ISIs and to unpredictable targets in the random ISI condition. Square markers represent the mean SRT at the target step according to group membership. Lines connect the mean SRTs as a function of target sequence in the experimental trial. Errors bars show mean \pm standard deviation. Horizontal SRT line at 90 ms denotes the separation between predictive and reactive saccades. Predict saccades were on average launched to metronome target by target steps 3–4. ADHD/BPD participants' mean SRT to target steps 2–16 in the random task show non-visually guided saccades toward temporally unpredictable targets.

SUPPLEMENTARY FIGURE 3

Accuracy of predict saccades depicted by the end of the saccade relative to target appearance ('end SRT'; vertical line at 0 ms). Histograms show kernel density estimates for predict saccades (SRT < 90 ms) made by participants (ADHD/BPD in dark blue, BPD in light blue, controls in gray) to the 5 metronome targets conditions and 1 randomized ISI condition. Participants tended to end their saccades 100–200 ms before the target appeared and this distribution became broader with longer ISI durations as well as with target unpredictability. No difference was observed in temporal accuracy \times subject group.

SUPPLEMENTARY FIGURE 4

(A) Blink probability relative to target onset (vertical line at 0 ms) on metronome trials when BPD participants (dark blue) and controls (gray) made a predict saccade (left panel), express saccade (middle panel), or regular saccade (right panel) to target. Shaded regions represent the 95% CIs of the individual mean blink probability averaged across subjects. (B) Effect sizes of the mean difference score of blink probabilities between BPD and control groups relative to target onset. The absolute values of the Cohen's d effect sizes are plotted with the shaded regions representing the 95% CI. Regions of statistically significant differences in blink probabilities between BPD and control groups are highlighted as tick marks with the color corresponding to which group had a higher blink probability at that timepoint. There are brief periods when BPD participants had significantly higher blink probabilities than controls during express and regular saccade trials (see light blue tick marks), however, this occurs for <100 consecutive ms. (C) and (D) reflect the same analysis for ADHD/BPD versus BPD participants.

- Caffier, P. P., Erdmann, U., and Ullsperger, P. (2003). Experimental evaluation of eye-blink parameters as a drowsiness measure. *Eur. J. Appl. Physiol.* 89, 319–325. doi: 10.1007/s00421-003-0807-5
- Calancie, O. G., Brien, D. C., Huang, J., Coe, B. C., Booi, L., Khalid-Khan, S., et al. (2022). Maturation of temporal saccade prediction from childhood to adulthood: predictive saccades, reduced pupil size, and blink synchronization. *J. Neurosci.* 42, 69–80. doi: 10.1523/JNEUROSCI.0837-21.2021
- Carr, L. A., Nigg, J. T., and Henderson, J. M. (2006). Attentional versus motor inhibition in adults with attention-deficit/hyperactivity disorder. *Neuropsychology* 20, 430–441. doi: 10.1037/0894-4105.20.4.430
- Cascone, L., Medaglia, C., Nappi, M., and Narducci, F. (2020). Pupil size as a soft biometrics for age and gender classification. *Pattern Recogn. Lett.* 140, 238–244. doi: 10.1016/j.patrec.2020.10.009
- Castellanos, F. X., Marvasti, F. F., Ducharme, J. L., Walter, J. M., Israel, M. E., Krain, A., et al. (2000). Executive function oculomotor tasks in girls with ADHD. *J. Am. Acad. Child Adolesc. Psychiatry* 39, 644–650. doi: 10.1097/00004583-200005000-00019
- Coors, A., Merten, N., Ward, D. D., Schmid, M., Breteler, M. M. B., and Ettinger, U. (2021). Strong age but weak sex effects in eye movement performance in the general adult population: evidence from the Rhineland study. *Vis. Res.* 178, 124–133. doi: 10.1016/j.visres.2020.10.004
- Covey, D. P., Juliano, S. A., and Garris, P. A. (2013). Amphetamine elicits opposing actions on readily releasable and reserve pools for dopamine. *PLoS One* 8:e60763. doi: 10.1371/journal.pone.0060763
- Cruz, A. A. V., Garcia, D. M., Pinto, C. T., and Cechetti, S. P. (2011). Spontaneous eyeblink activity. *Ocul. Surf.* 9, 29–41. doi: 10.1016/S1542-0124(11)70007-6
- Dalley, J. W., and Robbins, T. W. (2017). Fractionating impulsivity: neuropsychiatric implications. *Nat. Rev. Neurosci.* 18, 158–171. doi: 10.1038/nrn.2017.8
- Daugherty, T. K., Quay, H. C., and Ramos, L. (1993). Response perseveration, inhibitory control, and central dopaminergic activity in childhood behavior disorders. *J. Genet. Psychol.* 154, 177–188. doi: 10.1080/00221325.1993.9914731
- Demiral, Ş. B., Kure Liu, C., Benveniste, H., Tomasi, D., and Volkow, N. D. (2023). Activation of brain arousal networks coincident with eye blinks during resting state. *Cereb. Cortex* 33, 6792–6802. doi: 10.1093/cercor/bhad001
- Demiral, Ş. B., Manza, P., Biesecker, E., Wiers, C., Shokri-Kojori, E., McPherson, K., et al. (2022). Striatal D1 and D2 receptor availability are selectively associated with eye-blink rates after methylphenidate treatment. *Commun. Biol.* 5:1015. doi: 10.1038/s42003-022-03979-5
- Deravet, N., Orban de Xivry, J. J., Ivanoiu, A., Bier, J. C., Segers, K., Yüksel, D., et al. (2021). Frontotemporal dementia patients exhibit deficits in predictive saccades. *J. Comput. Neurosci.* 49, 357–369. doi: 10.1007/s10827-020-00765-2
- Dorris, M. C., and Munoz, D. P. (1998). Saccadic probability influences motor preparation signals and time to saccadic initiation. *J. Neurosci.* 18, 7015–7026. doi: 10.1523/jneurosci.18-17-07015.1998
- Eckstein, M. K., Guerra-Carrillo, B., Miller Singley, A. T., and Bunge, S. A. (2017). Beyond eye gaze: what else can eyetracking reveal about cognition and cognitive development? *Dev. Cogn. Neurosci.* 25, 69–91. doi: 10.1016/j.dcn.2016.11.001
- Ellis, C. J. K. (1981). The pupillary light reflex in normal subjects. *Br. J. Ophthalmol.* 65, 754–759. doi: 10.1136/bjo.65.11.754
- Feifel, D., Farber, R. H., Clementz, B. A., Perry, W., and Anllo-Vento, L. (2004). Inhibitory deficits in ocular motor behavior in adults with attention-deficit/hyperactivity disorder. *Biol. Psychiatry* 56, 333–339. doi: 10.1016/j.biopsych.2004.06.019
- Fischer, B., and Boch, R. (1983). Saccadic eye movements after extremely short reaction times in the rhesus monkey. *Brain Res.* 260, 21–26. doi: 10.1016/0006-8993(83)90760-6
- Fischer, B., and Ramsperger, E. (1984). Human express saccades: extremely short reaction times of goal directed eye movements. *Exp. Brain Res.* 57, 191–195. doi: 10.1007/BF00231145
- Fossati, A., Gratz, K. L., Maffei, C., and Borroni, S. (2014). Impulsivity dimensions, emotion dysregulation, and borderline personality disorder features among Italian nonclinical adolescents. *Borderline Personal. Disord. Emot. Dysregulation* 1:5. doi: 10.1186/2051-6673-1-5
- Fried, M., Tsitsiashvili, E., Bonneh, Y. S., Sterkin, A., Wygnanski-Jaffe, T., Epstein, T., et al. (2014). ADHD subjects fail to suppress eye blinks and microsaccades while anticipating visual stimuli but recover with medication. *Vis. Res.* 101, 62–72. doi: 10.1016/j.visres.2014.05.004
- Gaymard, B., Rivaud, S., Cassarini, J. F., Dubard, T., Rancurel, G., Agid, Y., et al. (1998). Effects of anterior cingulate cortex lesions on ocular saccades in humans. *Exp. Brain Res.* 120, 173–183. doi: 10.1007/s002210050391
- Gibaldi, A., and Sabatini, S. P. (2021). The saccade main sequence revisited: a fast and repeatable tool for oculomotor analysis. *Behav. Res. Methods* 53, 167–187. doi: 10.3758/s13428-020-01388-2
- Gooding, D. C., and Basso, M. A. (2008). The tell-tale tasks: a review of saccadic research in psychiatric patient populations. *Brain Cogn.* 68, 371–390. doi: 10.1016/j.bandc.2008.08.024
- Gould, T. D., Bastain, T. M., Israel, M. E., Hommer, D. W., and Castellanos, F. X. (2001). Altered performance on an ocular fixation task in attention-deficit/hyperactivity disorder. *Biol. Psychiatry* 50, 633–635. doi: 10.1016/S0006-3223(01)01095-2
- Groen, Y., Borger, N. A., Koerts, J., Thome, J., and Tucha, O. (2017). Blink rate and blink timing in children with ADHD and the influence of stimulant medication. *J. Neural Transm.* 124, 27–38. doi: 10.1007/s00702-015-1457-6
- Grootens, K. P., van Lijstelaar, G., Buitelaar, J. K., van der Laan, A., Hummelen, J. W., and Verkes, R. J. (2008). Inhibition errors in borderline personality disorder with psychotic-like symptoms. *Prog. Neuro Psychopharmacol. Biol. Psychiatry* 32, 267–273. doi: 10.1016/j.pnpbp.2007.08.020
- Guittion, D., Buchtel, H. A., and Douglas, R. M. (1985). Frontal lobe lesions in man cause difficulties in suppressing reflexive glances and in generating goal-directed saccades. *Exp. Brain Res.* 58, 455–472. doi: 10.1007/BF00235863
- Gunderson, J. G., Herpertz, S. C., Skodol, A. E., Torgersen, S., and Zanarini, M. C. (2018). Borderline Personality Disorder. *Nat. Rev. Dis. Prim.* 41, xiii–xixv. doi: 10.1016/j.psc.2018.09.001
- Hakvoort Schwerdtfeger, R. M., Alahyane, N., Brien, D. C., Coe, B. C., Stroman, P. W., and Munoz, D. P. (2013). Preparatory neural networks are impaired in adults with attention-deficit/hyperactivity disorder during the antisaccade task. *NeuroImage Clin.* 2, 63–78. doi: 10.1016/j.nicl.2012.10.006
- Hasegawa, R. P., Peterson, B. W., and Goldberg, M. E. (2004). Prefrontal neurons coding suppression of specific saccades. *Neuron* 43, 415–425. doi: 10.1016/j.neuron.2004.07.013
- Herpertz, S. C., and Koetting, K. (2005). Startle response in inpatients with borderline personality disorder vs. healthy controls. *J. Neural Transm.* 112, 1097–1106. doi: 10.1007/s00702-004-0249-1
- Herpertz, S. C., Nagy, K., Ueltzhöffer, K., Schmitt, R., Mancke, F., Schmahl, C., et al. (2017). Brain mechanisms underlying reactive aggression in borderline personality disorder—sex matters. *Biol. Psychiatry* 82, 257–266. doi: 10.1016/j.biopsych.2017.02.1175
- Hess, E. H., and Polt, J. M. (1960). Pupil size as related to interest value of visual stimuli. *Science* 132, 349–350. doi: 10.1126/science.132.3423.349
- Huang, L. Y., Jackson, B. S., Rodrigue, A. L., Tammimga, C. A., Gershon, E. S., Pearson, G. D., et al. (2022). Antisaccade error rates and gap effects in psychosis syndromes from bipolar-schizophrenia network for intermediate phenotypes 2 (B-SNIP2). *Psychol. Med.* 52, 2692–2701. doi: 10.1017/S003329172000478X
- Hutton, S. B., and Ettinger, U. (2006). The antisaccade task as a research tool in psychopathology: a critical review. *Psychophysiology* 43, 302–313. doi: 10.1111/j.1469-8986.2006.00403.x
- Jacob, G. A., Gutz, L., Bader, K., Lieb, K., Tüscher, O., and Stahl, C. (2010). Impulsivity in borderline personality disorder: impairment in self-report measures, but not behavioral inhibition. *Psychopathology* 43, 180–188. doi: 10.1159/000304174
- Jongkees, B. J., and Colzato, L. S. (2016). Spontaneous eye blink rate as predictor of dopamine-related cognitive function—a review. *Neurosci. Biobehav. Rev.* 71, 58–82. doi: 10.1016/j.neubiorev.2016.08.020
- Kaiser, D., Jacob, G. A., van Zutphen, L., Siep, N., Sprenger, A., Tuschen-Caffier, B., et al. (2019). Biased attention to facial expressions of ambiguous emotions in borderline personality disorder: an eye-tracking study. *J. Personal. Disord.* 33, 671–690. doi: 10.1521/pedi_2019_33_363
- Kaminer, J., Powers, A. S., Horn, K. G., Hui, C., and Evinger, C. (2011). Characterizing the spontaneous blink generator: an animal model. *J. Neurosci.* 31, 11256–11267. doi: 10.1523/JNEUROSCI.6218-10.2011
- Kandel, E. R., Schwartz, J. H., Jessell, T. M., Siegelbaum, S., Hudspeth, A. J., and Mack, S. (2000). *Principles of neural science*. New York: McGraw-hill.
- Karatekin, C., Bingham, C., and White, T. (2010). Oculomotor and pupillometric indices of pro- and antisaccade performance in youth-onset psychosis and attention deficit/hyperactivity disorder. *Schizophr. Bull.* 36, 1167–1186. doi: 10.1093/schbul/sbp035
- Koçer, E., Koçer, A., Özsütçü, M., Dursun, A. E., and Kirpınar, I. (2015). Dry eye related to commonly used New antidepressants. *J. Clin. Psychopharmacol.* 35, 411–413. doi: 10.1097/JCP.0000000000000356
- Lampe, K., Konrad, K., Kroener, S., Fast, K., Kunert, H. J., and Herpertz, S. C. (2007). Neuropsychological and behavioural disinhibition in adult ADHD compared to borderline personality disorder. *Psychol. Med.* 37, 1717–1729. doi: 10.1017/S0033291707000517
- LeDoux, M. S., Lorden, J. F., Smith, J. M., and Mays, L. E. (1998). Serotonergic modulation of eye blinks in cat and monkey. *Neurosci. Lett.* 253, 61–64. doi: 10.1016/S0304-3940(98)00616-8
- Leichsenring, F., Leibing, E., Kruse, J., New, A. S., and Leweke, F. (2011). Borderline personality disorder. *Lancet* 377, 74–84. doi: 10.1016/S0140-6736(10)61422-5
- Limberg, A., Barnow, S., Freyberger, H. J., and Hamm, A. O. (2011). Emotional vulnerability in borderline personality disorder is cue specific and modulated by traumatization. *Biol. Psychiatry* 69, 574–582. doi: 10.1016/j.biopsych.2010.10.024
- Liversedge, S., Gilchrist, I., and Everling, S. (2011). *The Oxford handbook of eye movements*. Oxford University Press. Oxford.

- Loewenfeld, I. E. (1999). *The pupil: Anatomy, physiology, and clinical applications*. Boston: Butterworth-Heinemann.
- Luna, B., Velanova, K., and Geier, C. F. (2008). Development of eye-movement control. *Brain Cogn.* 68, 293–308. doi: 10.1016/j.bandc.2008.08.019
- Marino, R. A., Levy, R., and Munoz, D. P. (2015). Linking express saccade occurrence to stimulus properties and sensorimotor integration in the superior colliculus. *J. Neurophysiol.* 114, 879–892. doi: 10.1152/jn.00047.2015
- Marino, R. A., and Munoz, D. P. (2009). The effects of bottom-up target luminance and top-down spatial target predictability on saccadic reaction times. *Exp. Brain Res.* 197, 321–335. doi: 10.1007/s00221-009-1919-x
- McCormick, B., Blum, N., Hansel, R., Franklin, J. A., St. John, D., Pfohl, B., et al. (2007). Relationship of sex to symptom severity, psychiatric comorbidity, and health care utilization in 163 subjects with borderline personality disorder. *Compr. Psychiatry* 48, 406–412. doi: 10.1016/j.comppsy.2007.05.005
- McDowell, J. E., Dyckman, K. A., Austin, B. P., and Clementz, B. A. (2008). Neurophysiology and neuroanatomy of reflexive and volitional saccades: evidence from studies of humans. *Brain Cogn.* 68, 255–270. doi: 10.1016/j.bandc.2008.08.016
- Moeller, F. G., Barratt, E. S., Ph, D., Dougherty, D. M., Ph, D., Schmitz, J. M., et al. (2001). Reviews and overviews psychiatric aspects of impulsivity. *Am. J. Psychiatry* 158, 1783–1793. doi: 10.1111/j.1467-789X.2011.00899.x
- Monti, J. M. (2011). Serotonin control of sleep-wake behavior. *Sleep Med. Rev.* 15, 269–281. doi: 10.1016/j.smrv.2010.11.003
- Munoz, D. P., Broughton, J. R., Goldring, J. E., and Armstrong, I. T. (1998). Age-related performance of human subjects on saccadic eye movement tasks. *Exp. Brain Res.* 121, 391–400. doi: 10.1007/s002210050473
- Munoz, D. P., and Wurtz, R. H. (1995). Saccade-related activity in monkey superior colliculus I. characteristics of burst and buildup cells. *J. Neurophysiol.* 73, 2313–2333. doi: 10.1152/jn.1995.73.6.2313
- Naicker, P., Anoopkumar-Dukie, S., Grant, G. D., Neumann, D. L., and Kavanagh, J. J. (2016). Central cholinergic pathway involvement in the regulation of pupil diameter, blink rate and cognitive function. *Neuroscience* 334, 180–190. doi: 10.1016/j.neuroscience.2016.08.009
- Nielsen, E. B., and Andersen, P. H. (1992). Dopamine receptor occupancy *in vivo*: behavioral correlates using NNC-112, NNC-687 and NNC-756, new selective dopamine D1 receptor antagonists. *Eur. J. Pharmacol.* 219, 35–44. doi: 10.1016/0014-2999(92)90577-Q
- Nigg, J. T., Butler, K. M., Huang-Pollock, C. L., and Henderson, J. M. (2002). Inhibitory processes in adults with persistent childhood onset ADHD. *J. Consult. Clin. Psychol.* 70, 153–157. doi: 10.1037/0022-006X.70.1.153
- Nigg, J. T., Silk, K. R., Stavro, G., and Miller, T. (2005). Disinhibition and borderline personality disorder. *Dev. Psychopathol.* 17, 1129–1149. doi: 10.1017/S0954579405050534
- Osman, A., Bagge, C., Gutierrez, P., Lonick, L., Kopper, B., and Barrios, F. (2001). The suicidal behaviors questionnaire-revised (SBQ-R): validation with clinical and nonclinical samples. *Psychol. Assess.* 8, 443–454. doi: 10.1177/107319110100800409
- Paré, M., and Munoz, D. P. (1996). Saccadic reaction time in the monkey: advanced preparation of oculomotor programs is primarily responsible for express saccade occurrence. *J. Neurophysiol.* 76, 3666–3681. doi: 10.1152/jn.1996.76.6.3666
- Parr, A. C., Calancie, O. G., Coe, B. C., Khalid-Khan, S., and Munoz, D. P. (2022). Impulsivity and emotional dysregulation predict choice behavior during a mixed-strategy game in adolescents with borderline personality disorder. *Front. Neurosci.* 15, 1–21. doi: 10.3389/fnins.2021.667399
- Peltsch, A., Hemraj, A., Garcia, A., and Munoz, D. P. (2011). Age-related trends in saccade characteristics among the elderly. *Neurobiol. Aging* 32, 669–679. doi: 10.1016/j.neurobiolaging.2009.04.001
- Philipsen, A., Limberger, M. F., Lieb, K., Feige, B., Kleindienst, N., Ebner-Priemer, U., et al. (2008). Attention-deficit hyperactivity disorder as a potentially aggravating factor in borderline personality disorder. *Br. J. Psychiatry* 192, 118–123. doi: 10.1192/bjp.bp.107.035782
- Pierrot-Deseilligny, C., Müri, R. M., Ploner, C. J., Gaymard, B., Demeret, S., and Rivaud-Pechoux, S. (2003). Decisional role of the dorsolateral prefrontal cortex in ocular motor behaviour. *Brain* 126, 1460–1473. doi: 10.1093/brain/awg148
- Pierrot-deseilligny, C. H., Rivaud, S., Gaymard, B., and Agid, Y. (1991). Cortical control of reflexive visually-guided saccades. *Brain* 114, 1473–1485. doi: 10.1093/brain/114.3.1473
- Rentrop, M., Backenstrass, M., Jaentsch, B., Kaiser, S., Roth, A., Unger, J., et al. (2008). Response inhibition in borderline personality disorder: performance in a go/Nogo task. *Psychopathology* 41, 50–57. doi: 10.1159/000110626
- Riek, H. C., Brien, D. C., Coe, B. C., Huang, J., Perkins, J. E., Yep, R., et al. (2023). Cognitive correlates of antisaccade behaviour across multiple neurodegenerative diseases. *Brain Commun.* 5, 1–15. doi: 10.1093/braincomms/fcad049
- Riffer, F., Farkas, M., Streibl, L., Kaiser, E., and Sprung, M. (2019). Psychopharmacological treatment of patients with borderline personality disorder: comparing data from routine clinical care with recommended guidelines. *Int. J. Psychiatry Clin. Pract.* 23, 178–188. doi: 10.1080/13651501.2019.1576904
- Rommelse, N. N. J., Van der Stigchel, S., and Sergeant, J. A. (2008). A review on eye movement studies in childhood and adolescent psychiatry. *Brain Cogn.* 68, 391–414. doi: 10.1016/j.bandc.2008.08.025
- Ross, R. G., Olincy, A., Harris, J. G., Radant, A., Adler, L. E., and Freedman, R. (1998). Anticipatory saccades during smooth pursuit eye movements and familial transmission of schizophrenia. *Biol. Psychiatry* 44, 690–697. doi: 10.1016/S0006-3223(98)00052-3
- Rubia, K., Noorloos, J., Smith, A., Gunning, B., and Sergeant, J. (2003). Motor timing deficits in community and clinical boys with hyperactive behavior: the effect of methylphenidate on motor timing. *J. Abnorm. Child Psychol.* 31, 301–313. doi: 10.1023/A:1023233630774
- Rubia, K., Taylor, E., Smith, A. B., Oksannen, H., Overmeyer, S., and Newman, S. (2001). Neuropsychological analyses of impulsiveness in childhood hyperactivity. *Br. J. Psychiatry* 179, 138–143. doi: 10.1192/bjp.179.2.138
- Rubia, K., Taylor, A., Taylor, E., and Sergeant, J. A. (1999). Synchronization, anticipation, and consistency in motor timing of children with dimensionally defined attention deficit hyperactivity behaviour. *Percept. Mot. Ski.* 89, 1237–1258.
- Schmahmann, J. D. (2000). The role of the cerebellum in affect and psychosis. *J. Neurolinguistics* 13, 189–214. doi: 10.1016/S0911-6044(00)00011-7
- Schmolsky, M. T., Wang, Y., Hanes, D. P., Thompson, K. G., Leutgeb, S., Schall, J. D., et al. (1998). Signal timing access the macaque visual system. *J. Neurophysiol.* 79, 3272–3278. doi: 10.1152/jn.1998.79.6.3272
- Schneider, M. F., Krick, C. M., Retz, W., Hengesch, G., Retz-Junginger, P., Reith, W., et al. (2010). Impairment of fronto-striatal and parietal cerebral networks correlates with attention deficit hyperactivity disorder (ADHD) psychopathology in adults - a functional magnetic resonance imaging (fMRI) study. *Psychiatry Res. Neuroimaging* 183, 75–84. doi: 10.1016/j.pscychres.2010.04.005
- Schulze, L., Schmah, C., and Niedtfeld, I. (2016). Neural correlates of disturbed emotion processing in borderline personality disorder: a multimodal Meta-analysis. *Biol. Psychiatry* 79, 97–106. doi: 10.1016/j.biopsych.2015.03.027
- Scott, L. N., Zalewski, M., Beeney, J. E., Jones, N. P., and Stepp, S. D. (2017). Pupillary and affective responses to maternal feedback and the development of borderline personality disorder symptoms. *Dev. Psychopathol.* 29, 1089–1104. doi: 10.1017/S0954579416001048
- Seitz, K. I., Leitenstorfer, J., Krauch, M., Hillmann, K., Boll, S., Ueltzhoeffer, K., et al. (2021). An eye-tracking study of interpersonal threat sensitivity and adverse childhood experiences in borderline personality disorder. *Borderline Personal. Disord. Emot. Dysregulat.* 8, 2–12. doi: 10.1186/s40479-020-00141-7
- Sforza, C., Rango, M., Galante, D., Bresolin, N., and Ferrario, V. F. (2008). Spontaneous blinking in healthy persons: an optoelectronic study of eyelid motion. *Ophthalmic Physiol. Opt.* 28, 345–353. doi: 10.1111/j.1475-1313.2008.00577.x
- Sparks, D. L. (1978). Functional properties of neurons in the monkey superior colliculus: coupling of neuronal activity and saccade onset. *Brain Res.* 156, 1–16. doi: 10.1016/0006-8993(78)90075-6
- Spinella, M. (2007). Normative data and a short form of the Barratt impulsiveness scale. *Int. J. Neurosci.* 117, 359–368. doi: 10.1080/00207450600588881
- Stepp, S. D., Smith, T. D., Morse, J. Q., Hallquist, M. N., and Pilkonis, P. A. (2012). Prospective associations among borderline personality disorder symptoms, interpersonal problems, and aggressive behaviors. *J. Interpers. Violence* 27, 103–124. doi: 10.1177/0886260511416468
- Swarztrauber, K., and Fujikawa, D. G. (1998). An electroencephalographic study comparing maximum blink rates in schizophrenic and nonschizophrenic psychiatric patients and nonpsychiatric control subjects. *Biol. Psychiatry* 43, 282–287. doi: 10.1016/S0006-3223(97)00028-0
- Tadori, Y., Forbes, R. A., McQuade, R. D., and Kikuchi, T. (2009). Receptor reserve-dependent properties of antipsychotics at human dopamine D2 receptors. *Eur. J. Pharmacol.* 607, 35–40. doi: 10.1016/j.ejphar.2009.02.007
- Taylor, J. R., Elsworth, J. D., Lawrence, M. S., Sladek, J. R., Roth, R. H., and Redmond, D. E. (1999). Spontaneous blink rates correlate with dopamine levels in the caudate nucleus of MPTP-treated monkeys. *Exp. Neurol.* 158, 214–220. doi: 10.1006/exnr.1999.7093
- Tekin, K., Sekeroglu, M. A., Kiziltoprak, H., Doguizi, S., Inanc, M., and Yilmazbas, P. (2018). Static and dynamic pupillometry data of healthy individuals. *Clin. Exp. Optom.* 101, 659–665. doi: 10.1111/cxo.12659
- Thakkar, K. N., and Rolf, M. (2019). Disrupted corollary discharge in schizophrenia: evidence from the oculomotor system. *Biol. Psychiatry Cogn. Neurosci. Neuroimaging* 4, 773–781. doi: 10.1016/j.bpsc.2019.03.009
- Thakkar, K. N., Schall, J. D., Boucher, L., Logan, G. D., and Park, S. (2011). Response inhibition and response monitoring in a saccadic countermanding task in schizophrenia. *Biol. Psychiatry* 69, 55–62. doi: 10.1016/j.biopsych.2010.08.016
- Vaca-Palomares, I., Brien, D. C., Coe, B. C., Ochoa-Morales, A., Martínez-Ruano, L., Munoz, D. P., et al. (2019). Implicit learning impairment identified via predictive saccades in Huntington's disease correlates with extended cortico-striatal atrophy. *Cortex* 121, 89–103. doi: 10.1016/j.cortex.2019.06.013
- Wainstein, G., Rojas-Libano, D., Crossley, N. A., Carrasco, X., Aboitiz, F., and Ossandón, T. (2017). Pupil size tracks attentional performance in attention-deficit/hyperactivity disorder. *Sci. Rep.* 7, 1–9. doi: 10.1038/s41598-017-08246-w

- Walker, R., Husain, M., Hodgson, T. L., Harrison, J., and Kennard, C. (1998). Saccadic eye movement and working memory deficits following damage to human prefrontal cortex. *Neuropsychologia* 36, 1141–1159. doi: 10.1016/S0028-3932(98)00004-9
- Wang, C. A., Boehnke, S. E., Itti, L., and Munoz, D. P. (2014). Transient pupil response is modulated by contrast-based saliency. *J. Neurosci.* 34, 408–417. doi: 10.1523/JNEUROSCI.3550-13.2014
- Wang, C. A., Brien, D. C., and Munoz, D. P. (2015). Pupil size reveals preparatory processes in the generation of pro-saccades and anti-saccades. *Eur. J. Neurosci.* 41, 1102–1110. doi: 10.1111/ejn.12883
- Wang, C.-A., Huang, J., Yep, R., and Munoz, D. P. (2018). Comparing pupil light response modulation between saccade planning and working memory. *J. Cogn.* 1:33. doi: 10.5334/joc.33
- Weber, H., Aiple, F., Fischer, B., and Latanov, A. (1992). Dead zone for express saccades. *Exp. Brain Res.* 89, 214–222. doi: 10.1007/BF00229018
- White, B. J., Kan, J. Y., Levy, R., Itti, L., and Munoz, D. P. (2017). Superior colliculus encodes visual saliency before the primary visual cortex. *Proc. Natl. Acad. Sci. U. S. A.* 114, 9451–9456. doi: 10.1073/pnas.1701003114
- Wright, A. G. C., Zalewski, M., Hallquist, M. N., Hipwell, A. E., and Stepp, S. D. (2016). Developmental trajectories of borderline personality disorder symptoms and psychosocial functioning in adolescence. *J. Personal. Disord.* 30, 351–372. doi: 10.1521/pedi_2015_29_200
- Yep, R., Smorenburg, M. L., Riek, H. C., Calancie, O. G., Kirkpatrick, R. H., Perkins, J. E., et al. (2022). Interleaved pro/anti-saccade behavior across the lifespan. *Front. Aging Neurosci.* 14, 1–15. doi: 10.3389/fnagi.2022.842549
- Yep, R., Soncin, S., Brien, D. C., Coe, B. C., Marin, A., and Munoz, D. P. (2018). Using an emotional saccade task to characterize executive functioning and emotion processing in attention-deficit hyperactivity disorder and bipolar disorder. *Brain Cogn.* 124, 1–13. doi: 10.1016/j.bandc.2018.04.002



OPEN ACCESS

EDITED BY

Xuemin Li,
Peking University Third Hospital, China

REVIEWED BY

Poppy Watson,
University of New South Wales, Australia
Naomi Kakoschke,
Commonwealth Scientific and Industrial
Research Organisation (CSIRO), Australia

*CORRESPONDENCE

Jang-Han Lee
✉ clipsy@cau.ac.kr

RECEIVED 23 January 2023

ACCEPTED 23 June 2023

PUBLISHED 13 July 2023

CITATION

Woo J-M, Lee G-E and Lee J-H (2023)
Attentional bias for high-calorie food cues by
the level of hunger and satiety in individuals
with binge eating behaviors.
Front. Neurosci. 17:1149864.
doi: 10.3389/fnins.2023.1149864

COPYRIGHT

© 2023 Woo, Lee and Lee. This is an
open-access article distributed under the terms
of the [Creative Commons Attribution License
\(CC BY\)](https://creativecommons.org/licenses/by/4.0/). The use, distribution or reproduction
in other forums is permitted, provided the
original author(s) and the copyright owner(s)
are credited and that the original publication in
this journal is cited, in accordance with
accepted academic practice. No use,
distribution or reproduction is permitted which
does not comply with these terms.

Attentional bias for high-calorie food cues by the level of hunger and satiety in individuals with binge eating behaviors

Ji-Min Woo, Gi-Eun Lee and Jang-Han Lee*

Department of Psychology, Chung-Ang University, Seoul, Republic of Korea

Introduction: The abnormal hyperreactivity to food cues in individuals with binge eating behaviors could be regulated by hedonic or reward-based system, overriding the homeostatic system. The aim of the present study was to investigate whether attentional bias for food cues is affected by the level of hunger, maintaining the normal homeostatic system in individuals with binge eating behaviors.

Methods: A total of 116 female participants were recruited and divided into four groups: hungry-binge eating group (BE) ($n = 29$), satiated BE ($n = 29$), hungry-control ($n = 29$), satiated control ($n = 29$). While participants completed a free-viewing task on high or low-calorie food cues, visual attentional processes were recorded using an eye tracker.

Results: The results revealed that BE group showed longer initial fixation duration toward high-calorie food cues in both hunger and satiety condition in the early stage, whereas the control group showed longer initial fixation duration toward high-calorie food cues only in hunger conditions. Moreover, in the late stage, the BE group stared more at the high-calorie food cue, compared to control group regardless of hunger and satiety.

Discussion: The findings suggest that automatic attentional bias for food cues in individuals with binge eating behaviors occurred without purpose or awareness is not affected by the homeostatic system, while strategic attention is focused on high-calorie food. Therefore, the attentional processing of food cues in binge eating group is regulated by hedonic system rather than homeostatic system, leading to vulnerability to binge eating.

KEYWORDS

binge eating, hunger and satiety, food cues, incentive salience, attentional bias

1. Introduction

In clinical settings, the consumption of a relatively large amount of food within a short period compared to usual, along with a subjective difficulty in controlling eating behavior during this time, is defined as binge eating behavior (American Psychiatric Association, 2013). This binge eating behavior is a core symptom observed in eating disorders such as binge eating disorder (BED), the binge-purge subtype of anorexia nervosa (AN), and bulimia nervosa (BN). Binge eating behavior often leads individuals to consume more energy than the actual amount of calories needed, resulting in imbalances related to the body and weight, causing excessive weight gain and associated psychological distress (Tanofsky-Kraff and Yanovski, 2004; Wonderlich et al., 2009). Problematic binge eating behavior can be explained by one of the important theories in addiction called the incentive-sensitization theory (Robinson and Berridge, 1993; Berridge and Robinson, 2016). The incentive-sensitization theory was proposed to explain substance abuse, such as drug addiction, and suggests that when individuals are repeatedly exposed to stimuli, such as specific substances, that provide

rewarding experiences, pleasure is induced and dopamine is activated, stimulating the brain and strengthening the connection between the stimulating substance and the rewarding response of pleasure. With the reinforcement of this connection over time, individuals can become conditioned to engage in behaviors that continuously seek out and consume the rewarding stimuli. In other words, the behavior of individuals who excessively seek and consume food in binge eating and those who exhibit problematic substance addiction, characterized by excessive preoccupation and approach toward addictive substances, share the same dopamine neural pathway, indicating that cravings for specific substances or food and the triggering of such cravings may have similarities (Schulte et al., 2016; Novelle and Diéguez, 2018). In essence, similar to substance addiction, repetitive and persistent binge eating behavior is suggested to induce sensitization in the mesocorticolimbic dopamine system (Berridge, 2009). Therefore, for individuals engaging in binge eating behavior, the importance of food stimuli or cues that trigger rewarding experiences after consumption gradually increases in their daily lives or environment.

In fact, the act of human food consumption appears to rely on both a pathway that maintains physiological homeostasis and a pathway that pursues psychological satisfaction in contrast (Lutter and Nestler, 2009). For instance, the pathway aimed at maintaining physiological homeostasis is essentially a system that regulates the body's energy balance, and when energy stores are depleted, it increases appetite and motivation to seek food. On the other hand, the activation of the non-homeostatic pathway, triggered by food stimuli or cues, disregards the regulation of the system for maintaining bodily homeostasis, leading to excessive food intake, and triggering binge eating behavior, which can manifest as symptoms of overweight or obesity-related eating disorders (Berthoud, 2012; Dileone et al., 2012; Witt and Lowe, 2014; Yu et al., 2015). Particularly, individuals who engage in binge eating behavior, influenced by the hedonic system, have been found to prefer high-calorie foods and show a tendency to consume them in greater quantities compared to non-binge eating behaviors (Raymond et al., 2003). This is believed to be because high-calorie foods elicit stronger reward-related responses in the brain, leading individuals to experience a heightened sense of reward or pleasure when consuming these foods.

As mentioned earlier in the incentive-sensitization theory, food cues and rewarding experiences can be conditioned through associative and reinforcement learning processes (Berridge and Robinson, 2003). In other words, specific food cues that are consistently paired with rewarding experiences after consumption can become attractive and desired stimuli that more easily and quickly capture an individual's attention, triggering cravings. The tendency of individuals who have become sensitive to these incentive stimuli is often measured by behavioral responsiveness, such as their reaction time to specific stimuli. Particularly, the most fundamental characteristic of attention, which is the underlying process guiding individual behavior, can be more accurately and sensitively measured through attention bias (Schag et al., 2013; Popien et al., 2015). Methods such as the go/no-go paradigm (Veling et al., 2017) or the dot-probe paradigm (Fenske and Raymond, 2006; Chen et al., 2016) are useful

for measuring behavioral responsiveness by observing which stimuli among various stimuli presented in the environment receive more attention or focus. However, these methods have limitations when it comes to assessing more immediate and automatic responsiveness to specific stimuli, as participants may learn during the task about certain stimuli or processes presented to them. The free-viewing paradigm using eye-tracking is an appropriate method for investigating attentional responses to food in individuals exhibiting binge eating behavior (Cisler and Koster, 2010). Enhanced attention refers to the rapid detection of salient stimuli through automatic processing in the early stages, while disengagement involves strategic processing during the maintenance of attention. Therefore, difficulty in disengagement represents sustained attention to food-related cues. Results in adults with binge eating disorder reflect longer attentional dwell time on food stimuli, indicating extended gaze duration on food cues, and eye-tracking studies have yielded mixed results regarding initial direction biases (Schag et al., 2013; Popien et al., 2015; Schmidt et al., 2016; Sperling et al., 2017). For instance, one study using the free-viewing paradigm and anti-saccade tasks found that individuals with binge eating disorder who were obese or overweight displayed longer gaze durations on food stimuli compared to individuals with obesity without binge eating disorder and normal-weight participants. However, all participants exhibited initial fixations occurring more frequently on food cues (Schag et al., 2013). Another study found that adults without binge eating disorder showed longer fixations and dwell times on both high-calorie and low-calorie food items (Popien et al., 2015). In adolescents with binge eating disorder, gaze durations were longer, but no directional biases were observed (Schmidt et al., 2016). Finally, while both positive and control groups did not differ in initial fixation locations, the positive group showed greater interest in food. There were no differences in detection times between groups in the visual search task, but the detection bias toward food cues was only found in the overall binge eating disorder (Sperling et al., 2017).

In addition, as emphasized in the incentive-sensitization theory, two key concepts are highlighted (Pool et al., 2015, 2016). First, the subjective value of incentives can vary depending on individuals' circumstances. For example, a stimulus that is rewarding to one person may be perceived as aversive or costly to another person. Second, individual circumstances and relational states are important factors that modulate sensitivity to incentives. For instance, individuals may become more sensitive to stimuli that can induce certain states they require. This is exemplified by individuals who require satiety being more sensitive to food cues or stimuli (Zhang et al., 2009; Robinson and Berridge, 2013). Evidence regarding the modulation of attentional patterns to food cues by hunger has been obtained through studies involving normal-weight and individuals with obesity (Nijs et al., 2010; Loeber et al., 2013). Normal-weight individuals showed biased attention toward food cues when hungry but not when satiated, indicating that attentional processing in healthy individuals is modulated by the homeostatic system (Piech et al., 2010; Loeber et al., 2013). However, in obese and overweight groups, no differences in attentional patterns were observed between hungry and satiated

states, and in some cases, results were contrary to those of the normal-weight group (Nijs et al., 2010). The evidence considering hunger and satiety factors in individuals with binge eating is limited. Given the mixed results regarding whether hunger can trigger binge eating, it is necessary to consider both hunger and satiety factors in individuals with binge eating disorder (Stice et al., 2008).

Due to a lack of control over hunger levels, there may be mixed results in the early stages of attention, as previous studies have shown (Schag et al., 2013; Schmidt et al., 2016; Sperling et al., 2017). For instance, one study found that individuals with binge eating disorder (BED) reported significantly higher levels of hunger, more depressive symptoms, and less positive emotional responses to food cues compared to a control group (Sperling et al., 2017). Another study focusing on adolescents with BED showed that attentional biases toward food cues were only associated with increased hunger in the BED group. These results differ from previous evidence of general biases toward food stimuli in control groups, suggesting that hunger levels may have influenced the attention patterns of the control group (Schag et al., 2013; Schmidt et al., 2016). The existing evidence regarding orientation biases is not conclusive because it did not employ a competitive paradigm involving three types of stimuli in complex naturalistic scenes. Additionally, the findings regarding the early stage of attentional processes are not certain due to the relatively long duration of stimulus presentation (8 s), which may not adequately measure early covert attention (Popien et al., 2015).

In the context of the incentive-sensitization theory, incentive salience refers to the implicit motivation to obtain a reward (i.e., wanting). Therefore, it is necessary to investigate the clear results of early attentional processes, which reflect relatively automatic attention patterns (Fox et al., 2001). The brain circuitry underlying the psychological processes of the reward system consists of two components: “wanting” and “liking” (Berridge and Robinson, 2016). “Wanting” represents the motivation to obtain a reward, while “liking” refers to the pleasure experienced during consumption (Berridge, 2009). The theory suggests that “wanting” and “liking” can be independent in psychopathological conditions such as addiction or binge eating (Finlayson et al., 2007; Pool et al., 2016). Unlike “liking”, it is proposed that explicit and implicit “wanting” rely on different psychological mechanisms (Berridge and Robinson, 2003; Anselme and Robinson, 2015). Implicit “wanting” is expected to be associated with the early stage of attention, while explicit “wanting” is more closely related to overt attention, which is measured in the later stages of attention (Fox et al., 2001; Pool et al., 2016). In this study, attentional bias indicating implicit “wanting” and self-reported explicit “wanting” and “liking” was measured.

The objective of this study is to investigate the influence of hunger and satiety on visual attentional bias toward food cue images in individuals with binge eating disorder. The research hypotheses are as follows: (1) In the hunger condition, both individuals with binge eating disorder and weight-matched controls will exhibit attentional bias toward high-calorie food cues compared to both low-calorie food cues and non-food cues. (2) In the satiety condition, individuals with binge eating disorder will continue to display attentional bias, whereas the

control group will show reduced attention toward high-calorie food cues.

2. Materials and methods

2.1. Participants

Prior to the experiment, candidate participants were recruited through an internet bulletin board of universities in Seoul, Korea. As an initial screening for the binge eating (BE) problem group and control group, a total of 435 female undergraduates completed the Eating Disorder Diagnostic Scale (EDDS; Stice et al., 2000) and Eating Disorder Examination Questionnaire (EDE-Q; Fairburn and Beglin, 1994). All group members with BE reported an average at least one BE episode per week for the past 3 months without compensatory behavior following BE episodes. These individuals, who have not received an official diagnosis of BED, but demonstrate relatively high scores on measures assessing symptoms of binge eating, refer to individuals with a propensity for binge eating behaviors. By contrast, none of the control group members reported BE episodes per week during the past 3 months and a history of other eating disorder symptoms. Exclusion criteria in this study were as follows: (1) diagnosis of other eating disorders, (2) recurrent use of inappropriate compensatory behavior, and (3) reported the presence of any illness, or the use of any pharmacological treatment, that might influence eating behavior, body weight, or that would not allow a 12-h fast. Eventually, 116 eligible females agreed to participate: 58 participants were in the BE group and 58 participants were in the control group, and the BE group was matched with the control group by weights. Each group was assigned to hunger or satiety condition randomly. Finally, there were four groups: hungry BED ($N = 29$), satiated BED ($N = 29$), hungry control ($N = 29$), and satiated control ($N = 29$) (Table 1). The study protocol was approved by an Institutional Review Board of Chung-Ang University, Seoul, Republic of Korea (no. 1041078-201910-HRSB-320-01).

2.2. Measurement

2.2.1. Self-report questionnaires

The Eating Disorder Diagnostic Scale (EDDS) is a 22-item self-report scale based on DSM criteria for anorexia nervosa, bulimia nervosa, and binge eating disorder (Stice et al., 2000). The Korean version of the EDDS (K-EDDS) was used (Bang et al., 2018b). It was used to identify BE participants and rule out an eating disorder among those in the control group. An overall symptom is calculated from the sum of scores for the first 18 EDDS items. In this study, the Cronbach's α was 0.807.

The Eating Disorder Examination Questionnaire (EDE-Q) is a 36-item self-report measure that assesses the presence and severity of eating disorder psychopathology (Fairburn and Beglin, 1994). The Korean version of EDE-Q version 6.0 was used (Bang et al., 2018a). It consists of a global score and four subscales: eating concern scale, restraint scale, shape concern scale, and weight concern scale. In this study, Cronbach's α was 0.938.

TABLE 1 Demographic and clinical characteristics of each group.

Measure	BE group		Control group		Test statistics (F)
	Hungry condition (N = 29)	Satiated condition (N = 29)	Hungry condition (N = 29)	Satiated condition (N = 29)	
Age (yrs)	21.103 (1.915)	21.276 (1.944)	21.207 (2.144)	21.241 (1.976)	0.404*
BMI	21.310 (2.157)	21.456 (2.242)	21.131 (2.001)	21.144 (2.032)	0.154*
EDE-Q	115.414 (38.652)	117.483 (32.068)	55.103 (28.821)	52.069 (22.399)	39.706*
BDI	12.241 (5.097)	11.207 (4.872)	4.897 (4.821)	5.448 (4.748)	17.659*
STAI-T	60.517 (6.733)	59.103 (7.575)	51.897 (6.915)	50.586 (6.339)	15.265*
STAI-S	60.690 (8.553)	57.414 (10.287)	49.759 (8.761)	49.483 (8.114)	11.345*
Hunger	69.759 (17.870)	15.241 (15.044)	66.000 (18.188)	18.759 (17.492)	85.086*

Mean (standard deviation); *p < 0.001; BE group, binge eating group; control group, weight-matched control. Age, years.

BMI, body mass index; EDE-Q, Eating Disorder Examination Questionnaire; BDI, Beck Depression Inventory; STAI-T, State-Trait Anxiety Inventory-Trait; STAI-S, State-Trait Anxiety Inventory-State; HUNGER, The level of hunger measured by visual analog scale.

The Beck Depression Inventory (BDI) is a 21-item questionnaire that was originally developed for use with the clinical population, assessing the presence and severity of depression symptoms (Beck et al., 1988). The validated Korean version of BDI was used (Lee et al., 1995). The scale is used to assess the cognitive, emotional, and somatic symptoms of depression. Each item has four choices that describe the severities of each symptom, respectively. Participants choose one option they think to be closest to the state during the past week. In this study, Cronbach's α was 0.821.

The State-Trait Anxiety Inventory (STAI; Spielberger et al., 1970) is used to trait anxiety and state anxiety. The trait version (STAI-T) measures the trait of anxiety, while the state version (STAI-S) measures the state of anxiety. The Korean version of STAI was used (Hahn et al., 1996). The total scores of each subscale are from 20 to 80. The STAI includes 20 items, with greater scores indicating more severe anxiety. In this study, Cronbach's α was 0.834 for STAI-T and 0.750 for STAI-S.

To measure the level of hunger and satiety, the visual analog scale (VAS) ranging from 0 to 100 mm was used. The VAS items consist of a question with “not at all” to “very much”. Participants responded with their own levels of hunger and satiety. Furthermore, to measure the level of wanting and liking, applying the incentive salience model for the rewarding value of food, VAS ranging from 0 to 100 mm was used. The VAS items consist of a question with “not at all” to “very much”. The question to determine wanting was “How much do you want to eat this item right now?”. Liking was determined to the question “How much do you like this item, not considering if you want to eat it right now?” (Stevenson et al., 2017).

The body mass index (BMI) was used to measure participants' physical information. BMI was calculated by dividing weight (kg) by height (m^2). It is an index that reflects the total amount of body fat. Weight was measured in kilograms, and height was measured

in meters using height and weight measuring tools available in the laboratory.

2.2.2. Free-viewing task

Eye-movement data were collected using an eye tracker (Tobii TX300, Tobii Technology AB, Danderyd, Sweden). There were three types of stimuli: high-calorie food, low-calorie food, and non-food cues. Each stimuli type consists of nine images. The high-calorie food cues were items that contained a large amount of fats and sugar, such as hamburgers, ice creams, and chocolates. The low-calorie food cues contained various types of vegetables and fruits. The neutral stimuli included some stationery and household objects. High- and low-calorie cues were determined based on the actual and perceived calories of specific foods, as rated, and standardized in the FATIS (Seo et al., 2020). The FATIS is a database of pictures with normed ratings on addictive images including food, alcohol, nicotine, and non-addictive neutral items. The pair of stimuli was matched using an inspection with respect to complexity, shape, color, brightness, and viewing distance of food cues. Totally, 27 pairs were made (high-calorie food vs. non-food, low-calorie food vs. non-food, high-calorie food vs. low-calorie food). Each pair was presented in a counterbalanced order, and cues were presented twice over on the left and right side of the monitor, conducted 54 trials (Kim et al., 2016). Each pair of cues was presented at a size of 80×100 mm with their centers 200 mm apart. Followed by a pair of pictures for 4,000 ms, each trial began with a fixation for 1,000 ms. The eye movements of participants were recorded by an eye-tracking system during the free-viewing task. The eye-tracking data were measured at 120 Hz. All participants performed the free-viewing task in a lighted room, and the size of the monitor was 23 inch with a distance of 60~75 cm between the eyes and monitor. The eye-tracking equipment was calibrated for participants by presenting the five moving dots on the screen, and

then the pairs of cues were presented. The software (Tobii TX300, Tobii Technology AB, Danderyd, Sweden) provided a variety of gaze information, involving initial fixation latency score, initial fixation duration score, and gaze duration score.

2.3. Procedures

Participants were asked not to consume any food, except water, for approximately 12 h prior to the start of the experiment. Upon arrival, participants were provided with information regarding their rights and the procedure. The experiment was scheduled between 8:00 and 10:00 a.m. to align participants' fasting and satiety states as closely as possible. Ultimately, all participants visited the laboratory before 10:00 a.m., and the manipulation checks for the fasting state were based on participants' self-reported responses. When participants arrived at the laboratory, they received instructions on the approved consent form from the Institutional Review Board and voluntarily signed the consent form. Then, participants were randomly assigned to either the hunger or satiety condition, matched for age and body mass index. For the satiety condition, a standard meal was provided at the laboratory to standardize satiety levels. The standard meal consisted of a "gimbap", approximately 350 kcal, which is a meal consisting of rice, radish, carrots, spinach, and other vegetables wrapped in seaweed. This was done to control participants' satiety levels. All participants in the satiety condition completed hunger and satiety visual analog scales (VASs) before and after the meal to assess their hunger and satiety levels. Participants in the hunger condition completed the hunger VAS only once. Afterward, participants were asked to complete the free-viewing task (Figure 1). All participants were instructed to freely view the computer monitor while minimizing movement during the task. The task consisted of a total of 54 trials. Following the task, participants completed self-report questionnaires. Finally, all participants were provided with a debriefing regarding the experiment. The experimental procedure took approximately 40 min, and all participants received a monetary reward of 10,000 Korean won (approximately 10 USD).

2.4. Data analyses

The required sample size for this study was calculated using G*Power 3.1.9.4 (University of Dusseldorf, Dusseldorf, Germany), with an alpha error probability of 0.05 and a power of 0.95. A large effect size of 0.40 was expected with the current sample size. For data analysis, a one-way analysis of variance (ANOVA) was conducted to analyze the differences in the characteristics among the hungry BE, satiated BE, hungry control, and satiated control groups. To examine the differences in attentional bias pattern, three dependent measures were derived from eye-movement data: initial fixation latency, initial fixation duration, and gaze duration. Each score of eye movement data was calculated as the difference between the attentional bias score for high- and low-calorie food cues, and high-calorie food cues and neutral cues. In addition, based on the analysis of the basic characteristics between groups,

significant differences were found in the levels of depression and anxiety among the groups. To account for these differences, depression and anxiety levels were set as covariates, and subsequent analyses were conducted. Hypothesis-driven analyses of attentional bias scores were conducted using Group 2 (BE, Control) x Condition 2 (hunger, satiety) two-way analysis of covariance (ANCOVA). Moreover, Group 2 (BE, Control) x Condition 2 (hunger, satiety) x Cue type (high calorie, low calorie) three-way ANCOVA was conducted on self-report wanting and liking VAS. All statistical analyses were conducted using IBM SPSS version 25.0 for Windows, v. 11.0.

3. Results

3.1. Sample characteristics

A total of 116 participants participated in this study: 29 in the hungry BE group, 29 in the satiated BE group, 29 in the hungry control group, and 29 in the satiated control group. Table 1 shows the group characteristics of the participants analyzed in this study. According to the criteria of matching, there were no significant differences in the mean age [$F_{(3,112)} = 0.40, p = 0.750$] and the mean BMI [$F_{(3,112)} = 0.15, p = 0.927$] between the groups. However, there were significant effects of the group for EDE-Q [$F_{(3,112)} = 39.71, p = 0.0001, \eta^2 = 0.515$], BDI [$F_{(3,112)} = 17.70, p = 0.0001, \eta^2 = 0.321$], STAI-T [$F_{(3,112)} = 15.27, p = 0.0001, \eta^2 = 0.290$], and STAI-S [$F_{(3,112)} = 11.35, p = 0.0001, \eta^2 = 0.233$]. Two BE groups had significantly higher eating disorder symptoms, depression, trait anxiety, and state anxiety than did the other two groups. As expected, hungry BE and control groups showed higher hunger than satiated BE and control groups [$F_{(3,112)} = 85.09, p = 0.0001, \eta^2 = 0.695$], indicating that manipulation was appropriate.

3.2. Manipulation check

Table 2 shows the subjective hunger rating before and after consuming a standardized meal. There was no statistically significant interaction between the group and the meal [$F_{(1,56)} = 0.59, p = 0.446, \eta^2 = 0.01$], and the main effect on the group [$F_{(1,56)} = 2.37, p = 0.129, \eta^2 = 0.04$]. It is suggested that there was no difference in the hunger level between BE and control groups. Subjective hunger rating using VAS showed a statistically significant main effect of the meal [$F_{(1,56)} = 156.35, p = 0.0001, \eta^2 = 0.736$], indicating that both BE and control groups showed higher level of hunger before consuming a standardized meal than after the meal.

3.3. Free-viewing task

To examine attentional bias toward food cues, three eye movement scores, involving initial fixation latency score, initial fixation duration score, and gaze duration score, were analyzed for two pairs of cues. The analysis accounted for the potential influence of depressive and anxiety levels (BDI, STAI-T, and STAI-S) by controlling for them as covariates during the analysis, considering that they could be emotional states that can affect

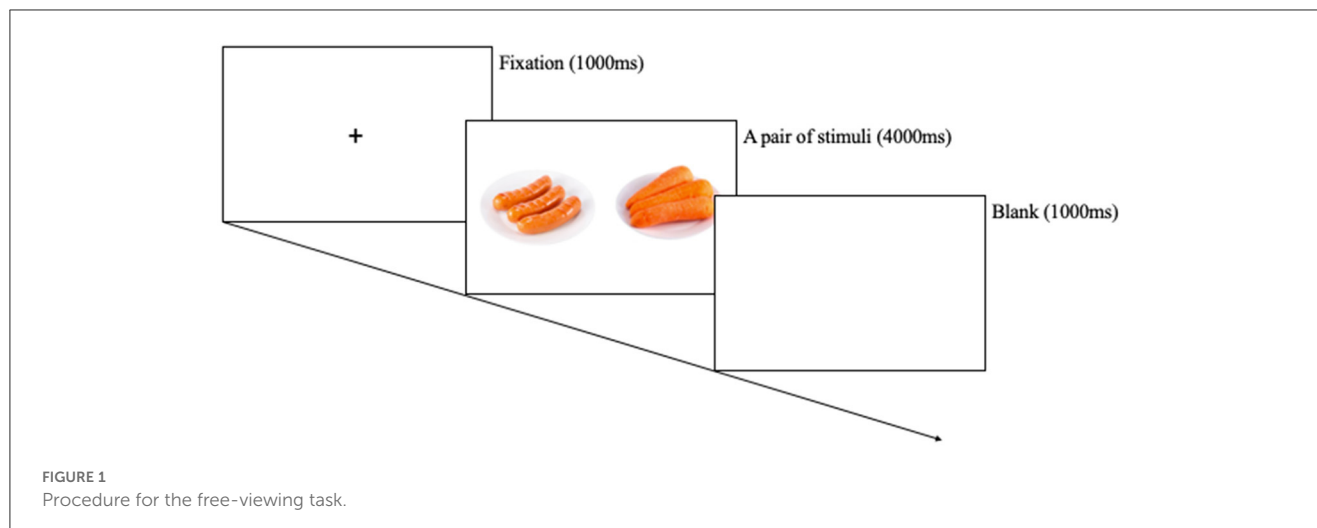


TABLE 2 Subjective hunger rating before and after consuming a standardized meal.

Measure	Satiated BE (N = 29)		Satiated control (N = 29)		Test statistics (F)
	Before meal	After meal	Before meal	After meal	
Hunger	55.552 (24.606)	15.241 (15.044)	64.345 (21.729)	18.759 (17.492)	0.590

Mean (standard deviation). BE group, binge eating group; control group, weight-matched control group.

TABLE 3 Comparison of attentional bias toward high-calorie cues vs. low-calorie cues among groups.

Measure	BE group		Control group		Test statistics (F)
	Hungry condition (N = 29)	Satiated condition (N = 29)	Hungry Condition (N = 29)	Satiated Condition (N = 29)	
Initial fixation latency (ms)	-128.569 (152.115)	-84.903 (171.463)	-118.178 (124.776)	-115.250 (120.016)	0.362
Initial fixation duration (ms)	61.465 (81.323)	68.504 (108.823)	64.625 (107.625)	-9.816 (77.947)	5.267*
Gaze duration (ms)	632.452 (466.479)	424.906 (414.676)	311.595 (441.079)	255.397 (491.451)	0.739

Mean (standard deviation); In milliseconds (ms) * $p < 0.05$. BE group, binge eating group; control group, weight-matched control group.

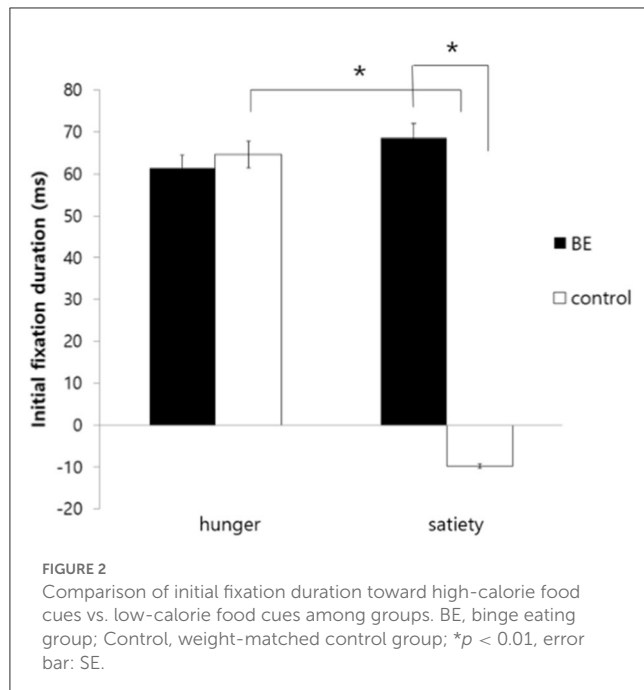
attention processes (Smith et al., 2020). Each score of eye-tracking data was calculated as the difference between the score for high- and low-calorie food cues, and high-calorie food cues and neutral cues. Group (BE, control) \times Condition (hunger, satiety) two-way ANCOVA was conducted. Furthermore, if there were significant interaction effects, *post hoc* analyses were conducted, and degrees of freedom were adjusted using the Greenhouse–Geisser epsilon to correct for violations of the assumption of sphericity.

3.3.1. Attentional bias toward high-calorie food cues vs. low-calorie food cues among the groups

To examine whether each group exhibits an attentional bias toward high-calorie food cues compared to low-calorie food cues under the hunger condition, the initial fixation latency and initial

fixation duration of each group were analyzed. Table 3 shows the mean and standard deviation values of attentional bias toward high-calorie cues vs. low-calorie cues among the groups. First, for the initial fixation latency score, there was no significant interaction between the group and condition [$F_{(1,109)} = 0.36$, $p = 0.549$, *n.s.*]. Moreover, there was no significant main effect on the group [$F_{(1,109)} = 1.81$, $p = 0.182$, *n.s.*] and the condition [$F_{(1,109)} = 0.90$, $p = 0.345$, *n.s.*]. The results indicated that both BE and control groups did not detect high-calorie food cues more quickly than they did the low-calorie food cues, regardless of hunger and satiety.

Second, for initial fixation duration, there was significant interaction between the group and the condition [$F_{(1,109)} = 5.27$, $p = 0.024$, $\eta^2 = 0.046$]. To determine the source of the interaction, a simple main effects analysis was performed. As a result, there was no difference between hunger and satiety condition in the BE group [$F_{(1,53)} = 0.004$, $p = 0.947$, *n.s.*]. In contrast, the control

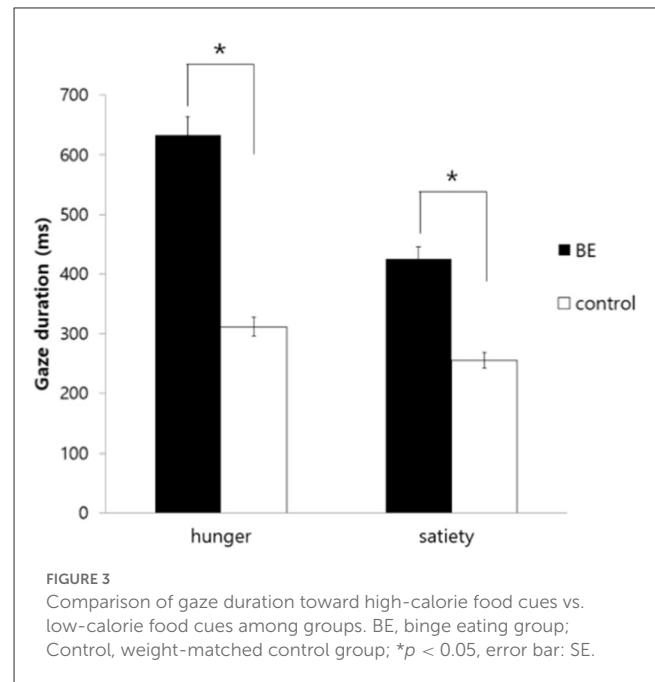


group showed higher initial fixation duration to high-calorie food cues compared to low-calorie food cues in the hungry condition, but they were more likely to look initially at low-calorie food in satiated condition [$F_{(1,53)} = 9.22, p = 0.004, \eta^2 = 0.048$]. Moreover, there was no difference between the BE group and control group in hunger condition [$F_{(1,53)} = 1.79, p = 0.186, n.s.$], but the BE group showed higher initial fixation duration to high-calorie food cues vs. low-calorie food cues than the control group in satiated condition [$F_{(1,53)} = 8.15, p = 0.006, \eta^2 = 0.033$]. It is indicated that the BE group showed persistent initial attentional bias toward high-calorie food cues both in the hunger and satiety condition, but the control group showed attentional bias only in the hunger condition. On the other hand, there were no significant effects observed for the condition [$F_{(1,109)} = 3.54, p = 0.063, \eta^2 = 0.031$] and the group [$F_{(1,109)} = 0.90, p = 0.337, n.s.$] (Figure 2).

To investigate whether participants demonstrating problematic binge eating behaviors under the satiety condition exhibit longer gaze duration toward high-calorie food cues compared to low-calorie food cues, the gaze duration toward food stimuli of each group was analyzed. As a result, there was no significant interaction between the group and the condition [$F_{(1,109)} = 0.739, p = 0.392, n.s.$] and there was no significant main effect on the condition [$F_{(1,109)} = 2.61, p = 0.109, n.s.$]. However, there was a significant main effect on the group indicating that the BE group looked at high-calorie food cues longer than low-calorie food cues compared to the control group [$F_{(1,109)} = 4.37, p = 0.039, \eta^2 = 0.039$] (Figure 3).

3.3.2. Attentional bias toward high-calorie food cues vs. neutral cues among the groups

To examine whether each group exhibits attentional bias toward high-calorie food cues compared to non-food cues under the hunger condition, initial fixation latency, and initial



fixation duration of each group were analyzed. Table 4 shows the mean and standard deviation values of attentional bias toward high-calorie cues vs. neutral cues. First, for the initial fixation latency score, there was no significant interaction between the group and the condition [$F_{(1,109)} = 0.90, p = 0.344, n.s.$], and the main effect on the group [$F_{(1,109)} = 1.81, p = 0.182, n.s.$]. However, there was a significant difference in the condition [$F_{(1,109)} = 7.01, p = 0.009, \eta^2 = 0.060$] presenting that all participants showed faster attention engagement in high-calorie food cues when hungry rather than satiated (Figure 4).

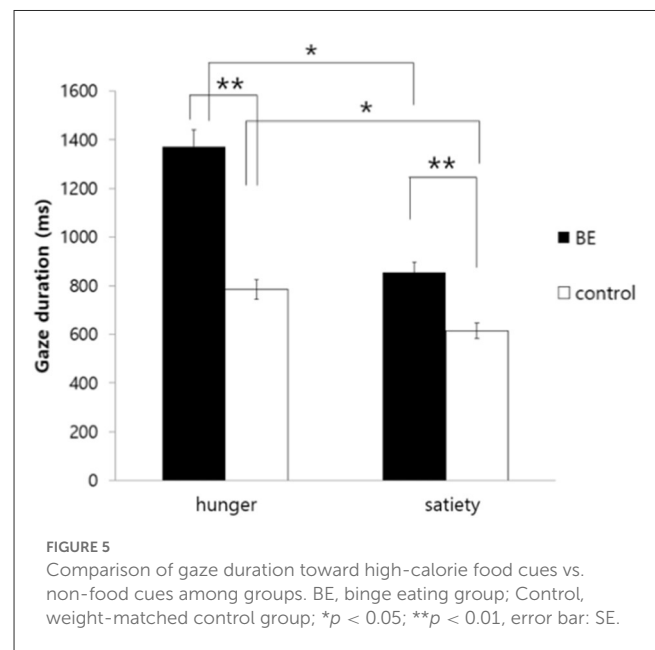
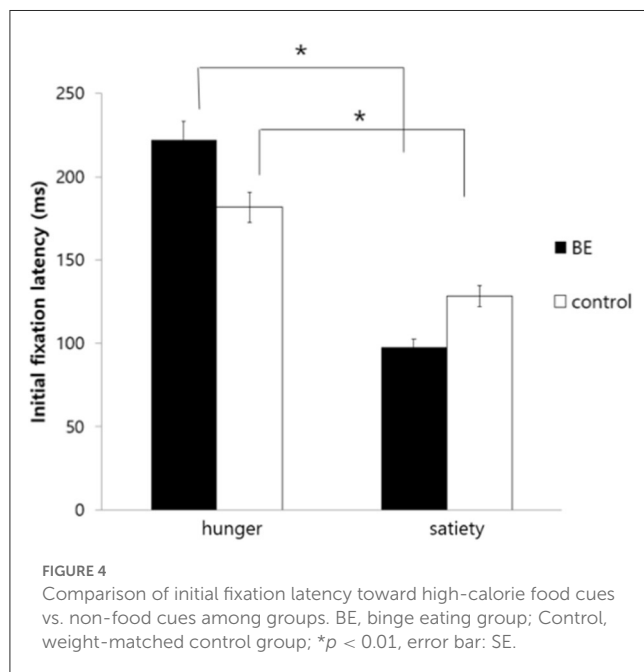
Second, for initial fixation duration, there was no significant interaction between the group and the condition [$F_{(1,109)} = 0.03, p = 0.855, n.s.$], and the main effect on the group [$F_{(1,109)} = 1.62, p = 0.206, n.s.$]. Although not statistically significant, there was a tendency observed for the condition [$F_{(1,109)} = 3.19, p = 0.077, \eta^2 = 0.028$], suggesting a cautious implication that participants may have a higher likelihood of viewing high-calorie food cues for a longer duration in the hunger condition compared to the satiety condition.

To investigate whether participants having problematic binge eating behaviors under the satiety condition exhibit longer gaze duration toward high-calorie food cues compared to non-food cues, the gaze duration toward food stimuli of each group was analyzed. As a result, there was no significant interaction between the group and the condition [$F_{(1,109)} = 1.91, p = 0.170, n.s.$]. However, there was a significant main effect on the group [$F_{(1,109)} = 4.75, p = 0.031, \eta^2 = 0.042$], indicating that the BE group showed attentional bias toward high-calorie food cues vs. neutral cues compared to the control group regardless of hunger and satiety. Moreover, there was a significant main effect on the condition [$F_{(1,109)} = 7.06, p = 0.009, \eta^2 = 0.061$], as all hungry participants looked at the high-calorie food cues for a longer time than satiated participants (Figure 5).

TABLE 4 Comparison of attentional bias toward high-calorie food cues vs. non-food cues among groups.

Measure	BE group		Control group		Test statistics (F)
	Hungry condition (N = 29)	Satiated condition (N = 29)	Hungry condition (N = 29)	Satiated condition (N = 29)	
Initial fixation latency (ms)	−222.226 (198.515)	−97.433 (180.317)	−181.692 (176.181)	−128.336 (181.347)	0.903
Initial fixation duration (ms)	140.072 (180.618)	98.361 (134.095)	76.754 (163.446)	17.499 (83.797)	0.033
Gaze duration (ms)	1,371.691 (710.136)	854.256 (612.703)	784.701 (827.218)	614.542 (695.017)	1.907

Mean (standard deviation); In milliseconds (ms). BE group, binge eating group; control group, weight-matched control group.



3.4. Explicit wanting and liking

To assess participants' explicit wanting and liking for high-calorie and low-calorie food cues, their self-reported values on a visual analog scale (VAS) were analyzed. Table 5 shows the mean and standard deviation values for explicit wanting and liking toward high-calorie and low-calorie food cues.

First, in terms of wanting level, the analysis revealed that there was no significant interaction between the group and the condition in wanting for high-calorie food cues [$F_{(1,109)} = 0.21$, $p = 0.647$, $n.s.$]. There was a main effect on the condition for high-calorie food cues [$F_{(1,109)} = 17.01$, $p = 0.0001$, $\eta^2 = 0.135$]. It is indicated that all participants reported higher explicit wanting for high-calorie food when they are hungry rather than satiated. However, there was no significant effect of the group on explicit wanting for high-calorie food cues [$F_{(1,109)} = 3.54$, $p = 0.63$, $n.s.$]. Furthermore, there was no significant interaction between the group and the condition in wanting low-calorie food cues [$F_{(1,109)} = 0.79$, $p = 0.377$, $n.s.$]. There was a main effect on the condition [$F_{(1,109)} = 12.03$, $p = 0.0008$, $\eta^2 = 0.099$] for low-calorie food cues, indicating that both

the BED group and the control group reported higher explicit wanting for low-calorie food cues when hungry than satiated. There was no significant main effect on the group [$F_{(1,109)} = 0.44$, $p = 0.510$, $n.s.$].

Second, for liking level, there was no significant interaction between the group and the condition in liking both for high-calorie [$F_{(1,109)} = 0.03$, $p = 0.865$, $n.s.$] and low-calorie food cues [$F_{(1,109)} = 0.23$, $p = 0.636$, $n.s.$]. There was no significant main effect on the group [$F_{(1,109)} = 0.66$, $p = 0.420$, $n.s.$] and the condition [$F_{(1,109)} = 1.08$, $p = 0.30$, $n.s.$] for high-calorie food cues. Moreover, there was no significant main effect on the group [$F_{(1,109)} = 0.42$, $p = 0.519$, $n.s.$] and the condition [$F_{(1,109)} = 0.001$, $p = 0.976$, $n.s.$] for low-calorie food cues. It is suggested that there was no difference in liking for high-calorie food cues and low-calorie food cues between the BE group and control group, or between the hunger condition and satiety condition.

4. Discussion

This study aimed to examine whether attentional bias for food cues was affected by hunger and satiety maintaining homeostasis

TABLE 5 Comparison of wanting and liking levels toward high-calorie food cues and low-calorie food cues among groups.

Measure	BE group		Control group		Test statistics (F)
	Hungry condition (N = 29)	Satiated condition (N = 29)	Hungry condition (N = 29)	Satiated condition (N = 29)	
Wanting_high-calorie	58.395 (21.004)	43.693 (21.621)	47.943 (19.763)	30.395 (18.184)	0.211
Wanting_low-calorie	45.839 (18.115)	37.487 (18.104)	42.969 (18.124)	29.161 (16.327)	0.377
Liking_high-calorie	69.406 (15.958)	65.421 (19.725)	65.441 (17.418)	62.701 (18.205)	0.029
Liking_low-calorie	53.475 (16.635)	54.766 (18.678)	52.812 (14.445)	51.939 (15.376)	0.225

Mean (standard deviation). BE group, binge eating group; control group, weight-matched control group.

Wanting_high-calorie: average of wanting VAS for high-calorie food stimulus, Wanting_low-calorie: average of wanting VAS for low-calorie food stimulus, Liking_high-calorie food cues: average of liking VAS for high-calorie food stimulus, Liking_low-calorie food cues: average of liking VAS for low-calorie food stimulus.

in individuals with BE. The result of this study showed that the BE group showed attentional bias toward high-calorie food cues over low-calorie food cues in both hunger and satiety conditions in the early stage of attentional processing. However, the control group showed attentional bias toward high-calorie food cues when hungry, but when satiated they were more likely to look at the low-calorie food cues. In the late stage of attentional processing, the BE group looked at the high-calorie food cues for longer than they did at the low-calorie food cues compared to the control group. Moreover, the BE group reported higher explicit wanting for high-calorie food than the control group did. All participants reported higher explicit wanting for high-calorie food when they are hungry rather than satiated. Finally, there was no difference in explicit liking for the group and the condition.

The main result of this study is that both the BE and control groups showed early attentional bias toward high-calorie food cues over low-calorie food cues in the hunger condition. In the satiety condition, BE participants showed persistent orientation bias toward high-calorie food images, whereas the control group did not. As hypothesized, the effect of the hedonic pathway overriding the homeostatic pathway contributes to the development and maintenance of BE (Novelle and Diéguez, 2018). Normal-weight group showed incentive salience to high-calorie food cues only when hungry according to the homeostasis pathway (Lutter and Nestler, 2009). While it is adaptive to quickly detect and allocate attention toward high-calorie food during energy depletion, it is inappropriate to show the attentional bias toward high-calorie food cues, regardless of the condition in the BE group. In addition, the continuous hyperreaction of high-calorie food cues suggests why the majority of people with BED are overweight or obese (Field et al., 2013).

This result supported the main hypothesis that the reward system activity is abnormally enhanced as exposure to palatable food cues in individuals with binge eating behaviors (Pool et al., 2016). In line with the incentive-sensitization theory, high-calorie food seems to be more salient than low-calorie food in the BE group because it is the reward-related cues. The attentional bias in the early stage of attentional processing presented the automatic engagement in high-calorie food cues, reflecting the implicit motivation to obtain a reward (Fox et al., 2001). As the

cues triggered reactivity to high-calorie food cues may be due to conditioning systems, attentional bias limited to high-calorie food cues may be caused by a personal history of binge eating (Berridge and Robinson, 2003). The study examining food selection and intake of overweight women with BED showed that participants with BED consumed a greater percentage of energy as fat and a lesser percentage as protein than did participants without BED during the binge meal (Yanovski et al., 1992). Moreover, it is suggested that palatable food containing sugar and fat, most of which are high-calorie foods, have addictive properties (Gearhardt et al., 2011; Smith and Robbins, 2013). The results may be the evidence of addiction such as the consumption of palatable food in individuals with binge eating behaviors.

The study shows that initial orientation bias toward high-calorie food cues vs. neutral cues appeared in all participants when hungry. The absence of group differences in participants' orientation bias toward high-calorie food cues vs. non-food is consistent with other eye-tracking studies in adults and adolescents who binge eat (Schag et al., 2013; Sperling et al., 2017). However, preferential orientation bias toward food stimuli was found in adults with BE episodes in real scenes (Popien et al., 2015) and in studies using reaction time-based measures (Schmitz et al., 2014, 2015; Sperling et al., 2017). The difference in results might be explained by the use of different experimental procedures and stimulus types. Moreover, another reason why this study did not show any difference between high-calorie food cues and neutral cues may be because of the ceiling effect. The ceiling effect may have occurred, as paying attention to high-calorie food cues is the most important issue for survival when hungry.

As expected, the longer gaze duration for high-calorie food cues compared to low-calorie food cues or neutral food cues in individuals with BE was replicated in our study. There were relatively consistent results that people with BE showed slower disengagement of food cues (Schag et al., 2013; Popien et al., 2015; Schmidt et al., 2016; Sperling et al., 2017). However, like the control group, the BE group also showed longer gaze duration for high-calorie food cues vs. neutral food cues when they were hungry than when they were satiated in this study. The result is different from those of the group with obesity that may be related to the reward system dysregulation (Nijs et al., 2010). As the maintained stage of

attention measures more strategic attention (Fox et al., 2001), the BE group can also be affected by hunger and satiety in explicit desire (i.e., explicit wanting). This has something in common with the result of self-reported explicit wanting, applying the classification of explicit and implicit wanting in the incentive-sensitization theory. The BE group reported higher explicit wanting for high-calorie food than the control group did, and all participants reported higher explicit wanting for high-calorie food when they are hungry rather than satiated. The results may suggest that computations of wanting to incorporated the current physiological state in the BE group (Zhang et al., 2009). Another possible explanation is that there may be a risk of binge eating or loss of control when hungry rather than satiated. It is consistent with the result that dietary restraint would predict binge eating episodes (Freeman and Gil, 2004).

When comparing high-calorie cues with low-calorie cues, the late stage of attentional bias toward high-calorie food cues is still evident in the BE group. This supports, to some extent, the approach-avoidance bias presented in previous studies (Schmidt et al., 2016). The results were different from other eating disorders, such as AN and BN (Brooks et al., 2011). For example, the eye-tracking studies showed that AN and BN attended to food cues for a shorter time than the control group did (Blechert et al., 2011). Moreover, the eye-tracking study demonstrated that the bulimic tendency group detected high-calorie food cues faster than neutral food cues initially and avoided attentional maintenance (Kim et al., 2016). People with BE are more similar to people with obesity that showed consistent attentional bias in the early and late stages. While people with obesity tend to allocate their attention to both high-calorie and low-calorie food cues, BE showed attentional bias only for the high-calorie food cues (Nijs et al., 2010). This demonstrated that, unlike people with obesity, intervention focusing on the high-calorie food cues may be required in individuals with binge eating behaviors.

There are several limitations in this study. First, in this study, the participants had a BMI index of approximately 21, which is within the average range for individuals in Korea and indicates that they did not exhibit issues of obesity or overweight. Therefore, we assumed that consuming “gimbap,” which is commonly regarded as a typical Korean meal, would induce a basic level of satiety. Although both the BE group and the control group reported reduced hunger after the meal, individual differences in the degree of satiety may exist, suggesting the possibility that participants did not fully experience satiety. Therefore, in future studies, it would be beneficial to use various physiological and psychological measures (e.g., blood samples), rather than relying solely on self-report evaluations, to assess the participants’ level of hunger in a more objective manner. Second, the food images formed a homogeneous category, whereas non-food images depicted items from various categories. Thus, it is possible that more attention may be paid to food stimulus because they were of the same category. However, an overriding consideration in selecting the stimuli was within each picture pair, in which the food and neutral cues were matched as closely as possible for complexity, color, and brightness. In future, it would seem desirable to select non-food images from a single category. Third, this study did not consider food intake to examine BE

after an attentional bias toward high-calorie food cues. In a future study, having a bogus taste test could provide additional evidence of BE.

To conclude, the current study offers a suggestion that high-calorie food perception is biased in individuals with binge eating behaviors vs. weight-matched female controls. This is the first evidence to examine the differences in attentional patterns between BE and weight-matched control groups in the consideration of demands of the internal milieu based on the incentive-sensitization theory. As visual food cues are particularly prominent in society, understanding the cognitive process of exposure to visual food cues in BE is of great importance in developing potential behavioral therapies, environmental alterations, and public health measures. Moreover, based on the results, attention bias modification could be implemented to modify the specific attentional bias to high-calorie food cues.

Data availability statement

The original contributions presented in the study are included in the article/supplementary material, further inquiries can be directed to the corresponding author.

Ethics statement

The studies involving human participants were reviewed and approved by Chung-Ang University IRB. The patients/participants provided their written informed consent to participate in this study.

Author contributions

J-MW: conceptualization, methodology, validation, formal analysis, investigation, data curation, writing, and visualization. J-HL: conceptualization, methodology, validation, resources, supervision, project administration, and funding acquisition. G-EL: secondary writing, visualization, and modified the submitted version. All authors contributed to the article and approved the submitted version.

Funding

This research was supported by the Ministry of Education of the Republic of Korea and the National Research Foundation of Korea (NRF-2017S1A5B4055761).

Conflict of interest

The authors declare that the research was conducted in the absence of any commercial or financial relationships that could be construed as a potential conflict of interest.

Publisher's note

All claims expressed in this article are solely those of the authors and do not necessarily represent those of their affiliated

organizations, or those of the publisher, the editors and the reviewers. Any product that may be evaluated in this article, or claim that may be made by its manufacturer, is not guaranteed or endorsed by the publisher.

References

- American Psychiatric Association (2013). *Diagnostic and Statistical Manual of Mental Disorders (5th ed.)*. Arlington, VA: American Psychiatric Publishing. doi: 10.1176/appi.books.9780890425596
- Anselme, P., and Robinson, M. J. (2015). "Wanting," "liking," and their relation to consciousness. *J. Exp. Psychol.* 42, 123–140. doi: 10.1037/xan0000090
- Bang, E., Han, C., Joen, Y., and Kim, Y. (2018b). The Korean version of eating disorder diagnostic scale DSM-5 (K-EDDS DSM-5): a reliability and validity study. *Anxiety Mood.* 14, 127–134. doi: 10.24986/anxmod.2018.14.2.127
- Bang, E., Han, C., Kim, Y., Kim, M., Lee, Y., Heo, S., et al. (2018a). A reliability and validity study of the Korean version of the eating disorder examination questionnaire version 6.0 (EDE-Q version 6.0) and the clinical impairment assessment questionnaire (CIA). *Korean J. Psychosomatic Med.* 26, 152–163. doi: 10.22722/KJPM.2018.26.2.152
- Beck, A. T., Steer, R. A., and Garbin, M. G. (1988). Psychometric properties of the Beck depression inventory: twenty-five years of evaluation. *Clin. Psychol. Rev.* 8, 77–100. doi: 10.1016/0272-7358(88)90050-5
- Berridge, K. C. (2009). 'Liking' and 'wanting' food rewards: brain substrates and roles in eating disorders. *Physiol. Behav.* 97, 537–550.
- Berridge, K. C., and Robinson, T. E. (2003). Parsing reward. *Trends Neurosci.* 26, 507–513. doi: 10.1016/S0166-2236(03)00233-9
- Berridge, K. C., and Robinson, T. E. (2016). Liking, wanting, and the incentive-sensitization theory of addiction. *Am. Psychol.* 71, 670–679. doi: 10.1037/amp0000059
- Berthoud, H. R. (2012). The neurobiology of food intake in an obesogenic environment. *Proc. Nutr. Soc.* 71, 478–487. doi: 10.1017/S0029665112000602
- Blechert, J., Feige, B., Joos, A., Zeeck, A., and Tuschen-Caffier, B. (2011). Electrocortical processing of food and emotional pictures in anorexia nervosa and bulimia nervosa. *Psychosom. Med.* 73, 415–421. doi: 10.1097/PSY.0b013e318211b871
- Brooks, S., Prince, A., Stahl, D., Campbell, I. C., and Treasure, J. (2011). A systematic review and meta-analysis of cognitive bias to food stimuli in people with disordered eating behaviour. *Clin. Psychol. Rev.* 31, 37–51. doi: 10.1016/j.cpr.2010.09.006
- Chen, S., Yao, N., Qian, M., and Lin, M. (2016). Attentional biases in high social anxiety using a flanker task. *J. Behav. Ther. Exp. Psychiatry* 51, 27–34.
- Cisler, J. M., and Koster, E. H. (2010). Mechanisms of attentional biases towards threat in anxiety disorders: An integrative review. *Clin. Psychol. Rev.* 30, 203–216.
- Dileone, R. J., Taylor, J. R., and Picciotto, M. R. (2012). The drive to eat: comparisons and distinctions between mechanisms of food reward and drug addiction. *Nat. Neurosci.* 15, 1330–1335. doi: 10.1038/nn.3202
- Fairburn, C. G., and Beglin, S. J. (1994). Assessment of eating disorders: Interview or self-report questionnaire? *Int. J. Eating Disord.* 16, 363–370. doi: 10.1002/1098-108X(199412)16:4<363::AID-EAT2260160405>3.0.CO;2-#
- Fenske, M. J., and Raymond, J. E. (2006). Affective influences of selective attention. *Curr. Dir. Psychol.* 15, 312–316.
- Field, A. E., Camargo, C. A., and Ogino, S. (2013). The merits of subtyping obesity: One size does not fit all. *J. Am. Med. Assoc.* 310, 2147–2148. doi: 10.1001/jama.2013.281501
- Finlayson, G., King, N., and Blundell, J. E. (2007). Liking vs. wanting food: importance for human appetite control and weight regulation. *Neurosci. Biobehav. Rev.* 31, 987–1002. doi: 10.1016/j.neubiorev.2007.03.004
- Fox, E., Russo, R., Bowles, R., and Dutton, K. (2001). Do threatening stimuli draw or hold visual attention in subclinical anxiety? *J. Exp. Psychol.* 130, 681–700. doi: 10.1037/0096-3445.130.4.681
- Freeman, L. Y., and Gil, K. M. (2004). Daily stress, coping, and dietary restraint in binge eating. *Int. J. Eating Disord.* 36, 204–212. doi: 10.1002/eat.20012
- Gearhardt, A. N., Davis, C., Kuschner, R., and Brownell, K. D. (2011). The addiction potential of hyperpalatable foods. *Curr. Drug Abuse Rev.* 4, 140–145. doi: 10.2174/1874473711104030140
- Hahn, D., Lee, C., and Chon, K. (1996). Korean adaptation of Spielberger's STAI (K-STAI). *Korean J. Health Psychol.* 1, 1–14.
- Kim, J., Kim, K., and Lee, J. (2016). Time course of visual attention to high-calorie virtual food in individuals with bulimic tendencies. *Cyberpsychol., Behav. Social Network.* 19, 28–33. doi: 10.1089/cyber.2015.0090
- Lee, M., Lee, Y., Park, S., Sohn, C., Hong, S., Lee, B., et al. (1995). Reliability and factor analysis: a standardization study of Beck depression inventory I Korean version (K-BDI). *Korean J. Psychopathol.* 4, 77–95.
- Loeber, S., Grosshans, M., Herpertz, S., Kiefer, F., and Herpertz, S. C. (2013). Hunger modulates behavioral disinhibition and attention allocation to food-associated cues in normal-weight controls. *Appetite.* 71, 32–39. doi: 10.1016/j.appet.2013.07.008
- Lutter, M., and Nestler, E. J. (2009). Homeostatic and hedonic signals interact in the regulation of food intake. *J. Nutr.* 139, 629–632. doi: 10.3945/jn.108.097618
- Nijs, I. M., Muris, P., Euser, A. S., and Franken, I. H. (2010). Differences in attention to food and food intake between overweight/obese and normal-weight females under conditions of hunger and satiety. *Appetite.* 54, 243–254. doi: 10.1016/j.appet.2009.11.004
- Novelle, M. G., and Diéguez, C. (2018). Food addiction and binge eating: lessons learned from animal models. *Nutrients.* 10, 71. doi: 10.3390/nu10010071
- Piech, R. M., Pastorino, M. T., and Zald, D. H. (2010). All I saw was the cake. Hunger effects on attentional capture by visual food cues. *Appetite.* 54, 579–582. doi: 10.1016/j.appet.2009.11.003
- Pool, E., Delplanque, S., Coppin, G., and Sander, D. (2015). Is comfort food really comforting? Mechanisms underlying stress-induced eating. *Food Res. Int.* 76, 207–215. doi: 10.1016/j.foodres.2014.12.034
- Pool, E., Sennwald, V., Delplanque, S., Brosch, T., and Sander, D. (2016). Measuring wanting and liking from animals to humans: a systematic review. *Neurosci. Biobehav. Rev.* 63, 124–142. doi: 10.1016/j.neubiorev.2016.01.006
- Popien, A., Frayn, M., von Ranson, K. M., and Sears, C. R. (2015). Eye gaze tracking reveals heightened attention to food in adults with binge eating when viewing images of real-world scenes. *Appetite.* 91, 233–240. doi: 10.1016/j.appet.2015.04.046
- Raymond, N. C., Neumeyer, B., Warren, C. S., Lee, S. S., and Peterson, C. B. (2003). Energy intake patterns in obese women with binge eating disorder. *Obes. Res.* 11, 869–879. doi: 10.1038/oby.2003.120
- Robinson, M. J., and Berridge, K. C. (2013). Instant transformation of learned repulsion into motivational "wanting". *Curr. Biol.* 23, 282–289. doi: 10.1016/j.cub.2013.01.016
- Robinson, T. E., and Berridge, K. C. (1993). The neural basis of drug craving: an incentive-sensitization theory of addiction. *Brain Res. Rev.* 18, 247–291. doi: 10.1016/0165-0173(93)90013-P
- Schag, K., Teufel, M., Junne, F., Preissl, H., Hautzinger, M., Zipfel, S., et al. (2013). Impulsivity in binge eating disorder: Food cues elicit increased reward responses and disinhibition. *PLoS ONE.* 8, e76542. doi: 10.1371/journal.pone.0076542
- Schmidt, R., Lüthold, P., Kittel, R., Tetzlaff, A., and Hilbert, A. (2016). Visual attentional bias for food in adolescents with binge-eating disorder. *J. Psychiatr. Res.* 80, 22–29. doi: 10.1016/j.jpsychires.2016.05.016
- Schmitz, F., Naumann, E., Biehl, S., and Svaldi, J. (2015). Gating of attention towards food stimuli in binge eating disorder. *Appetite.* 95, 368–374. doi: 10.1016/j.appet.2015.07.023
- Schmitz, F., Naumann, E., Trentowska, M., and Svaldi, J. (2014). Attentional bias for food cues in binge eating disorder. *Appetite.* 80, 70–80. doi: 10.1016/j.appet.2014.04.023
- Schulte, E. M., Grilo, C. M., and Gearhardt, A. N. (2016). Shared and unique mechanisms underlying binge eating disorder and addictive disorders. *Clin. Psychol. Rev.* 44, 125–139. doi: 10.1016/j.cpr.2016.02.001
- Seo, C. L., Kim, D., and Lee, J. (2020). "A study on the development of FATIS: Food, alcohol, and tobacco image system," in *Personality and Individual Differences* (Vol. 157). Oxford: Pergamon-Elsevier Science Ltd.
- Smith, D. G., and Robbins, T. W. (2013). The neurobiological underpinnings of obesity and binge eating: a rationale for adopting the food addiction model. *Biol. Psychiatry* 73, 804–810. doi: 10.1016/j.biopsych.2012.08.026
- Smith, K. E., Mason, T. B., Juarascio, A., Weinbach, N., Dvorak, R., Crosby, R. D., et al. (2020). The momentary interplay of affect, attention bias, and expectancies as predictors of binge eating in the natural environment. *Int. J. Eating Disord.* 53, 586–594. doi: 10.1002/eat.23235

- Sperling, I., Baldofski, S., Lüthold, P., and Hilbert, A. (2017). Cognitive food processing in binge-eating disorder: an eye-tracking study. *Nutrients*. 9, 903–915. doi: 10.3390/nu9080903
- Spielberger, C. D., Gorsuch, R. L., and Lushene, R. E. (1970). *Manual for the State-Trait Personality Inventory (Self-Evaluation Questionnaire)*. Palo Alto, CA: Consulting Psychologist Press.
- Stevenson, R. J., Francis, H. M., Attuquayefio, T., and Ockert, C. (2017). Explicit wanting and liking for palatable snacks are differentially affected by change in physiological state, and differentially related to salivation and hunger. *Physiol. Behav.* 182, 101–106. doi: 10.1016/j.physbeh.2017.10.007
- Stice, E., Davis, K., Miller, N. P., and Marti, C. N. (2008). Fasting increases risk for onset of binge eating and bulimic pathology: a 5-year prospective study. *J. Abnorm. Psychol.* 117, 941–946. doi: 10.1037/a0013644
- Stice, E., Telch, C. F., and Rizvi, S. L. (2000). Development and validation of the Eating Disorder Diagnostic Scale: a brief self-report measure of anorexia, bulimia, and binge-eating disorder. *Psychol. Assess.* 12, 1040–3590. doi: 10.1037/1040-3590.12.2.123
- Tanofsky-Kraff, M., and Yanovski, S. Z. (2004). Eating disorder or disordered eating? Non-normative eating patterns in obese individuals. *Obesity Res.* 12, 1361–1366. doi: 10.1038/oby.2004.171
- Veling, H., Lawrence, N. S., Chen, Z., van Koningsbruggen, G. M., and Holland, R. W. (2017). What is trained during food go/no-go training? A review focusing on mechanisms and a research agenda. *Curr. Addict. Rep.* 4, 35–41.
- Witt, A. A., and Lowe, M. R. (2014). Hedonic hunger and binge eating among women with eating disorders. *Int. J. Eating Disord.* 47, 273–280. doi: 10.1002/eat.22171
- Wonderlich, S. A., Gordon, K. H., Mitchell, J. E., Crosby, R. D., and Engel, S. G. (2009). The validity and clinical utility of binge eating disorder. *Int. J. Eating Disord.* 42, 687–705. doi: 10.1002/eat.20719
- Yanovski, S. Z., Leet, M., Yanovski, J. A., Flood, M. N., Gold, P. W., Kissileff, H. R., et al. (1992). Food selection and intake of obese women with binge-eating disorder. *Am. J. Clin. Nutr.* 56, 975–980. doi: 10.1093/ajcn/56.6.975
- Yu, Y. H., Vasselli, J. R., Zhang, Y., Mechanick, J. I., Korner, J., and Peterli, R. (2015). Metabolic vs. hedonic obesity: a conceptual distinction and its clinical implications. *Obesity Rev.* 16, 234–247. doi: 10.1111/obr.12246
- Zhang, S., Ang, M., Xiao, W., and Tham, C. K. (2009). Detection of activities by wireless sensors for daily life surveillance: eating and drinking. *Sensors*. 9, 1499–1517. doi: 10.3390/s90301499



OPEN ACCESS

EDITED BY

Xuemin Li,
Peking University Third Hospital, China

REVIEWED BY

Francesco Ascì,
Mediterranean Neurological Institute
Neuromed (IRCCS), Italy
Luca Marsili,
University of Cincinnati, United States

*CORRESPONDENCE

Yasuo Terao
✉ yterao@ks.kyorin-u.ac.jp

RECEIVED 08 April 2023

ACCEPTED 18 July 2023

PUBLISHED 11 August 2023

CITATION

Terao Y, Tokushige S-i, Inomata-Terada S,
Miyazaki T, Kotsuki N, Fisicaro F and
Ugawa Y (2023) How do patients with
Parkinson's disease and cerebellar ataxia read
aloud? -Eye-voice coordination in text reading.
Front. Neurosci. 17:1202404.
doi: 10.3389/fnins.2023.1202404

COPYRIGHT

© 2023 Terao, Tokushige, Inomata-Terada,
Miyazaki, Kotsuki, Fisicaro and Ugawa. This is
an open-access article distributed under the
terms of the [Creative Commons Attribution
License \(CC BY\)](#). The use, distribution or
reproduction in other forums is permitted,
provided the original author(s) and the
copyright owner(s) are credited and that the
original publication in this journal is cited, in
accordance with accepted academic practice.
No use, distribution or reproduction is
permitted which does not comply with these
terms.

How do patients with Parkinson's disease and cerebellar ataxia read aloud? -Eye-voice coordination in text reading

Yasuo Terao^{1,2*}, Shin-ichi Tokushige^{1,3}, Satomi Inomata-Terada^{1,2},
Tai Miyazaki³, Naoki Kotsuki³, Francesco Fisicaro⁴ and
Yoshikazu Ugawa⁴

¹Department of Neurology, Graduate School of Medicine, University of Tokyo, Tokyo, Japan,

²Department of Medical Physiology, Kyorin University, Mitaka, Japan, ³Department of Neurology, Kyorin University, Mitaka, Japan, ⁴Department of Human Neurophysiology, Fukushima Medical University, Fukushima, Japan

Background: The coordination between gaze and voice is closely linked when reading text aloud, with the gaze leading the reading position by a certain eye-voice lead (EVL). How this coordination is affected is unknown in patients with cerebellar ataxia and parkinsonism, who show oculomotor deficits possibly impacting coordination between different effectors.

Objective: To elucidate the role of the cerebellum and basal ganglia in eye-voice coordination during reading aloud, by studying patients with Parkinson's disease (PD) and spinocerebellar degeneration (SCD).

Methods: Participants were sixteen SCD patients, 18 PD patients, and 30 age-matched normal subjects, all native Japanese speakers without cognitive impairment. Subjects read aloud Japanese texts of varying readability displayed on a monitor in front of their eyes, consisting of Chinese characters and hiragana (Japanese phonograms). The gaze and voice reading the text was simultaneously recorded by video-oculography and a microphone. A custom program synchronized and aligned the gaze and audio data in time.

Results: Reading speed was significantly reduced in SCD patients (3.53 ± 1.81 letters/s), requiring frequent regressions to compensate for the slow reading speed. In contrast, PD patients read at a comparable speed to normal subjects (4.79 ± 3.13 letters/s vs. 4.71 ± 2.38 letters/s). The gaze scanning speed, excluding regressive saccades, was slower in PD patients (9.64 ± 4.26 letters/s) compared to both normal subjects (12.55 ± 5.42 letters/s) and SCD patients (10.81 ± 4.52 letters/s). PD patients' gaze could not far exceed that of the reading speed, with smaller allowance for the gaze to proceed ahead of the reading position. Spatial EVL was similar across the three groups for all texts (normal: 2.95 ± 1.17 letters/s, PD: 2.95 ± 1.51 letters/s, SCD: 3.21 ± 1.35 letters/s). The ratio of gaze duration to temporal EVL was lowest for SCD patients (normal: 0.73 ± 0.50 , PD: 0.70 ± 0.37 , SCD: 0.40 ± 0.15).

Conclusion: Although coordination between voice and eye movements and normal eye-voice span was observed in both PD and SCD, SCD patients made frequent regressions to manage the slowed vocal output, restricting the ability for advance processing of text ahead of the gaze. In contrast, PD patients experience restricted reading speed primarily due to slowed scanning, limiting their maximum reading speed but effectively utilizing advance processing of upcoming text.

KEYWORDS

eye-voice coordination, eye tracking, Parkinson's disease, spinocerebellar degeneration, reading

Introduction

Speech production involves the coordination of various motor activities, such as respiration, phonation, articulation, resonance, and prosody (Fabbri et al., 2017; Dashtipour et al., 2018). Voice disorders refer to conditions that affect the production or quality of the voice, impacting pitch, loudness, resonance, and overall voice quality. Speech disorders, on the other hand, involve difficulties in producing speech sounds or using language effectively, affecting articulation, fluency, or voice quality during speaking. Neurological disorders like cerebellar ataxia and parkinsonism can involve both aspects of vocal output disorder (Suppa et al., 2015, 2020).

When reading aloud, eye movements synchronize with the actions of the vocal organs to gather visual information from the text. This information undergoes lexical and phonological processing and is then converted into spoken words through articulation and vocal output production. The coordination between eye movements and vocal output during oral reading is known as “eye-voice coordination.” Studying gaze movement during oral reading helps us understand the process of converting written words into spoken language.

Typically, when reading aloud, individuals focus their gaze slightly ahead of the current word being spoken (referred to as eye-voice lead [EVL] or eye-voice span [EVS]). This means there are differences between the words they fixate on and the words they pronounce. The gaze input is used to visually process upcoming letters in the text, converting them into lexical and phonological information. This information is temporarily stored in memory or the “verbal sketchpad” (De Luca et al., 1999, 2002, 2013; Rayner, 2009; Baddeley and Hitch, 2019), while the acquired information is simultaneously processed and transformed into speech output for vocal output/verbal expression.

Early studies by Buswell (1921) and Fairbanks (1937) showed that the gaze position over the text precedes the position read by the voice by approximately 10–15 letters in space (spatial EVL) or 0.5–1 s in time (temporal EVL). These studies relied on the “light-off” method, which estimated the preceding gaze based on the number of words that could be articulated after the room or monitor light was turned off. However, they did not directly record eye movements and instead made speculations as to the amount of letters processed by preceding gaze.

Recent advancements in eye-tracking technology have allowed us to gain a better understanding of the precise coordination between eye movements and vocalization in normal individuals. By recording both voice and eye movements simultaneously, researchers have been able to examine eye-voice coordination in normal subjects and shed light

on the underlying pathophysiological processes in reading disabilities like dyslexia.

De Luca et al. (2013) conducted a study in which they had native Italian speakers with dyslexia read Italian texts aloud and compared their performance to that of normal subjects. They found that dyslexic readers exhibited slower reading compared to control peers. Dyslexic readers showed more silent pauses, sounded-out behaviors, and slightly longer word articulation times. Additionally, they showed reduced EVL compared to normal subjects. Similarly, individuals with autistic spectrum disorder (ASD) also displayed reduced EVL when asked to quickly name numbers arranged in rows (rapid automatic naming tasks, RAN). This reduction in EVL was associated with slower naming and indicated a reduced capacity of the “verbal sketchpad” in these individuals (Zoccolotti et al., 2013; Hogan-Brown et al., 2014). These findings suggest that reduced EVL reflects a diminished capacity of the “verbal sketchpad” in these patients, leading to less efficient reading.

In individuals without reading difficulties, enhanced eye-voice span (EVL) has been linked to increased automation in reading skills, such as proficient reading and faster reading speed or word naming. How does the length of EVL contribute to faster or more automatic reading? The eyes tend to move ahead of the articulatory system because visual processing is quicker than processing the articulation of the perceived word (Laubrock and Kliegl, 2015). One advantage of the eyes leading the voice is that the longer interval between the eyes and the voice aids in reading faster or more automatically. In typically developing individuals, extensive practice establishes automaticity in reading-related skills, such as in RAN, by reducing the need for attentional control and freeing up various attentional processes, such as working memory. However, Inhoff argues that the eyes do not necessarily have to move ahead of the voice but can instead wait until the voice catches up, especially when reading at a very slow pace (Inhoff et al., 2011; Laubrock and Kliegl, 2015; Silva et al., 2016).

If the reader uses the initial gaze time on the text ahead of the currently uttered word or syllable, the time can be used to finish the processing of the currently gazed part of the text as well, that is, parallel processing of the two components (or words) in the text can take place at the same time (Jones et al., 2008, 2016; Protopapas et al., 2013; Laubrock and Kliegl, 2015). Additionally, buffering of the material that can be rapidly decoded and translated from graphemic input into a phonological code also allows faster reading through processing of word articulation into chunks. Thus, longer EVL helps subjects read automatically or faster, whereas subjects can read faster by “stretching” the EVL while reading. Shorter EVL in individuals with dyslexia or ASD can disrupt automaticity in language-related skills as the diminished EVL hampers parallel processing (Silva et al., 2016).

Few studies to date have examined the impact of impaired oculomotor control on reading aloud (Schattka et al., 2010; Stock et al., 2020). Reading difficulties during oral reading are often observed in individuals with neurological disorders like Parkinsonism

Abbreviations: EVL, eye-voice lead; EVS, eye-voice span; RAN, rapid automatic naming; SCD, spinocerebellar degeneration; SCA, spinocerebellar ataxia; PD, Parkinson's disease; ASD, autistic spectrum disorder; MSAC, multiple system atrophy cerebellar-type; ANOVA, analysis of variance; UPDRS, Unified Parkinson's Disease Rating Scale.

and cerebellar ataxia. The coordination between eye movements and voice involves multiple brain regions, particularly the cerebellum, which controls the movements of these two components (Miall and Jenkinson, 2005; Nitschke et al., 2005; Stoodley and Stein, 2013; Modroño et al., 2020; Rizzo et al., 2020). Therefore, cerebellar pathology can impact this coordination associated with deficits in oculomotor control.

Basal ganglia disorders can impact gaze movement during reading in a distinct manner. Individuals with Parkinson's disease (PD) often experience various abnormalities in their eye movements while reading. These include an increased number of both forward and backward eye movements (saccades) and longer periods of fixation, leading to a slower scanning of the text (Stock et al., 2020).

In PD, the basal ganglia excessively inhibit the oculomotor system, causing the amplitude of eye movements while scanning the text to be smaller (hypometric) compared to individuals without the disorder. Additionally, the frequency of these eye movements per unit of time also decreases (Terao et al., 2011; 2013; Matsumoto et al., 2011a,b; Tokushige et al., 2018). As a result, the speed at which the gaze scans the text is slower, leading to a decrease in reading speed (Waldthaler et al., 2018).

No spaces are usually inserted between words in Japanese, this may make Japanese reading an exceptional case as opposed to Western and other languages. However, reading in the RAN context (with space intervals) and those reading a normal text represents a different context in terms of reading, with the latter more emphasis for eye movements (eye jumps between words). Here we focused on the overall time course of natural, continuous reading of Japanese instead of discrete fixations on each word.

This study aimed to explore the impact of gaze on natural and continuous oral reading (reading aloud) in individuals with Parkinsonism and cerebellar ataxia. By investigating the role of gaze in this specific reading behavior, we aimed to shed light on the underlying pathophysiology. Although silent reading has received more attention in research, this coordination is crucial even in silent reading, as it involves subvocalization as a latent output. Here, we conducted a study to examine the coordination between eye movements and voice in native Japanese patients with Parkinson's disease (PD) as they read Japanese text of varying readability. We compared their performance with that of age-matched healthy individuals and patients with spinocerebellar degeneration (SCD). The participants read Japanese texts displayed on a monitor screen, and we analyzed the coordination between their gaze and voice while reading. We simultaneously recorded and tracked their eye movements and voice utterances to assess the fundamental relationship between eye and voice during reading. Additionally, we investigated how the subjects adjusted their eye movements, voice latency, and reading speed in response to changes in the text's readability according to the demands of the text.

Methods

Subjects

Subjects were native Japanese speakers. Study participants were 16 SCD patients (11 males, 5 females; age 62.2 ± 9.5 years); 9 multiple system atrophy cerebellar-type (MSAC), 5 spinocerebellar ataxia

(SCA6 4, SCA31, unknown 1) and 18 PD patients (11 males, 8 females, age 70.1 ± 4.4 years). The patients were recruited at the outpatient and inpatient sections of the University of Tokyo Hospital. Initially, 18 SCD patients were recruited, but two subjects were excluded because of poor recording. Thirty age-matched normal subjects (11 males, 17 females, age 70.8 ± 3.7 years) were also recruited to obtain age-matched control data. The following experiments were conducted according to the declaration of Helsinki, after obtaining written informed consent from the subjects. The procedures of the experiment were approved by the local ethical committee [Reference number: 2411-(10)]. None of the subjects had mental or cognitive problems, and all had a Mini-Mental State Examination score above 25. There were no dysmorphisms or paramorphisms in the subjects.

The inclusion criteria of SCD patients were adult patients with MSAC and SCD patients with predominant cerebellar manifestation, and the exclusion criteria were those with hearing loss that interfered with verbal communication, severe dysarthria that prevented the subjects from performing the reading task, or severe cognitive impairment that they prevented them from understanding or performing the task procedure, or severe orthostatic hypotension that they cannot keep seated for 1 h.

All SCD patients presented predominantly with cerebellar ataxia with minimal parkinsonism. Among them, the diagnosis of MSA was based on Gilman's criteria (Gilman et al., 1999, 2008). Selection of other SCD patients in this study was based on pure progressive cerebellar symptoms throughout the follow-up period but no brainstem involvement, as also demonstrated by cerebellar atrophy and preservation of brainstem in neuroimaging. The disease stage of SCD patients was assessed according to the ataxia scale of Schmitz-Hübsch et al. (2006), as in our previous studies (Terao et al., 2016, 2017). Stage 0 represents no gait difficulty, whereas stage 1 represents patients at disease onset, as defined by onset of gait difficulties. At stage 2, patients lose their independent gait, necessitating the use of a walking aid or a supporting arm to walk. At stage 3, patients are permanently confined to a wheelchair. Stages in between were given intermediate scores (such as 2.5).

PD patients were diagnosed according to the British Parkinson's Disease Society Brain Bank Criteria. H-Y stage of the patients was 1.6 ± 0.9 on average. The disease stage of motor symptoms was 14.9 ± 1.9 on average as assessed by means of the Unified Parkinson's Disease Rating Scale (UPDRS) Scale motor score (UPDRS-III). Subject information is summarized in Table 1. None of the patients received DBS surgery. PD patients continued to take their medication as usual, and were examined approximately 3–4 h after drug intake in the morning, which would minimize the effects on eye movements according to our previous study (Yugeta et al., 2008). Levodopa equivalent dose was 321.3 ± 131.9 mg on average. For SCD patients, the drug patients took was taltirelin hydrate in most cases, while some patients were taking clonazepam, L-threo-DOPS, midodrine hydrochloride, diphenidol hydrochloride as drugs potentially acting on the central nervous system. L-dopa or other dopaminergic drugs were not taken by any of the SCD patients.

Task procedure

Subjects read aloud Japanese texts (Table 2 and Figure 1) presented on a 17-inch monitor screen with a refresh rate of 60 Hz (Dell

TABLE 1 Details of included subjects.

Diagnosis	No. of cases	Male	Female	Age (yrs)	Duration (yrs)	Disease stage*	H-Y stage	UPDRS motor score	LEDD (mg)
Normal	30	13	17	70.8 ± 3.7	–	–		–	
SCD	16	11	5	62.1 ± 9.5	7.3 ± 5.6	1.7 ± 0.7			
PD	18	11	7	70.1 ± 4.3	3.8 ± 0.8	–	1.6 ± 0.9	14.9 ± 1.9	321.3 ± 131.9

*Stage 0 represents no gait difficulty, whereas Stages 1 represent patients at disease onset, as defined by onset of gait difficulties. At Stage 2, patients lose independent gait, and needs a walking aid or a supporting arm to walk with. At Stage 3, patients come to be permanently confined to a wheel chair. Stages in between were scored intermediate (such as 2.5).

TABLE 2 Text used in the study.

Text number	Vocabulary level in Japanese	Readability level	Font size
Text1	350	Entry level	24
Text2		Elementary level (low grades)	24
Text3	500	Elementary level (high grades)	24
Text4	800	Pre-intermediate	24
Text5		Pre-intermediate	32
Text6		Pre-intermediate	32
Text7	1000	Intermediate level	24
Text8		Intermediate level	32
Text9		Intermediate level	32
Text10		Intermediate level	32
Text11		Intermediate level	16
Text12		Intermediate level	16
Text13		Intermediate level	16
Text14	2000	Japanese modern literature	16
Text15	Above 2000	Extracts from medical textbooks	24
Text16		Japanese premodern writings	32
Text17	–	Random sequence of Japanese ancient writings	30
Text18	–	Random sequence of Japanese phonograms	24
Text19	–	Random sequence of Japanese phonograms	16
Text20	–	Arranged list of words (hiragana words)	24
Text21	–	Arranged list of words (kanji compounds)	24
Text22	–	Japanese syllabary (list of hiragana phonograms)	24

Vocabulary level in Japanese, text readability and font sizes of each text used in the present study. Texts 1–19 are typical Japanese texts, without spaces between words, and are arranged in order of decreasing readability (from easier to more difficult to read) in this table. Texts 20–22 are arranged word lists (texts 20, 21): arranged list of Kanji words (Kanji compounds), with spaces in between, or Japanese syllabary (text 22).

E173FPb, Dell, Kawasaki, Japan, screen resolution 1024 × 768). Head movement was restricted by the chin and forehead rests of the eye tracker, although some slight movements were noted when the subjects read the text aloud. The monitor was positioned vertically at a viewing distance of 50 cm in front of their eyes.

The subjects had to read the text clearly at their natural and comfortable speed and usual prosody. The eye movement data was recorded from the dominant eye, although when recording from the dominant eye was not stable, the non-dominant eye was recorded instead. The gaze location on the screen was measured simultaneously by a video-based eye tracking system (EyeLink 1000, SR Research, Mississauga, Ontario, Canada) at a sampling rate of 1000 Hz, and

spatial resolution of less than 0.04°. The output from the microphone was fed to a PC a short-latency ASIO driver that connected the microphone input directly to a USB audio interface (M-track M-audio, M-audio Japan, Tokyo, Japan) with a recording latency of 2–6 ms, and also interfaced to the eye tracker by the EyeLink Experiment Builder software. Eye movement data was fed to the EyeLink Host computer via an analog board, and was then fed to the Experiment builder computer through an ethernet cable.

Tasks were created using the SR Research Experiment Builder software, version 1.5.58. The gaze position on the monitor screen was recorded using a video-based eye tracking system (EyeLink 1000, SR Research, Mississauga, Ontario, Canada), while the voice

simultaneously digitally recorded by a headset with a microphone. Prior to the experiments, the subjects performed a nine-point gaze calibration procedure to map the ocular fixation position onto screen coordinates. The calibration was considered to be valid if the maximum spatial error was less than 1° and the average error was less than 0.5° .

Stimulus

Japanese texts of 5–14 lines in length, written in the horizontal direction from left to right with Chinese characters and Japanese phonetic lettering intermingled, were presented for 45 s each (Table 2 and Figure 1). Each letter subtended a visual angle of 0.6 – 1.3 degrees (0.85 cm on the screen, corresponding to approximately 1° of visual angle). Texts of various reading difficulty levels and letter sizes were used. Most of the texts presented were taken from those frequently adopted in Japanese textbooks. These texts were selected since they use standard Japanese text styles and are actually used for teaching Japanese to foreigners living in Japan (Hayashi and NPO Tadoku Supporters, 2012; Kio and NPO Tadoku Supporters, 2012; Koizumi and NPO Tadoku Supporters, 2012; Sakai and NPO Tadoku Supporters, 2014). The text levels reflecting the overall reading difficulty was defined according to the frequency of words and grammar structures included in the text. Correspondence to grades of reading levels in ordinary Japanese schools were made based on this information; the texts ranged in difficulty from the first grade of elementary school to the university/academic level. The two most difficult texts were taken from a Japanese medical textbook, in which the included medical terminology was unfamiliar to the subject, and from pre-modern Japanese writing, which was written in the style of the Edo-Meiji era (1700–1800), understandable to many contemporary Japanese people but using words and grammar of a pre-modern style, thus increasing the reading difficulty.

To account for the spaces between words that are present in Western languages, we also presented word lists in both hiragana phonograms and kanji graphemes, separated by spaces [text 20: arranged list of hiragana words, text 21: arranged list of kanji words (kanji compounds)]. Also, we presented the Japanese syllabary, separated by spaces and consisting of 50 different hiragana graphemes ordered in a sequence. This Japanese is learned at the beginning of school (Text 22), just as the alphabet is learned for Western languages. When reading this text, the subjects did not actually “read” it since they are expected to access it from memory.

Data processing

The gaze position data were processed using EyeLink Data Viewer software (Data Viewer ver. 1.3.137., SR Research, Mississauga, Ontario, Canada). Based on the input from the microphone and the gaze data output from the EyeLink, two parallel datasets were generated: an eye movement dataset and a sound file in the wave format. Eye movement and audio input data were synchronized and put in the register in time using a custom program operating on Experiment builder that was obtained from the support page of SR research, which was provided by De Luca et al. (2013). The time relationship between audio recordings and gaze position (EVL) was

analyzed offline using a custom-made program produced using Visual Studio 2015 (Microsoft, Redmond, Washington). The voice-line recording onset and offset was automatically overlaid on the timeline of the eye movements recording output (Figure 2). From the overlaid timelines of the eye movements recording and voice recordings, we analyzed for each moment, (1) Where the gaze was looking at, to place the x-coordinates of the gaze (gaze position), and (2) the read positions on the text (uttered voice position). Both data were then put together.

Saccade reports generated by the Data Viewer software provided data such as the saccade amplitude, x- and y-coordinates of the start and end positions of the saccade, and start and end times of saccades, whereas the fixation report contained the x- and y-coordinates of each fixation, the start and end time of the fixation, and the duration of individual fixation in each trial (each text reading).

Based on these, we calculated the following saccade parameters for each trial (text): the average number of saccades made per second (saccade frequency), mean amplitude of saccades, mean saccade duration, mean fixation duration, and proportion of regressive saccades made during reading (%). Gaze duration was defined as the sum of fixation and saccade duration.

By listening to the recording as the text was read aloud, the text position the subject was currently reading (reading or uttered position) was marked on the screenshot interface along the timeline interface of the program and the time was recorded simultaneously. Listening to the wave files, fixation positions were mapped onto letter positions over the screenshot of the three-line sentence to determine which graphemes in the passage were fixated.

Reading speed was defined as the average speed that the uttered position (x- and y-coordinates of the screen position in pixels) moved over the text as reading proceeded from left to right, excluding positions where there were line changes in the text. The EVL was the distance by which the eye moved ahead of the voice during reading aloud. More specifically, it refers to differences between fixated and uttered words, which is related to processing difficulty at a given point in time (when the gaze lagged behind the voice the eye-EVL was negative), as the subjects read each text.

Since the overall general level of spatial EVL was relatively stable for each text, even adjusting for different text sizes (see Results), we took the average EVL as an overall indicator for both onset and offset EVL. This parameter corresponds to spatial EVS in previous literature (Laubrock and Kliegl, 2015), as opposed to temporal EVS, which is frequently discussed in previous literature. Temporal EVL has been defined at both the onset of gaze in a certain word (onset EVL) and the offset of gaze from the word (offset EVL) (Silva et al., 2016). However, since there is no space between words in typical Japanese texts, except at explicit punctuations, we could not clearly define clear onset or offset EVLs. Instead, we took the average spatial EVL as an overall indicator for spatial EVL, since the overall general level of EVL was relatively stable for each text. In view of the relatively stable EVL for each text and the relatively stable reading speed for each text, we calculated the temporal EVL by dividing the former by the latter. Reading parameters, such as reading velocity and EVL, were expressed in letter values where appropriate.

The instantaneous location of the text gazed at by the eyes (gaze position), from the eye tracker appeared simultaneously on the interface timeline. In this way, the instantaneous gaze and reading positions (x- and y-coordinates) were marked consecutively at each

Text 1

あつ、桜のつぼみ！もうすぐ桜が咲きます。
九州、四国、本州、北海道はまだ寒いんです。
桜は南から北へ。咲きました。学校にも桜が咲きました。
みんなで、お花見をしましょう。
桜井の下でお弁当を食べます。
お酒を飲みます。歌を歌います。
今も。昔も。
4月。学校が、始まります。桜と一緒に、始まります。
桜の前で、写真を撮りましょう。
桜は、一週間ぐらいで散ります。桜は北へ、北へ。
5月 北海道で、桜が咲きます。

Text 15

小脳皮質は外表から分子層、プルキンエ細胞層、顆粒層の三層に分かれている。分子層は主として神経細胞の突起からなる。プルキンエ細胞の樹状突起は分子層内で扇状に広がって存在し、軸索は白質を通り歯状核などの小脳核へ到達して、その細胞に信号を伝達する。小脳では外部と連絡する線維が束をつくって存在しており、上・中・下小脳脚と呼ばれる。上小脳脚は主として小脳からの出力成分で、小脳葉状核から出て赤核・視床に至る線維からなる。中小脳脚の大部分は橋核の神経細胞から小脳に至る線維である。下小脳脚は様々な入力系の成分からなり、主なものとして下オリブ核から小脳に至るオリブ小脳路、脊髄からの後脊髄小脳路などがある。

Text 16

美登利はかの日を始めて生れかはりし様の身の振舞、用ある折は廊の姉のもとにこそ通へ、かけても町に遊ぶ事をせず、友達さびしがりて誘ひにと行けば今に今にと空約束はてし無く、さしにも中よし成けれど正太とさへに親しまず、いつも恥かし氣に顔のみ赤めて筆やの店に手踊の活潑さは再び見るに難く成ける、人は怪しがりて病ひの故かと危ぶむも有れども母親一人ほゝ笑みては、今にお供(きやん)の本性は現れます、これは中休みと子細わけありげに言はれて、知らぬ者には何の事とも思はれず、女らしい温順(おとな)しう成つたと褒めるもあれば折角の面白い子を種なしにしたと誹るもあり。

Text 18

いえぬをよつらよれたえへろにりつねはたひ
つれちえいえぬをよついらよれろろにりえら
うねなつなよたねつへりえへつなたわつるえ
かとりにりえらうねなつなよたねつむひなれ
えにりれなぬるへわつへえよたたよたねつ
むひなれえちわれなのなつぬろえにかつち
をえにわれそへおつひちわれなのなつぬろ
ねりかえろちつにえぬよつねむわえつへち
たねえりはろつりかえろちつにえぬ

Text 21

草花	北風	広場	雨雲	坂道
野原	谷底	海辺	米俵	口紅
目印	物音	建物	昼間	親子
朝市	割引	骨身	針金	品切
小銭	書留	昔話	厚手	積立
塩焼	古巣	裏側	島国	遠浅
型紙	花束	指輪	名札	小包

Text 22

あ	い	う	え	お
か	き	く	け	こ
さ	し	す	せ	そ
た	ち	つ	て	と
な	に	ぬ	ね	の
は	ひ	ふ	へ	ほ
ま	み	む	め	も
や	い	ゆ	え	よ
わ		を		ん

FIGURE 1

Examples of texts presented in the study. **Text 1**: Transcript of Japanese conversation, entry level (entry level, word level 350), **Text 15**: Japanese medical textbook (word level 2000), **Text 16**: Japanese pre-modern literature (word level 2000), **Text 18**: random sequence of Japanese phonograms (hiragana), **Text 21**: arranged list of words (Kanji compounds), **Text 22**: Japanese syllabary arranged from top to bottom in each column and from left to right columns.

moment over the screenshot as pixels on the screen. This information was integrated into a single plot, depicting the gaze and reading positions as a function of time (Figure 1). From this plot, the distance by which the gaze position led the reading position was calculated at each moment of the recording (EVL).

From the data, reading speed (letters/s) was calculated as the mean speed of reading the text in number of letters, excluding positions of the text where line changes took place. Although gaze movements actually comprise discrete movements (saccades) intervening with fixation periods, the overall speed of gaze scanning the text was also calculated, excluding where line changes occurred and where regressive eye movements occurred. This was defined as the product of saccade frequency and saccade amplitude multiplied by the proportion of non-regressive saccades, a parameter reflecting the speed of gaze scanning the text, excluding the contribution of regressive saccades.

To assess the degree to which parallel processing was taking place during reading, for the word gazed at and the word to be uttered, we calculated the ratio of gaze duration to temporal EVL according to Silva et al. (2016). This ratio reflects the higher weight of different processing stages (gaze-dependent vs. gaze-independent) within the onset EVS, with a higher ratio associated with more weight in the gaze-dependent process (see Discussion).

We also measured saccade parameters during the reading-aloud task: the number of saccades per unit time, the mean amplitude of saccades, such as the mean duration of fixation (ms), mean saccade duration (ms), mean saccade amplitude (deg), number of saccades made per unit time (/s), proportion of regression (regressive saccades among the total number of saccades [%]), and finally EVL (in pixels or number of letters). EVL (in letters) was defined as the amount of time by which gaze preceded the voice and was compared among the subject groups (PD, SCD patients, and normal subjects).

Statistical analysis

Statistical analyses were performed using a commercial software (version 19.0; SPSS Inc., Chicago, IL). To analyze the saccade and reading parameters (saccade amplitude, saccade frequency, frequency of regression, EVL), repeated measures analysis of variance (ANOVA) was conducted with a within-subject factor: subject group (3 levels, PD, SCD patients, and normal subjects) and a between-subject factor: the read text (22 levels), where appropriate. The significance criteria were set at a *p*-value of less than 0.05. Contingent on the significance of analyzed effects, *post hoc* analyses were also conducted, using the Bonferroni/Dunn's correction for multiple comparisons. We also analyzed the correlation between disease stage and the parameters within the two patient groups using the Spearman's rank correlation in both SCD and PD groups.

Results

Eye–hand coordination during reading

Figure 1 shows typical examples of eye–voice coordination during reading, in which the abscissa gives the time and the ordinate the gaze (blue curves) read positions (green curves) of the text (x-coordinate of the monitor screen). SCD patients exhibited a slower reading speed compared with normal subjects and PD patients, as reflected in the flatter slope of the plot depicting the reading positions as a function of time. During the course of reading, gaze was sometimes directed backwards (from right to left), which was termed *regression* or *regressive saccades*. Although slightly more frequent in SCD patients, regression was observed in all subject groups.

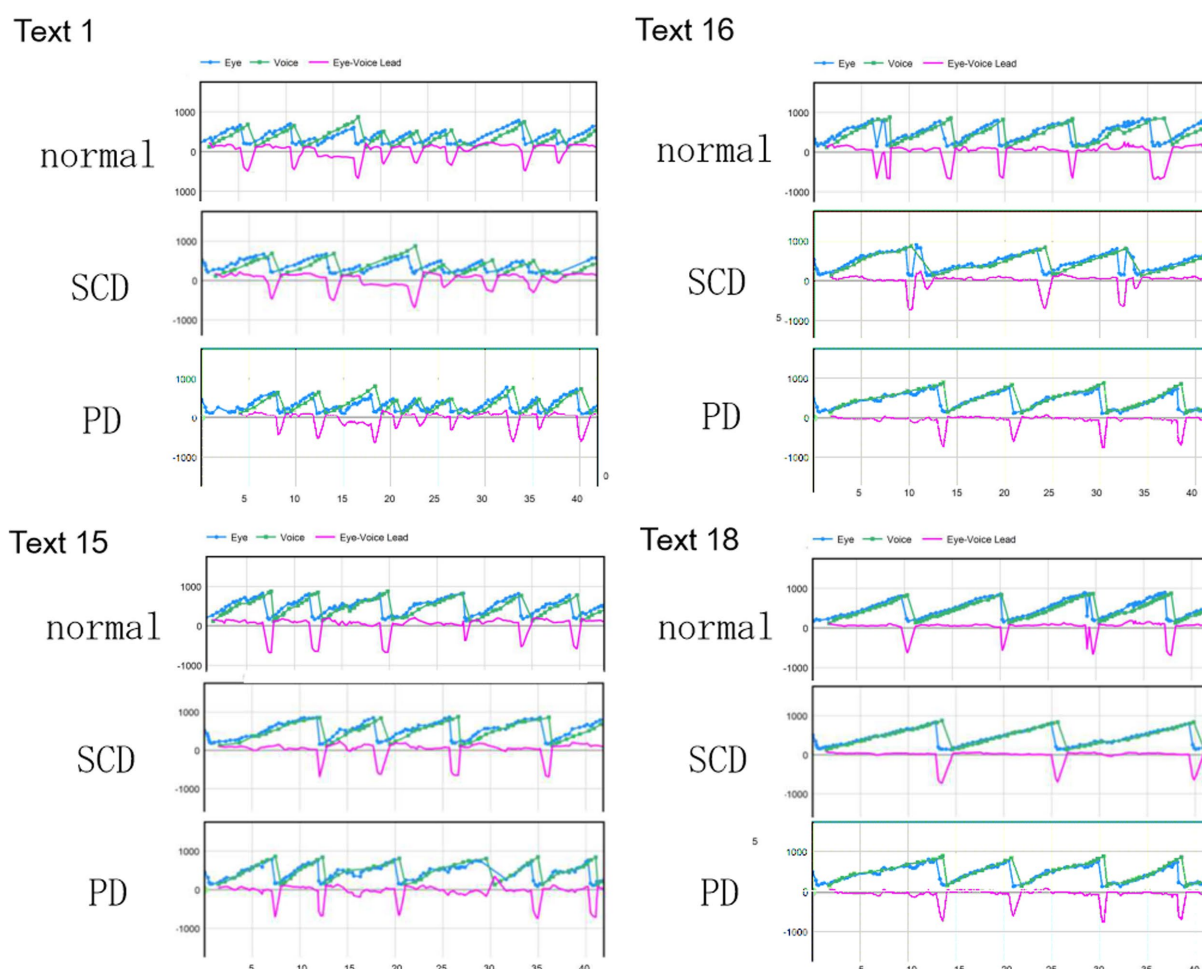


FIGURE 2

Typical examples of eye-voice coordination during reading aloud. The abscissa shows the time and the ordinate shows the gaze (blue curves) and read positions (green curves) of the text (x-coordinate of the monitor screen). Plots for each text (texts 1, 15, 16, and 21) are given separately for normal subjects (top row), SCD (middle row), and PD patients (bottom row). Note that the gaze position precedes the read (uttered position) except where line changes occur. The pink curve in each figure shows the spatial eye-voice lead (EVL), i.e., the distance by which the gaze position preceded the reading position. The pink curve in each figure shows the spatial EVL, i.e., the distance by which the gaze position preceded the read (uttered) position. Normal: normal subjects, PD: patients with Parkinson's disease, SCD: patients with spinocerebellar degeneration.

In all subject groups, the similar slope of curves for the gaze (blue curves) and voice (green curves) indicated that the overall reading speed and gaze movements were similar, although they showed some variability. The pink curve in each figure shows the spatial EVL, that is, the distance by which the gaze position preceded the position of the uttered letter at each moment. For all groups of subjects, on average, the gaze led the uttered letter almost constantly by 2.9 to 3.2 letters throughout the text reading (Table 3), except at locations where line changes occurred.

Except where line changes occurred, EVL was relatively stable during text reading, as shown by the slope of the correlation between time and EVL. However, after closer inspection, there were occasions on which the gaze position temporarily led the reading position largely, especially at the beginning of the texts in normal subjects and SCD patients, but later decreasing to zero. In contrast, the gaze of PD would occasionally lag behind the reading position, resulting in slightly negative EVL.

For all subject groups, the reading speed as well as the EVL reliably decreased as the readability of the text decreased and texts

were more difficult to read or could be read only at slower speed. For increasing number of texts (as shown in Figure 2), text readability decreased, that is, the text became more difficult to read speedily. Although reading speed expressed in pixels over the monitor screen was also slower as the individual letter size became smaller, reading speed was similar across texts with similar levels of text readability when expressed in terms of the number of letters. Thus, in the following analyses, the reading speed was expressed in terms of the letters in each text (letters/s).

Parameters of reading in normal subjects and neurological patients

Quantitative analyses corroborated the above visual inspection (reading and saccade parameters summarized in Table 3). For statistical assessment, we separately analyzed typical Japanese texts without spaces [text between words (texts 1–19 in Table 2)] and a word list arranged with spaces (texts 20–22 in Table 2;

statistical results summarized in [Tables 4, 5](#), for analyses of SCD patients restricting to MSAC patients, [Tables 4_2, 5_2](#), respectively).

Excluding places where line changes occurred, reading speed was significantly slower in SCD patients compared with normal subjects and even PD patients ([Figure 3A](#), *post hoc* analysis: normal vs. SCD $p < 0.0001$, PD vs. SCD $p = 0.0017$). This trend persisted even when we restricted the analysis of SCD patients to MSAC patients ([Figure 3_2A](#), *post hoc* analysis: normal vs. SCD $p = 0.0002$, PD vs. SCD $p = 0.0016$). In PD, reading speed was comparable to normal subjects. The general trend was similar for the three texts that

consisted of an arranged list of words or phonograms with spaces in between (text 20–22), although the reading speed was slightly faster for PD, followed by normal subjects and then SCD patients ([Figure 4A](#); *post hoc* analysis: normal vs. PD $p = 0.0162$, normal vs. SCD $p = 0.0006$, PD vs. SCD $p < 0.0001$). This trend also held true when we restricted our analysis of SCD patients to MSAC patients ([Figure 4_2A](#), *post hoc* analysis: normal vs. SCD $p = 0.0018$, PD vs. SCD $p < 0.0001$).

Reading speed correlated negatively with disease stage in SCD patients (correlation results with disease stage are presented in [Table 6](#) for texts 1–19, and [Table 7](#) for texts 20–22). This was true even restricting the analysis of SCA patients to MSAC patients (rightmost columns of [Tables 6, 7](#)). In PD patients, there was a slight negative correlation between disease stage (UPDRS motor score) and average reading speed across texts, but this correlation failed to reach significance.

Saccade parameters during reading in normal subjects and neurological patients

We looked at the saccade parameters of gaze movements during oral reading and compared them among the three subject groups ([Tables 4, 5](#)). The mean saccade amplitude was slightly reduced in SCD and PD patients compared to normal subjects, but these differences did not reach significance ([Figures 5A, 6A](#); restricting the analysis of SCD patients to MSAC patients [Figures 5_2A, 6_2A](#)). In contrast, saccade frequency was significantly lower in PD patients than in both normal subjects and SCD patients ([Figures 5B, 6B](#); *post hoc* analysis: texts 1–19: normal vs. PD $p < 0.0001$, PD vs. SCD $p = 0.00241$; texts 20–22: normal vs. PD $p < 0.0001$, PD vs. SCD $p < 0.0001$; restricting the analysis of SCD patients to MSAC patients [Figures 5_2B, 6_2B](#), normal vs. MSAC $p = 0.0018$, PD vs. MSAC $p < 0.0001$). Saccade frequency did not correlate significantly with disease stage in either PD and SCD patients for either texts 1–19 ([Table 6](#)) or texts 20–22 ([Table 7](#)). This held even restricting the

TABLE 3 Reading and saccade parameters during reading.

Parameter	Normal	PD	SCD
Reading vel (letter/s)	4.71 ± 2.38	4.79 ± 3.13	3.53 ± 1.81
Saccade amplitude (deg)	3.88 ± 1.62	3.38 ± 1.28	3.56 ± 1.14
Saccade frequency (/s)	5.06 ± 1.21	2.84 ± 0.51	3.80 ± 0.71
Fixation duration (ms)	236.8 ± 70.4	304.0 ± 66.2	293.3 ± 60.9
Saccade duration (ms)	74.3 ± 38.9	58.9 ± 35.1	57.3 ± 30.8
Gaze duration (ms)	309.5 ± 61.1	356.8 ± 60.1	365.0 ± 69.9
Scanning speed (letter/s)	12.55 ± 5.42	9.64 ± 4.26	10.81 ± 4.52
Regression (%)	22.9 ± 6.6	23.6 ± 6.7	27.1 ± 8.5
Eye voice lead (EVL) (letter)	2.95 ± 1.17	2.95 ± 1.51	3.21 ± 1.35
Eye voice lead (EVL) (ms)	664 ± 242	683 ± 493	1041 ± 404

Values represent mean ± standard deviation.

TABLE 4 Analysis of variance results for reading and saccade parameters with disease stage (texts 1–19).

Variable	Group		Text		Group X Text	
	$F_{(2,124)}$	p	$F_{(21,1302)}$	p	$F_{(42,2604)}$	p
Reading velocity	$F = 10.433$	$p = 0.0002^*$	$F = 224.890$	$p < 0.0001^{**}$	$F = 2.161$	$p = 0.0001^*$
Saccade amplitude	$F = 1.674$	$p = 0.1964$	$F = 115.781$	$p < 0.0001^{**}$	$F = 1.695$	$p = 0.0068^*$
Saccade frequency	$F = 14.273$	$p < 0.0001^{**}$	$F = 0.423$	$p = 0.6560$	$F = 1.069$	$p = 0.3755$
Fixation duration	$F = 0.327$	$p = 0.7222$	$F = 16.536$	$p < 0.0001^{**}$	$F = 3.023$	$p < 0.0001^{**}$
Saccade duration	$F = 1.343$	$p = 0.2691$	$F = 7.152$	$p < 0.0001^{**}$	$F = 1.098$	$p = 0.3196$
Gaze duration	$F = 0.554$	$p = 0.5781$	$F = 12.876$	$p < 0.0001^{**}$	$F = 2.649$	$p < 0.0001^{**}$
Regression	$F = 3.531$	$p = 0.0341^*$	$F = 13.697$	$p < 0.0001^{**}$	$F = 2.537$	$p < 0.0001^{**}$
Scanning speed	$F = 11.813$	$p < 0.0001^{**}$	$F = 88.019$	$p < 0.0001^{**}$	$F = 3.65$	$p < 0.0001^{**}$
Scanning – reading speed	$F = 5.589$	$p = 0.0070$	$F = 29.196$	$p < 0.0001^{**}$	$F = 2.167$	$p = 0.0001^*$
Eye voice lead (EVL)	$F = 0.716$	$p = 0.4948$	$F = 51.891$	$p < 0.0001^{**}$	$F = 0.995$	$p = 0.4785$
Variability of EVL	$F = 0.775$	$p = 0.4682$	$F = 1.130$	$p = 0.3176$	$F = 1.123$	$p = 0.2887$
Gaze duration/ temporal EVL	$F = 4.834$	$p = 0.0135^*$	$F = 3.978$	$p < 0.0001^{**}$	$F = 1.138$	$p = 0.0810$

*Significance at $p < 0.05$; **Significance at $p < 0.0001$.

TABLE 4_2 Analysis of variance results for reading and saccade parameters with disease stage (analysis of SCD patients restricted to MSAC patients, texts 1–19).

Variable	Group		Text		Group X Text	
	$F_{(2,110)}$	p	$F_{(21,1155)}$	p	$F_{(42,2310)}$	p
Reading velocity	$F = 8.924$	$p = 0.0007^*$	$F = 215.495$	$p < 0.0001^{**}$	$F = 1.680$	$p = 0.0084^*$
Saccade amplitude	$F = 1.961$	$p = 0.1508$	$F = 82.309$	$p < 0.0001^{**}$	$F = 1.648$	$p = 0.0101^*$
Saccade frequency	$F = 11.876$	$p < 0.0001^{**}$	$F = 10.579$	$p < 0.0001^{**}$	$F = 1.672$	$p = 0.0084$
Fixation duration	$F = 0.144$	$p = 0.8659$	$F = 11.967$	$p < 0.0001^{**}$	$F = 2.662$	$p < 0.0001^{**}$
Saccade duration	$F = 1.185$	$p = 0.3137$	$F = 7.032$	$p < 0.0001^{**}$	$F = 1.222$	$p = 0.1755$
Gaze duration	$F = 0.238$	$p = 0.7888$	$F = 9.120$	$p < 0.0001^{**}$	$F = 2.302$	$p < 0.0001^{**}$
Regression	$F = 2.276$	$p = 0.1131$	$F = 11.330$	$p < 0.0001^{**}$	$F = 2.347$	$p < 0.0001^{**}$
Scanning speed	$F = 13.324$	$p < 0.0001^{**}$	$F = 65.461$	$p < 0.0001^{**}$	$F = 3.529$	$p < 0.0001^{**}$
Scanning – reading speed	$F = 5.472$	$p = 0.0083^*$	$F = 9.443$	$p < 0.0001^{**}$	$F = 2.247$	$p < 0.0001^{**}$
Eye voice lead (EVL)	$F = 0.143$	$p = 0.8674$	$F = 37.813$	$p < 0.0001^{**}$	$F = 1.070$	$p = 0.3619$
Variability of EVL	$F = 0.654$	$p = 0.5270$	$F = 0.7550$	$p = 0.7541$	$F = 0.899$	$p = 0.6395$
Gaze duration/ temporal EVL	$F = 2.178$	$p = 0.1288$	$F = 3.038$	$p < 0.0001^{**}$	$F = 0.840$	$p = 0.7342$

*Significance at $p < 0.05$; **Significance at $p < 0.0001$.**TABLE 5** Analysis of variance results for reading and saccade parameters with disease stage (texts 20–22).

Parameter	Group		Text		Group X Text	
	$F_{(2,124)}$	p	$F_{(21,1302)}$	p	$F_{(42,2604)}$	p
Reading velocity	$F = 15.085$	$p < 0.0001^{**}$	$F = 151.667$	$p < 0.0001^{**}$	$F = 15.845$	$p < 0.0001^{**}$
Saccade amplitude	$F = 1.417$	$p = 0.2504$	$F = 66.275$	$p < 0.0001^{**}$	$F = 2.238$	$p = 0.0689$
Saccade frequency	$F = 12.190$	$p < 0.0001^{**}$	$F = 14.518$	$p < 0.0001^{**}$	$F = 1.465$	$p = 0.0389^*$
Fixation duration	$F = 2.511$	$p = 0.0870$	$F = 6.372$	$p = 0.0023^*$	$F = 1.005$	$p = 0.4079$
Saccade duration	$F = 0.356$	$p = 0.7018$	$F = 0.450$	$p = 0.6387$	$F = 0.555$	$p = 0.6960$
Gaze duration	$F = 2.539$	$p = 0.0875$	$F = 4.190$	$p = 0.0175^*$	$F = 0.997$	$p = 0.4120$
Regression	$F = 2.961$	$p = 0.0595$	$F = 2.714$	$p = 0.0704$	$F = 1.258$	$p = 0.2906$
Scanning speed	$F = 8.879$	$p = 0.0004^*$	$F = 53.479$	$p < 0.0001^{**}$	$F = 1.874$	$p < 0.0001^{**}$
Scanning – reading speed	$F = 31.521$	$p < 0.0001^{**}$	$F = 53.177$	$p < 0.0001^{**}$	$F = 14.154$	$p < 0.0001^{**}$
Eye–voice lead (EVL)	$F = 1.891$	$p = 0.1607$	$F = 73.782$	$p < 0.0001^{**}$	$F = 5.436$	$p = 0.0005$
Variability of EVL	$F = 0.797$	$p = 0.4572$	$F = 36.832$	$p < 0.0001^{**}$	$F = 1.915$	$p = 0.1149$
Gaze duration/temporal EVL	$F = 3.323$	$p = 0.0434^*$	$F = 52.716$	$p < 0.0001^{**}$	$F = 6.252$	$p = 0.0001$

*Significance at $p < 0.05$; **Significance at $p < 0.0001$.

analysis of SCA patients to MSAC patients (rightmost columns of Tables 6, 7).

In both SCD and PD patients, the fixation duration and saccade duration, though slightly shorter, were not significantly different from those of normal subjects (Tables 4, 5 and Figures 5C,D, 6C,D; restricting the analysis of SCD patients to MSAC patients Tables 4_2, 5_2, Figures 5_2C,D, 6_2C,D). Fixation gaze duration showed a significant negative correlation with disease stage only for texts 1–19 in SCD patients but not PD patients (Tables 6, 7). The lack of correlation held when restricting the analysis of SCD patients to MSAC patients. In SCD and PD patients, gaze duration was slightly

but not significantly shorter than in normal subjects (Figures 5E, 6E; restricting the analysis of SCD patients to MSAC patients Figures 5_2E, 6_2E). Gaze durations showed a significant negative correlation with disease stage only for texts 1–19 in SCD patients but not PD patients. This significant correlation was lost when the analysis of SCD patients were restricted to MSAC patients.

For all subject groups, the position of gaze over the text led the uttered position of the text by approximately 3 letters on average (EVL, Table 3), consistent with the notion that the text was first scanned by the gaze and the visual input was transformed into vocal output (voice). EVL was statistically comparable among the three subject

Figure 3

Texts 1-19

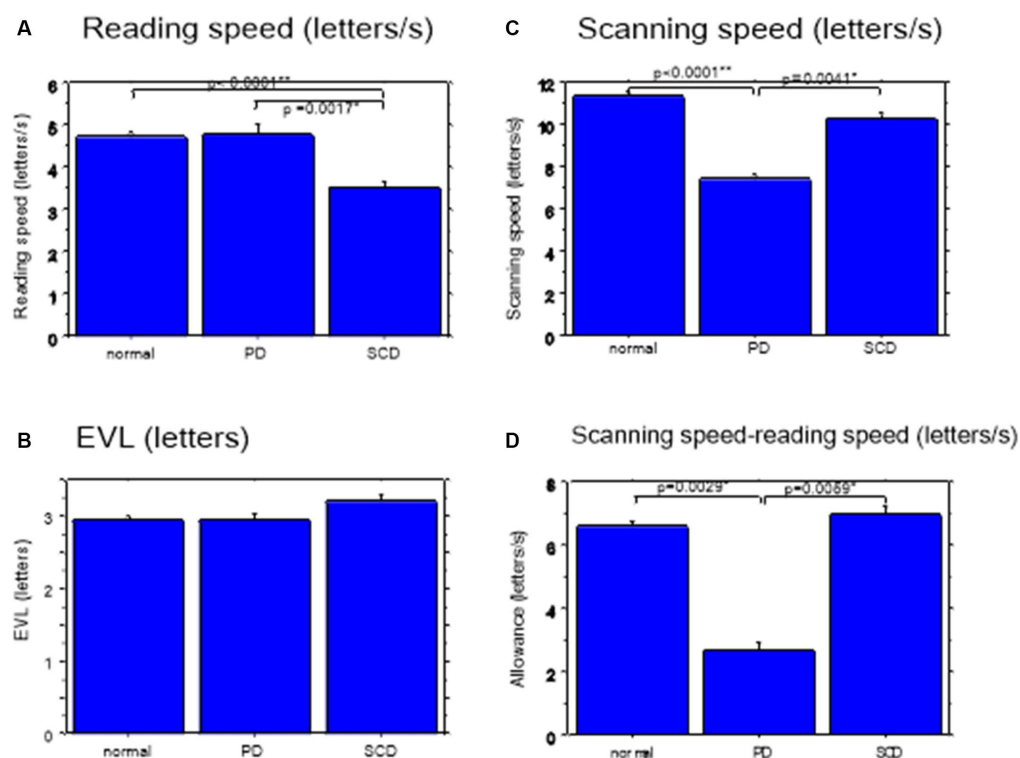


Figure 3_2

Texts 1-19

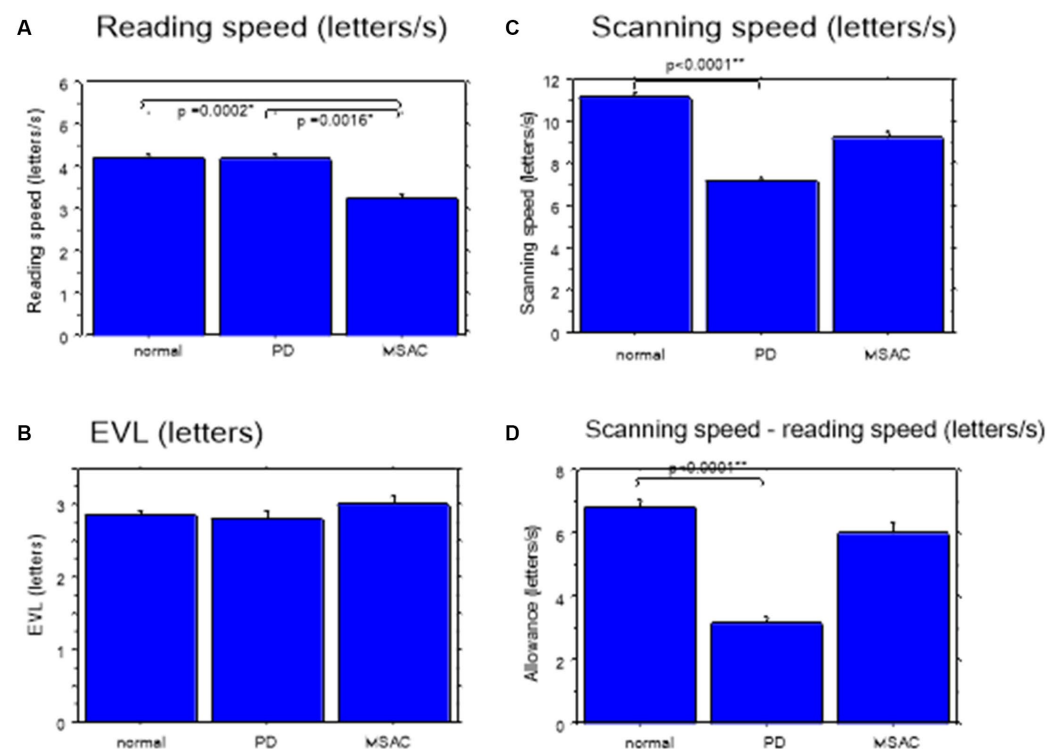


FIGURE 3

Reading parameters for reading texts in normal subjects, PD and SCD patients (text 1–19). (A) Reading speed (letters/s), (B) Eye-voice lead (EVL) (letters), (C) Scanning speed (letters/s), (D) Scanning speed-reading speed (letters/s). Normal: normal subjects, PD: patients with Parkinson's disease, SCD: patients with spinocerebellar degeneration. Error bars show standard errors. Asterisks indicate significant difference at * $p < 0.05$, or ** $p < 0.0001$.

(Continued)

FIGURE 3 (Continued)

3_2 (lower four figures): Reading parameters for reading texts in normal subjects, PD and MSAC patients (text 1–19). Similar figures with conventions as in Figure 3 when the analysis of SCD patients were restricted to MSAC patients. MSAC, multiple system atrophy cerebellar-type.

TABLE 5_2 Analysis of variance results for reading and saccade parameters with disease stage (analysis of SCD patients restricted to MSAC patients, texts 20–22).

Parameter	Group		Text		Group X Text	
	$F_{(2,110)}$	p	$F_{(2,110)}$	p	$F_{(4,220)}$	p
Reading velocity	$F = 12.147$	$p < 0.0001^{**}$	$F = 97.150$	$p < 0.0001^{**}$	$F = 14.926$	$p < 0.0001^{**}$
Saccade amplitude	$F = 1.782$	$p = 0.1781$	$F = 57.751$	$p < 0.0001^{**}$	$F = 2.082$	$p = 0.0881$
Saccade frequency	$F = 13.139$	$p < 0.0001^{**}$	$F = 0.564$	$p = 0.5705$	$F = 0.900$	$p = 0.4669$
Fixation duration	$F = 2.060$	$p = 0.1374$	$F = 4.872$	$p = 0.0094^{*}$	$F = 0.540$	$p = 0.7065$
Saccade duration	$F = 0.360$	$p = 0.6991$	$F = 0.868$	$p = 0.9346$	$F = 0.868$	$p = 0.4859$
Gaze duration	$F = 2.029$	$p = 0.1416$	$F = 4.552$	$p = 0.0130^{*}$	$F = 0.595$	$p = 0.6673$
Regression	$F = 1.644$	$p = 0.2027$	$F = 2.714$	$p = 0.0700$	$F = 1.306$	$p = 0.2723$
Scanning speed	$F = 9.204$	$p = 0.0004^{*}$	$F = 33.485$	$p < 0.0001^{**}$	$F = 2.057$	$p = 0.0917$
Scanning - reading speed	$F = 27.641$	$p < 0.0001^{**}$	$F = 34.086$	$p < 0.0001^{**}$	$F = 12.516$	$p < 0.0001^{**}$
Eye-voice lead (EVL)	$F = 3.296$	$p = 0.0454$	$F = 42.454$	$p < 0.0001^{**}$	$F = 5.563$	$p = 0.0004^{*}$
Variability of EVL	$F = 0.724$	$p = 0.4914$	$F = 21.063$	$p < 0.0001^{**}$	$F = 1.859$	$p = 0.1263$
Gaze duration/temporal EVL	$F = 2.116$	$p = 0.1314$	$F = 34.128$	$p < 0.0001^{**}$	$F = 5.735$	$p = 0.0003$

*Significance at $p < 0.05$; **Significance at $p < 0.0001$.

groups (Tables 4, 5 and Figures 3B, 4B; restricting the analysis of SCD patients to MSAC patients Tables 4_2, 5_2, Figures 3_2B, 4_2B). EVL, both spatial and temporal, did not correlate significantly with disease stage in either SCD or PD patients for any of the texts, except for texts 20–22 in SCD patients (Tables 6, 7). This significant correlation did not persist when the analysis of SCD patients were restricted to MSAC patients (right most columns in Tables 6, 7).

Except where line changes occurred, EVL was relatively stable during text reading. To assess the group differences, we studied the correlation between time and EVL. The slope of this correlation was not significantly different from 0 (slope: normal -0.26 ± 2.78 pixel/s, SCD -0.41 ± 1.8 pixel/s, PD -0.10 ± 0.80 pixel/s) and there were no differences in the slopes and intercept among subject groups (slope: effect of group: $F(2,124) = 0.252$, $p = 0.7788$; effect of text: $F(21,1302) = 3.271$, $p < 0.0001$, subject group X text: $F(42,2604) = 1.183$, $p = 0.2074$, intercept: effect of group: $F(2,124) = 0.060$, $p = 0.9416$; effect of text: $F(21,1302) = 4.696$, $p < 0.0001$, subject group X text: $F(42,2604) = 1.558$, $p = 0.0150$). The variability of EVL (standard deviation of EVL) across time was also similar for all groups across all texts, reflecting the overall similar EVL ($p > 0.05$) (not showed in Tables).

Gaze scanning the text sometimes involved regressive movements from right to left instead of proceeding progressively from left to right. Overall, the frequency of regression was significantly higher in SCD patients compared with normal subjects and PD patients for texts 1–19, but not for texts 20–22 (Tables 4, 5 and Figures 5F, 6F; *post hoc* analysis: texts 1–19: normal vs. SCD $p = 0.0120$; restricting the analysis to MSA patients Tables 4_2, 5_2; Figures 5_2F, 6_2F). The frequency of regression did not show significant correlation with

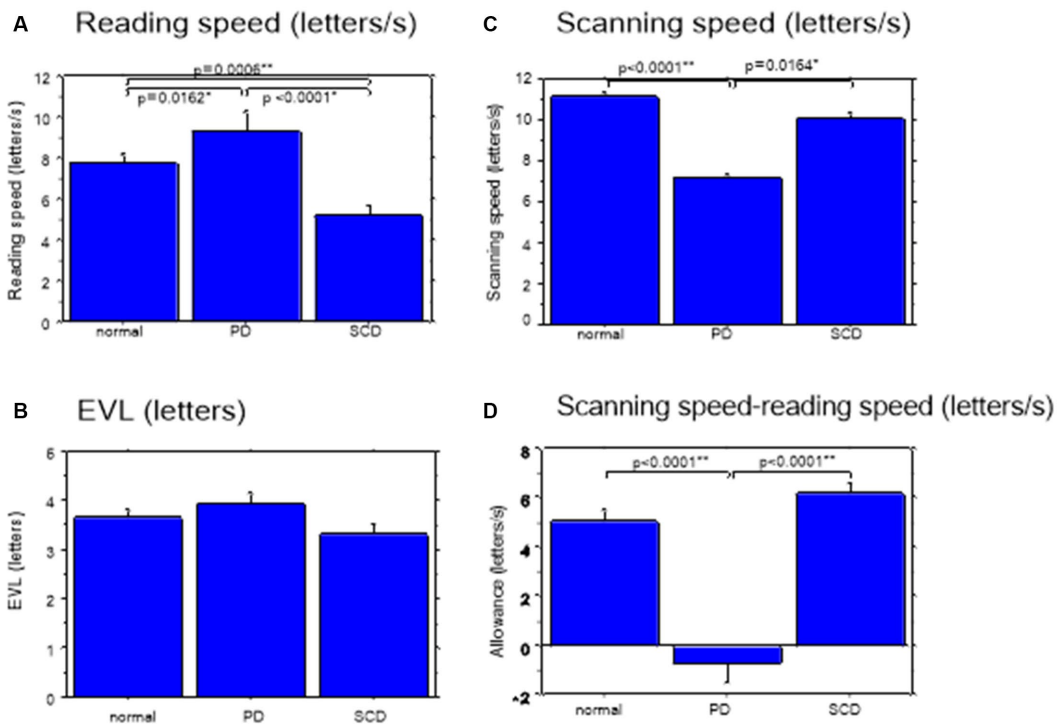
disease stage or UPDRS motor score in either SCD or PD patients (Tables 4, 5).

These regressive saccades may impair rather than help advance processing of the text ahead. Thus, we considered the product of saccade amplitude multiplied by the frequency of saccades per unit time as an index of the potential speed of gaze scanning the text (hereafter termed “scanning speed”). This measure would approximately reflect the overall slope of the blue curves in Figure 1, excluding regressions. The scanning speed was reduced in PD patients relative to normal subjects and SCD patients (Figures 3C, 4C, *post hoc* analysis: texts 1–19 normal vs. PD $p < 0.0001$, normal vs. SCD $p = 0.2342$, SCD vs. PD $p = 0.0041$; texts 20–22 normal vs. PD $p < 0.0001$, normal vs. SCD $p = 0.2227$, SCD vs. PD $p = 0.0164$; restricting the analysis to MSA patients Figures 3_2C, 4_2C). Scanning speed significantly decreased progressively with disease stage in SCD patients for texts 1–19, also showing a tendency to decrease with UPDRS motor score in PD patients not reaching statistical significance (Tables 6, 7). This significant correlation did not persist when the analysis of SCD patients were restricted to MSAC patients (right most columns in Tables 6, 7).

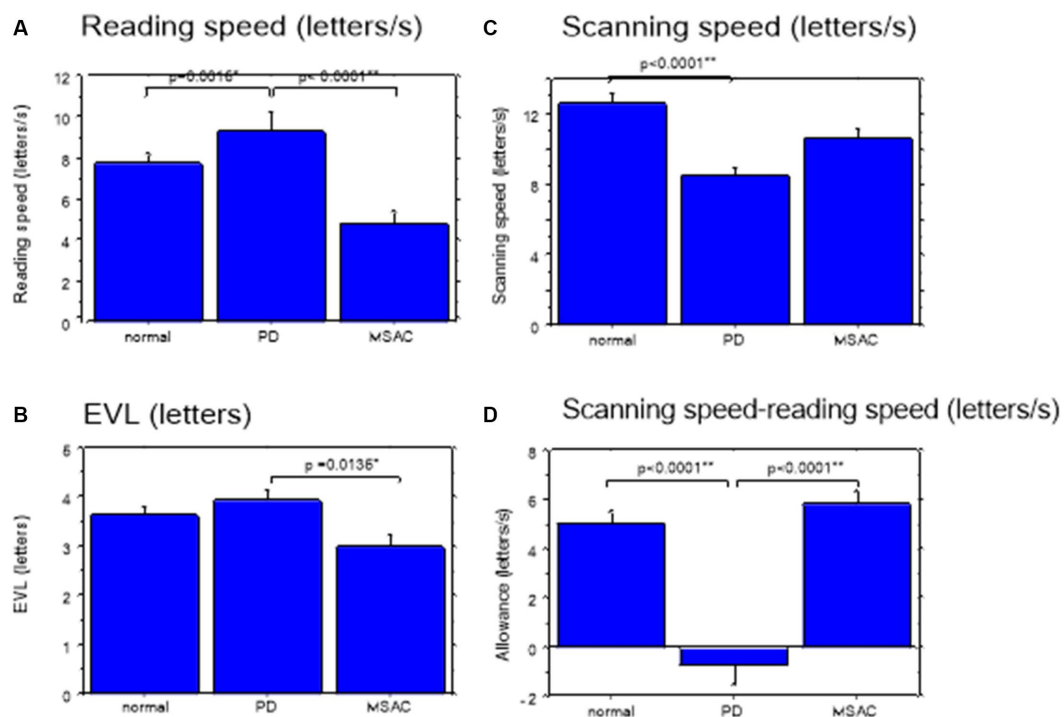
How much the gaze position scanning the text could potentially precede the uttered text position was calculated by subtracting reading speed from scanning speed, that is, the allowance for the gaze to precede the uttered word position. This measure was reduced in PD patients relative to normal subjects and SCD patients (Figures 3D, 4D; *post hoc* analysis: text 1–19 normal vs. PD $p = 0.0029$, normal vs. SCD $p = 0.8512$, SCD vs. PD $p = 0.0059$; text 1–20–22 normal vs. PD $p < 0.0001$, normal vs. SCD $p = 0.2447$, SCD vs. PD $p < 0.0001$). This significant difference was seen also when the analysis of SCD patients were restricted to MSAC

Figure 4

Texts 20–22

**Figure 4_2**

Texts 20–22

**FIGURE 4**

Reading parameters in normal subjects, PD and SCD patients (text 20–22). Similar figures with conventions as in Figure 3. (A) Reading speed (letters/s), (B) Eye–voice lead (EVL) (letters), (C) Scanning speed (letters/s), (D) Scanning speed–reading speed (letters/s). 4_2 (lower four figures): Reading parameters for reading texts in normal subjects, PD and MSAC patients (text 20–22). Similar figures with conventions as in Figure 4 when the analysis of SCD patients were restricted to MSAC patients. MSAC, multiple system atrophy cerebellar-type.

TABLE 6 Statistical results for the correlation analyses between saccade parameters and disease stage (texts 1–19).

Parameters	PD		SCD		MSAC	
	<i>r</i>	<i>p</i>	<i>r</i>	<i>p</i>	<i>r</i>	<i>p</i>
Reading speed	<i>r</i> = −0.334	<i>p</i> = 0.1648	<i>r</i> = −0.571	<i>p</i> = 0.0246*	<i>r</i> = 0.775	<i>p</i> = 0.0211*
Saccade amplitude	<i>r</i> = −0.333	<i>p</i> = 0.1659	<i>r</i> = −0.484	<i>p</i> = 0.0670	<i>r</i> = 0.135	<i>p</i> = 0.7613
Saccade duration	<i>r</i> = −0.393	<i>p</i> = 0.0965	<i>r</i> = 0.144	<i>p</i> = 0.6161	<i>r</i> = 0.019	<i>p</i> = 0.9660
Fixation duration	<i>r</i> = 0.347	<i>p</i> = 0.1479	<i>r</i> = 0.495	<i>p</i> = 0.0599	<i>r</i> = 0.225	<i>p</i> = 0.6095
Gaze duration	<i>r</i> = −0.180	<i>p</i> = 0.4658	<i>r</i> = 0.597	<i>p</i> = 0.0170*	<i>r</i> = 0.234	<i>p</i> = 0.5934
Saccade frequency	<i>r</i> = −0.258	<i>p</i> = 0.2901	<i>r</i> = −0.425	<i>p</i> = 0.1161	<i>r</i> = 0.038	<i>p</i> = 0.9323
Scanning speed (saccade amplitude × saccade frequency)	<i>r</i> = −0.416	<i>p</i> = 0.0465	<i>r</i> = −0.649	<i>p</i> = 0.0073*	<i>r</i> = 0.178	<i>p</i> = 0.6872
Frequency of regression	<i>r</i> = 0.469	<i>p</i> = 0.0418	<i>r</i> = −0.241	<i>p</i> = 0.3951	<i>r</i> = 0.577	<i>p</i> = 0.1413
Eye–voice lead (EVL)	<i>r</i> = 0.208	<i>p</i> = 0.3993	<i>r</i> = −0.208	<i>p</i> = 0.4636	<i>r</i> = 0.078	<i>p</i> = 0.8618
Eye–voice lead (temporal EVL)	<i>r</i> = 0.418	<i>p</i> = 0.0847	<i>r</i> = 0.092	<i>p</i> = 0.7494	<i>r</i> = 0.545	<i>p</i> = 0.1344
Gaze duration/temporal EVL	<i>r</i> = −0.363	<i>p</i> = 0.1284	<i>r</i> = −0.024	<i>p</i> = 0.9343	<i>r</i> = −0.662	<i>p</i> = 0.0750

*Significance at *p* < 0.05.

TABLE 7 Statistical results for the correlation analyses between saccade parameters and disease stage (texts 20–22).

Parameters	PD		SCD		MSAC	
	<i>r</i>	<i>p</i>	<i>r</i>	<i>p</i>	<i>r</i>	<i>p</i>
Reading speed	<i>r</i> = −0.274	<i>p</i> = 0.2757	<i>r</i> = −0.593	<i>p</i> = 0.0236*	<i>r</i> = −0.317	<i>p</i> = 0.4636
Saccade amplitude	<i>r</i> = −0.416	<i>p</i> = 0.0860	<i>r</i> = −0.352	<i>p</i> = 0.2232	<i>r</i> = 0.184	<i>p</i> = 0.6767
Saccade duration	<i>r</i> = −0.067	<i>p</i> = 0.7953	<i>r</i> = 0.344	<i>p</i> = 0.2349	<i>r</i> = 0.252	<i>p</i> = 0.5650
Fixation duration	<i>r</i> = −0.192	<i>p</i> = 0.4508	<i>r</i> = −0.057	<i>p</i> = 0.8511	<i>r</i> = 0.320	<i>p</i> = 0.4584
Gaze duration	<i>r</i> = −0.132	<i>p</i> = 0.6066	<i>r</i> = 0.153	<i>p</i> = 0.6083	<i>r</i> = 0.362	<i>p</i> = 0.3966
Saccade frequency	<i>r</i> = 0.010	<i>p</i> = 0.9684	<i>r</i> = −0.339	<i>p</i> = 0.2418	<i>r</i> = −0.024	<i>p</i> = 0.9581
Scanning speed (saccade amplitude × saccade frequency)	<i>r</i> = −0.340	<i>p</i> = 0.1696	<i>r</i> = −0.456	<i>p</i> = 0.1025	<i>r</i> = 0.170	<i>p</i> = 0.7009
Frequency of regression	<i>r</i> = 0.357	<i>p</i> = 0.1476	<i>r</i> = −0.241	<i>p</i> = 0.3951	<i>r</i> = 0.623	<i>p</i> = 0.1028
Eye–voice lead (spatial EVL)	<i>r</i> = 0.131	<i>p</i> = 0.6101	<i>r</i> = −0.606	<i>p</i> = 0.0199*	<i>r</i> = −0.368	<i>p</i> = 0.3886
Eye–voice lead (temporal EVL)	<i>r</i> = 0.404	<i>p</i> = 0.0967	<i>r</i> = −0.110	<i>p</i> = 0.7028	<i>r</i> = −0.277	<i>p</i> = 0.4852
Gaze duration/temporal EVL	<i>r</i> = −0.422	<i>p</i> = 0.0718	<i>r</i> = 0.069	<i>p</i> = 0.8183	<i>r</i> = 0.105	<i>p</i> = 0.8138

*Significance at *p* < 0.05.

patients (Figures 3_2D, 4_2D). This implied that the potential scanning position of gaze led the uttered voice position in SCD patients and normal subjects more evidently than in PD patients.

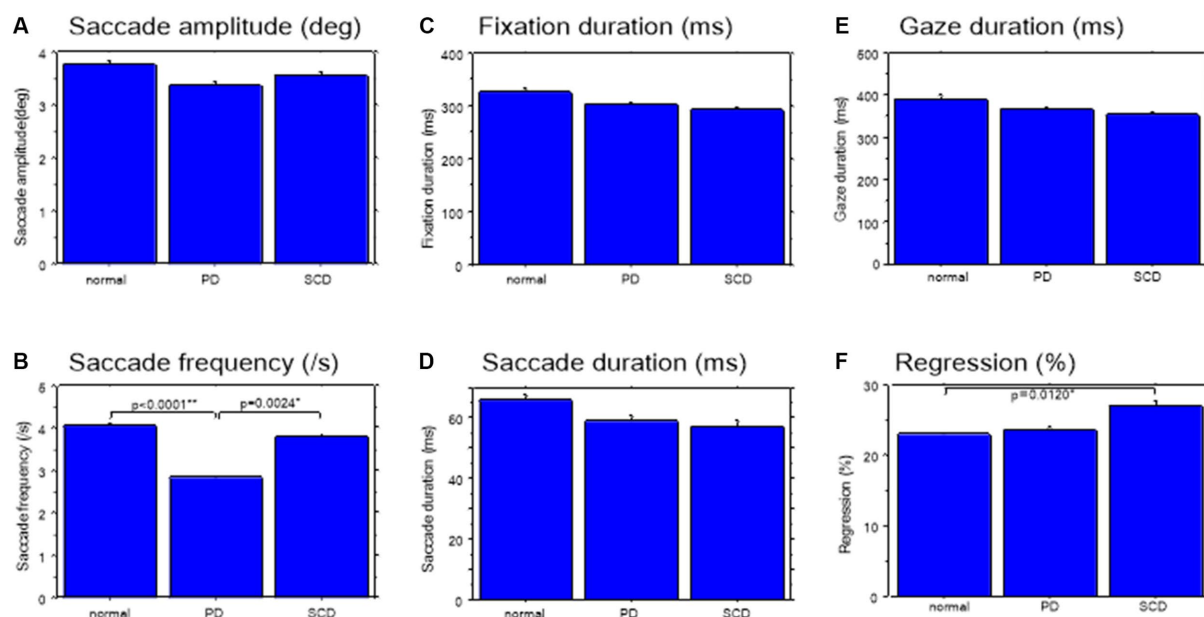
Reading and scanning speeds as a function of text readability

We studied how the reading and saccade parameters changed with varying text readability (Tables 4, 5; restricting the analysis to MSA patients Tables 4_2, 5_2). Reading speed, as expected, decreased significantly with decreasing text readability (text becoming difficult to read) (Figures 7A, 8A; restricting the analysis to MSA patients Figures 7_2A, 8_2A). There was a significant interaction between subject group and text, reflecting the finding that, compared to PD patients and normal subjects, the reading speed of SCD patients was slower, especially for texts that were relatively easy-to-read and could be read faster (Tables 4, 5; restricting the analysis to MSA patients Tables 4_2, 5_2). In contrast, reading speed of PD patients was comparable to normal subjects for all texts (*p* = 0.6407), except for text 22, a Japanese syllabary.

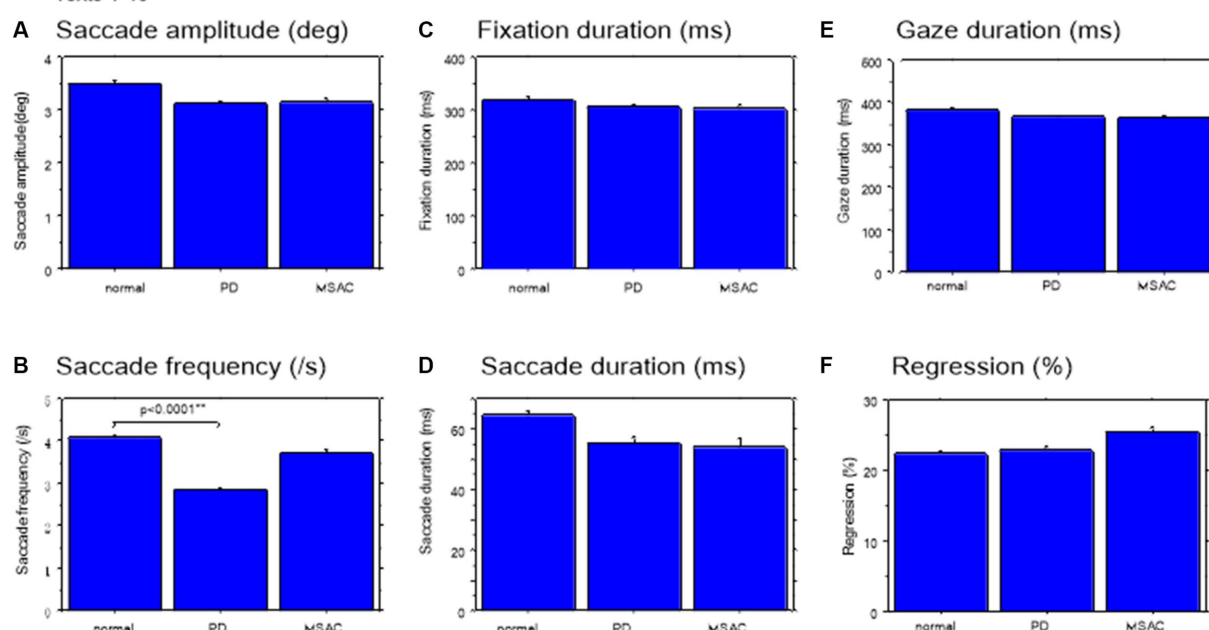
Saccade amplitude reliably decreased as the text became difficult to read, but was statistically comparable among the three groups, and the interaction between subject group and text readability did not reach significance (Figures 9A, 10A; Tables 4, 5; restricting the SCD analysis to MSA patients Figures 9_2A, 10_2A; Tables 4_2, 5_2). Saccade frequency also significantly decreased for text 20–22 as text became difficult to read (text readability decreased; Figures 9B, 10B; restricting the analysis to MSA patients Figures 9_2B, 10_2B), and was consistently smaller in PD patients than in the other two groups across all text readability. Scanning speed decreased with increasing text readability, and was reduced in PD and SCD patients relative to normal subjects (Figures 7B, 8B; restricting the SCD analysis to MSA patients Figures 7_2B, 8_2B). The allowance of scanning speed minus the reading speed was smallest for PD patients than in normal controls and SCD patients for all texts (Figures 7C_2C, 8C_2C). Fixation, saccade, and gaze durations varied slightly across text readability but were comparable among different subject groups for all texts (Figures 9C,D,E, 10C,D,E; restricting the analysis to MSA patients Figures 9_2C,D,E, 10_2C,D,E). The proportion of regressive saccades was slightly higher in SCD patients across all text readability than in

Figure 5

Texts 1–19

**Figure 5_2**

Texts 1–19

**FIGURE 5**

Saccade parameters during reading in normal subjects, PD and SCD patients (text 1–19). (A) Saccade amplitude (deg), (B) Saccade frequency (/s), (C) Fixation duration (ms), (D) Saccade duration (ms), (E) Gaze duration (ms), (F) Proportion of regressive saccades (%). Normal: normal subjects, PD: patients with Parkinson's disease, SCD: patients with spinocerebellar degeneration. Error bars show standard errors. Asterisks indicate significant difference at $*p < 0.05$. 5_2: (lower two rows) Saccade parameters during reading in normal subjects, PD and MSAC patients (text 1–19). Similar figures with conventions as in Figure 5 when the analysis of SCD patients were restricted to MSAC patients. MSAC, multiple system atrophy cerebellar-type.

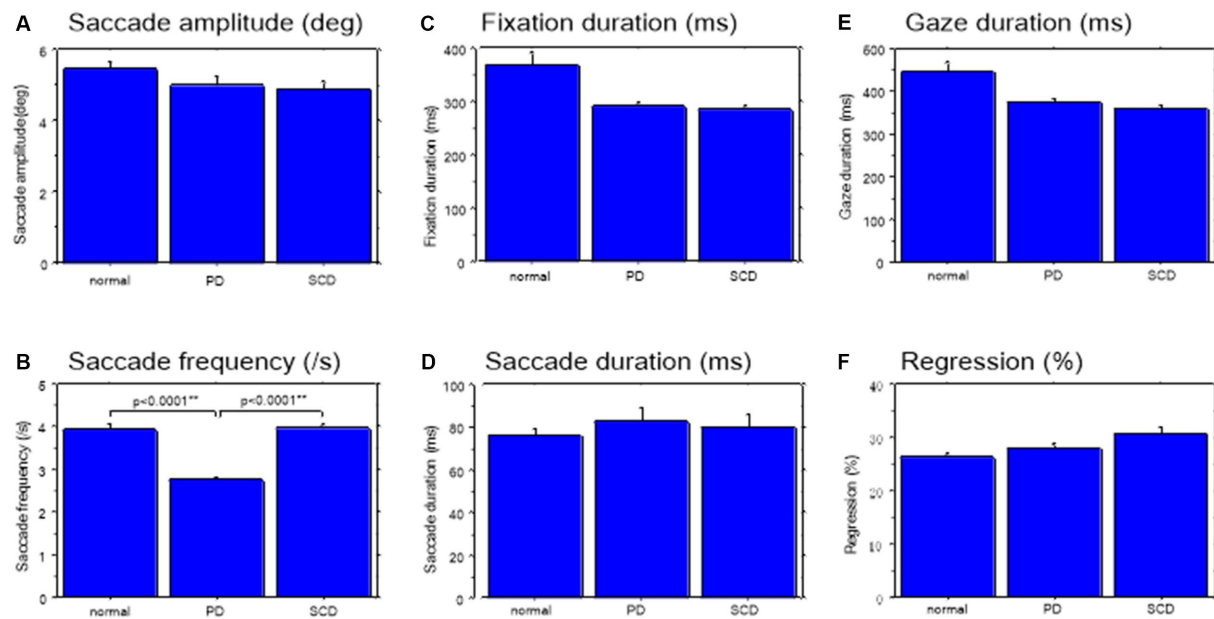
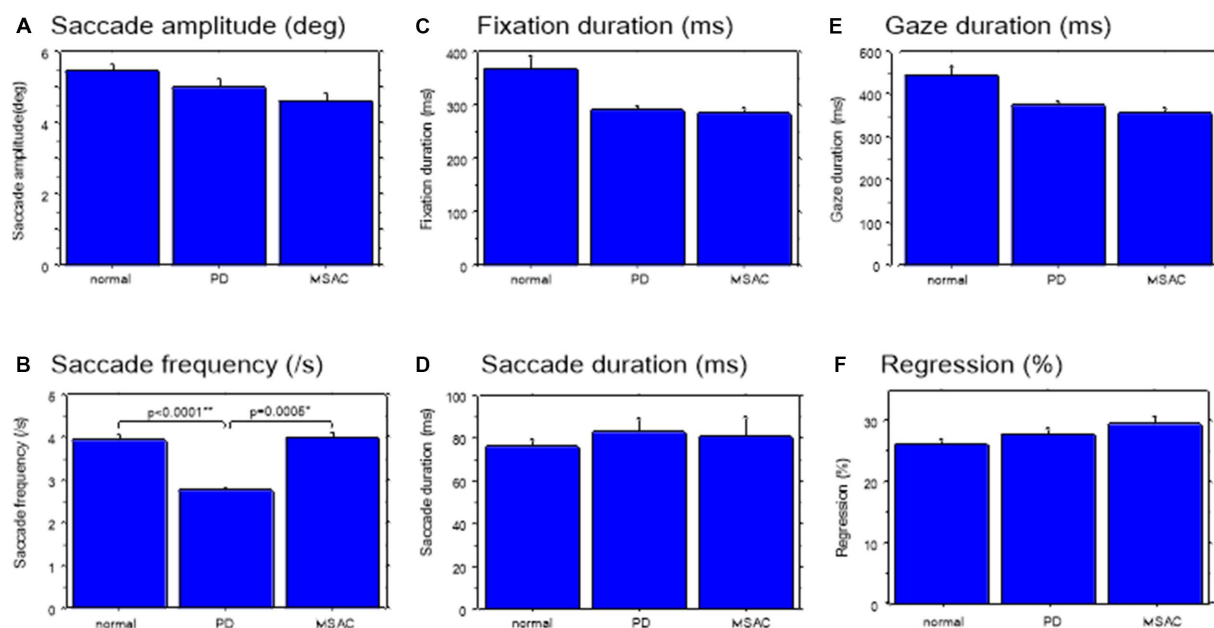
normal subjects and PD patients, and decreased with decreasing readability of the text, with no significant difference between groups (Figures 9F, 10F; Tables 4, 5; restricting the SCD analysis to MSA patients Figures 9_2F, 10_2F; Tables 4_2, 5_2). The gaze would go well ahead of the uttered text for texts that were difficult to read, such that regression occurred only infrequently to compensate for this.

EVL as an index of text readability and advance text processing

EVL became smaller as the text became more difficult to read (Tables 4, 5; restricting the SCD analysis to MSA patients Tables 4_2, 5_2). As the readability decreased and the reading speed was reduced,

Figure 6

Texts 20–22

**Figure 6_2****FIGURE 6**

Saccade parameters during reading in normal subjects, PD and SCD patients (texts 20–22). Similar figures with conventions as in Figure 4. (A) Saccade amplitude (deg), (B) Saccade frequency (/s), (C) Fixation duration (ms), (D) Saccade duration (ms), (E) Gaze duration (ms), (F) Proportion of regressive saccades (%). Error bars show standard errors. Asterisks indicate significant difference at $p < 0.05$. 6_2 (lower two rows): Saccade parameters during reading in normal subjects, PD and MSAC patients (text 20–22). Similar figures with conventions as in Figure 6 when the analysis of SCD patients were restricted to MSAC patients. MSAC, multiple system atrophy cerebellar-type.

EVL also decreased. There was a significant interaction between groups and text for texts 20–22. This indicated that, although overall EVL was comparable among the three subject groups for most texts, with the exception of text 22 (Japanese syllabary), for which EVL was smaller in SCD patients in comparison to PD patients and normal subjects (Figures 7_2D, 8D; restricting the SCD analysis to MSA patients Figures 7, 8_2D).

EVL has been shown to correlate with reading speed, which is related to the automaticity or speed of reading (see Introduction). Conversely, EVL decreases with increasing text difficulty or decreasing text readability. Across different subject groups, EVL showed a moderate to strong correlation with reading velocity across text readability and across all texts (normal $r = 0.79 \pm 0.02$, SCD $r = 0.78 \pm 0.04$, PD $r = 0.64 \pm 0.08$; Figure 11A). The slopes of this correlation (reading speed

Figure 7

Texts 1-19

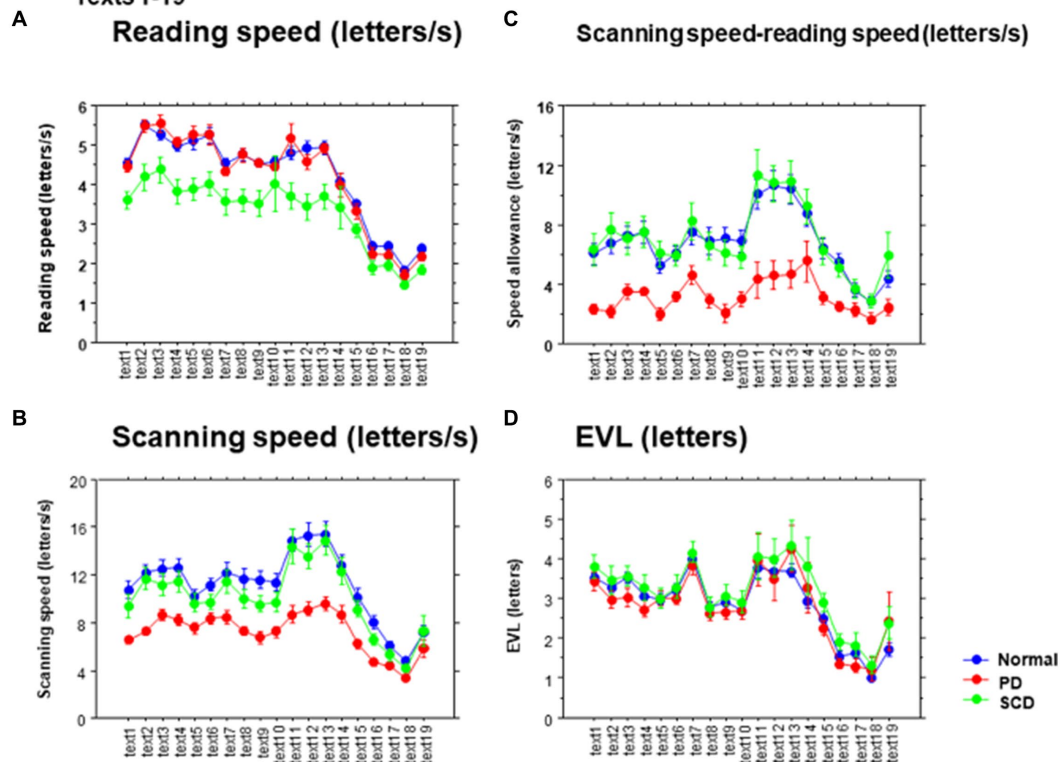


Figure 7_2

Texts 20-22

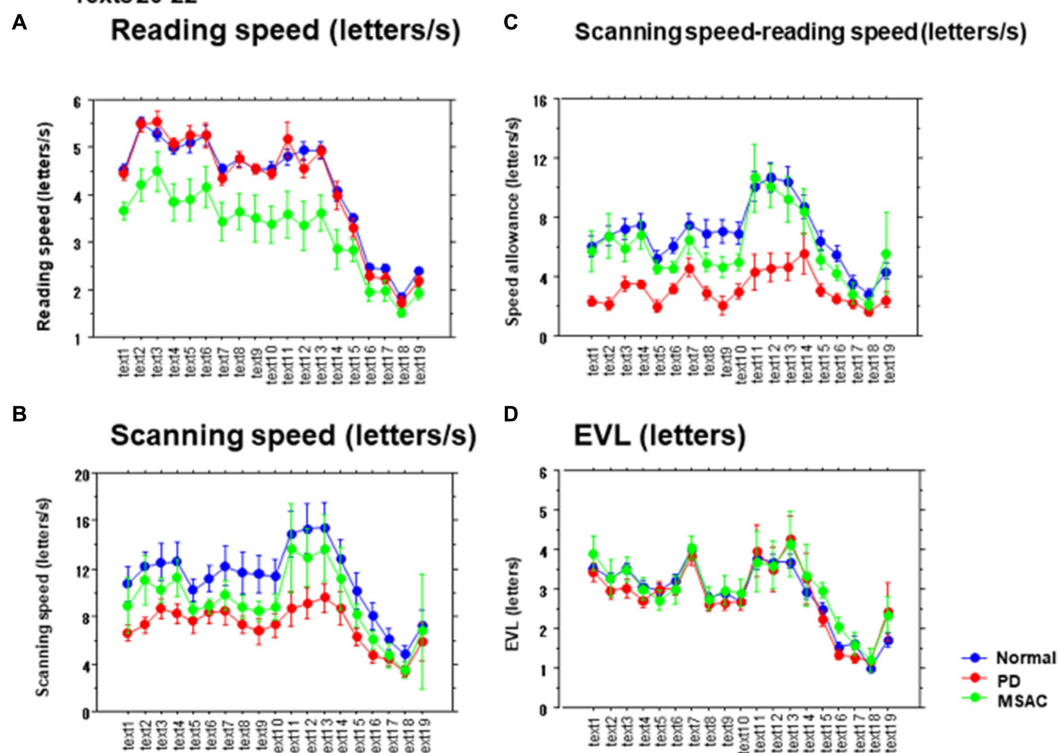
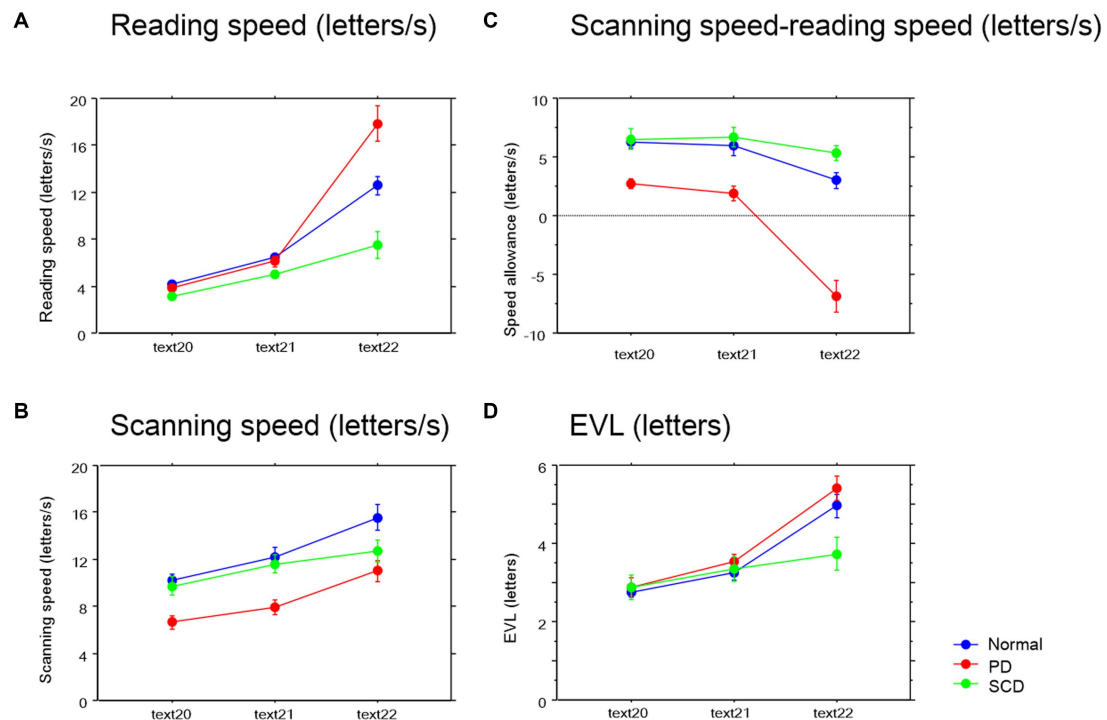


FIGURE 7

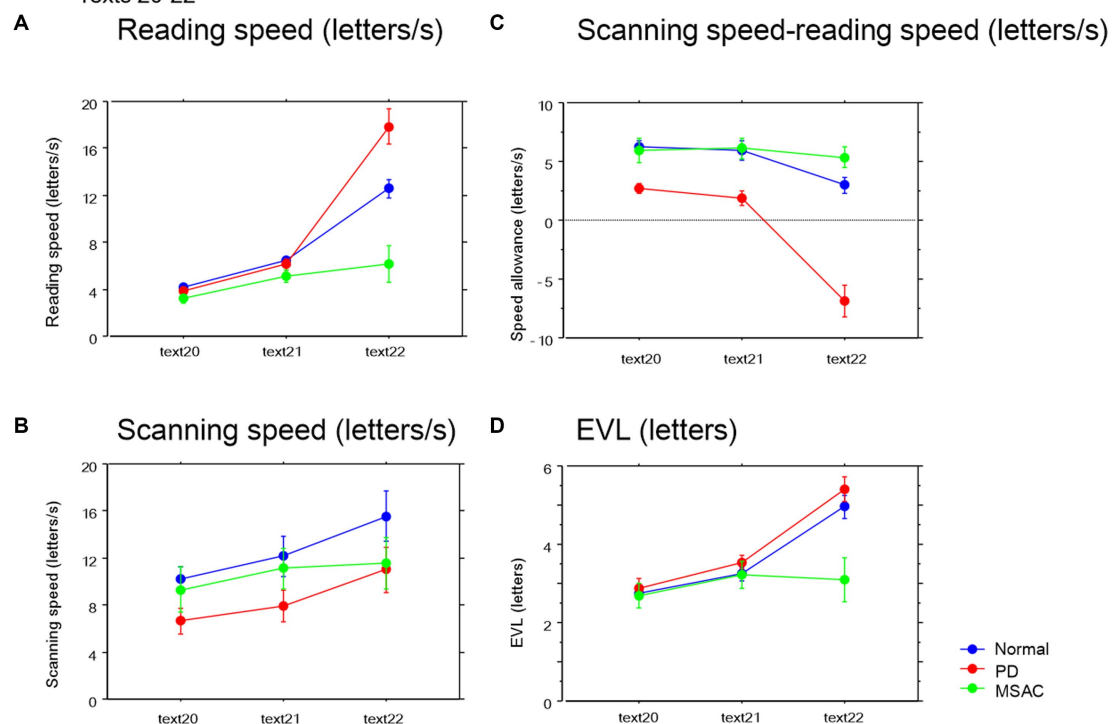
Reading parameters as a function of text readability (texts 1–19). (A) Reading speed (letters/s), (B) Scanning speed (letters/s), (C) Scanning speed-reading speed (letters/s), (D) Eye–voice lead (EVL, letters). Normal: normal subjects; PD: patients with Parkinson's disease; SCD: patients with spinocerebellar degeneration. Text readability decreases from left to right along the ordinate. Error bars show standard errors. **7_2** (lower four figures): Reading parameters as a function of text readability (text 1–19). Similar figures with conventions as in Figure 7 when the analysis of SCD patients were restricted to MSAC patients. MSAC, multiple system atrophy cerebellar-type.

Figure 8

Texts 20–22

**Figure 8_2**

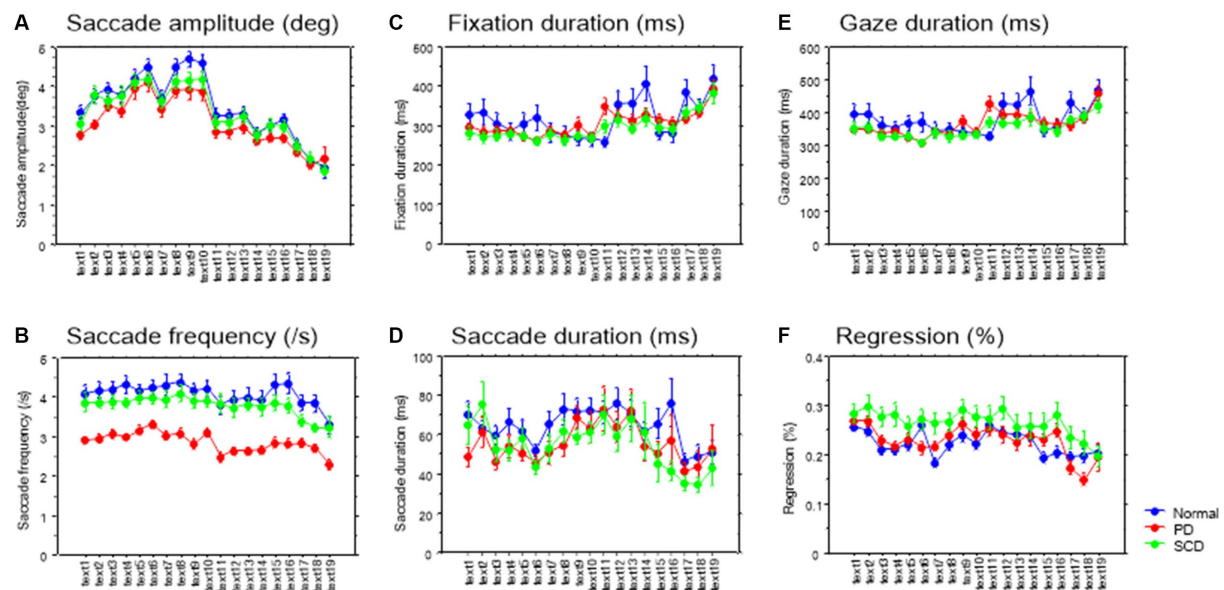
Texts 20–22

**FIGURE 8**

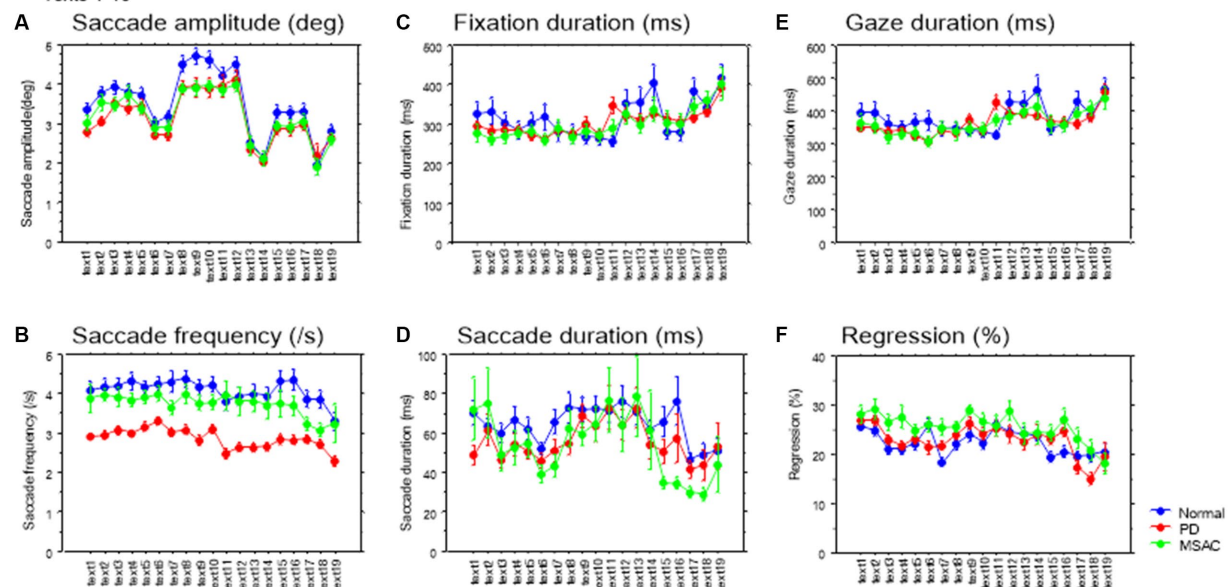
Reading parameters as a function of text readability (texts 20–22). Similar figures with conventions as in Figure 6. (A) Reading velocity (letters/s), (B) Scanning speed (letters/s), (C) Scanning speed-reading speed (letters/s), (D) Eye-voice lead (EVL, letters). **8_2** (lower four figures): Reading parameters as a function of text readability (text 20–22). Similar figures with conventions as in Figure 8 when the analysis of SCD patients were restricted to MSAC patients. MSAC, multiple system atrophy cerebellar-type.

Figure 9

Texts 1–19

**Figure 9_2**

Texts 1–19

**FIGURE 9**

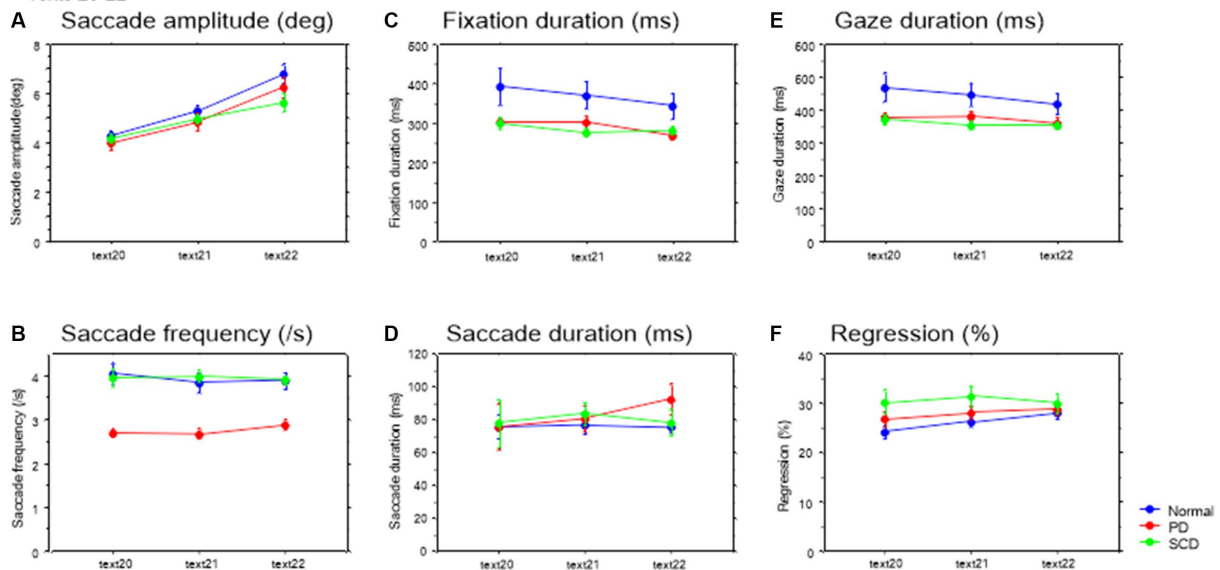
Saccade parameters as a function of text readability (texts 1–19). (A) Saccade amplitude (deg), (B) Saccade frequency (/s), (C) Fixation duration (ms), (D) Saccade duration (ms), (E) Gaze duration (ms), (F) Proportion of regressive saccades (%). Normal: normal subjects; PD: patients with Parkinson's disease; SCD: patients with spinocerebellar degeneration. Text readability decreases from left to right along the ordinate. Error bars show standard errors. **9_2** (lower row): Saccade parameters as a function of text readability (text 1–19). Similar figures with conventions as in Figure 9 when the analysis of SCD patients were restricted to MSAC patients. MSAC, multiple system atrophy cerebellar-type.

vs. spatial EVL) was small in SCD patients compared to normal subjects, but was comparable for PD patients and normal subjects (Figure 11B). This trend persisted when restricting the analysis of SCD patients to MSAC patients, although the difference between normal vs. SCD and PD vs. SCD failed to reach significance (Figure 11_2A; effect of group: $F(2,124) = 4.261$, $p = 0.0189$; *post hoc* analysis normal vs. SCD $p = 0.0057$, normal vs. PD $p = 0.6256$). Meanwhile, the intercept of the correlation was significantly higher for PD patients than for SCD patients and normal subjects across all texts (Figure 11C). The same was true when restricting the SCD patients to MSAC patients, although again, the

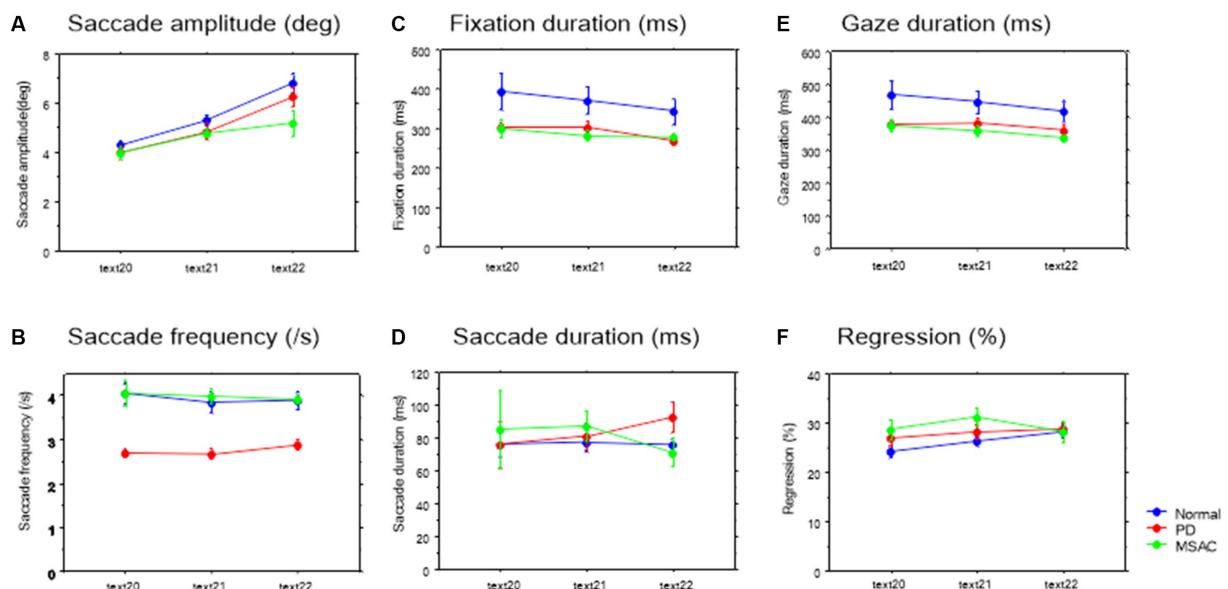
difference between normal vs. SCD and PD vs. SCD failed to reach significance (Figure 11_2B; effect of group: $F(2,124) = 4.887$, $p = 0.0109$; *post hoc* analysis normal vs. PD $p = 0.0033$, PD vs. SCD $p = 0.0055$). This suggested that, in PD patients, reading speed was faster already at a small EVL, but they improved by a smaller amount with increasing EVL compared to normal subjects. In SCD patients, reading speed was comparable to normal subjects at smaller EVL levels, but again improved by a similar amount with increasing EVL than in normal subjects. As a result, the reading speed of SCD patients was smaller for all text readability than the other two groups.

Figure 10

Texts 20–22

**Figure 10_2**

Texts 20–22

**FIGURE 10**

Saccade parameters as a function of text readability (texts 20–22). Similar figures with conventions as in Figure 8. (A) Saccade amplitude (deg),

(B) Saccade frequency (/s), (C) Fixation duration (ms), (D) Saccade duration (ms), (E) Gaze duration (ms), (F) Proportion of regressive saccades (%). **10_2** (lower row): Saccade parameters as a function of text readability (text 20–22). Similar figures with conventions as in Figure 10 when the analysis of SCD patients were restricted to MSAC patients. MSAC, multiple system atrophy cerebellar-type.

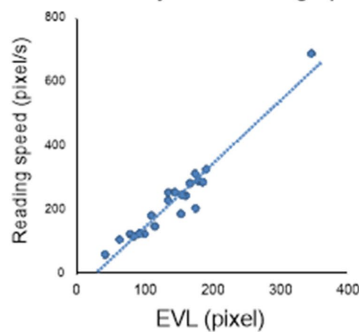
The ratio of gaze duration/temporal EVL, a measure reflecting the weight of different processing stages (gaze-dependent vs. gaze-independent) within the onset EVS (Silva et al., 2016; see *Data Processing* section in the Methods), and thus the degree of parallel processing of the currently fixated word with the following word, was significantly smaller in SCD patients compared to other groups of subjects, while the difference between PD and SCD patients reached a trend but failed to reach significance for texts 1–19. This indicated lesser gaze-dependent factor in SCD patients (Figure 12; *post hoc* analysis: texts 1–19: normal vs. SCD $p=0.0043$, SCD vs. PD $p=0.0293$, texts 20–22: normal vs. SCD $p=0.0127$). However, the difference between normal subjects and MSAC

patients and between PD and MSAC patients did not reach significance when restricting the SCD patients to MSAC patients (Figure 12_2).

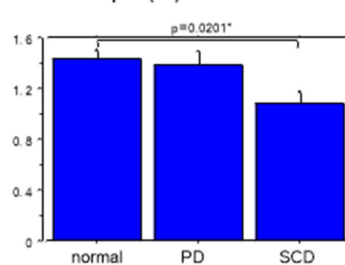
Discussion

Eye–voice coordination in reading aloud in normal subjects

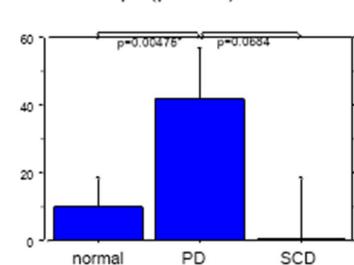
When Japanese texts are read aloud by normal subjects, the gaze position in the text is consistently located spatially before the reading

Figure 11**A** Correlation between text readability and reading speed**Figure 11_2****B**

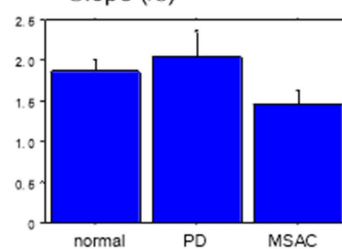
Slope (/s)

**C**

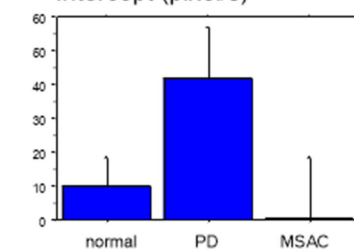
Intercept (pixel/s)

**A**

Slope (/s)

**B**

Intercept (pixel/s)

**FIGURE 11**

Slope and intercept of the linear correlation for reading speed as a function of EVL in the three groups of subjects. (A) Typical plot showing the correlation between spatial EVL (in pixels) and reading speed in a normal subject. (B) Slope, (C) Intercept of this correlation in different subject groups. Error bars show standard errors. Normal: normal subjects; PD: patients with Parkinson's disease; SCD: patients with spinocerebellar degeneration. Asterisks indicate significant difference at $*p < 0.05$. **11_2** (lower two figures): Slope and intercept of the linear correlation for reading speed as a function of EVL in the three groups of subjects. Similar figures with conventions as in [Figure 11](#) when the analysis of SCD patients were restricted to MSAC patients. (A) Slope, (B) Intercept of this correlation in different subject groups. MSAC, multiple system atrophy cerebellar-type.

position by about 1 to 4 letters for all groups studied (spatial EVL). This is in contrast to the findings of [Buswell \(1921\)](#) and [De Luca et al. \(2013\)](#) in Western languages, where the EVL was reported to be between 12 and 18 letters. The discrepancy in EVL may be attributed to the difference between Western and Japanese writing systems. Japanese writing consists of a combination of hiragana (phonograms) and Chinese characters, with each phonogram generally corresponding to two or more letters in Western languages, and even more letters for Chinese characters. Additionally, Japanese texts typically do not have spaces between words. On the other hand, the temporal EVL, which refers to the time lag between gaze and reading position, is approximately 0.5–1.0 s ahead, consistent with previous findings in Western languages (as observed by [Inhoff et al., 2011](#)).

Even in the absence of the explicit segmentation of words and spaces in between in Japanese texts, stable eye-voice correlation with similar spatial and temporal EVL was observed for texts that consisted only or predominantly of hiragana, or texts consisting a mixture of hiragana and Chinese characters, with the latter possibly serving as a marker for the beginning of a word.

EVL was relatively stable throughout the texts, except where line changes took place, but varied depending on the overall readability of each text [text grade ([Table 2](#))]. As the text became difficult to read (i.e., text grade increased), both the reading speed and the spatial EVL decreased and there was a significant correlation between them, consistent with previous reports that text reading automaticity

correlates with text reading speed ([Silva et al., 2016](#)); enlarging EVL would serve to leverage the reading speed.

[Laubrock and Kliegl \(2015\)](#) suggested that the changes in text scanning speed with text difficulty are primarily modulated by saccade amplitude rather than saccade frequency, since saccade frequency remains relatively stable across different texts. In our study, when the reading speed is significantly slowed, individuals' gaze almost remained fixated at a similar position or even make regressive eye movements toward the left. This occurred in texts in which graphemes were arranged in a randomized order, limiting the ability to process the text ahead of the gaze or chunk it into words or phrases. In such cases, the average reading speed dropped to 1.2–2.3 letters, whereas for other texts, it ranged from 2.3 to 3.7 letters. Even in these difficult texts, reading approached, if not reached, a "letter by letter" level, in which EVL is reduced down to a single letter level ([Figure 8](#)).

Reading speed in PD and SCD patients

According to [Figure 2](#), the reading position over time showed a flatter slope for SCD patients compared to the other two groups. This indicates that SCD patients exhibited a slower reading speed regardless of the readability of the text. The slower reading speed can be attributed to the impact on vocal output processing, affecting articulation in these patients. Even when presented with texts that had spaced intervals, such as text 22, SCD patients were unable to increase

Figure 12

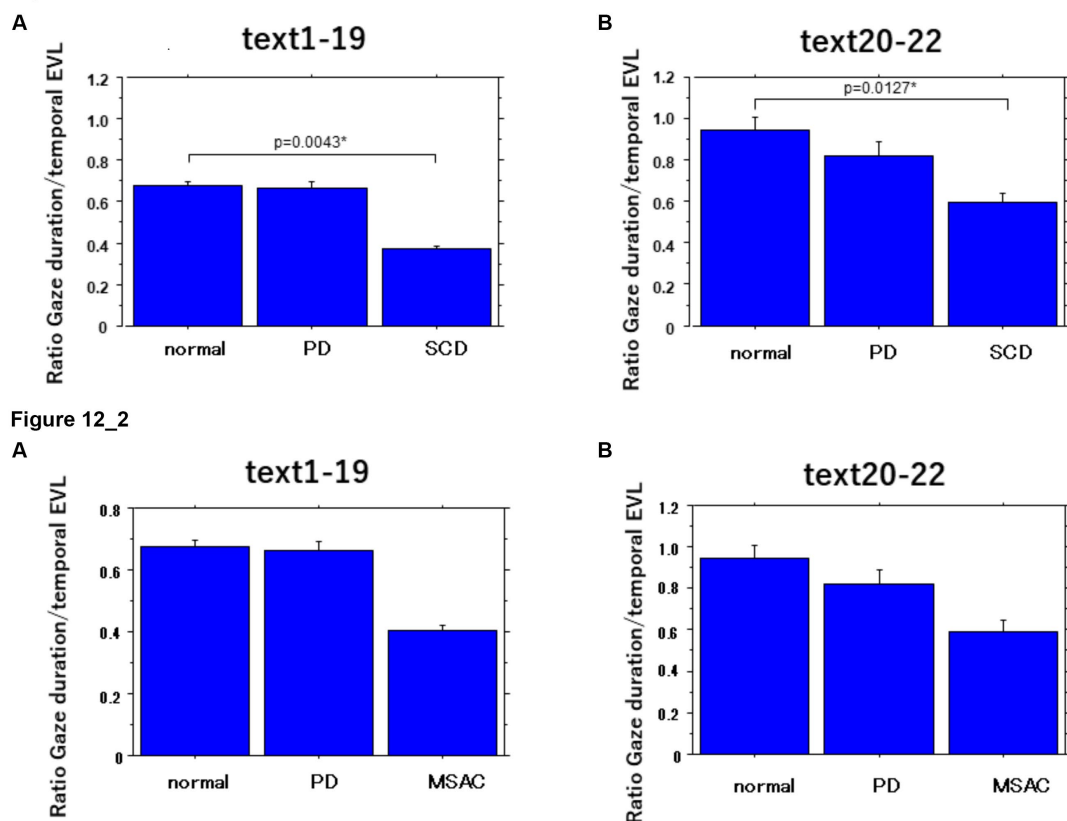


FIGURE 12

Ratio of gaze duration to temporal EVL in the three subject groups. Error bars show standard errors. Normal: normal subjects; PD: patients with Parkinson's disease; SCD: patients with spinocerebellar degeneration. Asterisks indicate significant difference at $*p < 0.05$. **12_2** (lower two figures): Ratio of gaze duration to temporal EVL in the three subject groups. Similar figures with conventions as in Figure 12 when the analysis of SCD patients were restricted to MSAC patients. MSAC, patients with spinocerebellar degeneration.

their reading speed to match those of normal subjects or PD patients. Additionally, the reading speed in SCD patients decreased as the severity of the disease progressed.

We expected the reading speed of PD patients to be slowed as well, considering the bradykinesia observed in these patients. However, reading speed was actually comparable or even be slightly more accelerated compared to normal subjects for texts with spaced intervals between words or phonograms (texts 20–22), nor did it decline with disease stage. Parkinsonian speech is characterized by hypophonia and dysprosody, sometimes with hastening, which worsens with disease progression, but not with slowness of vocal output (Skodda and Schlegel, 2008; Waldthaler et al., 2018; Stock et al., 2020).

Interaction between text scanning speed and reading speed in PD and SCD patients

How does the altered gaze behavior in PD and SCD patients affect the eye–voice coordination during reading? In SCD patients, the speed of gaze scanning the text, excluding regressions, was only slightly slower than normal, contrasting with the reading speed that was much slower. As a result, the gaze could sometimes go well ahead of the voice, especially at the beginning of texts, such that regressions occurred frequently to keep pace with the slowly proceeding voice for

most texts. Frequent occurrence of regressions may hamper advance text processing ahead of the gaze, degrading the visual input, and may lead to various reading impairments in SCD, such as letter reversals (adjacent, non-adjacent), letter insertion, word omission, addition, and verbal substitution (Moretti et al., 2002, 2003a,b). During visual search, patients with hereditary pure cerebellar ataxia exhibit a larger number of repeated fixations (re-fixations) of the target compared with normal subjects, because SCD patients may be unable to properly process and interpret what they are seeing on the first try (Matsuda et al., 2014).

Silva et al. (2016) reported a higher weight of different processing stages (gaze-dependent vs. gaze-independent) within the onset EVS, with a higher ratio associated with more weight in the gaze-dependent process. Namely, a higher ratio indicated more contribution of the parallel processing of words N (word fixated) and $N+1$ (word to the right of the word fixated) to the complete processing (naming latency) of a given word N . In our study, the ratio of gaze duration to temporal EVL was lowest for SCD patients compared to the other two subject groups. This suggests that less parallel processing was taking place in SCD patients with less weight in the gaze-dependent process.

In contrast, PD patients exhibited almost normal reading speed. The frequency of saccades was significantly reduced in PD patients compared to normal subjects and SC patients, leading to significantly

lower scanning speed. This may represent an oculomotor correlate of akinesia/bradykinesia. Consequently, the scanning speed of PD patients, on average, barely exceeded the reading speed in PD patients for all texts, and could not speed up further. The allowance for scanning gaze to precede the reading position was thus smaller for these patients, even for easy-to-read texts. Frequently, the gaze of PD patients scanning the text would even lag behind the read position of the text (Figure 1). The ratio of gaze duration to temporal EVL was comparable to normal subjects, indicating that parallel processing of words N and N + 1 was taking place as usual.

Regulating reading speed by varying EVL for texts with various text readability

Similarly to normal subjects, the basic structure of eye–voice coordination was preserved in both SCD and PD patients, with the gaze preceding the voice by an approximately similar fixed amount of spatial separation (spatial EVL). Furthermore, PD and SCD patients as well as normal subjects exhibited a preserved ability to systematically modulate EVL according to text readability, and to keep this value relatively stable within each text reading.

EVL asymptoted to a certain level for easier texts, and became comparable among the three subject groups at around 2.5–4 letters (Figures 8, 9), where the maximal memory buffer size would have been reached. Even though the gaze theoretically could have gone farther ahead of the voice, subjects would have avoided overloading the memory load of the verbal sketchpad by restricting EVL within some range. At the other extreme end of text readability, in which hiragana was arranged in a randomized order, the letter to follow was unpredictable and reading was least “automatic.” For these texts, reading approximated “letter by letter” in all three subject groups and EVL became minimal at a single letter level, that is, the gaze would be at almost the same position as the uttered text.

In previous studies, EVL (eye voice lead) and EVS (eye voice span) have been found to be correlated with the automaticity of reading. Faster and more automatic reading is associated with a larger EVL size. The speed of naming during tasks like RAN is also influenced by EVS, but this correlation is observed mainly in highly automated processes such as digit naming, but not in less automated processes like dice naming (Pan et al., 2013; Silva et al., 2016).

In our current study, we investigated the relationship between reading speed and spatial EVL for different groups of participants. We found a significant correlation between reading speed and EVL in each subject group. However, the slope of this correlation, which represents the increase in reading speed with larger EVL, was lower in SCD patients compared to other groups. This suggests that SCD patients were unable to fully utilize a strategy of leveraging EVL to increase reading speed due to their inherent difficulty with fast articulation; despite their ability to move their gaze ahead of the reading position, they could not effectively employ this leverage strategy.

On the other hand, the intercept of the correlation (the starting point) was higher for PD patients with compared to both normal subjects and SCD patients. This indicates that even though PD patients had limited potential for increasing reading speed by “stretching” their EVL, they could still accommodate an EVL of 2.5–4 letters, as mentioned earlier.

Our research indicates that individuals with SCD encounter obstacles when it comes to effectively utilizing EVL for faster reading.

This is primarily due to their difficulty in swift articulation. On the other hand, PD patients, despite their limited scanning speed, are able to operate within a defined range of EVL and sustain their reading speed. The difference in eye–voice coordination may also impact verbal processing. In SCD patients, the gaze sometimes moved well ahead of the voice, leading to more regressions and less parallel processing of words. This suggests that SCD patients had difficulties integrating word N + 1 while processing word N, with the gaze-dependent process playing a lesser role in their reading comprehension.

Paradoxically, when presented with a list of words arranged with spaces in between (Text 22, consisting of a Japanese syllabary with phonograms arranged in a predetermined order that the subjects had already memorized). PD patients actually showed a slightly faster reading speed compared to patients with SCD patients and normal subjects. This finding suggests that the reading speed itself was not inherently slowed in PD patients, but in some cases, it can even be potentially accelerated. PD patients may have utilized the spaced words or phonograms as external cues to enhance their reading speed, without the need for lexical processing of the phonograms. Interestingly, although the eye movements of PD patients were slightly delayed compared to their reading speed (as depicted in Figure 8C), this did not significantly hinder their overall reading performance.

Limitations of the study

The study studied a limited number of subjects, particularly SCD patients, despite a recruitment period of over 5 years in a hospital that focuses on medical care for neurodegenerative disorders. The majority of SCD patients in the study presented with pure cerebellar manifestation or multiple system atrophy, which have distinct differences in their underlying causes. While both groups demonstrated a similar trend in eye–voice coordination, studying a larger number of subjects may reveal additional differences between these two types of disorders.

Another limitation would be the potential effect of medication, including levodopa and other dopaminergic drugs on the eye movement and vocal output, which cannot be completely discounted. We could not withdraw the medication completely due to ethical and clinical reasons. Although PD patients were examined approximately 3–4 h after drug intake which would have minimized the effects of l-dopa according to our previous studies, other dopaminergic drugs could not be completely washed out and we cannot exclude their persisting effects. In SCD patients, most of the drug taken was tartirelin hydrate, but there were some patients who were taking drugs that could have affected the central nervous system.

Both PD and SCD can affect eye movement and vocal output. Therefore, it is difficult to determine which of the two mainly affects eye–voice coordination. Our analysis showed that the relative contribution between these two were very different. The contrast between PD and SCD patients, with the scanning speed affected in the former and vocal output affected in the latter, allowed us to address the interaction of voice output and eye movements to scan the text.

Finally, the experimental design we used did not take into account certain intrinsic factors that could have influenced the correlation between eye movements and voice utterances. For instance, we did not compare reading aloud to silent reading, nor did we differentiate between reading meaningful and meaningless words, or between

reading single words and reading complete sentences. Exploring these factors in future studies would provide valuable insights into the coordination between eye movements and voice outputs.

Conclusion

EVL has been considered to reflect the size of the information included in the verbal sketch pad, a presumed biomarker for the amount of information that can be held in working memory while reading aloud. EVL was shown to be relatively intact in SCD and PD patients compared to normal subjects. Furthermore, these patients demonstrated the ability to adjust their reading speed by modulating EVL based on the demands of the text.

The process of reading aloud involves complex computations in different parts of the brain. It begins with converting a written letter string into a sequence of spoken sounds. Both familiar and unfamiliar words are processed using different pathways (Dehaene and Cohen, 2011). Processing of known words rely on the lexical route, which is influenced by word frequency. On the other hand, processing of novel words are constructed letter by letter through the sublexical route, which is sensitive to orthographic reading. Woolnough et al. (2022) conducted a study using fMRI to investigate the spatiotemporal map of reading aloud and identified a reading network involving several brain regions. This network includes the medial fusiform gyrus (mFus), inferior frontal gyrus (IFG), inferior parietal cortex (IPS), precentral sulcus, and the motor cortex. The findings suggest that reading involves simultaneous processing through the lexical route, from mFus (sensitive to word frequency) to IFG, and the sublexical route, from IPS and precentral sulcus to anterior IFG (sensitive to orthographic processing). The lexical route may support automatic and faster reading and enhance activity in the IFG and frontal eye fields, which are responsible for eye movement.

In this context, English is an alphabetic language, in which the sublexical pathway is primarily employed for reading regular words. However, learned irregular words may utilize the lexical pathway. On the other hand, reading Chinese characters heavily relies on the lexical pathway since the pronunciation of each character is learned through rote memorization; Chinese characters are logograms, which means they represent words or concepts directly, rather than individual sounds. Japanese text, however, represents a unique combination of phonograms (representing a phoneme) and morphemes (Chinese characters). This distinct composition makes Japanese a language that warrants further examination in future studies, allowing for a better understanding of the different use of lexical and sublexical pathways.

Instead of looking at the difference in character-based or phoneme/morpheme processing, here we looked at eye-voice coordination by changing the level of readability and looking at its impact on eye-voice coordination in PD and SCD patients. The interaction between eye movements and voice utterance differed in these two disorders, despite similar EVL comparable to normal subjects. While SCD patients experienced slowed eye movement scanning the text and vocal output, PD patients were able to maintain a relatively smooth reading process despite their inherent slowness in the text scanning speed. This finding holds potential significance as it highlights a distinct difference between PD patients and SCD patients in terms of eye-voice coordination during reading aloud. This discrepancy may serve as a potential disease biomarker for SCD

and parkinsonism when reading aloud, although further research is needed to determine if it applies to all types of cerebellar ataxia and Parkinsonism disorders.

Data availability statement

The original contributions presented in this study are included in the article/supplementary material. Further inquiries can be directed to the corresponding author.

Ethics statement

The studies involving human participants were reviewed and approved by Ethics Committee of Graduate School of Medicine, University of Tokyo. The patients/participants provided their written informed consent to participate in this study.

Author contributions

YT and S-iT performed the experiments, collected the data, and prepared the figures. YT wrote the main manuscript text and carried out patient recruitment. SI-T wrote the custom program for analyzing the data. All authors reviewed the manuscript and contributed to the discussion.

Funding

YT was supported by a Research Project Grant in-aid for Scientific Research from the Ministry of Education, Culture, Sports, Science and Technology of Japan (18H05523) and Communications R&D Promotion Programme from the Ministry of Internal Affairs and Communications, Japan (B203060001). These funders were not involved in the study design, collection, analysis, interpretation of data, the writing of this article, or the decision to submit it for publication. YU received grants from the Ministry of Education, Culture, Sports, Science and Technology of Japan (Nos. 25293206, 15H05881, 16H05322, and 18K10821), Research Committee on the Medical Basis of Motor Ataxias, Health and Labour Sciences Research Grants, Ministry of Health, Labour and Welfare of Japan, Support Center for Advanced Telecommunications Technology Research, Association of Radio Industries Businesses and Novartis Foundation (Japan) for the Promotion of Science. S-iT was supported by a Research Project Grant-in-aid for Scientific Research from the Ministry of Education, Culture, Sports, Science and Technology of Japan (Nos. 19K17046, 21K15687).

Conflict of interest

The authors declare that the research was conducted in the absence of any commercial or financial relationships that could be construed as a potential conflict of interest.

Publisher's note

All claims expressed in this article are solely those of the authors and do not necessarily represent those of their affiliated

References

- Baddeley, A. D., and Hitch, G. J. (2019). The phonological loop as a buffer store: an update. *Cortex* 112, 91–106. doi: 10.1016/j.cortex.2018.05.015
- Buswell, G. T. (1921). The relationship between eye-perception and voice-response in reading. *J. Educ. Psychol.* 12, 217–227. doi: 10.1037/h0070548
- Dashtipour, K., Tafreshi, A., Lee, J., and Crawley, B. (2018). Speech disorders in Parkinson's disease: pathophysiology, medical management and surgical approaches. *Neurodegener. Dis. Manag.* 8, 337–348. doi: 10.2217/nmt-2018-0021
- De Luca, M., Borrelli, M., Judica, A., Spinelli, D., and Zoccolotti, P. (2002). Reading words and pseudowords: an eye movement study of developmental dyslexia. *Brain Lang.* 80, 617–626. doi: 10.1006/brln.2001.2637
- De Luca, M., Di Pace, E., Judica, A., Spinelli, D., and Zoccolotti, P. (1999). Eye movement patterns in linguistic and non-linguistic tasks in developmental surface dyslexia. *Neuropsychologia* 37, 1407–1420. doi: 10.1016/S0028-3932(99)00038-X
- De Luca, M., Pontillo, M., Primativo, S., Spinelli, D., and Zoccolotti, P. (2013). The eye-voice lead during oral reading in developmental dyslexia. *Front. Hum. Neurosci.* 7:696. doi: 10.3389/fnhum.2013.00696
- Dehaene, S., and Cohen, L. (2011). The unique role of the visual word form area in reading. *Trends Cogn. Sci.* 15, 254–262. doi: 10.1016/j.tics.2011.04.003
- Fabbri, M., Guimaraes, I., Cardoso, R., Coelho, M., Guedes, L. C., Rosa, M. M., et al. (2017). Speech and voice response to a levodopa challenge in late-stage Parkinson's disease. *Front. Neurol.* 8:432. doi: 10.3389/fneur.2017.00432
- Fairbanks, G. (1937). The relation between eye-movements and voice in the oral reading of good and poor silent readers. *Psychol. Monograph* 48, 78–107. doi: 10.1037/h0093394
- Gilman, S., Low, P. A., Quinn, N., Albanese, A., Ben-Shlomo, Y., Fowler, C. J., et al. (1999). Consensus statement on the diagnosis of multiple system atrophy. *J. Neurol. Sci.* 163, 94–98. doi: 10.1016/S0022-510X(98)00304-9
- Gilman, S., Wenning, G. K., Low, P. A., Brooks, D. J., Mathias, C. J., Trojanowski, J. Q., et al. (2008). Second consensus statement on the diagnosis of multiple system atrophy. *Neurology* 71, 670–676. doi: 10.1212/01.wnl.0000324625.00404.15
- Hayashi, N., NPO Tadoku Supporters (Eds.) (2012). *Japanese graded readers*. Level 1. Tokyo, Japan: ask publishers.
- Hogan-Brown, A. L., Hoedemaker, R. S., Gordon, P. C., and Losh, M. (2014). Eye-voice span during rapid automatized naming: evidence of reduced automaticity in individuals with autism spectrum disorder and their siblings. *J. Neurodev. Disord.* 6:33. doi: 10.1186/1866-1955-6-33
- Inhoff, A. W., Solomon, M., Radach, R., and Seymour, B. A. (2011). Temporal dynamics of the eye-voice span and eye movement control during oral reading. *J. Cogn. Psychol.* 23, 543–558. doi: 10.1080/20445911.2011.546782
- Jones, M. W., Kuipers, J. R., and Thierry, G. (2016). ERPs Reveal the time-Course of aberrant visual-phonological binding in developmental dyslexia. *Front. Hum. Neurosci.* 10:71. doi: 10.3389/fnhum.2016.00071
- Jones, M. W., Obregon, M., Louise Kelly, M., and Branigan, H. P. (2008). Elucidating the component processes involved in dyslexic and non-dyslexic reading fluency: an eye-tracking study. *Cognition* 109, 389–407. doi: 10.1016/j.cognition.2008.10.005
- Kio, C., NPO Tadoku Supporters (Eds.). (2012). *Japanese graded readers*. Level 0. Tokyo, Japan: ask publishers.
- Koizumi, B., NPO Tadoku Supporters (Eds.). (2012). *Japanese graded readers*. Level 3. Tokyo, Japan: ask publishers.
- Laubrock, J., and Kliegl, R. (2015). The eye-voice span during reading aloud. *Front. Psychol.* 6:1432. doi: 10.3389/fpsyg.2015.01432
- Matsuda, S., Matsumoto, H., Furubayashi, T., Fukuda, H., Emoto, M., Hanajima, R., et al. (2014). Top-down but not bottom-up visual scanning is affected in hereditary pure cerebellar ataxia. *PLoS One* 9:e116181. doi: 10.1371/journal.pone.0116181
- Matsumoto, H., Terao, Y., Furubayashi, T., Yugeta, A., Fukuda, H., Emoto, M., et al. (2011a). Small saccades restrict visual scanning area in Parkinson's disease. *Mov. Disord.* 26, 1619–1626. doi: 10.1002/mds.23683
- Matsumoto, H., Terao, Y., Yugeta, A., Fukuda, H., Emoto, M., Furubayashi, T., et al. (2011b). Where do neurologists look when viewing brain CT images? An eye-tracking study involving stroke cases. *PLoS One* 6:e28928. doi: 10.1371/journal.pone.0028928
- Miall, R. C., and Jenkinson, E. W. (2005). Functional imaging of changes in cerebellar activity related to learning during a novel eye-hand tracking task. *Exp. Brain Res.* 166, 170–183. doi: 10.1007/s00221-005-2351-5
- Modroño, C., Socas, R., Hernández-Martín, E., Plata-Bello, J., Marcano, F., Pérez-González, J. M., et al. (2020). Neurofunctional correlates of eye to hand motor transfer. *Hum. Brain Mapp.* 41, 2656–2668. doi: 10.1002/hbm.24969
- Moretti, R., Bava, A., Torre, P., Antonello, R. M., and Cazzato, G. (2002). Reading errors in patients with cerebellar vermis lesions. *J. Neurol.* 249, 461–468. doi: 10.1007/s004150200040
- Moretti, R., Torre, P., Antonelli, R. M., and Cazzato, G. A. Bava Acquired reading disruptions caused by cerebellar vermis lesions. In: R Moretti, P Torre, R. M. Antonelli, G Cazzato and A Bava(eds.) *The cerebellum and the reading process*. Nova Biomedical Books: New York. (2003a). Pp. 21–33.
- Moretti, R., Torre, P., Antonelli, R. M., and Cazzato, G. A. Bava. Reading and writing performance in patients with multiple system atrophy having predominant cerebellar features. In: R Moretti, P Torre, R. M. Antonelli, G Cazzato and A Bava (eds.) *The cerebellum and the reading process*. Nova Biomedical Books: New York. (2003b). Pp. 21–33.
- Nitschke, M. F., Arp, T., Stavrou, G., Erdmann, C., and Heide, W. (2005). The cerebellum in the cerebro-cerebellar network for the control of eye and hand movements -an fMRI study. *Prog. Brain Res.* 148, 151–164. doi: 10.1016/S0079-6123(04)48013-3
- Pan, J., Yan, M., Laubrock, J., Shu, H., and Kliegl, R. (2013). Eye-voice span during rapid automatized naming of digits and dice in Chinese normal and dyslexic children. *Dev. Sci.* 16, 967–979. doi: 10.1111/desc.12075
- Protopapas, A., Altani, A., and Georgiou, G. K. (2013). Development of serial processing in reading and rapid naming. *J. Exp. Child Psychol.* 116, 914–929. doi: 10.1016/j.jecp.2013.08.004
- Rayner, K. (2009). Eye movements and attention in reading, scene perception, and visual search. *Q J Exp Psychol* 62, 1457–1506. doi: 10.1080/17470210902816461
- Rizzo, J. R., Beheshti, M., Naeimi, T., Feiz, F., Fatterpekar, G., Balcer, L. J., et al. (2020). The complexity of eye-hand coordination: a perspective on cortico-cerebellar cooperation. *Cerebellum Ataxias* 7:14. doi: 10.1186/s40673-020-00123-z
- Sakai, K., NPO Tadoku Supporters (Eds.). (2014). *Japanese graded readers*. Level 2. Tokyo, Japan: ask publishers.
- Schattka, K. I., Radach, R., and Huber, W. (2010). Eye movement correlates of acquired central dyslexia. *Neuropsychologia* 48, 2959–2973. doi: 10.1016/j.neuropsychologia.2010.06.005
- Schmitz-Hübsch, T., du Montcel, S. T., Baliko, L., Berciano, J., Boesch, S., Depondt, C., et al. (2006). Scale for the assessment and rating of ataxia: development of a new clinical scale. *Neurology* 66, 1717–1720. doi: 10.1212/01.wnl.0000219042.60538.92
- Silva, S., Reis, A., Casaca, L., Petersson, K. M., and Faisca, L. (2016). When the eyes no longer lead: familiarity and length effects on eye-voice span. *Front. Psychol.* 7:1720. doi: 10.3389/fpsyg.2016.01720
- Skodda, S., and Schlegel, U. (2008). Speech rate and rhythm in Parkinson's disease. *Mov. Disord.* 23, 985–992. doi: 10.1002/mds.21996
- Stock, L., Krüger-Zechlin, C., Deeb, Z., Timmermann, L., and Waldthaler, J. (2020). Natural reading in Parkinson's disease with and without mild cognitive impairment. *Front. Aging Neurosci.* 12:120. doi: 10.3389/fnagi.2020.00120
- Stoodley, C. J., and Stein, J. F. (2013). Cerebellar function in developmental dyslexia. *Cerebellum* 12, 267–276. doi: 10.1007/s12311-012-0407-1
- Suppa, A., Asci, F., Saggio, G., Marsili, L., Casali, D., Zarezaheh, Z., et al. (2020). Voice analysis in adductor spasmodic dysphonia: objective diagnosis and response to botulinum toxin. *Parkinsonism Relat. Disord.* 73, 23–30. doi: 10.1016/j.parkreldis.2020.03.012
- Suppa, A., Marsili, L., Giovannelli, F., Di Stasio, F., Rocchi, L., Upadhyay, N., et al. (2015). Abnormal motor cortex excitability during linguistic tasks in adductor-type spasmodic dysphonia. *Eur. J. Neurosci.* 42, 2051–2060. doi: 10.1111/ejn.12977
- Terao, Y., Fukuda, H., and Hikosaka, O. (2017). What do eye movements tell us about patients with neurological disorders? - an introduction to saccade recording in the clinical setting. *Proc. Jpn. Acad. Ser. B Phys. Biol. Sci.* 93, 772–801. doi: 10.2183/pjab.93.049
- Terao, Y., Fukuda, H., Tokushige, S. I., Inomata-Terada, S., and Ugawa, Y. (2016). How saccade intrusions affect subsequent motor and oculomotor actions. *Front. Neurosci.* 10:608. doi: 10.3389/fnins.2016.00608
- Terao, Y., Fukuda, H., Ugawa, Y., and Hikosaka, O. (2013). New perspectives on the pathophysiology of Parkinson's disease as assessed by saccade performance: a clinical review. *Clin. Neurophysiol.* 124, 1491–1506. doi: 10.1016/j.clinph.2013.01.021
- Terao, Y., Fukuda, H., Yugeta, A., Hikosaka, O., Nomura, Y., Segawa, M., et al. (2011). Initiation and inhibitory control of saccades with the progression of Parkinson's disease

- changes in three major drives converging on the superior colliculus. *Neuropsychologia*. 49, 1794–1806. doi: 10.1016/j.neuropsychologia.2011.03.002

Tokushige, S. I., Matsuda, S. I., Oyama, G., Shimo, Y., Umemura, A., Sasaki, T., et al. (2018). Effect of subthalamic nucleus deep brain stimulation on visual scanning. *Clin. Neurophysiol.* 129, 2421–2432. doi: 10.1016/j.clinph.2018.08.003

Waldthaler, J., Tsitsi, P., Seimyr, G. O., Benfatto, M. N., and Svenningsson, P. (2018). Eye movements during reading in Parkinson's disease: a pilot study. *Mov. Disord.* 33, 1661–1662. doi: 10.1002/mds.105

Woolnough, O., Donos, C., Curtis, A., Rollo, P. S., Roccaforte, Z. J., Dehaene, S., et al. (2022). A spatiotemporal map of reading aloud. *J. Neurosci.* 42, 5438–5450. doi: 10.1523/JNEUROSCI.2324-21.2022

Yugeta, A., Terao, Y., Fukuda, H., and Ugawa, Y. (2008). Effects of levodopa on saccade performance in Parkinson's disease. *Mov. Disord.* 23:S296.

Zoccolotti, P., De Luca, M., Lami, L., Pizzoli, C., Pontillo, M., and Spinelli, D. (2013). Multiple stimulus presentation yields larger deficits in children with developmental dyslexia: a study with reading and RAN-type tasks. *Child Neuropsychol.* 19, 639–647. doi: 10.1080/09297049.2012.718325



OPEN ACCESS

EDITED BY

Xuemin Li,
Peking University Third Hospital, China

REVIEWED BY

Kotaro Yuge,
Kurume University Hospital, Japan
Giorgia Bussu,
Uppsala University, Sweden

*CORRESPONDENCE

Xuerong Luo
✉ luoxuerong@csu.edu.cn
Jianping Lu
✉ szlujianping@126.com

[†]These authors have contributed equally to this work

RECEIVED 21 February 2023

ACCEPTED 17 August 2023

PUBLISHED 15 September 2023

CITATION

Meng F, Li F, Wu S, Yang T, Xiao Z, Zhang Y, Liu Z, Lu J and Luo X (2023) Machine learning-based early diagnosis of autism according to eye movements of real and artificial faces scanning. *Front. Neurosci.* 17:1170951. doi: 10.3389/fnins.2023.1170951

COPYRIGHT

© 2023 Meng, Li, Wu, Yang, Xiao, Zhang, Liu, Lu and Luo. This is an open-access article distributed under the terms of the [Creative Commons Attribution License \(CC BY\)](#). The use, distribution or reproduction in other forums is permitted, provided the original author(s) and the copyright owner(s) are credited and that the original publication in this journal is cited, in accordance with accepted academic practice. No use, distribution or reproduction is permitted which does not comply with these terms.

Machine learning-based early diagnosis of autism according to eye movements of real and artificial faces scanning

Fanchao Meng^{1,2†}, Fenghua Li^{3†}, Shuxian Wu², Tingyu Yang², Zhou Xiao⁴, Yujian Zhang⁵, Zhengkui Liu³, Jianping Lu^{4*} and Xuerong Luo^{2*}

¹The National Clinical Research Center for Mental Disorder & Beijing Key Laboratory of Mental Disorders, Beijing Anding Hospital, Capital Medical University, Beijing, China, ²Department of Psychiatry, and National Clinical Research Center for Mental Disorders, The Second Xiangya Hospital of Central South University, Changsha, Hunan, China, ³Key Lab of Mental Health, Institute of Psychology, Chinese Academy of Sciences, Beijing, China, ⁴Department of Child Psychiatry, Kangning Hospital of Shenzhen, Shenzhen Mental Health Center, Shenzhen, Guangdong, China, ⁵Sichuan Cancer Hospital & Institute, Sichuan Cancer Center, Chengdu, Sichuan, China

Background: Studies on eye movements found that children with autism spectrum disorder (ASD) had abnormal gaze behavior to social stimuli. The current study aimed to investigate whether their eye movement patterns in relation to cartoon characters or real people could be useful in identifying ASD children.

Methods: Eye-tracking tests based on videos of cartoon characters and real people were performed for ASD and typically developing (TD) children aged between 12 and 60 months. A three-level hierarchical structure including participants, events, and areas of interest was used to arrange the data obtained from eye-tracking tests. Random forest was adopted as the feature selection tool and classifier, and the flattened vectors and diagnostic information were used as features and labels. A logistic regression was used to evaluate the impact of the most important features.

Results: A total of 161 children (117 ASD and 44 TD) with a mean age of 39.70 ± 12.27 months were recruited. The overall accuracy, precision, and recall of the model were 0.73, 0.73, and 0.75, respectively. Attention to human-related elements was positively related to the diagnosis of ASD, while fixation time for cartoons was negatively related to the diagnosis.

Conclusion: Using eye-tracking techniques with machine learning algorithms might be promising for identifying ASD. The value of artificial faces, such as cartoon characters, in the field of ASD diagnosis and intervention is worth further exploring.

KEYWORDS

autism spectrum disorder, eye-tracking, cartoon character, machine learning, random forest

Introduction

Social interaction impairment is the most common clinical manifestation of autism spectrum disorder (ASD), which is characterized by verbal and nonverbal communication difficulties as well as stereotyped obsessive behaviors (Volkmar et al., 2004). Abnormal eye contact during social situations is among the most noticeable manifestations of social interaction difficulties for those with ASD (Leekam et al., 1998; Spezio et al., 2007). Early screening remains one of the major challenges in ASD research. According to a recent meta-analysis involving 30 studies with over 60,000 ASD participants from 35 countries, the age for diagnosis occurred at approximately 60 months of age, which was late for early intervention to be initiated (Van't Hof et al., 2021). Delayed diagnosis and intervention will have a negative impact on children's prognoses and may lead to lifelong unpleasant outcomes, posing a significant burden on families and society.

Tremendous efforts have been made by clinical workers to create techniques for the early screening of ASD, and there are numerous tools available (Sappok et al., 2015). However, due to the popularity of existing instruments and incorrect operating methods, some missed diagnoses may occur in places with exceptionally large populations and few or no community health workers (James et al., 2014). The results have aroused the attention of professionals involved in the early detection of ASD.

Eye-tracking technology has become an increasingly important tool in the early screening and diagnosis of ASD in recent years. In contrast to electroencephalography (EEG) and magnetic resonance imaging (MRI), which are time-consuming and difficult to perform, eye-tracking is regarded as a very child-friendly tool that enables a variety of original designs for the investigation of visual exploration patterns and their underlying mechanisms. Evidence proved that eye-tracking techniques combined with machine learning algorithms might be promising in the early and objective diagnosis of ASD (Kollias et al., 2021). Because of ASD children's difficulties in social interaction, the complexity of social interaction is lacking, and eye-tracking technology can capture the distinctions between high and low social significance stimulation in ASD children via the stimulation paradigm. Studies investigating the factors influencing social attention in ASD found a decrease in gaze to stimuli with high social significance and an increase in gaze to stimuli with low social significance (Chita-Tegmark, 2016a; Frazier et al., 2017). For example, there was decreased attention to the entire face and upper face regions, increased attention to body regions and other unimportant or extraneous aspects of stimuli, and decreased attention to the lower face (mouth) (Chita-Tegmark, 2016b; Frazier et al., 2017).

The total time of gaze fixation with low social significance (such as geometric figures) has been successfully applied as a criterion to distinguish ASD (Shi et al., 2015; Pierce et al., 2016; Moore et al., 2018). Multiple studies for ASD identification using machine learning with eye-tracking data exhibited accuracies of 67–98% in non-toddler groups (Kollias et al., 2021). To the best of our knowledge, there were no studies combining eye tracking using cartoons as stimuli with machine learning algorithms. Using cartoons as stimuli has several advantages. First, it might better capture the attention of toddlers who can be easily influenced by the outside environment, especially when they are not interested in the proposed stimuli (Masedu et al., 2022). Second, a recent study found that ASD children had lower levels of

social orientation (SO) than TD children in the realistic task but comparable levels in the cartoon task. Nonetheless, their findings indicated that the cartoon task effectively captured developmental and adaptive delay by demonstrating numerous correlations with visual exploration parameters such as social prioritization, fixation duration, and percentage of SO (Robain et al., 2022). In addition, studies investigating factors that influence social attention in ASD found that ASD children seem to process cartoon faces in a similar manner that typical development (TD) children do; they tend to look more at cartoon characters than at other objects in cartoon situations (Van der Geest et al., 2002). The differences between these groups make it simpler for us to capture the complexities of ASD social interaction and then infer the difference between ASD and TD children in social interaction, which becomes a diagnostic signal. Therefore, given that developmental delay and abnormal gaze are early markers of ASD, we hypothesized that the cartoon task, as well as other minimally social stimuli, could be a useful tool for early screening.

Methods

Participants

Participants were recruited between 2019 and 2021 in Changsha and Shenzhen, China. The inclusion criteria for children with ASD were as follows: (1) those aged 12–60 months; (2) those who met the diagnosis of ASD according to the Diagnostic and Statistical Manual of Mental Disorders, fifth edition (DSM-V) (American Psychological Association, 2009) and the Autism Diagnostic Observation Schedule (ADOS) confirmed the diagnosis (Lord et al., 1999); and (3) children with normal vision and hearing who can complete the eye movement tests. Those with other major mental disorders or serious physical health problems were excluded. Toddlers who participated when they were younger than 24 months old were classified as global developmental failures based on their performance on the Chinese version of the Gesell development scale (GDS) (Yang, 2016). They were followed and diagnosed every 3–6 months until they were 2 years old. TD children aged 12–60 months were recruited without gender restrictions. According to their parents/caregivers, they had no evidence of developmental disabilities or neuropsychiatric conditions.

The research was carried out in accordance with the Declaration of Helsinki's ethical principles. The experimental procedures had been explained to all participants' parents or caregivers, and written informed consent was obtained from all of them. The ethics committee of the Second Xiangya Hospital, Central South University, reviewed and approved the study (No. 2017YFC1309904).

Clinical assessments

Autism diagnostic observation schedule

ADOS is a semi-structured, standardized observational tool that is frequently used as a diagnostic indicator for ASD. It can accurately assess and diagnose ASD using a variety of play-based activities that focus on communication, social engagement, play, and innovative use of materials, as well as restricted and repetitive behaviors (González et al., 2019).

Chinese version of GDS

GDS was used to assess the development of children. It is composed of five domains: adaptability, gross motor, fine motor, language, and social-emotional responses (Yang, 2016). Participants' development quotient (DQ) in each domain was calculated. Using the full-scale DQ, the development was classified as normal ($DQ \geq 85$), deficient ($DQ \leq 75$), or borderline ($75 \sim 85$). In this field, DQ in any single domain less than 75 was considered deficient.

Eye-tracking acquisition and processing

The eye-tracking tests were carried out in a quiet environment. A SensoMotoric Instruments Red500 remote eye tracker (Teltow, Germany) was attached to the frame of a $1,680 \times 1,050$ 22-inch LCD stimulus presentation monitor. The highest spatial resolution and gaze position accuracy were 0.1 and 0.4, respectively. The capture range for eye movement was 40° horizontally ($\pm 20^\circ$) and 60° vertically ($\pm 40^\circ$). The tracking range of the head motion is 40×20 cm when the man-machine distance is 70 cm. Throughout the experiment, two 5-point calibrations were obtained at fixed times.

Eight videos were played in the SMI Experiment Center. Each video has two large rectangular areas side by side, and the screen is also divided into the left and right sides. There was a cartoon character on the left (or right) side playing actions such as dancing, nodding, blowing a kiss, scratching the neck, clapping hands, bouncing, skipping rope, and nodding while stretching thumbs. The opposite side presented a real person. This person imitates the cartoon character. During the imitation process, the person tried to match the expression (smiling or no obvious expression), movement, clothing (clothing color and accessories), character size, and appearance (half body or whole body) with the cartoon pattern (Figures 1A–H). All of the videos were soundless, and the SMI Experiment Center software was created using a random playback option so that each child would see the eight videos in a different order.

Data organization

A three-level hierarchical structure [participants, events, and area of interest (AOI)] was used to arrange the data obtained by the SMI BeGaze program (Figure 2). Each participant had eight event data entities, matching one of the eight videos used in the trials. A total of 24 data items, including fixation frequency, saccade amplitude, count, frequency, average latency, fixation dispersion, saccade length, saccade velocity, and total, average, maximum, and minimum values of fixation time, were recorded for each event data entity. Three events (nodding, clapping hands, and nodding while stretching thumbs) had four AOIs (cartoon, people, people's heads, and people's bodies) (Figure 3). Five events (dancing, blowing a kiss, scratching the neck, bouncing, and skipping rope) had two AOIs (cartoon and people) (Figure 4). Each AOI contained a set of 14 data items. The 14 data items within each AOI data entity were as follows: entry time, visible time (equivalent to the duration of the event in this study), net dwell time (time of all gazes that hit the AOI), dwell time (sum of net dwell time and time of saccades that hit the AOI), glance duration (sum of dwell time and duration of saccade entering the AOI), and diversion duration (sum of glance duration and duration of saccade leaving the

AOI). In this study, gaze refers to the non-saccade movement status, and fixation refers to a cluster of gaze points that are close in space and time (60 ms).

Data analysis

We flattened each participant's hierarchical data structure into a single vector with a length of 688 elements in order to thoroughly investigate the data items collected from the participants. Therefore, an array of event items and AOI entities from a single participant were arranged consecutively (Figure 5). Flatten vectors and diagnostic information were used as features and labels, and random forest (RF) was used as the feature selection method and classifier.

RF is a common ensemble classifier and feature-selection technique (Menze et al., 2009; Boulesteix et al., 2012; Biau and Scornet, 2016). Multiple independent decision trees make up an RF. Each decision tree uses a random subset of the input features from a random subset of the training examples to fit itself during the training phase. The predictions of all the fitted trees were averaged to determine the final classification of an RF. In addition to the final choice, an RF also produces a significant value for each feature (entropy decrease, Gini impurity, etc.).

In our research, we created equal-sized autistic and healthy groups using the undersampling technique and constructed RF models. Gini impurity was utilized as the split criterion, and there were 800 decision trees. The ratio of training to validation cases was 7:3. The average accuracy, precision, and recall were obtained after 500 iterations of the fitting process (Powers, 2020). Additionally, we plotted the receiver operating characteristic curve (ROC) using all the prediction findings and determined the area under the curve (AUC). The undersampling and training-validation splits were randomized before each of the 500 fitting processes.

A logistic regression was applied to examine if the features were related to the diagnoses. Forward stepwise factor selection was used to build the logistic regression model. Features in the RF models were used as independent variables in the regression model. Features were added to the model one at a time. A feature was chosen if statistical significance could be found in the feature itself or if the statistical significance of previously added features was unaffected by the new feature. Python 3.8.10, sci-kit learn 1.1.1, and the R language 4.1.1 were used for all data organization and analysis.

Results

The characteristics of the participants are presented in Table 1. A total of 161 children with a mean age of 39.70 ± 12.27 months were recruited, and 47 of them were girls. Among them, 117 were diagnosed with ASD and 44 with TD. There were 91 boys and 26 girls in the ASD group and 23 boys and 21 girls in the TD group. The children in the ASD group were significantly younger than those in the TD group. Children in the ASD group had significantly lower scores in the GDDS compared to their healthy controls.

The average accuracy, precision, and recall of the 500-time fitting validation were 0.73, 0.73, and 0.75, respectively, and the AUC was 0.81 (Figure 6). Randomized undersampling and the train-test split were performed before every fitting. The sizes of the ASD and TD

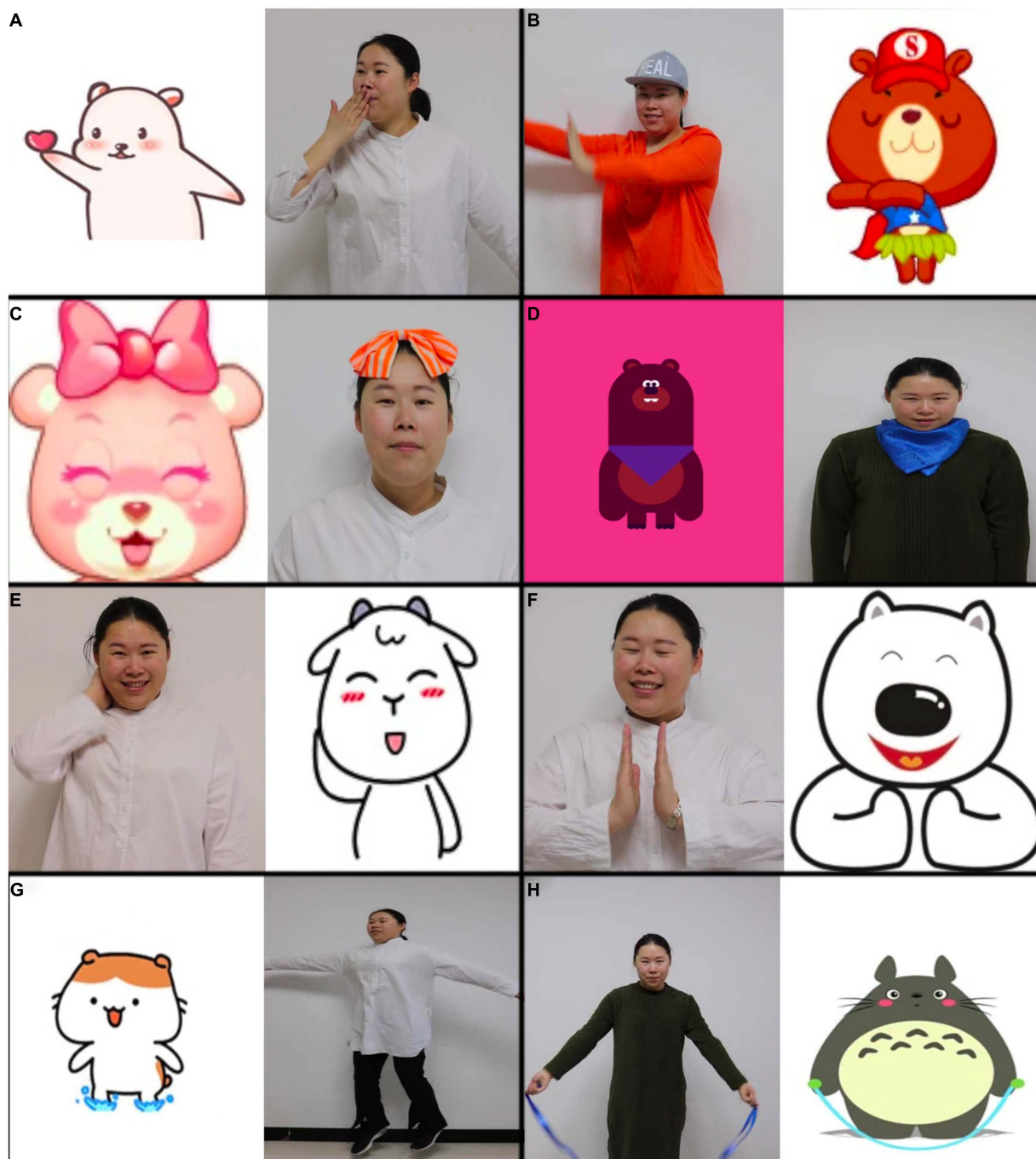


FIGURE 1
Pictures of eight videos used for eye-tracking tests, (A-H) represented different scenarios.

groups were both 44 after undersampling. The size ratio of the training and validation sets was 7:3.

In the logistic regression analysis, we first included age as the independent variable before the stepwise factor selection as children in the ASD and TD groups had significantly different ages. In addition to age, the best-fit logistic model found that nine features were significantly associated with an ASD diagnosis (Table 2). The features that were negatively associated with ASD were body-revisits and head-glance-duration when the cartoon

character makes the gesture of clapping hands, cartoon-sequence when scratching the neck, people-glances-count when nodding while stretching thumbs, and people-net-dwell-time when dancing. The features that were positively associated with ASD were people-first-fixation-duration when the people are dancing, cartoon-sequence when the character is nodding, and cartoon-fixation-time when blowing a kiss. In addition, the saccade velocity maximum has a positive correlation with ASD diagnoses (Table 2).

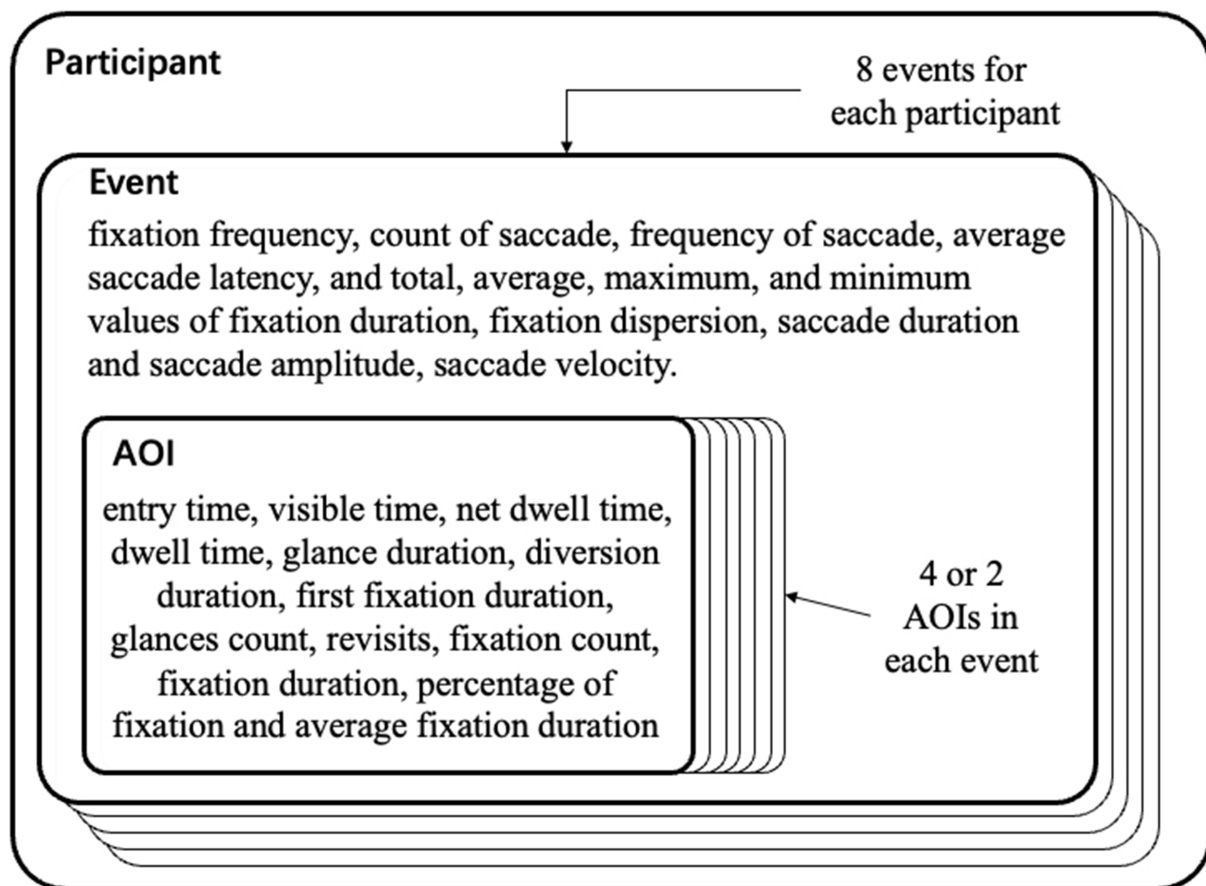


FIGURE 2
Three-level hierarchical structure and data item of each level.

Discussion

In this study, we developed a novel ASD identification framework for children using a specific cartoon paradigm, together with eye movement data for cartoon preferences and machine learning. We gave children a task based on [Pierce et al. \(2011\)](#), in which videotaped moving/dancing kids were pitted against geometric patterns moving repetitively. The cartoon and real human figures were used at the same time in the stimulus design to make sure the clothing and actions in the cartoon were comparable to those in the real figures. ASD and TD children had different visual preferences for cartoon and real human faces, and ASD children preferred cartoon faces much more than TD children ([Van der Geest et al., 2002](#); [Rosset et al., 2008](#)). According to the results, our stimulus paradigm had satisfactory efficacy in distinguishing ASD from TD children. The ML model has an average accuracy, precision, and recall ASD of 0.73, 0.73, and 0.75, respectively. As a classifier to differentiate between ASD and TD children, it has an AUC of 0.81.

Similar efforts have been made by some other studies combining eye-tracking technology with ML algorithms for the objective diagnosis of ASD. For example, [Liu et al. \(2016\)](#) used a data-driven approach to extract features from face scanning data, and a support vector machine (SVM) was applied in the data analysis. While this study showed a maximum classification accuracy of 88.5%, it had a

relatively small sample size with 29 ASD children included. [Kang et al. \(2020\)](#) recruited 77 low-functioning autistic children and 80 TD children to watch a random sequence of face photos. With SVM, they found a maximum classification accuracy of 72.5% (AUC=0.77). However, all of their participants were aged between 3 and 6 years, and no younger children were included. Consistent with previous findings ([Tao and Shyu, 2019](#); [Tsuchiya et al., 2021](#)), our study has the advantage of including the largest sample size of younger children under the age of three. Other researchers promote the research ideology that early diagnosis and special education can be accomplished through the use of computer-aided methods based on EEG signals and/or imaging; however, the results in different studies are not quite the same. [Wee et al. \(2014\)](#) reported the greatest accuracy of 96% using SVM as a classifier in a study utilizing sMRI (structural magnetic resonance image). [Haar et al. \(2016\)](#) conducted a large-scale investigation with 245 ASD and 245 control subjects, using cortical surface area as a feature and linear discriminant analysis as a classifier, and reported a low accuracy of 60%. [Rane et al. \(2017\)](#) conducted the largest fMRI study, with over a thousand participants. A low accuracy rate of 60.56% was obtained. [Wang et al. \(2019\)](#) had over a thousand participants as well and reported a higher accuracy of 93.59%. Although the research findings are highly exciting, we prefer to use eye movement in clinical promotion because the clinical operability of MRI is significantly more challenging.

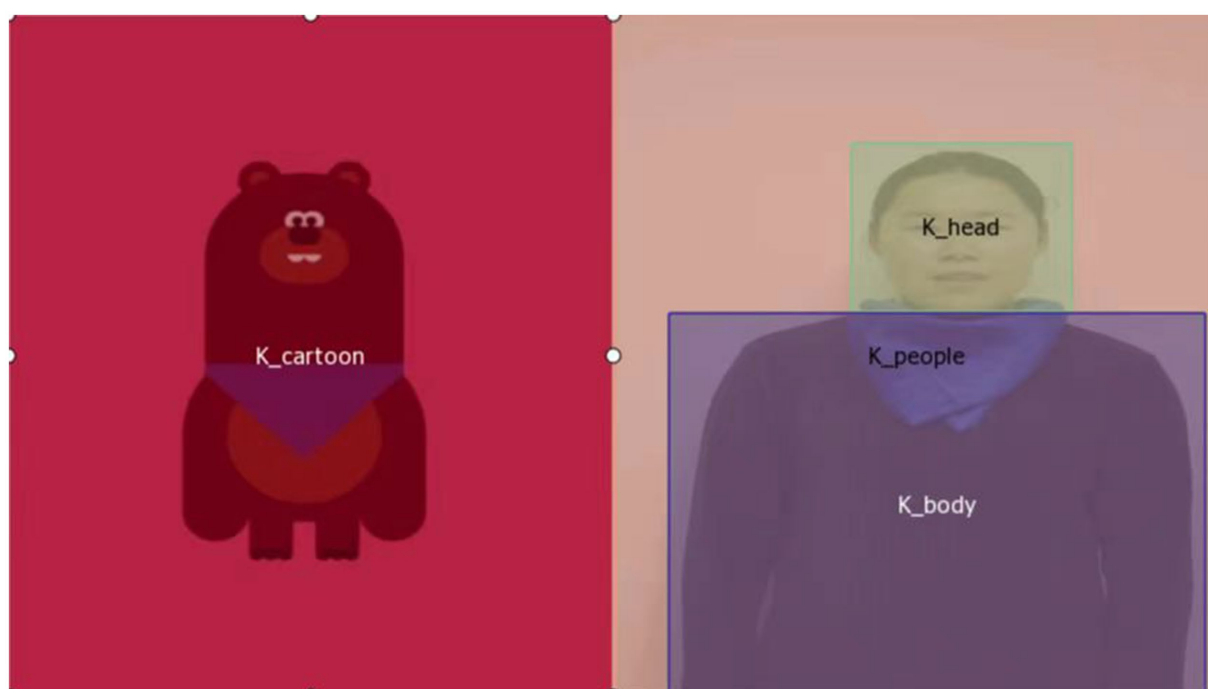


FIGURE 3
The four area of interests in the three events.



FIGURE 4
The two area of interests in the five events.

In the current study, we found several glancing behaviors that related to real humans or human parts, such as body-revisits, head-glance-duration, people-glance-count, and people-net-dwell-time,

were all negatively associated with ASD. In contrast, glancing behaviors that related to cartoon characters such as cartoon-sequence and cartoon-fixation-time were positively associated with ASD. These

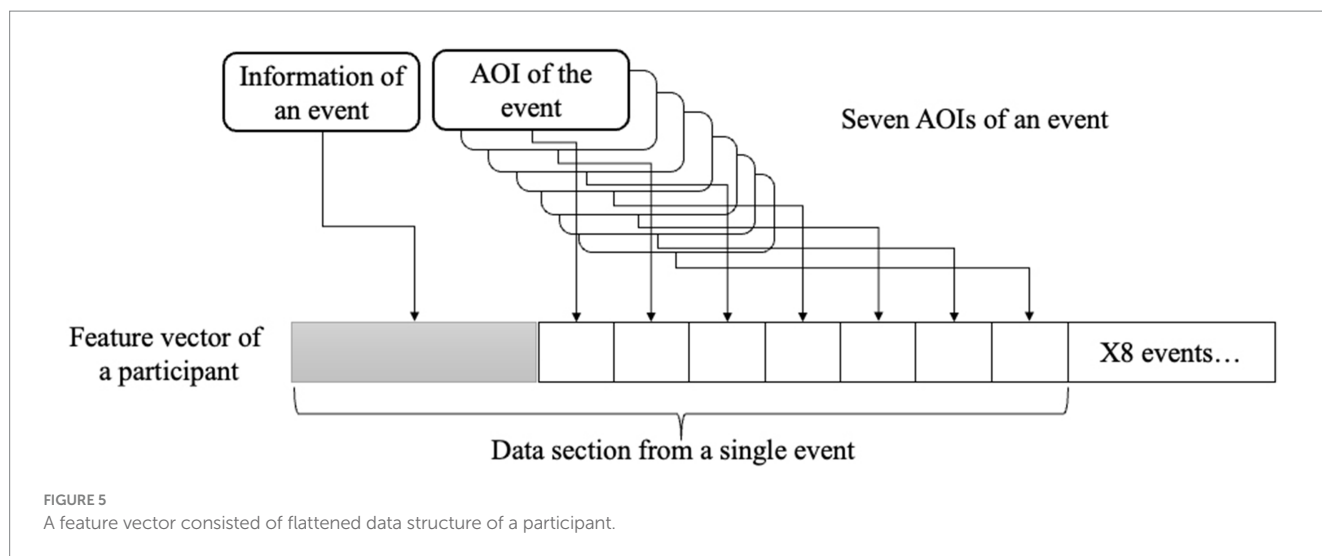


TABLE 1 Clinical characteristics of participants.

Characteristics	ASD (N = 117)	TD (N = 44)	Value of <i>p</i>
Female, <i>n</i> (%)	26 (22.2)	21 (47.7)	<0.001
Age, mean (SD), months	38.7 (12.8)	46.0 (11.9)	0.002
Adaptive behavior, mean (SD)	65.7 (16.8)	94.0 (9.5)	<0.001
Gross motor, mean (SD)	73.4 (15.2)	89.4 (14.6)	<0.001
Fine motor, mean (SD)	71.23 (19.5)	92.0 (8.9)	<0.001
Language, mean (SD)	46.9 (19.4)	98.7 (15.7)	<0.001
Personal-social behavior, mean (SD)	59.1 (18.1)	101.6 (10.1)	<0.001

ASD, autism spectrum disorder; SD, standard deviation; TD, typically developing.

behaviors had social significance. Children were more likely to have ASD when they were less interested in real humans or human parts and were more interested in cartoon characters. These results were similar to previous findings that adults with ASD were slow to respond to social stimuli, especially when there were non-social stimuli competing with social stimuli that were related to the narrow interests of ASD (Sasson and Touchstone, 2014; Wang et al., 2014). People with a higher degree of autistic features showed a greater interest in non-human social beings such as animals, robots, or cartoons (Atherton and Cross, 2018). One possible explanation for the cartoon preference of ASD children is that cartoons do not require social interaction. That is to say, the typicality of ASD in cartoon processing may be due to the damage to their social communication skills (Rosset et al., 2008).

Notwithstanding, we found that people-first-fixation-duration when dancing was positively associated with an ASD diagnosis. The reason under this might be that real people had a greater range of motion and children were more attracted to this motion. Another unexpected result was that when watching the video of scratching the neck, ASD children showed quick attention to the cartoon area, while when watching the video of nodding, they showed slow attention to the cartoon area. We compared these two videos and found that in the video of nodding, the face size of the cartoon character was

significantly larger than that of a real human. This result reminds us that although cartoon characters have lower social intensity than real people, ASD children also showed similar face avoidance when the face size was relatively large (Falck-Ytter and von Hofsten, 2011). This study utilizes non-linear machine learning models to select a series of indicators, which have been automatically summarized through multiple iterations of machine learning. These indicators possess strong data-driven characteristics and are not heavily reliant on the specific features of the selection method itself. According to our statistics, the predictive capabilities of each indicator decrease with the order of the indicator list. However, it is essential to note that this research utilizes a non-linear machine learning method (RF) for selection. While the authors attempted to provide explanations for the rationality of the selected indicators, their individual use or linear combination to construct predictive models may not necessarily achieve the same effect as when combined in the RF. This is determined by the working mechanism of the RF's decision trees, where the same indicator may be used multiple times based on different premises at different decision nodes.

There are several limitations to this study. First, the artificial undersampling may lead to an increase in false-positive judgments in an ecological setting, especially when the prevalence is extremely low. Nonetheless, the samples collected in this study differ significantly from the real-world prevalence of ASD (117 positive cases and 44 negative cases). Therefore, without the use of undersampling to balance the samples, it would not be possible to create a model that better adapts to large-scale screening. Moreover, an abundance of positive samples might mislead the model, which is another reason why we ultimately decided to use balanced samples. In future research, these extracted indicators should be applied to fit a screening model more suitable for ecological settings in larger-scale samples (such as screening studies at the provincial level). Second, the age and development level among ASD and TD children were different, and these differences might affect the face scanning patterns (Yi et al., 2014). We did not consider age in the prediction model, and we just focused on whether there was a discrepancy in task performance. With a balanced age distribution and cognitive levels, incorporating age range as a factor in the model would further improve its performance. However, due to the limitations of sample size and an imbalanced age

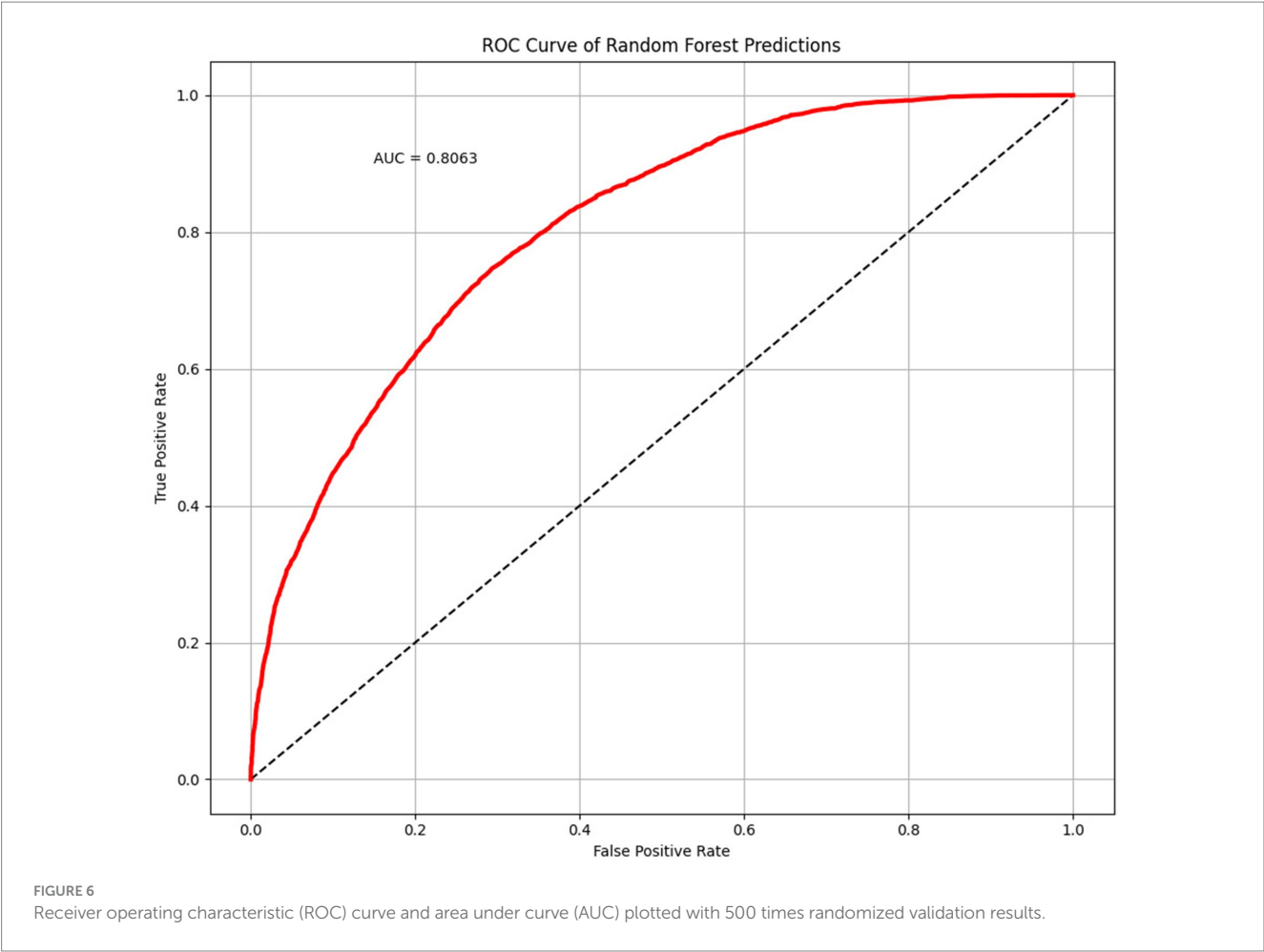


TABLE 2 The best-fit logistic regression model.

Features	Estimate	Std. error	z value	Value of <i>p</i>
(Intercept)	1.22	0.22	5.55	<0.001
Clapping hands: body-revisits	−0.41	0.20	−2.07	0.038
Clapping hands: head-glance-duration	−0.59	0.23	−2.52	0.012
Dancing: people-first-fixation-duration	1.04	0.27	3.80	0.000
Scratching the neck: cartoon-sequence	−0.62	0.21	−2.95	0.003
Nodding while stretching thumbs: people-glances-count	−0.95	0.24	−3.98	<0.001
Nodding: cartoon-sequence	0.54	0.21	2.58	0.010
Saccade velocity maximum	0.52	0.21	2.42	0.015
Blowing a kiss: cartoon-fixation-time	0.63	0.22	2.82	0.005
Dancing: people-net-dwell-time	−0.63	0.25	−2.54	0.011

distribution, this study has not been able to achieve this step. Third, though we found a correlation between eye movement features and ASD diagnosis, considering the complex nonlinear classification characteristics of RF, the actual eye movement patterns of ASD children were still not fully clear to us, especially when facing cartoon characters. Fourth, even though our study included the largest sample size of children under the age of three, a larger sample size is still needed in

future studies. In particular, those who are at high risk of ASD and younger than 2 years old are needed to validate our results and model. Despite these limitations, the current study demonstrated that using eye-tracking techniques with ML algorithms might be promising for identifying ASD. The value of artificial faces, such as cartoon characters in the field of ASD diagnosis and intervention is worth further exploring.

Data availability statement

The raw data supporting the conclusions of this article will be made available by the authors, without undue reservation.

Ethics statement

The studies involving humans were approved by the ethics committee of the Second Xiangya Hospital, Central South University, reviewed and approved the study (No. 2017YFC1309904). The studies were conducted in accordance with the local legislation and institutional requirements. Written informed consent for participation in this study was provided by the participants' legal guardians/next of kin.

Author contributions

FM, SW, TY, ZX, and YZ performed the experiments. FL and ZL performed the statistical analysis. FM revised the manuscript. JL drafted the manuscript. XL designed the study. All authors have given final approval for the version to be published.

References

- American Psychological Association. *Diagnostic and statistical manual of mental disorders*. 5th Edn. Washington, DC: American Psychological Association. (2009).
- Atherton, G., and Cross, L. (2018). Seeing more than human: autism and anthropomorphic theory of mind. *Front. Psychol.* 9:528. doi: 10.3389/fpsyg.2018.00528
- Biau, G., and Scornet, E. (2016). A random forest guided tour. *TEST* 25, 197–227. doi: 10.1007/s11749-016-0481-7
- Boulesteix, A. L., Janitzka, S., Kruppa, J., and König, I. R. (2012). Overview of random forest methodology and practical guidance with emphasis on computational biology and bioinformatics. *Wiley Interdiscipl. Rev.* 2, 493–507. doi: 10.1002/widm.1072
- Chita-Tegmark, M. (2016a). Social attention in ASD: a review and meta-analysis of eye-tracking studies. *Res. Dev. Disabil.* 48, 79–93. doi: 10.1016/j.ridd.2015.10.011
- Chita-Tegmark, M. (2016b). Attention allocation in ASD: a review and Meta-analysis of eye-tracking studies. *Rev. J. Autism Dev. Disord.* 3:400. doi: 10.1007/s40489-016-0089-6
- Falck-Ytter, T., and von Hofsten, C. (2011). How special is social looking in ASD: a review. *Prog. Brain Res.* 189, 209–222. doi: 10.1016/B978-0-444-53884-0.00026-9
- Frazier, T. W., Strauss, M., Klingemier, E. W., Zetzer, E. E., Hardan, A. Y., Eng, C., et al. (2017). A Meta-analysis of gaze differences to social and nonsocial information between individuals with and without autism. *J. Am. Acad. Child Adolesc. Psychiatry* 56, 546–555. doi: 10.1016/j.jaac.2017.05.005
- González, M. C., Vázquez, M., Hernández-Chávez, M. Autism spectrum disorder: Clinical diagnosis and ADOS Test. *Rev. Chil Pediatr.* (2019). 90(5), 485–491. doi: 10.32641/rchped.v90i5.872
- Haar, J., Han, X., Hu, J.-F., Behrmann, M., and Dinstein, I. (2016). Anatomical abnormalities in autism? *Cereb. Cortex* 26, 1440–1452. doi: 10.1093/cercor/bhu242
- James, L. W., Pizur-Barnekow, K. A., and Scheffkind, S. (2014). Online survey examining practitioners' perceived preparedness in the early identification of autism. *Am. J. Occup. Ther.* 68, e13–e20. doi: 10.5014/ajot.2014.009027
- Kang, J., Han, X., Hu, J.-F., Feng, H., and Li, X. (2020). The study of the differences between low-functioning autistic children and typically developing children in the processing of the own-race and other-race faces by the machine learning approach. *J. Clin. Neurosci.* 81, 54–60. doi: 10.1016/j.jocn.2020.09.039
- Kollias, K.-F., Syriopoulou-Delli, C. K., Sarigiannidis, P., and Fragulis, G. F. (2021). The contribution of machine learning and eye-tracking technology in autism spectrum disorder research: a systematic review. *Electronics* 10:2982. doi: 10.3390/electronics10232982
- Leekam, S. R., Hunnisett, E., and Moore, C. (1998). Targets and cues: gaze-following in children with autism. *J. Child Psychol. Psychiatry* 39, 951–962. doi: 10.1111/1469-7610.00398
- Liu, W., Li, M., and Yi, L. (2016). Identifying children with autism spectrum disorder based on their face processing abnormality: a machine learning framework. *Autism Res.* 9, 888–898. doi: 10.1002/aur.1615
- Lord, C., Rutter, M., DiLavore, P. C., and Risi, S. *Autism diagnostic observation schedule – WPS (ADOS-WPS)*. Los Angeles, CA: Western Psychological Services. (1999).
- Masedu, F., Vagnetti, R., Pino, M. C., Valenti, M., and Mazza, M. (2022). Comparison of visual fixation trajectories in toddlers with autism Spectrum disorder and typical development: a Markov chain model. *Brain Sci.* 12:10. doi: 10.3390/brainsci12010010
- Menze, B. H., Kelm, B. M., Masuch, R., Himmelreich, U., Bachert, P., Petrich, W., et al. (2009). A comparison of random forest and its Gini importance with standard chemometric methods for the feature selection and classification of spectral data. *BMC Bioinform.* 10, 1–16. doi: 10.1186/1471-2105-10-213
- Moore, A., Wozniak, M., Yousef, A., Barnes, C. C., Cha, D., Courchesne, E., et al. (2018). The geometric preference subtype in ASD: identifying a consistent, early-emerging phenomenon through eye tracking. *Mol. Autism.* 9:19. doi: 10.1186/s13229-018-0202-z
- Pierce, K., Conant, D., Hazin, R., Stoner, R., and Desmond, J. (2011). Preference for geometric patterns early in life as a risk factor for autism. *Arch. Gen. Psychiatry* 68, 101–109. doi: 10.1001/archgenpsychiatry.2010.113
- Pierce, K., Marinero, S., Hazin, R., McKenna, B. S., Barnes, C. C., and Malige, A. (2016). Eye tracking reveals abnormal visual preference for geometric images as an early biomarker of an autism Spectrum disorder subtype associated with increased symptom severity. *Biol. Psychiatry* 79, 657–666. doi: 10.1016/j.biopsych.2015.03.032
- Powers, D. M. (2020). Evaluation: From precision, recall and F-measure to ROC, informedness, markedness and correlation. *arXiv*. doi: 10.48550/arXiv.2010.16061
- Rane, S., Jolly, E., Park, A., Jang, H., and Craddock, C. (2017). Developing predictive imaging biomarkers using whole-brain classifiers: application to the ABIDE I dataset. *Res. Ideas Outcomes* 3:e12733. doi: 10.3897/rio.3.e12733
- Robain, F., Godel, M., Kojovic, N., Franchini, M., Journal, F., and Schaer, M. (2022). Measuring social orienting in preschoolers with autism spectrum disorder using cartoons stimuli. *J. Psychiatr. Res.* 156, 398–405. doi: 10.1016/j.jpsychires.2022.10.039
- Rosset, D. B., Rondan, C., Da Fonseca, D., Santos, A., Assouline, B., and Deruelle, C. (2008). Typical emotion processing for cartoon but not for real faces in children with autistic spectrum disorders. *J. Autism Dev. Disord.* 38, 919–925. doi: 10.1007/s10803-007-0465-2
- Sappok, T., Heinrich, M., and Underwood, L. (2015). Screening tools for autism spectrum disorders. *Adv. Autism* 1, 12–29. doi: 10.1108/AIA-03-2015-0001
- Sasson, N., and Touchstone, E. (2014). Visual attention to competing social and object images by preschool children with autism spectrum disorder. *J. Autism Dev. Disord.* 44, 584–592. doi: 10.1007/s10803-013-1910-z
- Shi, L., Zhou, Y., Ou, J., Gong, J., Wang, S., Cui, X., et al. (2015). Different visual preference patterns in response to simple and complex dynamic social stimuli in preschool-aged children with autism spectrum disorders. *PLoS One* 10:e0122280. doi: 10.1371/journal.pone.0122280

Funding

This work was supported by Youth Talent Training “Green Seedling Program of Beijing Hospital Management Center” (No. QML20231906 to FM), Shenzhen Fund for Guangdong Provincial High-level Clinical Key Specialties (No. SZGSP013 to JL), National Key R&D Program of China (No. 2017YFC1309900 to XL), and Key Research and Development Program of Hunan Province (No. 2019SK2081 to XL).

Conflict of interest

The authors declare that the research was conducted in the absence of any commercial or financial relationships that could be construed as a potential conflict of interest.

Publisher's note

All claims expressed in this article are solely those of the authors and do not necessarily represent those of their affiliated organizations, or those of the publisher, the editors and the reviewers. Any product that may be evaluated in this article, or claim that may be made by its manufacturer, is not guaranteed or endorsed by the publisher.

- Spezio, M. L., Huang, P.-Y. S., Castelli, F., and Adolphs, R. (2007). Amygdala damage impairs eye contact during conversations with real people. *J. Neurosci.* 27, 3994–3997. doi: 10.1523/JNEUROSCI.3789-06.2007
- Tao, Y., and Shyu, M.-L. (2019). SP-ASDNet: CNN-LSTM based ASD classification model using observer scanpaths. *IEEE*, 641–646. doi: 10.1109/ICMEW.2019.00124
- Tsuchiya, K. J., Hakoshima, S., Hara, T., Ninomiya, M., Saito, M., Fujioka, T., et al. (2021). Diagnosing autism spectrum disorder without expertise: a pilot study of 5- to 17-year-old individuals using Gazefinder. *Front. Neurol.* 11:603085. doi: 10.3389/fneur.2020.603085
- Van der Geest, J. N., Kemner, C., Camfferman, G., Verbaten, M., and van Engeland, H. (2002). Looking at images with human figures: comparison between autistic and normal children. *J. Autism Dev. Disord.* 32, 69–75. doi: 10.1023/A:1014832420206
- Van't Hof, M., Tisseur, C., van Berckleear-Onnes, I., van Nieuwenhuyzen, A., Daniels, A. M., Deen, M., et al. (2021). Age at autism spectrum disorder diagnosis: a systematic review and meta-analysis from 2012 to 2019. *Autism* 25, 862–873. doi: 10.1177/1362361320971107
- Volkmar, F. R., Lord, C., Bailey, A., Schultz, R. T., and Klin, A. (2004). Autism and pervasive developmental disorders. *J. Child Psychol. Psychiatry* 45, 135–170. doi: 10.1046/j.0021-9630.2003.00317.x
- Wang, C., Xiao, Z., Wang, B., and Wu, J. (2019). Identification of autism based on SVM-RFE and stacked sparse auto-encoder. *IEEE Access* 7, 118030–118036. doi: 10.1109/ACCESS.2019.2936639
- Wang, S., Xu, J., Jiang, M., Zhao, Q., Hurlmann, R., Adolphs, R., et al. (2014). Autism spectrum disorder, but not amygdala lesions, impairs social attention in visual search. *Neuropsychologia* 63, 259–274. doi: 10.1016/j.neuropsychologia.2014.09.002
- Wee, C. Y., Wang, L., Shi, F., Yap, P. T., and Shen, D. (2014). Diagnosis of autism spectrum disorders using regional and interregional morphological features. *Hum. Brain Mapp.* 35, 3414–3430. doi: 10.1002/hbm.22411
- Yang, Y. Rating scales for Children's developmental behavior and mental health version 1, Beijing: People's Medical Publishing House. (2016): 71.
- Yi, L., Feng, C., Quinn, P. C., Ding, H., Li, J., Liu, Y., et al. (2014). Do individuals with and without autism spectrum disorder scan faces differently? A new multi-method look at an existing controversy. *Autism Res.* 7, 72–83. doi: 10.1002/aur.1340

Frontiers in Neuroscience

Provides a holistic understanding of brain
function from genes to behavior

Part of the most cited neuroscience journal series
which explores the brain - from the new eras
of causation and anatomical neurosciences to
neuroeconomics and neuroenergetics.

Discover the latest Research Topics

See more →

Frontiers

Avenue du Tribunal-Fédéral 34
1005 Lausanne, Switzerland
frontiersin.org

Contact us

+41 (0)21 510 17 00
frontiersin.org/about/contact

